Artificial Chiral Metallo-pockets Including a Single Metal Serving as both structural Probe and Catalytic Center

Pinglu Zhang, Coralie Tugny, Jorge Meijide Suárez, Maxime Guitet, Etienne Derat, Nicolas Vanthuyne, Yongmin Zhang, Olivia Bistri, Virginie Mouriès-Mansuy, Mickaël Ménand, et al.

Artificial chiral metallo-pockets including a single metal serving as both structural probe and catalytic center

Pinglu Zhang,[a] Coralie Tugny,[a] Jorge Meijide Suárez,[a] Maxime Guitet,[a] Etienne Derat, Nicolas Vanthuyne,[b] Yongmin Zhang,[a] Olivia Bistri,[a] Virginie Mouriès-Mansuy,[a] Mickaël Ménand,[a] Sylvain Roland,[a] Louis Fensterbank, [a]* Matthieu Sollogoub [a]*†

[a]*Sorbonne Universités, UPMC Univ Paris 06, CNRS, Institut Parisien de Chimie Moléculaire (IPCM), UMR8232, 4, place Jussieu, 75005 Paris, France.*
[b]*Aix Marseille Univ, CNRS, Centrale Marseille, iSm2, Marseille, France*

Correspondence: louis.fensterbank@upmc.fr; matthieu.sollogoub@upmc.fr

Summary

A series of capped metallo-cyclodextrins were synthesized, affording a variety of artificial chiral metallo-pockets through modulation of the space around the metal. Carbene ligands were used as caps to place a silver, gold or copper center at a well-defined location inside the cyclodextrin cavity. Multiple weak interactions involving the d^{10} metal center and intra-cavity hydrogen atoms, including anagostic interactions, were observed in solution. Thus, the metal was used as a probe to assess intra-cavity metal–H distances to build 3D models revealing the very different shapes of capped α-, β- and γ-cyclodextrins and the unprecedented helical shape of the chiral pocket of some modified cyclodextrins. This series of NHC-based cyclodextrins were compared in gold-catalyzed cycloisomerization reactions for which the 3D models were used to rationalize the observed regio- and stereoselectivities.

Keywords

Metallo-pockets; Molecular shape; Cavity; N-heterocyclic carbenes (NHC); Cyclodextrin; Catalysis

Introduction

Encapsulating a metallic center in a cavity with a defined and specific shape is an efficient way to promote selectivity in catalytic processes. This is the strategy Nature uses in metalloenzymes, and it has naturally become a source of inspiration to the chemist.[1,2] Confinement of the metal has been achieved in many ways, for instance through confining of metal complex in a caged host, in ligand-forming cages, or through covalent binding to a cavity.[3] Molecular cavities are, most of the time, cyclic oligomers of identical monomeric rings: aromatic rings, sugars, etc. The atoms of these rings demarcate the upper and lower sides of the cavity. Hence, the metal has been placed either outside, in an extension of, or at the edge of the cavity to exploit the inclusion properties of the cavity as a second coordination sphere. Following Breslow's seminal work,[4] cyclodextrins (CDs) have become popular in this area as they provide a system with a well-defined naturally-occurring chiral cavity. The association of a CD with a metal has been thoroughly studied, and the mode of metal anchoring can be divided in two categories involving either a single linkage, or a bridge to form the so-called capped-CDs.[5,6] The clear advantage of the second mode is the precise positioning of the metal with regard to the cavity. When the ligand system positions the metal in close proximity to the cavity, the latter can play the role of host for an exogenous ligand and can constitute a second coordination sphere.[7] Interesting catalytic behaviors have been observed using metal-capped CDs, such as enantioselectivities,[8-11] regioselectivities,[8] and extremely high turnover numbers.[12] Notably, in all these examples, the CD rather served as a platform, a chiral environment or as a bulky ligand to promote unusual coordination modes to the metal but the effect of the CD cavity shape on the outcome of the reactions was scarcely investigated.

In the course of a study into the appending of *N*-heterocyclic carbenes (NHCs) on perbenzylated CDs,[13,14] we serendipitously uncovered a new type of CD-based ligand, an NHC-capped CD (Figure 1).[15] A thorough NMR study of group 11 metal complexes derived from NHC-capped α-CD (**α-ICyD**),

† Lead contact

showed that the metal center is literally wrapped inside the cavity, interacting with both H-5s and H-3s, which cover the inner wall of the cavity of the CD. This therefore stands out from the previously described cavity-linked metal complexes inasmuch as the cavity itself interacts with both the metal and its counterion hence playing the role of both first and second coordination sphere. Additionally, in this system, incoming reaction substrates are forced to interact with the cavity to access the metal (*endo*-approach), in contrast with previous metal-capped CDs where an *exo*-approach can take place (Figure 1).

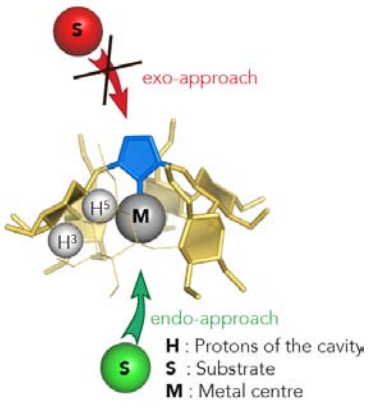

Figure 1. Representation of a carbene-capped cyclodextrin metal complex characterized by a well-defined placing of the metal inside the cavity. The carbene (NHC) is represented in blue. The cyclodextrin macrocycle is shown in beige.

Additionally, promising regio- and stereoselectivities were observed in a preliminary set of catalytic reactions. Remarkably, α- and β-CD derivatives promoted the formation of different products using the same starting material thus showing a strong connection between the selectivity of the reactions and the size of the CD macrocycle. Following this study, we hypothesized that the cavity shape should be crucial for reactivity and potential selectivities. The deformation of the conical shape of the CD has been reported for a metal-capped CD,[16] but its influence on the reactivity of the complex has never been studied. This prompted us to undertake an in-depth structural study of a series of CD-based metal complexes.

Herein we present a broad family of NHC-capped CDs as chiral metallo-pockets, and an original "inverse" approach to map the interior shape of their cavity in solution using NMR. Indeed, the cavity has been used many times as a probe to detect inclusion or ligand exchange in metal-capped CDs;[17] here we use the metal complex as a probe for the interior structure of the cavity through an original network of rare weak interactions. Consequently, we access a series of 3D models, in which the cavity shapes surrounding the metal are significantly different from each other, and are additionally quite distinct from the simplified classical conic representation of CDs. A comparative study of these NHC-capped CD ligands in gold-catalyzed reactions, demonstrates the relevance of these NHC-CD 3D models and the relationship between the shape of the chiral metallo-pockets and the selectivity of the reactions.

Results and discussion

We designed a series of seventeen NHC-capped α-, β- and γ-CD metal complexes to answer the following questions: What are the main factors influencing selectivity in reactions catalyzed by NHC-capped CD metal complexes? Is it the shape of the cavity surrounding the metal or the electronic properties of the capping ligand? or both? To which extend can the shape of the CDs be modified? What is the influence of the size of the CD rim on its shape? What is the influence of the length of the capping moiety? What is the influence of the positioning of the cap anchoring on the shape? Figure 2 shows the various modifications introduced on NHC-capped CDs to answer these questions.

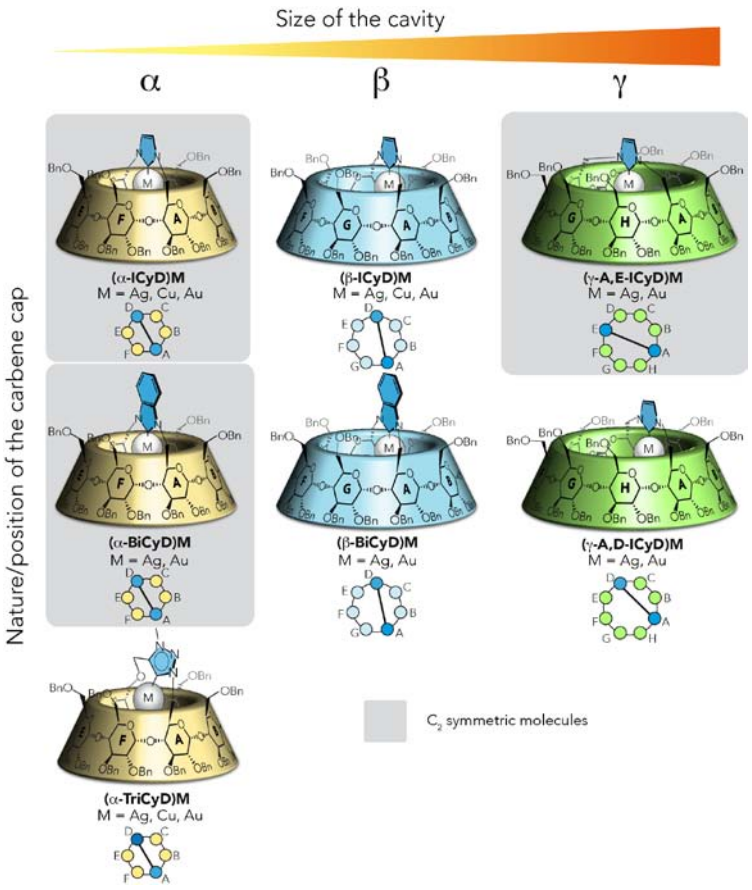

Figure 2. Presentation of all the studied carbene-capped CDs.

A first variation consisted in ***modulating the size of the rim*** using α, β, γ-CD with increasing number of glucose units (n= 6,7,8). A very simple and efficient 5 steps procedure was used to prepare **α, β, γ-ICyD** metal complexes starting from the corresponding native CDs: 1) benzylation , 2) double-debenzylation,[18-20] 3) mesylation, 4) azolium capping and 5) metalation (*see Schemes S1 and S2 and Supplemental Experimental Procedures*). Of note, in the γ-CD series, two different regioisomers are formed[21] **(γ-A,D-ICyD)MCl** and **(γ-A,E-ICyD)MCl** corresponding to two different anchorings of the capping NHC ligand on the CD core, thus allowing to study the effect of the ***variation of topology*** of the capping on the shape of the CD. To study the influence of electronic properties of the ligand, we changed ***the nature of the capping*** to benzimidazole, and synthesized **(α-BiCyD)M** and **(β-BiCyD)M** (M = Ag, Au) complexes using the same route. All these syntheses were achieved on large scale with high yields and the obtained complexes are remarkably stable (Scheme 1).

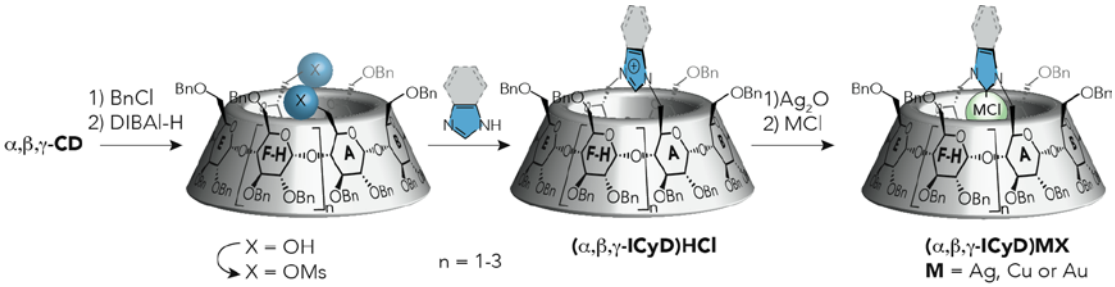

Scheme 1. General synthetic scheme.

In addition, a ***modulation of the length of the cap as well as its electronic properties*** was accessible by synthesizing an abnormal[22] or mesoionic carbene (MICs),[23-25] namely triazolylidene-capped α-CD complexes **(α-TriCyD)M** (M = Ag, Au, Cu). Their synthesis involved an intramolecular copper(I)-catalyzed alkyne-azide cycloaddition (CuAAC)[26] of an azido-alkyne derived CD, which

synthesis is based on recent developments on hetero-functionalisations of CDs[19,27-43] (*see Supplemental Scheme S3, and Supplemental Experimental Procedures*).

NMR study. We next studied the structure of this family of carbene-capped CD metal complexes by NMR and molecular modeling. In a first instance, we observed a NOESY cross-correlation between the acidic azolium proton Hα of all the precursors and some inner-cavity protons H-5 symptomatic of an introverted position of this proton (*see Figures S1-S6*). We then carefully characterized all carbene-capped CD complexes also by NMR. As we previously described on **α-ICyD** metal complexes, the inclusion of the metal inside the cavity induced the deshielding of H-5s and H-3s, carpeting the interior of the cavity (Figure 1), compared to the corresponding azoliums (*see Figures S7-S15*). The chemical shifts of the H-3s and H-5s of all the synthesized silver complexes are reported in table S1. A general trend appears: H-5s belonging to glucose units linked to the carbene metal complex are the most deshielded among the H-5s, while their H-3s are among the less deshielded compared to the other H-3s. For the H-3s, a general trend can be drawn depending on the symmetry of the complex, but in a first approximation the H-3s of the sugars situated clockwise (view from the primary rim) to the cap are the most deshielded (*for more details see SI*). Furthermore, benzimidazolylidene complexes **BiCyDs** display H-5s, which are more deshielded than the imidazole-derived **ICyDs**. The deshielding of the H-5s on **γ**-CDs is notably less important than for their α and β counterparts. We hypothesized that these shifts were related to the position of the inner-cavity protons relative to the complex and therefore to the shape of the cavity.

Molecular modeling of the shape. In order to understand this relationship to eventually deduce the 3D shape in solution of all our cavities, we first conducted an in-depth study of the structure of **(α-ICyD)AgCl** complex. We modeled **(α-ICyD)AgCl** using DFT calculations replacing benzyl groups by methyls. These calculations were performed with Turbomole,[44] at the B3LYP level[45-47] complemented by the D3 dispersion scheme[48] and with the def2-SV(P) basis set.[49] We then observed a good correlation between H-5/Ag, and H-3/Cl distances measured on this model and the relative chemical shifts of those protons (Table S1 and Figure 5): the closer the proton is to Ag or Cl in the model, the more deshielded are the corresponding protons on the NMR spectrum.

For H-3s the interaction is most certainly a C-H…X type weak hydrogen bonding with the halogen. For H-5s the situation is different because they interact with a metal, H-5^A/Ag distance is around 2.5 Å and C-$H5^A$-Ag angle is around 140°, which associated to deshielding, are a good diagnosis for anagostic interactions. Anagostic interactions, which differ from more usual agostic interactions,[50] are thought to be more electrostatic in nature, associated to longer H…M distances and larger C-H-M angles, as well as proton deshielding.[51] We also performed a NCI (Non-Covalent Interaction) analysis[52,53] and determined that attractive interactions were indeed observed between protons and proximal metal or halogen, with intensities in the same order as the chemical shifts (Figure 3).

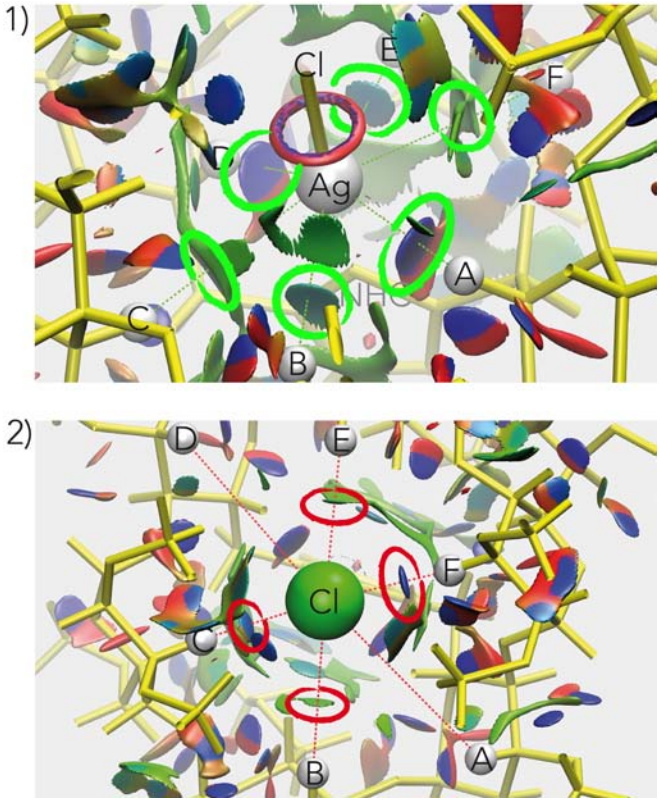

Figure 3. NCI analysis of **(α-ICyD)AgCl**; the molecular structure is displayed by the yellow backbone while the NCI layers are color-coded as follow: blue: strong interactions; green: weak interactions; red: repulsive interactions. 1) Anagostic interactions between H-5s and Ag, green circles, 2) Weak hydrogen bonds between H-3s and Cl, red circles.

Anagostic interactions have been mainly observed in square planar d^8 systems.[54-57] For d^{10} coinage metals, though richer in electrons, cases of reported anagostic interactions remain very scarce: a single one in the solid state involving Cu^{I}[58] and another one in solution with Au^{I}.[59] No anagostic interaction has been reported so far involving Ag^{I}. In fact, in the case of one reported NHC ligand, the interaction exists in the presence of Pd^{II}, but when this metal is replaced by Ag^{I}, the ligand changes its conformation and the anagostic interaction is not observed anymore.[60] In our case, the preorganization of the protons in the cavity forces anagostic interactions to take place. The metal here undergoes 6 anagostic interactions in addition to the halogen and NHC coordinations. Hence, through C-H-5…Ag and C-H-3…Cl interactions the walls of the cavity play the role of both first and second coordination spheres for the complex. This is a unique feature of the system compared to all other metals appended to cavities.

All chemical shifts observed for H-5s when ligands, metals or counterions are modified, can be accounted in light of anagostic interactions. Indeed, the less Lewis acidic metals give the strongest anagostic interaction and therefore the strongest deshielding of the H-5s.[61,62] First, we had previously shown that deshielding of the $H\text{-}5^{A}$ in the AgOAc complex is more important than in the case of the AgOTf complex where the triflate is less σ-donating in nature.[15] We also observed that the variation of $H\text{-}5^{A,D}$ deshielding depends on the nature of the metal $\delta_{H5A,D}$ Au > $\delta_{H5A,D}$ Cu > $\delta_{H5A,D}$ Ag (*See SI, Figures S7-S10, S13*). We can correlate this chemical shift variation with the nature of the NHC-metal bond. Bond strengths of group 11 NHC complexes follow the pattern Au > Cu > Ag. The NHC-Au bond is the strongest while NHC-Ag bond is relatively the weakest. At the same time, the bond length variation for the complexes follow the tendency Au < Cu < Ag, confirmed by both theoretical and single-crystal X-ray diffraction studies,[63-65] and explained by relativistic effects.[66] Finally, we observed that internal protons of **(α-BiCyD)AgCl** are deshielded by 0.28 ppm compared to **(α-ICyD)AgCl** (see *SI, Figure S14*). Benzimidazolylidene is a stronger σ-donating and π-accepting ligand than Imidazolylidene,[67] it is therefore difficult to predict its effect on the Lewis acidity of the metal. Anagostic interactions through H-5 chemical shift show that it decreases the Lewis acidity of the metal, which therefore implies that it is globally a stronger donor than imidazolylidene. The measure of the Lewis acidity through anagostic interactions complements the numerous techniques already to measure electronic properties of NHCs.[67-76] Therefore, the electron density of the metal influences H-5's chemical shift, and reversely, $H\text{-}5^{A,D}$'s chemical shifts can be a way to map the interior of the cavity.

Indeed, the mapping of the cavity is possible as a consequence of the direct relation between chemical shift of the H involved in an anagostic interaction or in a weak hydrogen bonding to its distance to the metal,[55] or to the halogen. Given the size of our systems for DFT calculations, using simple molecular mechanics to build models seems appropriate and practical for all molecules described here. Thus, we used Avogadro's[77] UFF force field[78] and adjusted the order of the distances to the metal and the halogen according to the order of the observed chemical shifts then allowed the system to reach a minimum. We then superimposed the model **(α-ICyD)AgCl** obtained in this manner with the one produced by DFT. As can be seen on figure 4, the two models give essentially the same structures, validating our approach.

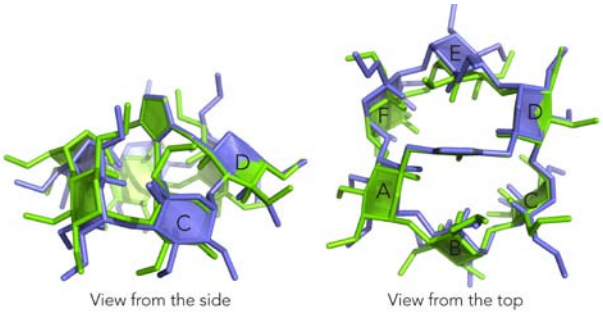

Figure 4. Superimposition of modeled **(α-ICyD)AgCl**, DFT green, MM blue

3D structure building of all metal complexes. We therefore decided to use the same methodology for all silver complexes. We built the model and minimized the structure for each of them. The distances in the obtained models were then adjusted in Avogadro followed by another minimization until the order of distances of the H-5s and H-3s to the metal and the halogen, respectively, corresponded to the order of the observed chemical shifts. The resulting models are presented in figure 5. We used the same optimized structures to build Cu^{I} and Au^{I} complexes having the same linear coordination.

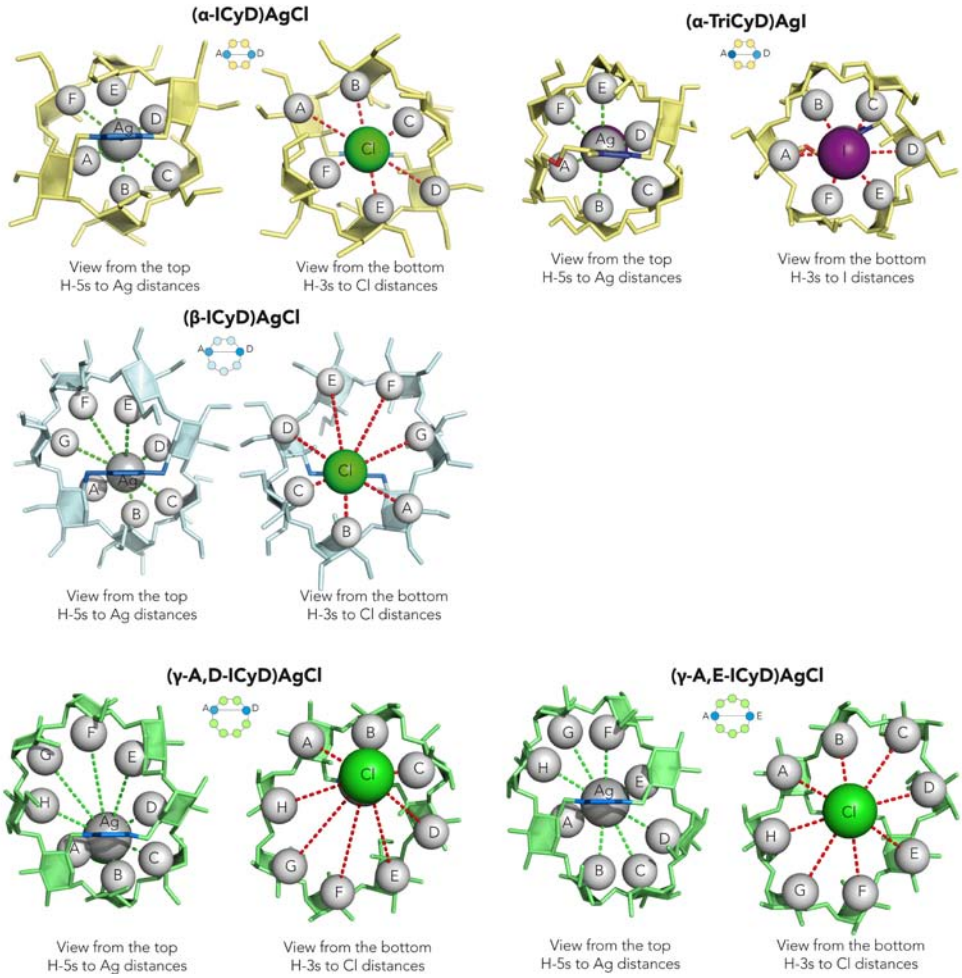

Figure 5. Models of **(α-ICyD)AgCl, (β-ICyD)AgCl, (α-TriCyD)AgCl, (γ-A,E-ICyD)AgCl, (γ-A,D-ICyD)AgCl** with Ag to H-5s distances (in green) and Cl to H-3s distances (in red) set in order according to their chemical shifts.

The shapes of the cavities imposed by both the bridging and the metal complex are revealed on Figure 6 by tracing their Connolly surface. At first glance, the conical shape has been substantially altered. All structures present a groove, a consequence of the tilting of sugar units linked by the cap, which is a direct translation of the chemical shifts of the H-5s and H-3s: H-5 closest to the metal, and H-3 farthest to the halogen. Remarkably, **α-**, **β-** and **γ-AD-ICyDs** feature asymmetric cavities. For instance, the cavity of the **α-ICyD** adopts the shape of a M-helix resembling to a propeller. This is directly related to the H-3/Cl distances observed by NMR and translated in the model. In the cases of **β-** and **γ-AD-ICyDs** the narrow side of the cavity forms a steep wall while the wide side also adopts a M-helical shape. Surprisingly, we can distinguish two structures in which the helicity is a lot less apparent: **(α-TriCyD)M** and, **(γ-AE-ICyD)M**. Apparently a long cap or a large CD do not induce an asymmetrical deformation of the CD cavity. This was rather unexpected, at least for the TriCyD derivative where the cap is unsymmetrical and was expected to yield a more twisted structure (Figure 6).

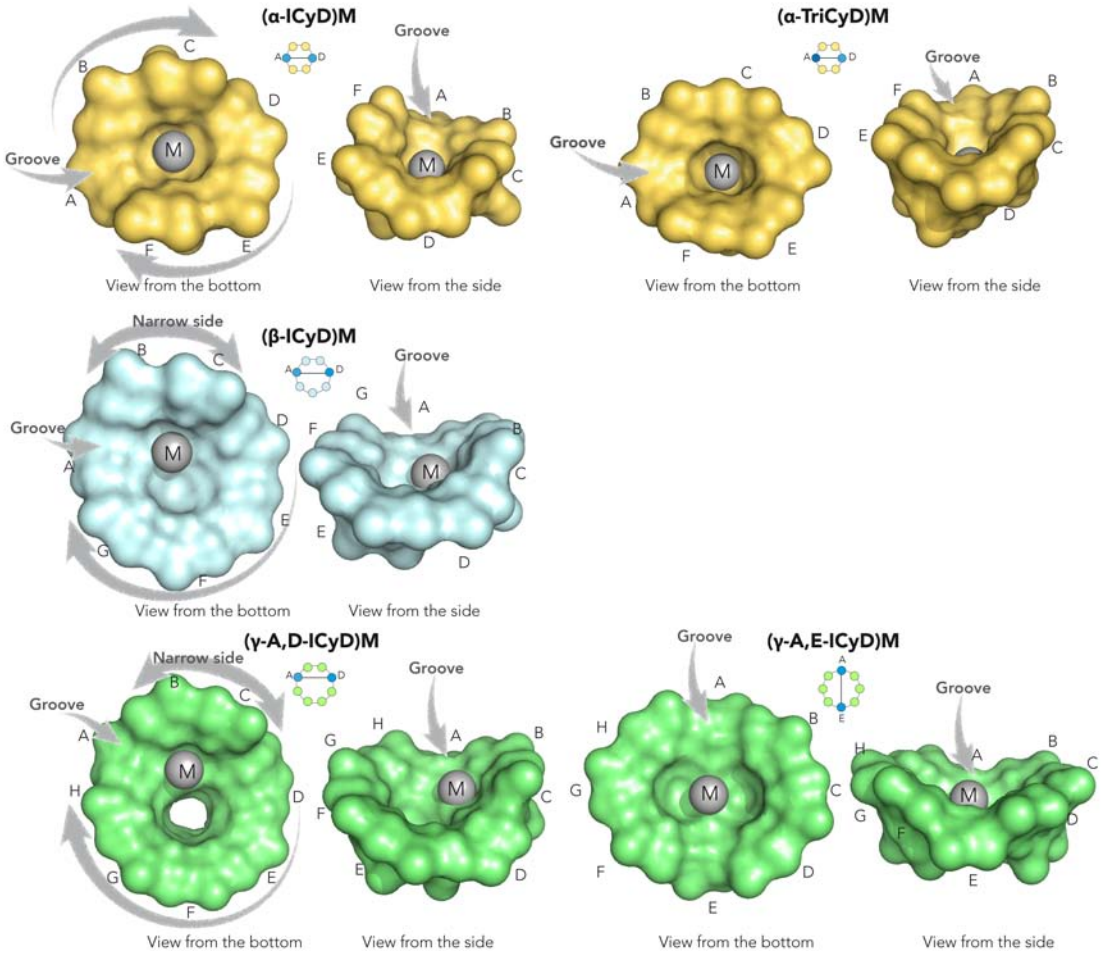

Figure 6. Estimated average shapes (Connolly surface) in solution of **(α-ICyD)MCl**, **(β-ICyD)MCl**, **(α-TriCyD)MCl**, **(γ-A,E-ICyD)MCl**, **(γ-A,D-ICyD)MCl**, arrows indicate the groove, the narrow side or the M-helix side, Cl has been omitted for clarity, Me groups were oriented in the same direction for comparison purposes.

Can we connect the CD shape to selectivity in metal-catalyzed reactions ? We then sought to validate our mapping of the morphologies of metal NHC-capped CD complexes by comparing the selectivities that each cavity shape induces in catalytic tests. Encapsulation of a gold metal center into a cavity appears interesting because it allows variation of the reactivity in catalysis.[79-84] Therefore, we anticipated that modularity of the cavity shape should affect the outcomes of the reactions in terms of regio- and stereoselectivity. We previously showed that **(α-ICyD)AuCl** and **(β-ICyD)AuCl** were able to catalyze cycloisomerization reactions.[15] The prototypical 1,6-enyne system **1** was initially chosen as a probe. Herein, its cycloisomerization with the synthesized series of new AuCl carbene-CD precatalysts, under identical conditions (CH_2Cl_2, rt, 18h) contrasted with findings in the literature data[85] and our previous findings.[15] While the α-CD environment, regardless of the ancillary carbene ligand (NHC or MIC) on gold(I), resulted in the formation of the usually prevailing cyclopentadienic products **2a/b**, the β-CD (**2**:**3**, 1:3.3), and to a lesser extent γ-CDs, gave the highest yields of the "endocyclization" cyclohexadiene product **3** recorded for gold catalysis in this reaction (Scheme 2).[85-88] It is worth noting that ICyD and BiCyD ligands yielded effectively the same results. This set of reactions clearly demonstrates that it is the variation of the size and therefore the shape of the cavity that influences the outcome of this cycloisomerization reaction and not the electronics of the ligand (Table 1).

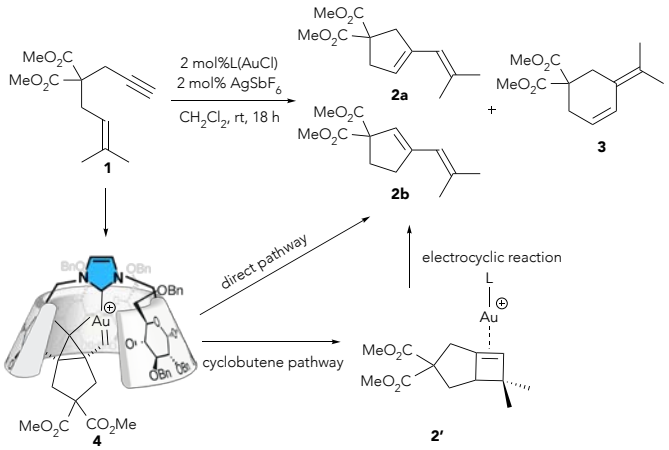

Scheme 2. Gold-catalyzed regioselective cycloisomerisation of enyne **1**

Table 1. Yields of the products of the gold-catalyzed regioselective cycloisomerisation of enyne **1**

Ligand	IPr	α-ICyD	β-ICyD	γ-A,D-ICyD	γ-A,E-ICyD	α-BiCyD	β-BiCyD	α-TriCyD
Yield	88%	52%	63%	80%	100%	87%	88%	78%
2 **(a:b)**	100% (1:0.7)	100% (1:0.7)	23% (1:0)	72% (1:0.56)	55% (1:0.14)	90% (1:0.2)	21% (1:0.6)	96% (1:0.8)
3	0%	0%	77%	28%	45%	10%	79%	4%

The mechanism of the reactions affording either 5- or 6-membered rings was studied in detail, both computationally and experimentally, by Echavarren.[89] In both cases, the reaction is believed to involve the formation of a cyclopropylcarbene intermediate such as **4**. From **4**, a direct pathway involving a skeletal rearrangement of the cyclopropyl affords either cyclopentene derivatives **2**[90] or cyclohexene derivative **3**.[91] Alternatively, **2** can be produced through a cyclobutenyl intermediate **2'** (Scheme 2).[92] This evolution is therefore altered in the confined medium of α- and β-CD derivatives. We therefore probed these mechanisms computationally by DFT modeling (B3LYP-D3/def2-SV(P)) the cyclopropylcarbene **4** in the case of both **α**- and **β-ICyD**. In the case of **α-ICyD**, the model of complex **4α** was found by DFT to spontaneously evolve into an opened carbocationic intermediate **4'α**, which affords the cyclobutenyl intermediate **2'α** via a transition state **TS2'α** of very low energy (0.95 kcal.mol^{-1}) (Scheme 3, and Figure S16). This pathway is consistent with the obtention of the cyclopentene derivatives **2**[92] as the major isomer with α-CD-based gold catalyst.

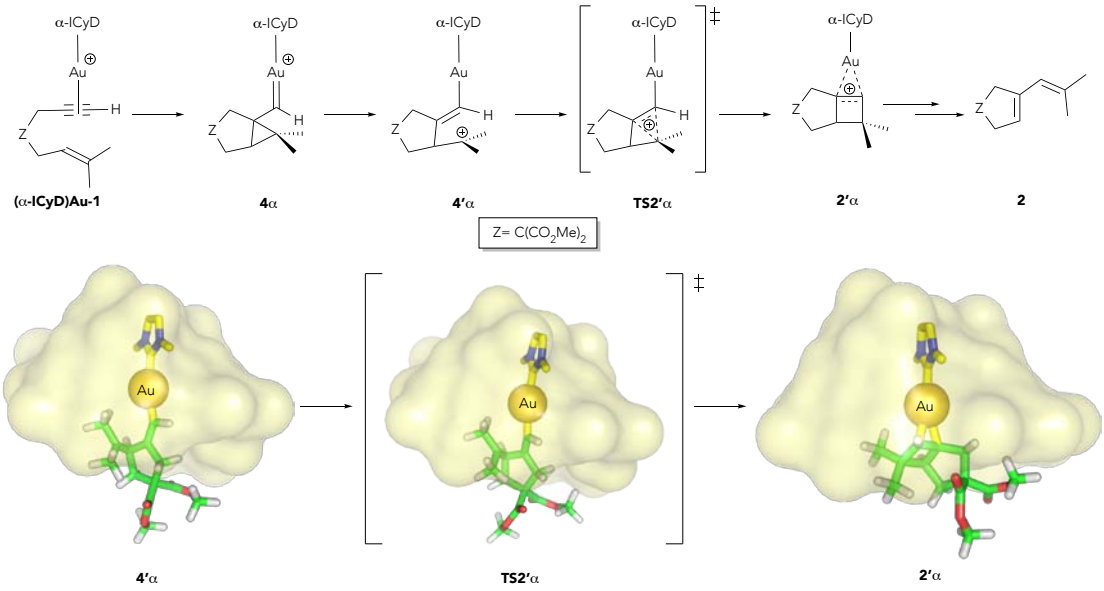

Scheme 3. Proposed mechanism of the Gold-catalyzed regioselective cycloisomerisation of enyne **1** using **α-ICyD**

Interestingly, in the case of **β-ICyD**, we found that complex **4β** corresponded to a local minimum, which therefore does not spontaneously evolve, but first gives a gold complex with a rather different conformation compared to that of the reactive complex obtained with **α-ICyD**. We next turned our attention to the different transition states **TS$_A$** and **TS$_B$** (Scheme 4, L=PMe$_3$) allowing the formation of **3** or **2** respectively published in the literature.[90-91] We observed that in the transition state en route to either 6- or 5-membered rings the bond becoming a double bond is anti-periplanar to the C-Au bond as shown in **TS$_A$** and **TS$_B$** respectively (red bonds in scheme 4). We therefore assumed that it is a difference of conformation imposed by the confinement of the β-CD that would orient the regioselectivity toward **2** or **3**. Hence, we calculated the energies of both conformers **A** and **B** (L=**β-ICyD**, scheme 4), obtained under constraint, relative to **4β** and found that conformer **A** was more energetically favored than **B** by 4.08 kcal.mol^{-1}. Thus, we attribute the formation of **3** as the major product with **β-ICyD** to the easier access to conformation **A** giving **TS$_A$**. Furthermore, we incidentally found that the unfavored conformer **B** led to **4'β** and therefore that the formation of the minor isomers **2**, in the case of β-CD-based catalyst should preferentially take place via the cyclobutene pathway (Scheme 4 and Figure S17). Therefore the different shapes of **α**- and **β-ICyDs** lead to different conformations of intermediate **4** that produce **2** or **3** as a major product.

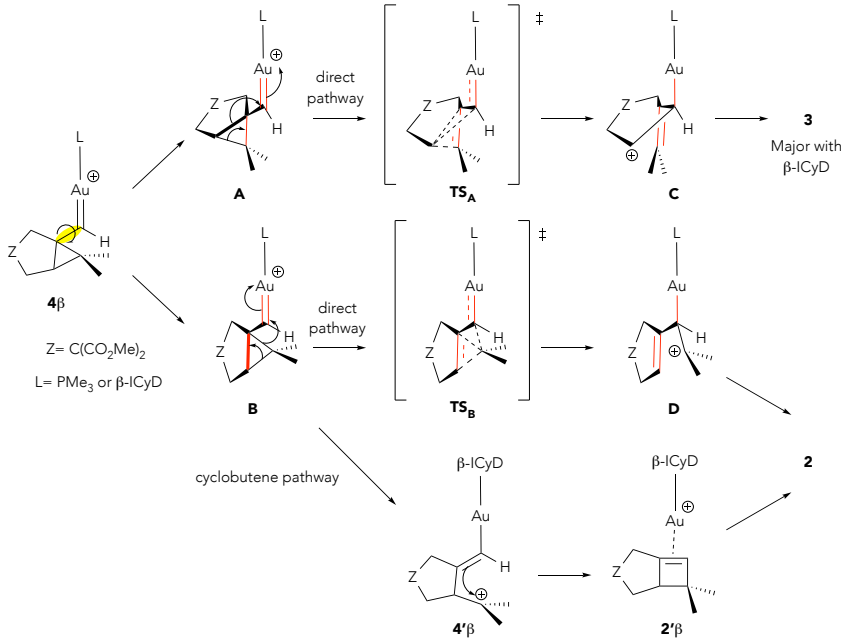

Scheme 4. Proposed mechanism of the Gold-catalyzed regioselective cycloisomerisation of enyne **1** using **β-ICyD**

The wrapping of the gold center into the chiral NHC-capped CD ligand offers an exciting opportunity to perform asymmetric gold catalysis, which still remains very challenging because of the linear coordination of gold(I) complexes.[93-95]We therefore examined the cycloisomerization of *N*-tethered enynes **5**[96-101] and **6**[102-103] (Scheme 5). Interestingly, α- and β-CD derivatives as well as the asymmetrically capped γ-A,D-CD induced ees and favored the formation of the same isomer. In striking contrast, the **(γ-AE-ICyD)AuCl** and **(α-TriCyD)AuCl** precatalysts provided only racemic mixtures with enyne **5** and notably an inversion of enantioselectivity was observed upon reaction of **6** with **(γ-AE-ICyD)AuCl**. The catalysts derived from β-CD, provided **7** and **8** with very promising ees around 60% and 80%, respectively. The more sterically hindered phenyl-substituted alkene **6** resulted in higher ees. By way of comparison, the best enantioselectivity observed in the metal-catalyzed cycloisomerization of **5** is 88% with rhodium(I) catalysis, and 80% for **6** (Scheme 5, Table 2).[102] While the influence of the nature of the NHC is very minor, the shape of the cavity seems to promote drastic differences in selectivities from 0 to 80% ee. The reaction kinetics were studied by ^{1}H NMR with **(IPr)AuCl**, **(α-ICyD)AuCl** and **(β-ICyD)AuCl** as catalysts, under the same standard conditions than those used for the catalytic tests: **(L)AuCl** (2 mol%), $AgSbF_6$ (2 mol%), enyne **6** 0.025 M in CD_2Cl_2, r.t. (*see Supplemental Experimental Procedures*). Under these conditions, the reaction rates are dramatically different, as clearly shown by the values of initial rates. The **IPr**-derived catalyst induced a much faster reaction (r_0 = 40.2 mM.s^{-1}) than both **ICyD**-based catalysts, emphasizing the steric hindrance induced by the CD around the gold center. Furthermore, the steric effect is also demonstrated by the difference in kinetics between CD derivatives, the **β-ICyD** ligand (r_0 = 1.2 mM.s^{-1}) leading to a much faster reaction than the **α**-

ICyD ligand, which is inactive at 300 K (r_0 = 0) (*see Figures S18-S19 and Supplemental Experimental Procedures*). Finally, cumulative turn-over numbers (TONs) were determined for **(IPr)AuCl** and **(β-ICyD)AuCl**-catalyzed reactions to assess their relative stability. Three cycles of reaction were run for each catalyst in a NMR tube, by keeping a constant Au complex concentration, and by adding increasing amounts of enyne **6** in the medium after the reaction is complete (see SI for the detailed procedure). From these experiments, it appears that the stability of the **β-ICyD**-derived Au^I complex is comparable to that of the very stable **IPr** complex with TONs reaching ∼800 in both cases. Interestingly, under these conditions, the **(β-ICyD)Au^I** complex is still active with comparable ee (79%) and a final catalyst loading lowered up to 0.1 mol % (starting from 2%) and a very high final concentration of substrate (0.5 M)(see *Figure S20 and Supplemental Experimental Procedures*).

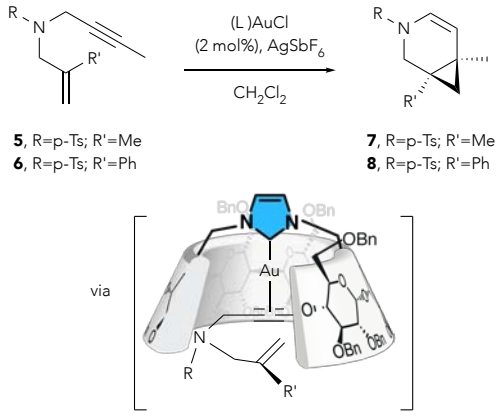

Scheme 5. Gold-catalyzed enantioselective cycloisomerisations of enynes **5, 6.**

Table 2. Yields and ees of the gold-catalyzed enantioselective cycloisomerisations of enynes **5, 6.**

Substrate	L	IPr	α-ICyD	β-ICyD	γ-A,D-ICyD	γ-A,E-ICyD	α-BiCyD	β-BiCyD	α-TriCyD
5	Yield of **7**	80%	83%	77%	77%	50%	63%	85%	58%
	ee	0%	43% (+)	59% (+)	7% (+)	0%	26% (+)	63% (+)	0%
6	Yield of **8**	74%	78%	99%	70%	99%			
	ee	0%	48% (+)	**80%** (+)	22% (+)	42% (-)			

We showed that we could rationalize the regioselectivities induced by our system thanks to the size of the cavity but the role of shape itself was difficult to apprehend. In the present case of stereoselecivity, electronic properties of the NHC, again, do not seem to have a significant effect whereas the nature of the CD and therefore its shape must have. We decided to confront our enantioselective catalytic results with the shapes of the cavities we obtained. The reaction starts with the complexation of the triple bond to the electrophilic gold center followed by the nucleophilic addition of the alkene to form the cyclopropane, and the formation of both new stereogenic centers.[104] The enantioselectivity is therefore ruled by the approach of the alkene. Hence, we were able to account for the obtained enantioselectivities of the cycloisomerisations of **5** and **6** using the shapes that we determined above and simply manually approaching the substrate like in a molecular model. It seems reasonable that the alkyne enters the groove with the alkene folding to overlap with the triple bond. In the case of **α-ICyD**, because of its C_2 symmetry, there are only two ways to fold for the enyne. In one case the phenyl of **6** or the methyl of **5** borne by the alkene clashes with the steeper side of the helix or with the lower one. The second approach gives the right stereoisomers **(+)-(*R*,*R*)-7** and **(+)-(*R*,*R*)-8**, the absolute configuration of the latter was determined using X-ray crystallography. (Figures 7A and 7B, see SI) The α-CD can be further simplified as a hexagon divided into six triangles, each corresponding to a sugar unit that makes up the CD. These triangles can be colored with a gradient of blue according to the proximity of the sugar unit to the reaction center; namely the darker blue the closer the sugar. (Figure 7B) It is also worth mentioning that when phenyl of enyne **6** is replaced by

a less hindered methyl in enyne **5**, the steric clash is less significant and therefore the ees are smaller. When looking at β-CD derivatives, the CD can be simplified as a heptagon with 7 triangles, shaded in the same manner. (Figure 7D) This time, on one side of the groove delineated by the light blue triangles, two dark blue triangles indicate the presence of the steep wall; the enyne can therefore not fold on this side. Two approaches are therefore possible as shown in Figure 7C and 7D, the one inducing the less steric clashes (on the left) produces the correct stereoisomer. We then confronted these simplified and static models with DFT calculations (B3LYP-D3/def2-SV(P)) optimizing all the proposed conformations. Our calculations found that the conformer leading to **(+)-(*R*,*R*)-8** is more energetically favored by 3.68 kcal.mol^{-1} for the **α-ICyD** and by 4.08 kcal.mol^{-1} for the **β-ICyD** (*see Figure S21*), which is in line with the experimental results. Finally, the very different behavior of both **(γ-AE-ICyD)AuCl** and **(α-TriCyD)AuCl** in terms of stereoselectivities also underlines the critical role of the critical shapes which visually differ from the others.

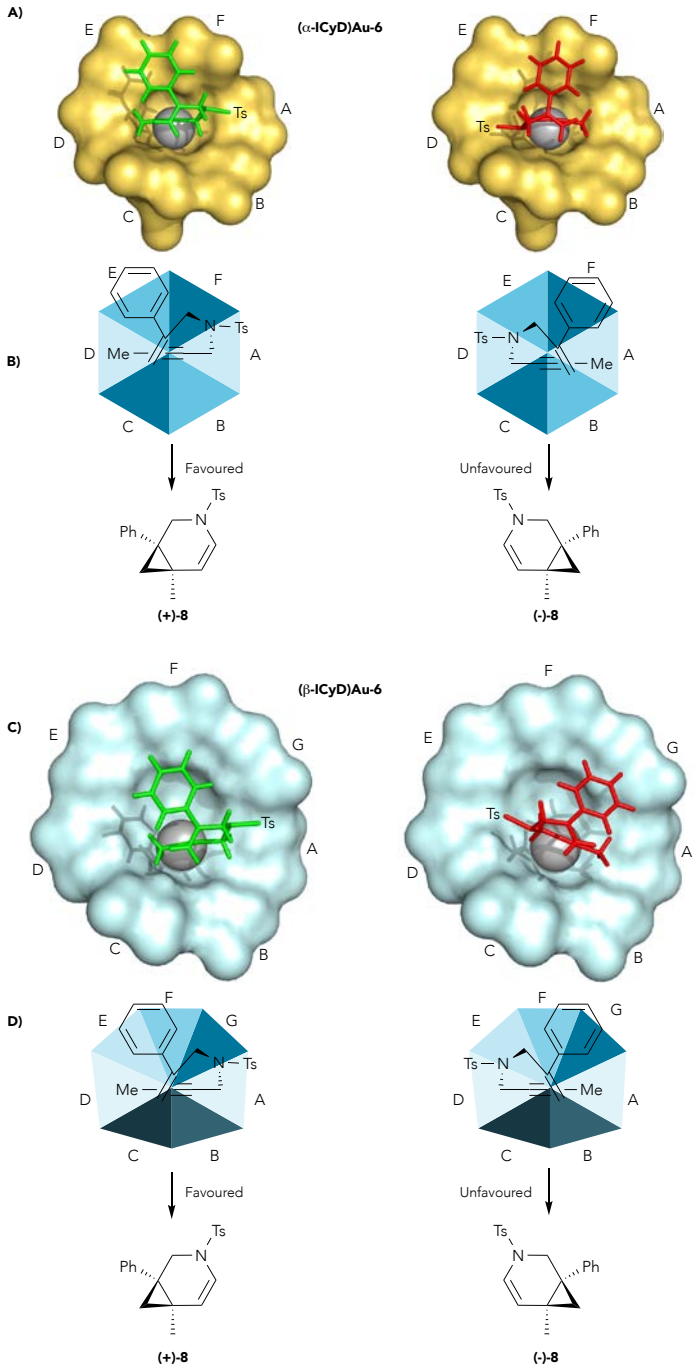

Figure 7. Rationalization of the enantioselectivities in the cycloisomerisation of **6**. A) Possible approaches of **6** on **(α-ICyD)Au**, manually constructed, in green the sterically favored approach, in red the sterically unfavored approach; B) The

corresponding simplified model; C) Possible approaches of **6** on **(β-ICyD)Au**, manually constructed, in green the sterically favored approach, in red the sterically unfavored approach; D) The corresponding simplified model.

Conclusions

We have synthesized a family of seventeen carbene-capped CDs metal complexes that present an original set of interactions, including numerous anagostic interactions together with weak hydrogen bonds. The ensemble of those two interactions allowed the mapping of the interior of the cavity and modeling of its shape for each complex. We showed that the precise positioning of a carbene cap on CDs led to a series of metallo-pockets of varied shape. Cavity modulation was found to be rather drastic, as the structures ranged from symmetrical to propeller-like. Compounds were then used as catalysts in cycloisomerisation reactions. The size and shape of the cavity induced cavity-dependent selectivities. A spectacular difference between the α and β-CDs appeared in the different regioselectivities that were observed in a cycloisomerisation yielding 5 or 6 membered rings. Enantioselectivities in a family of cycloisomerisations can reach 80% ee. We propose a rationalization of these results based on the topography of α and β-ICyDs. More generally, using modulation of the cavity and molecular modeling to reveal the shape variation, we have been able to understand some aspects of the reactivity of carbene-capped CDs highlighting their potential as tunable chiral metallo-pockets. Many aspects of these fascinating molecules should be further explored to precisely control their properties. We surmise that CD-NHC metal complexes have many assets to promote new applications in all aspects of selectivity in catalysis in particular on site-selective catalysis.

Author Contributions

PZ synthesized α- and β-BiCyD, β-ICyD and TriCyD derivatives and studied their NMR. CT did the catalysis experiments. JMS synthesized and studied the γ-CD derivatives. MG synthesized and studied α-ICyD. ED did the DFT calculations. NV determined the ees and the separated enantiomers. YZ supervised PZ and contributed in the analysis of the results. OB supervised JMS and contributed in the analysis of the results and spectral analysis. VMM supervised CT and did some catalysis experiments. MM supervised MG and contributed to the NMR analysis. SR supervised all the synthetic part of NHC-CDs of PZ and JMS. SR, VMM, and OB designed and did the kinetics experiments. LF designed the catalytic experiments. MS designed the study, supervised it and wrote the paper. All authors contributed to the writing of the paper.

Acknowledgements

The authors thank Cyclolab (Hungary) and Roquette (France) for generous supply of α-CD, β-CD, and γ-CD, Avassaya Vanitcha for a sample of compound 8, Aurélie Bernard for efficient assistance in NMR, LabEx MiChem part of French state funds managed by the ANR within the Investissements d'Avenir programme under reference ANR-11-IDEX-0004-02, and Agence Nationale de la Recherche (Supra-HierArchi Project ANR-Blanc SIMI 7-2012) for financial support and the China Scholarship Council for PhD grant (PZ).

Notes and references

1- Le Poul, N., Le Mest, Y., Jabin, I., and Reinaud, O. (2015). Supramolecular Modeling of Mono-copper Enzyme Active Sites with Calix[6]arene-based Funnel Complexes. Acc. Chem. Res. *48*, 2097-2106.

2- Rebilly, J.-N., Colasson, B., Bistri, O., Over, D., and Reinaud, O. (2015). Biomimetic cavity-based metal complexes. Chem. Soc. Rev. *44*, 467-489.

3- For a recent review on metal-catalysis in confined space see: Leenders, S. H. A. M., Gramage-Doria, R., de Bruin, B., and Reek, J. N. H. (2015). Transition metal catalysis in confined spaces. Chem. Soc. Rev. *44*, 433-448.

4- Breslow, R., and Overman, L. E. (1970). "Artificial enzyme" combining a metal catalytic group and a hydrophobic binding cavity. J. Am. Chem. Soc. *92*, 1075-1077.

5- Armspach, D., and Matt, D. (1999). Metal-capped α-cyclodextrins: the crowning of the oligosaccharide torus with precious metals. Chem. Commun. 1073-1074.

6- Engeldinger, E. , Armspach, D., and Matt, D. (2003). Capped Cyclodextrins. Chem. Rev. *103*, 4147-4173.

7- Gramage-Doria, R., Armspach, D., and Matt, D. (2013). Metallated cavitands (calixarenes, resorcinarenes, cyclodextrins) with internal coordination sites. Coord. Chem. Rev. *257*, 776-816.

8- Jouffroy, M., Gramage-Doria, R., Armspach, D., Sémeril, D., Oberhauser, W., Matt, D., and Toupet, L. (2014). Confining Phosphanes Derived from Cyclodextrins for Efficient Regio- and Enantioselective Hydroformylation. Angew. Chem. Int. Ed. *53*, 3937-3940.

9- Wong, Y. T., Yang, C., Ying, K.-C., and Jia, G. (2002). Synthesis of a Novel β-Cyclodextrin-Functionalized Diphosphine Ligand and Its Catalytic Properties for Asymmetric Hydrogenation. Organometallics *21,* 1782-1787.

10- Engeldinger, E., Armspach, D., Matt, D., Toupet, L., and Wesolek, M. (2002). Synthesis of large chelate rings with diphosphites built on a cyclodextrin scaffold. Unexpected formation of 1,2-phenylene-capped α-cyclodextrins. C. R. Chimie *5*, 359-372.

11- Guieu, S., Zaborova, E., Blériot, Y., Poli, G., Jutand, A., Madec, D., Prestat, G., and Sollogoub M. (2010). Can hetero-polysubstituted cyclodextrins be considered as inherently chiral concave molecules? Angew. Chem. Int. E d. *49*, 2314-2318

12- Zaborova, E., Deschamp, J., Guieu, S., Blériot, Y., Poli, G., Ménand, M., Madec, D., Prestat, G., and Sollogoub M. (2011). Cavitand supported Tetraphosphine: Cyclodextrin offers a useful platform for Suzuki-Miyaura cross-coupling. Chem. Commun*. 47*, 9206-9208.

13- Legrand, F.-X., Ménand, M., Sollogoub, M., Tilloy, S., and Monflier, E. (2011). N-Heterocyclic Carbene Ligand based on a β-cyclodextrin-Imidazolium Salt: Synthesis, Characterization of Organometallic Complexes and Suzuki Coupling. New J. Chem. *35*, 2061-2065.

14- Guitet, M., Marcelo, F., Adam de Beaumais, S., Zhang, Y., Jiménez-Barbero, J., Tilloy, S., Monflier, E., Ménand, M., and Sollogoub, M. (2013). Diametrically opposed Carbenes on an α-Cyclodextrin: synthesis, characterization of organometallic complexes and Suzuki-Miyaura coupling in ethanol and in water. Eur. J. Org. Chem. 3691-3699.

15- Guitet, M., Zhang, P., Marcelo, F., Tugny, C., Jiménez-Barbero, J., Buriez, O., Amatore, C., Mouriès-Mansuy, V., Goddard, J.-P., Fensterbank, L., Zhang, Y., Roland, S., Ménand, and M., Sollogoub, M. (2013). NHC-Capped Cyclodextrins (ICyDs): Insulated Metal Complexes, Comutable Multicoordination Sphere and Cavity-Dependant Catalytisis. Angew. Chem. Int. Ed. *52*, 7213-7218.

16- Armspach, D., and Matt, D. (2001). Metal-Capped α-Cyclodextrins: Squaring the Circle. Inorg. Chem. *40*, 3505-3509.

17- Engeldinger, E. , Armspach, D., and Matt, D. (2001). Cyclodextrin Cavities as Probes for Ligand-Exchange Processes. Angew. Chem. Int. Ed. *40*, 2526-2529.

18- Lecourt, T., Pearce, A. J., Herault, A., Sollogoub, M., and Sinaÿ, P. (2004). Triisobutylaluminium and diisobutylaluminium hydride as molecular scalpels: the regioselective stripping of perbenzylated sugars and cyclodextrins. Chem. Eur. J. *10*, 2960-2971.

19- Zaborova, E., Blériot, Y., and Sollogoub, M. (2010). μ-Waves Avoid Large Excesses of Diisobutyl-aluminium-hydride (DIBAL-H) in the Debenzylation of Perbenzylated α-Cyclodextrin. Tetrahedron Lett. *51*, 1254-1256.

20- Guieu, S., and Sollogoub, M. (2008). Multiple homo and hetero-functionalisations of α-cyclodextrin through oriented deprotections. J. Org. Chem. *73*, 2819-2828.

21- De-O-benzylation of perbenzylated γ-cyclodextrin affords a mixture of A,D and A,E diols which were separated after mesylation.

22- Mathew, P., Neels, A., and Albrecht. M. (2008). 1,2,3-Triazolylidenes as Versatile Abnormal Carbene Ligands for Late Transition Metals. J. Am. Chem. Soc. *130*, 13534-13535.

23- Guisado-Barrios, G., Bouffard, J., Donnadieu, B., and Bertrand. G. (2010). Crystalline 1H-1,2,3-Triazol-5-ylidenes: New Stable Mesoionic Carbenes (MICs). Angew. Chem., Int. Ed. *49*, 4759-4762.

24- Schuster, O., Yang, L., Raubenheimer, H. G., and Albrecht, M. (2009). Beyond Conventional N-Heterocyclic Carbenes: Abnormal, Remote, and Other Classes of NHC Ligands with Reduced Heteroatom Stabilization. Chem. Rev. *109*, 3445-3478.

25- Albrecht, M. (2014). Normal and Abnormal N-Heterocyclic Carbene Ligands: Similarities and Differences of Mesoionic C–Donor Complexes. Adv. Organomet. Chem. *62*, 111-158.

26- Rostovtsev, V. V., Green, L. G., Fokin, V. V., Sharpless, K. B. (2002). A Stepwise Huisgen Cycloaddition Process: Copper(I)-Catalyzed Regioselective "Ligation" of Azides and Terminal Alkynes. Angew. Chem. Int. Ed. *41*, 2596-2599.

27- Fujita, K., Matsunaga, A., Yamamura H., and Imoto, T. (1988). Complete sets of structurally determined 6A,6X-unsymmetrically disubstituted .beta.-cyclodextrins. 6A-S-phenyl-6X-O-(.beta.-naphthylsulfonyl)-6A-thio-.beta.-cyclodextrins and 6A-S-(tert-butyl)-6X-O-(.beta.-naphthylsulfonyl)-6A-thio-.beta.-cyclodextrins. J. Org. Chem. *53*, 4520-4522.

28- Tabushi, I., Nabeshima, T., Kitaguchi H., and Yamamura, K. (1982). Unsymmetrical introduction of two functional groups into cyclodextrin. Combination specificity by use of N-benzyl-N-methylaniline N-oxide cap. *J. Am. Chem. Soc. 104*, 2017-2019.

29- Fasella, E., Dong S. D., and Breslow, R. (1999). Reversal of optical induction in transamination by regioisomeric bifunctionalized cyclodextrins. Bioorg. Med. Chem. *7*, 709-714.

30- Yuan, D.-Q., Yamada T., and Fujita, K. (2001). Amplification of the reactivity difference between two methylene groups of cyclodextrins via a cap. Chem. Commun. 2706-2707.

31- Fukudome, M., Yuan, D.-Q., Fujita, K. (2005). Preparation of 2A,3A-alloepimino-2A,3A-dideoxy-β-cyclodextrin as a versatile scaffold candidate for the hetero-2A,3A-bifunctionalization. Tetrahedron Lett. *46*, 1115-1118.

32- Yuan, D.-Q., Y. Kitagawa, K. Aoyama, T. Douke, M. Fukudome, K. Fujita, *Angew. Chem. Int. Ed.* **2007**, *46*, 5024-5027.

33- Yu, H., Yuan, D.-Q., Makino, Y., Fukudome, M., Xie, R.-G., and Fujita, K. (2006). Clockwise–counterclockwise differentiation on the upper rim of a monofunctional γ-cyclodextrin: efficient topological control in the syntheses of capped cyclodextrins. Chem. Commun. 5057-5059.

34- Bistri, O., Sinaÿ, P., and Sollogoub, M. (2005). Diisobutylaluminium hydride (DIBAL-H) is promoting a selective clockwise debenzylation of perbenzylated 6A, 6D-dideoxy-α-Cyclodextrin. Tetrahedron Lett. *46*, 7757-7760.

35- Bistri, O., Sinaÿ, P., and Sollogoub, M. (2006). Pd-catalysed Capping Removal on a Tri-differentiated α-Cyclodextrin. Chem. Lett. *35*, 534-535.

36- Bistri, O., Sinaÿ, P., and Sollogoub, M. (2006). Expeditious Selective Synthesis of Primary Rim Tri-differentiated α-Cyclodextrin. Tetrahedron Lett. *47*, 4137-4139.

37- Bistri, O., Sinaÿ, P., Jiménez-Barbero, J., and Sollogoub, M. (2007). Chemical clockwise tridifferentiation of α- and β-cyclodextrins : Bascule-bridge or deoxy-sugars strategies. Chem. Eur. J. *13*, 9757-9774

38- Zaborova, E., Guitet, M., Prencipe, G., Blériot, Y., Ménand, M., and Sollogoub, M. (2013). An "Against-the-Rules" Double Bank Shot with Diisobutylaluminium Hydride allows Triple Functionalisation of α-Cyclodextrin. Angew. Chem. Int. Ed. *52*, 639-644.

39- Wang, B., Zaborova, E., Guieu, S., Petrillo, M., Guitet, M., Blériot, Y., Ménand, M., Zhang, Y., and Sollogoub, M. (2014). Site-selective hexa-hetero-functionalization of α-cyclodextrin an archetypical C_6-symmetric concave cycle. Nature Comms. *5*, 5354.

40- Guieu, S., and Sollogoub, M. (2008). Regiospecific Tandem Azide-Reduction/Deprotection To Afford Versatile Amino Alcohol-Functionalized α- and β-Cyclodextrins. Angew. Chem. Int. Ed. *47*, 7060-7063.

41- Petrillo, M., Marinescu, L., Rousseau, C., and Bols, M. (2009). Selective Discrimination of Cyclodextrin Diols Using Cyclic Sulfates. Org. Lett. *11*, 1983-1985.

42- Jouffroy, M., Gramage-Doria, R., Armspach, D., Matt, D., and Toupet, L. (2012). Regioselective opening of proximally sulfato-capped cyclodextrins. Chem. Commun. *48*, 6028-6030.

43- Bistri, O., Sinaÿ, P., and Sollogoub, M. (2006). Sequential Ring Closing/Opening Metathesis for the Highly Selective Synthesis of a Triply Bifunctionalized α-Cyclodextrin. Chem. Commun. 1112-1114.

44- Furche, F., Ahlrichs, R., Hättig, C., Klopper, W., Sierka, M., Weigend, F. (2013). Turbomole. WIREs Comput. Mol. Sci. *4*, 91–100.

45- Becke, A. D. (1993). Densityfunctional thermochemistry. III. The role of exact exchange. J. Chem. Phys. *98*, 5648–5653.

46- Becke, A. D. (1988). Density-functional exchange-energy approximation with correct asymptotic behavior. Phys. Rev. A *38*, 3098–3100.

47- Lee, C., Yang, W., and Parr, R. G. (1988). Development of the Colle-Salvetti correlation-energy formula into a functional of the electron density. Phys. Rev. B *37*, 785-789.

48- Grimme, S., Antony, J., Ehrlich, S., and Krieg, H. A consistent and accurate ab initio parametrization of density functional dispersion correction (DFT-D) for the 94 elements H-Pu. *J. Chem. Phys. 132*, 154104-1-154104-19.

49- Schäfer, A., Horn, H., and Ahlrichs, R. (1992). Fully optimized contracted Gaussian basis sets for atoms Li to Kr. J. Chem. Phys. *97*, 2571-2577.

50- For a recent example see : Rekhroukh, F., Estévez, L., Bijani, C., Miqueu, K., Amgoune, A., Bourissou, D. (2016). Experimental and Theoretical Evidence for an Agostic Interaction in a Gold(III) Complex. Angew. Chem. Int. Ed. *55*, 3414-3418.

51- Brookhart, M., Green, M. L. H., and Parkin, G. (2007). Agostic interactions in transition metal compounds. Proc. Natl. Acad. Sci. U.S.A. *104*, 6908-6914.

52- Johnson, E. R., Keinan, S., Mori-Sánchez, P., Contreras-García, J., Cohen, A. J., and Yang, W. (2010). Revealing Noncovalent Interactions. J. Am. Chem. Soc. *132*, 6498-6506.

53- Contreras-García, J., Johnson, E. R., Keinan, S., Chaudret, R., Piquemal, J.-P., Beratan, D. N., and Yang, W. (2011). NCIPLOT: A Program for Plotting Noncovalent Interaction Regions. J. Chem. Theory Comput. *7*, 625-632.

54- Yao, W., Eisenstein, O., and Crabtree, R. H. (1997). Interactions between C−H and N−H bonds and d^8 square planar metal complexes: hydrogen bonded or agostic? Inorg. Chim. Acta *254*, 105-111.

55- Zhang, Y., Lewis, J. C., Bergman, R., Ellman, J. A., and Oldfield, E. (2006). NMR Shifts, Orbitals, and M···H−X Bonding in d^8 Square Planar Metal Complexes. Organometallics *25*, 3515-3519.

56- Angamuthu, R., Gelauff, L. L., Siegler, M. A., Spekb, A. L., and Bouwman, E. (2009). A molecular cage of nickel(II) and copper(I): a $[\{Ni(L)_2\}_2(CuI)_6]$ cluster resembling the active site of nickel-containing enzymes. Chem. Commun. 2700-2702.

57- Yadav, M. K., Rajput, G., Prasad, L. B., Drew, M. G. B., and Singh, N. (2015). Rare intermolecular M···H–C anagostic interactions in homoleptic Ni(II)–Pd(II) dithiocarbamate complexes. New J. Chem. *39*, 5493-5499.

58- Willcocks, A. M., Johnson, A. L., Raithby, P. R., Schiffers, S., and Warren, J. E. (2011). Bis(tert-butyl isocyanide-κC)[4-fluoro-N-({2-[N-(4-fluoro-phenyl)-carbox-imido-yl]-cyclo-penta-2,4-dien-1-yl-idene}-methyl)-anilinido-κ2N,N′]copper(I). Acta Cryst. *C67*, m215–m217.

59- Schaper, L.-A., Wei, X., Hock, S. J., Pöthig, A., Öfele, K., Cokoja, M., Herrmann, W. A., and Kühn, F. E. (2013). Gold(I) Complexes with "Normal" 1,2,3-Triazolylidene Ligands: Synthesis and Catalytic Properties. Organometallics *32*, 3376-3384.

60- Teci, M., Brenner, E., Matt, D., Gourlaouen, C., and Toupet, L. (2015). N-Alkylfluorenyl-substituted N-heterocyclic carbenes as bimodal pincers. Dalton Trans. *44*, 9260-9268.

61- Han, Y., Huynh, H. V., Tan, G. K. (2007). Syntheses and Characterizations of Pd(II) Complexes Incorporating a N-Heterocyclic Carbene and Aromatic N-Heterocycles. Organometallics *26,* 6447-6452.

62- Huynh, H. V., Wong, L. R., and Ng, P. S. (2008). Anagostic Interactions and Catalytic Activities of Sterically Bulky Benzannulated N-Heterocyclic Carbene Complexes of Nickel(II). Organometallics *27,* 2231–2237.

63- Boehme, C., and Frenking, G. (1998). N-Heterocyclic Carbene, Silylene, and Germylene Complexes of MCl (M = Cu, Ag, Au). A Theoretical Study. Organometallics *17*, 5801-5809.

64- Nemcsok, D., Wichmann, K., and Frenking, G. (2004). The Significance of π Interactions in Group 11 Complexes with N-Heterocyclic Carbenes. Organometallics *23*, 3640-3646.

65- Hu, X., Castro-Rodriguez, I., Olsen, K., and Meyer, K. (2004). Group 11 Metal Complexes of N-Heterocyclic Carbene Ligands: Nature of the Metal-Carbene Bond. Organometallics *23*, 755-764.

66- Pyykkö, P. (2004). Theoretical Chemistry of Gold. Angew. Chem. Int. Ed. *43*, 4412-4456.

67- Vummaleti, S. V. C., Nelson, D. J., Poater, A., Gomez-Suarez, A., Cordes, D. B., Slawin, A. M. Z., Nolan, S. P., and Cavallo, L. (2015). What can NMR spectroscopy of selenoureas and phosphinidenes teach us about the π-accepting abilities of N-heterocyclic carbenes? Chem. Sci. *6*, 1895-1904.

68- Tolman, C. A. (1977). Steric effects of phosphorus ligands in organometallic chemistry and homogeneous catalysis. Chem. Rev. *77*, 313-348.

69- Chianese, A. R., Li, X., Janzen, M. C., Faller, J. W., and Crabtree, R. H. (2003). Rhodium and Iridium Complexes of N-Heterocyclic Carbenes via Transmetalation: Structure and Dynamics. Organometallics *22*, 1663-1667.

70- Chianese, A. R., Kovacevic, A., Zeglis , B. M., Faller, J. W., and Crabtree, R. H. (2004). Abnormal C5-Bound N-Heterocyclic Carbenes: Extremely Strong Electron Donor Ligands and Their Iridium(I) and Iridium(III) Complexes. Organometallics *23*, 2461–2468.

71- Altenhoff, G., Goddard, R., Lehmann, C. W., and Glorius, F. (2004). Sterically Demanding, Bioxazoline-Derived N-Heterocyclic Carbene Ligands with Restricted Flexibility for Catalysis. J. Am. Chem. Soc. *126*, 15195-15201.

72- Huynh, H. V., Han, Y., Jothibasu, R., and Yang, J. A. (2009). ^{13}C NMR Spectroscopic Determination of Ligand Donor Strengths Using N-Heterocyclic Carbene Complexes of Palladium(II). Organometallics *28*, 5395–5404.

73- Gusev D. G. (2009). Electronic and Steric Parameters of 76 N-Heterocyclic Carbenes in $Ni(CO)_3(NHC)$. Organometallics *28*, 6458–6461.

74- Dröge, T., and Glorius F. (2010). The Measure of All Rings—N-Heterocyclic Carbenes. Angew. Chem. Int. Ed. *49*, 6940-6952.

75- Back, O., Henry-Ellinger, M., Martin, C. D., Martin, D., and Bertrand, G. (2013). ^{31}P NMR chemical shifts of carbene-phosphinidene adducts as an indicator of the π-accepting properties of carbenes. Angew. Chem. Int. Ed. *52*, 2939-2943.

76- Liske, A., Verlinden, K., Buhl, H., Schaper, and K., Ganter, C. (2013). Determining the π-Acceptor Properties of N-Heterocyclic Carbenes by Measuring the ^{77}Se NMR Chemical Shifts of Their Selenium Adducts. Organometallics *32*, 5269-5272.

77- Hanwell, M. D., Curtis, D. E., Lonie, D. C., Vandermeersch, T., Zurek, E., and Hutchison, G. R. (2012). Avogadro: an advanced semantic chemical editor, visualization, and analysis platform. J. Cheminf. *4*, 17.

78- Rappé, A. K., Casewit, C. J., Colwell, K. S., Goddard, W. A., and Skiff, W. M. (1992). UFF, a full periodic table force field for molecular mechanics and molecular dynamics simulations. J. Am. Chem. Soc. *114*, 10024–10035.

79- Cavarzan, A., Scarso, A., Sgarbossa, P., Strukul, G., and Reek, J. N. H. (2011). Supramolecular Control on Chemo- and Regioselectivity via Encapsulation of (NHC)-Au Catalyst within a Hexameric Self-Assembled Host. *J. Am. Chem. Soc. 133*, 2848–2851.

80- Galli, M., Lewis, J. E. M., and Goldup, S. M. (2015). A Stimuli-Responsive Rotaxane–Gold Catalyst: Regulation of Activity and Diastereoselectivity. Angew. Chem. Int. Ed. *54*, 13545-13549.

81- Gramage-Doria, R., Hessels, J., Leenders, S. H. A. M., Tröppner, O., Dürr, M., Ivanovic-Burmazovic, I., and Reek, J. N. H. (2014). Gold(I) catalysis at extreme concentrations inside self-assembled nanospheres. Angew. Chem. Int. Ed. *53*, 13380-13384.

82- Cavarzan, A., Reek, J. N. H., Trentin, F., Scarso, A., and Strukul, G. (2013). Substrate selectivity in the alkyne hydration mediated by NHC–Au(I) controlled by encapsulation of the catalyst within a hydrogen bonded hexameric host. Catal. Sci. Technol. *3*, 2898-2901.

83- Wang, Z. J., Brown, C. J., Bergman, R. G., Raymond, K. N., and Toste, F. D. (2011). Hydroalkoxylation Catalyzed by a Gold(I) Complex Encapsulated in a Supramolecular Host. J. Am. Chem. Soc. *133*, 7358–7360.

84- Schramm, M. P., Kanaura, M., Ito, K., Ide, M., and Iwasawa, T. (2016). Introverted Phosphorus-Au Cavitands for Catalytic Use. Eur. J. Org. Chem. 813-820.

85- Bartolome, C., Ramiro, Z., Garcia-Cuadrado, D., Perez-Galan, P., Raducan, M., Bour, C., Echavarren, A. M., and Espinet, P. (2010). Luminescent Gold(I) Carbenes from 2-Pyridylisocyanide Complexes: Structural Consequences of Intramolecular versus Intermolecular Hydrogen-Bonding Interactions. Organometallics *29*, 951-956.

86- Ferrer, C., Raducan, M., Nevado, C., Claverie, C. K., Echavarren, A. M. (2007). Missing cyclization pathways and new rearrangements unveiled in the gold(I) and platinum(II)-catalyzed cyclization of 1,6-enynes. Tetrahedron *63*, 6306-6316.

87- Bartolome, C., Ramiro, Z., Perez-Galan, P., Bour, C., Raducan, M., Echavarren, A. M., and Espinet, P. (2008). Gold(I) Complexes with Hydrogen-Bond Supported Heterocyclic Carbenes as Active Catalysts in Reactions of 1,6-Enynes. Inorg. Chem. *47*, 11391-11397.

88- Raducan, M., Moreno, M., Bour, C., and Echavarren, A. M. (2012). Phosphate ligands in the gold(I)-catalysed activation of enynes. Chem. Commun. *48*, 52-54.

89- Obradors, C.,and Echavarren, A. M. (2014). Intriguing mechanistic labyrinths in gold(I) catalysis. Chem. Commun. *50*, 16-28 and references therein.

90- Nieto-Oberhuber, C., López, S., Muñoz, M. P., Cárdenas, D. J., Buñuel, E., Nevado, C., and Echavarren, A. M. (2005). Divergent Mechanisms for the Skeletal Rearrangement and [2+2] Cycloaddition of Enynes Catalyzed by Gold. Angew. Chem. Int. Ed. *44*, 6146-6148.

91- Cabello, N., Jiménez-Núñez, E., Buñuel, E., Cárdenas, D. J., and Echavarren, A. M. (2007). On the Mechanism of the Puzzling "Endocyclic" Skeletal Rearrangement of 1,6-Enynes. Eur. J. Org. Chem. 4217-4223.

92- Escribano-Cuesta, A., Pérez-Galán, P., Herrero-Gómez, E., Sekine, M., Braga, A. A. C., Maserasa, F., and Echavarren, A. M. (2012). The role of cyclobutenes in gold(I)-catalysed skeletal rearrangement of 1,6-enynes. Org. Biomol. Chem. *10*, 6105–6111.

93- Lopez, F., and Mascarenas, J. L. (2013). Gold(I)-catalyzed enantioselective cycloaddition reactions. Beilstein J. Org. Chem. *9*, 2250-2264.

94- Pradal, A., Toullec, P. Y., and Michelet, V. (2011). Recent Developments in Asymmetric Catalysis in the Presence of Chiral Gold Complexes. Synthesis 1501-1514.

95- Zi, W., and Toste, F. D. (2016). Recent advances in enantioselective gold catalysis. Chem. Soc. Rev. *45*, 4567-4589.

96- Fürstner, A., Stelzer, F., and Szillat, H. (2001). Platinum-Catalyzed Cycloisomerization Reactions of Enynes. J. Am. Chem. Soc. *123,* 11863-11869.

97- Kim, S. Y., and Chung, Y. C. (2010). Rhodium(I)-Catalyzed Cycloisomerization of 1,6-Enynes to Bicyclo[4.1.0]heptenes. J. Org. Chem. *75*, 1281-1284.

98- Sim, S. H., Lee, S. I., and Keun, Y. (2010). Iridium(I)-Catalyzed Cycloisomerization of Cyclohexadienyl Alkynes. Adv. Synth. Catal. *352*, 317-322.

99- Nishimura, T., Kawamoto, T., Nagaosa, M., Kumamoto, H., and Hayashi, T. (2001). Chiral Tetrafluorobenzobarrelene Ligands for the Rhodium-Catalyzed Asymmetric Cycloisomerization of Oxygen- and Nitrogen-Bridged 1,6-Enynes. Angew. Chem. Int. Ed. *49*, 1638-1641.

100- Jullien, H., Brissy, D., Brissy, R., Retailleau, P., Naubron, J.-V., Gladiali, S., and Marinetti, A. (2011). Cyclometalated N-Heterocyclic Carbene-Platinum Catalysts for the Enantioselective Cycloisomerization of Nitrogen-Tethered 1,6-Enynes. Adv. Synth. Catal. *353*, 1109-1124.

101- Nishiumura, T., Maeda, Y., and Hayashi, T. (2011). Chiral Diene-Phosphine Tridentate Ligands for Rhodium-Catalyzed Asymmetric Cycloisomerization of 1,6-Enynes. Org. Lett. *13*, 3674-3677.

102- Kim, S. T., and Chung, T. K. (2010). Rhodium(I)-Catalyzed Cycloisomerization of 1,6-Enynes to Bicyclo[4.1.0]heptenes. J. Org. Chem. *75*, 1281-1284.

103- Barbazanges, M., Augé, M., Moussa, J., Amouri, H., Aubert, C., Desmarets, C., Fensterbank, L., Gandon, V., Malacria, M., and Ollivier, C. (2011). Enantioselective Ir^{I}-Catalyzed Carbocyclization of 1,6-Enynes by the Chiral Counterion Strategy. Chem. Eur. J. *17*, 13789-13794.

104- Gorin, D. J., and Toste, F. D. (2007). Relativistic effects in homogeneous gold catalysis. Nature *446*, 395–403.

Supplemental figures

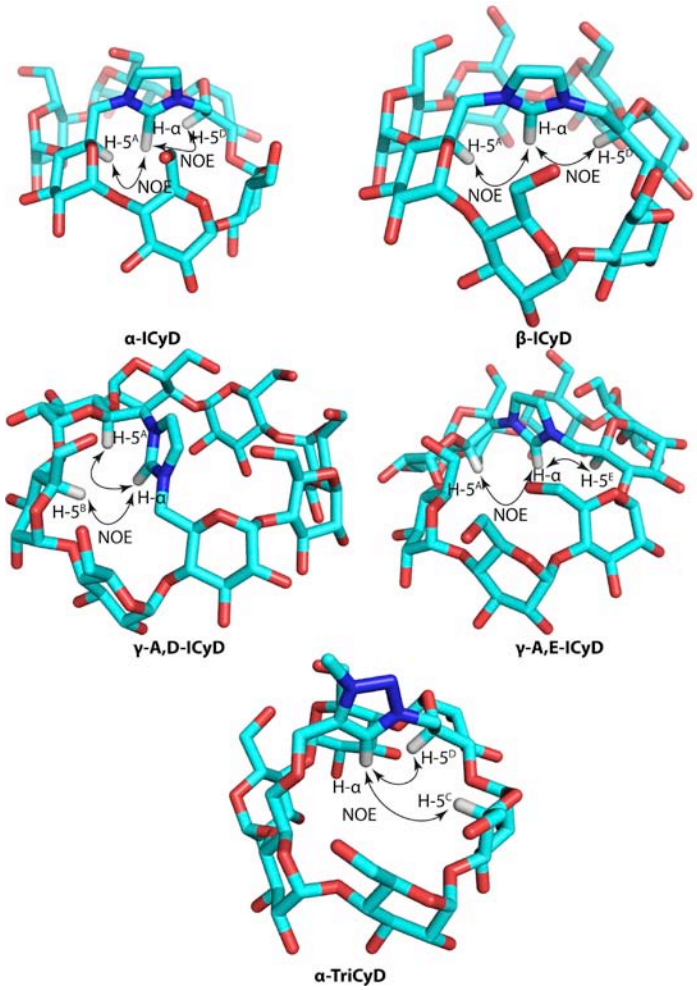

Figure S1. Selected NOEs between Hα of the azoliums and the introverted H-5s of the CD cavity

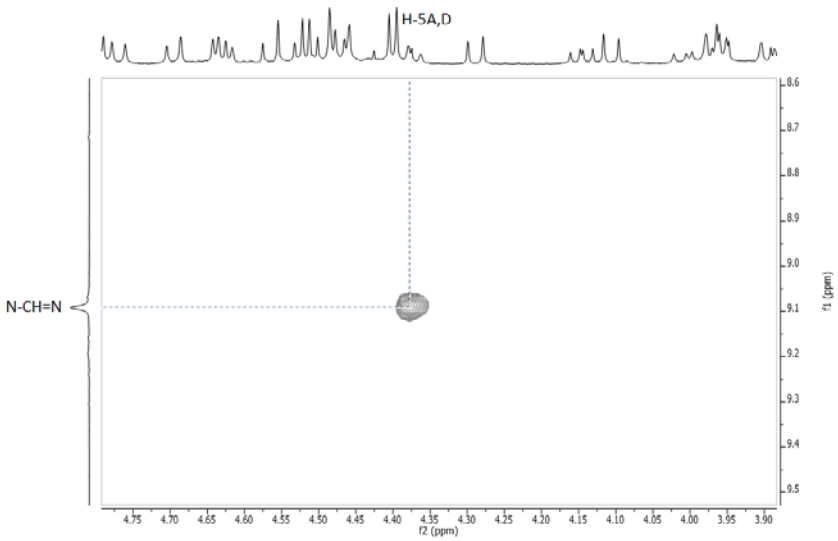

Figure S2. Key NOESY cross peak of imidazolium **(α-ICyD)HCl**, CD_3CN, 600 MHz, 300 K

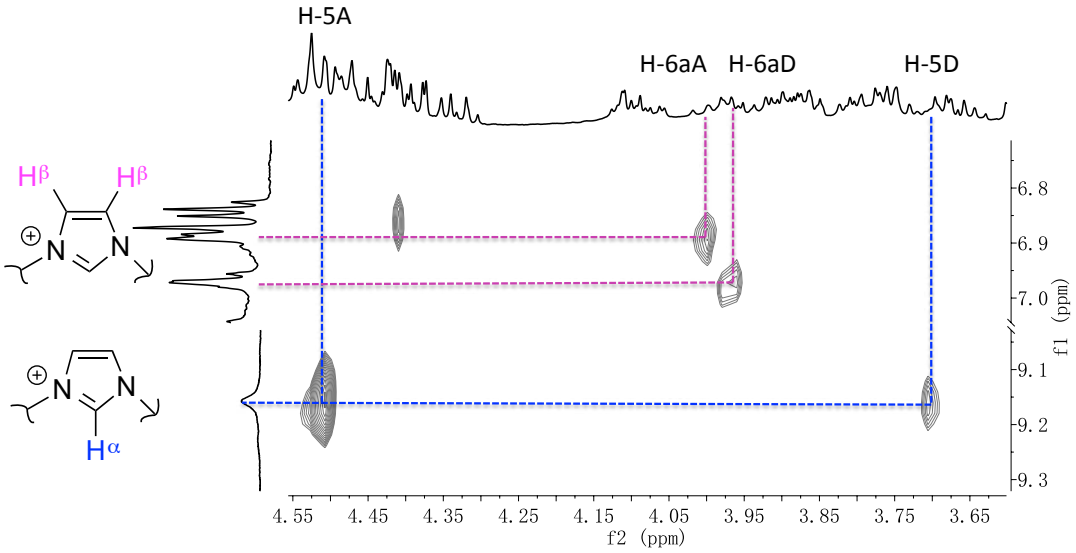

Figure S3. Key NOESY cross peaks of imidazolium **(β-ICyD)HCl**, CD_3CN, 600 MHz, 300 K

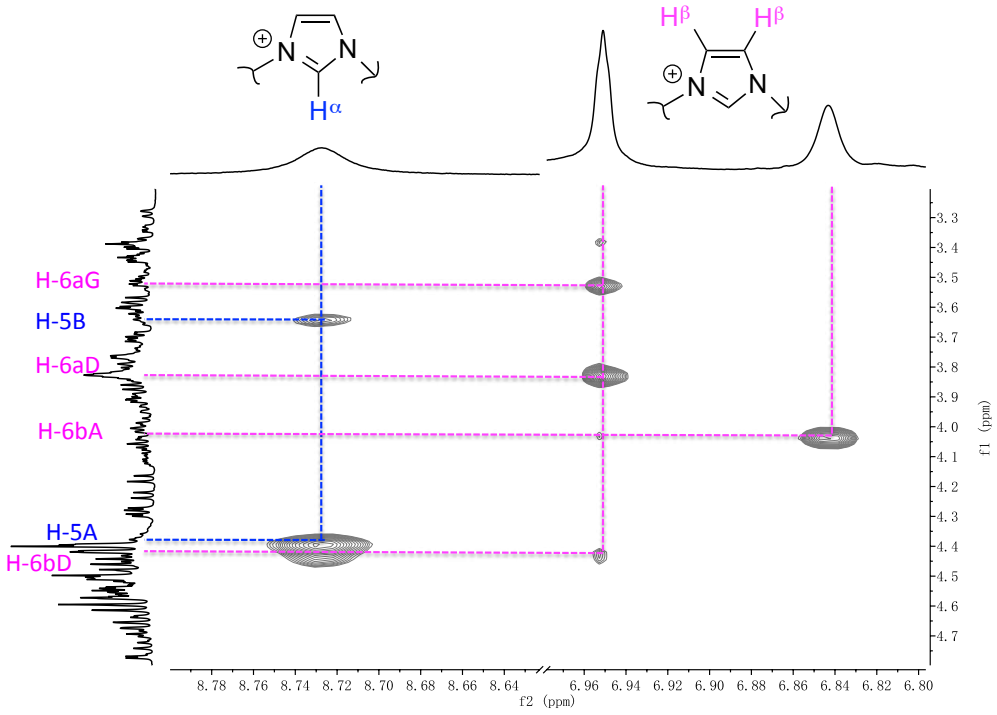

Figure S4. Key NOESY cross peaks of imidazolium **(γ-A,D-ICyD)HCl**, CD_3CN, 600 MHz, 300 K

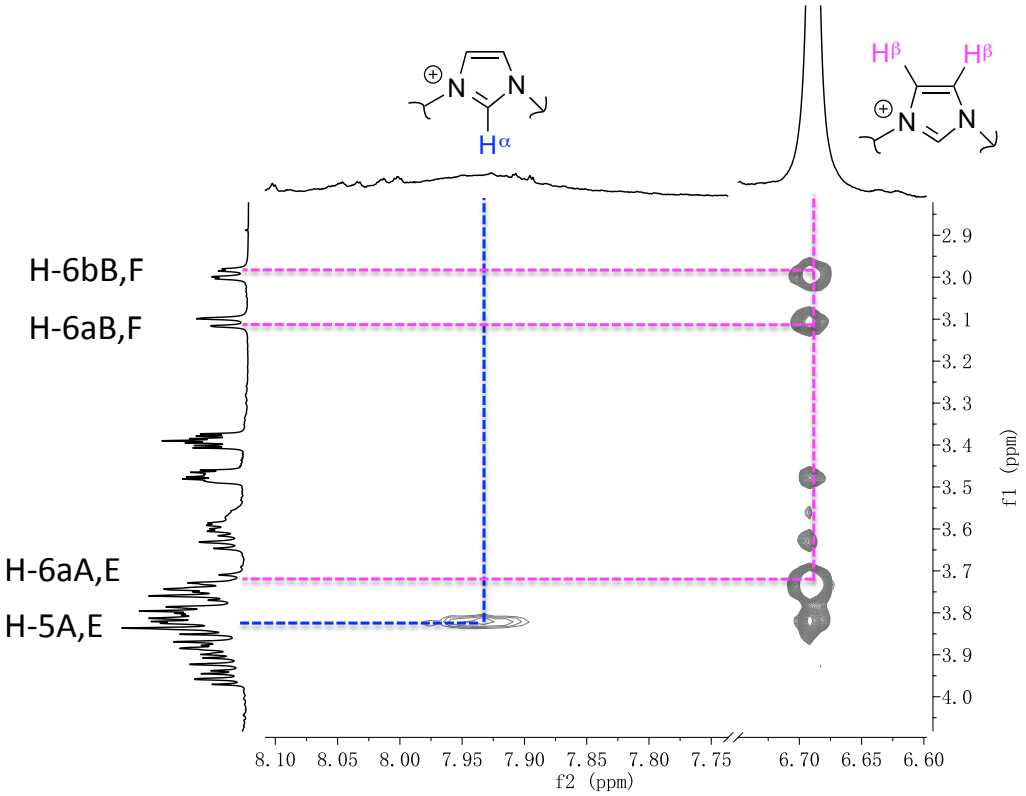

Figure S5. Key NOESY cross peaks of imidazolium **(γ-A,E-ICyD)HCl**, CD_3CN, 600 MHz, 300 K

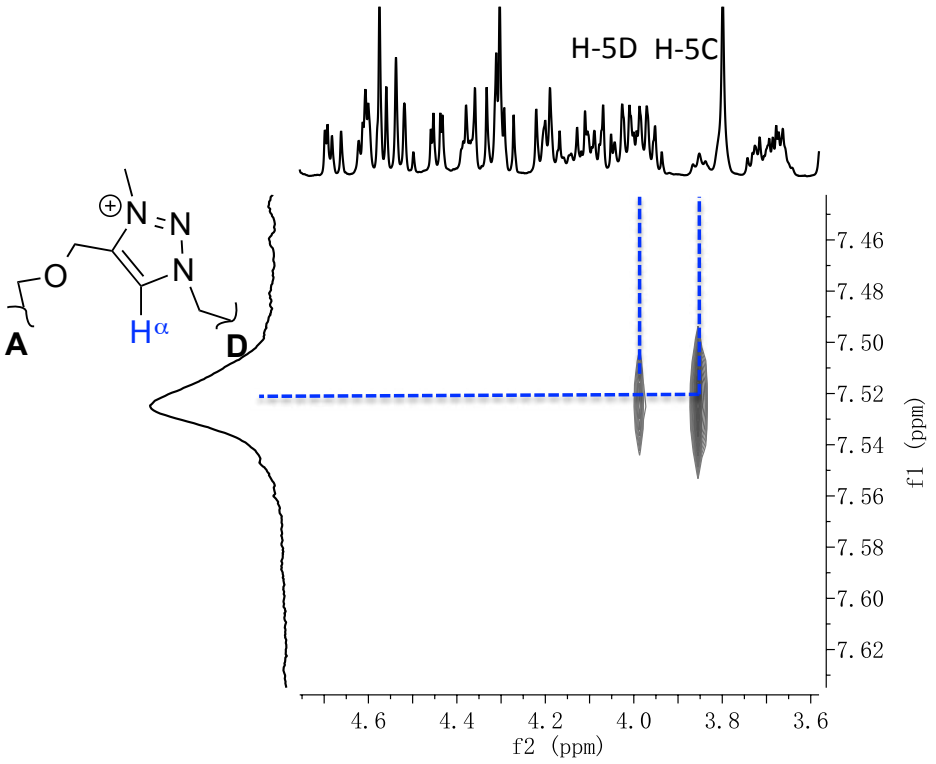

Figure S6. Key NOESY cross peaks of triazolium **(α-TriCyD)HI**, $CDCl_3$, 600 MHz, 300 K

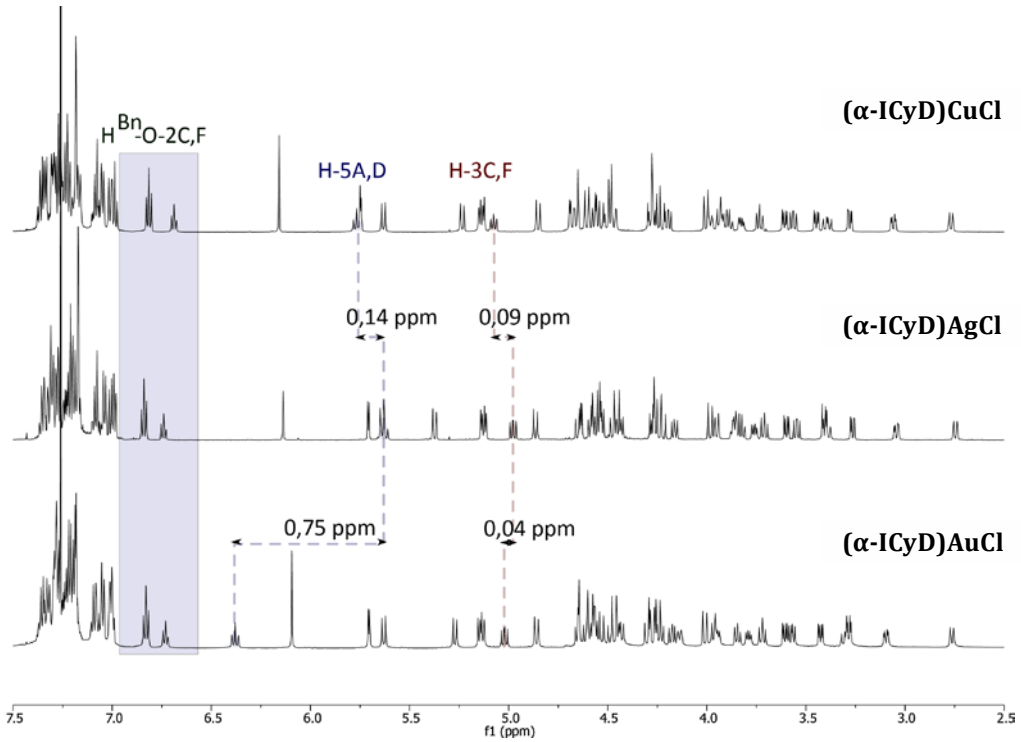

Figure S7. Stacked ^{1}H NMR spectra of **(α-ICyD)Cu**, **Ag** and **Au** complexes ($CDCl_3$, 600MHz, 300K)

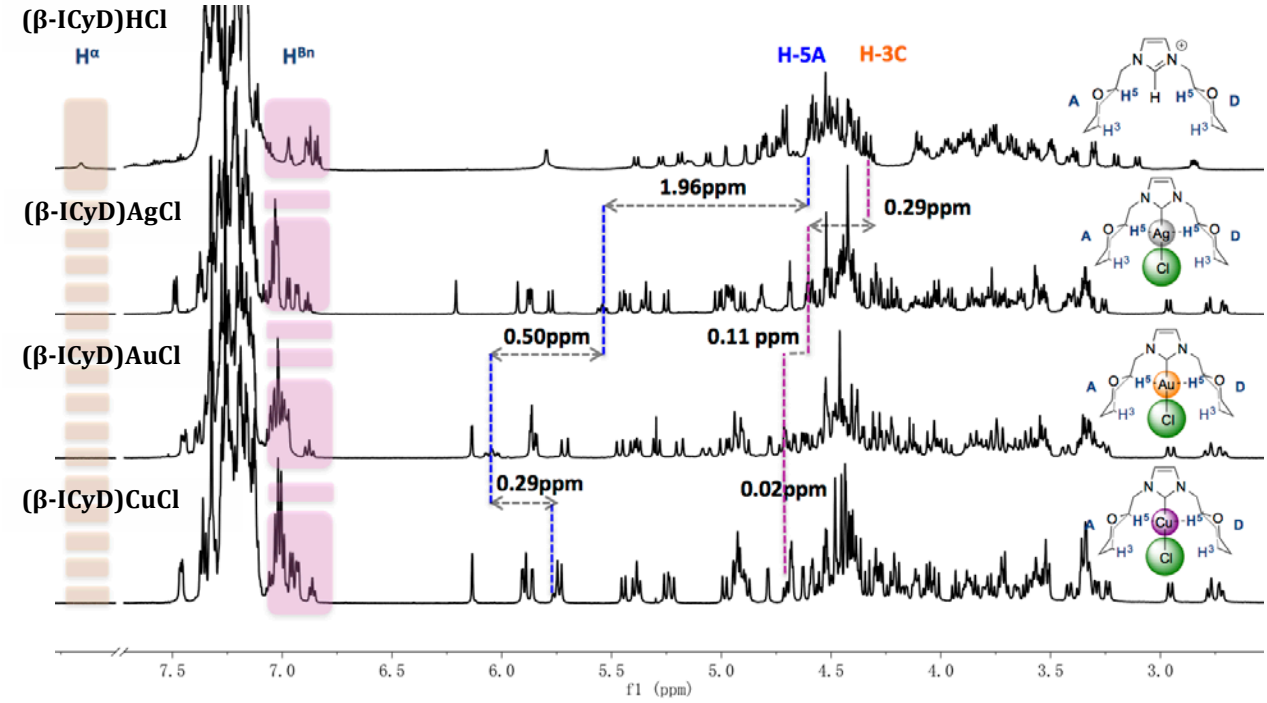

Figure S8. Stacked ^{1}H NMR spectra of **(β-ICyD)HCl** and **Cu**, **Ag** and **Au** complexes ($CDCl_3$, 600MHz, 300K)

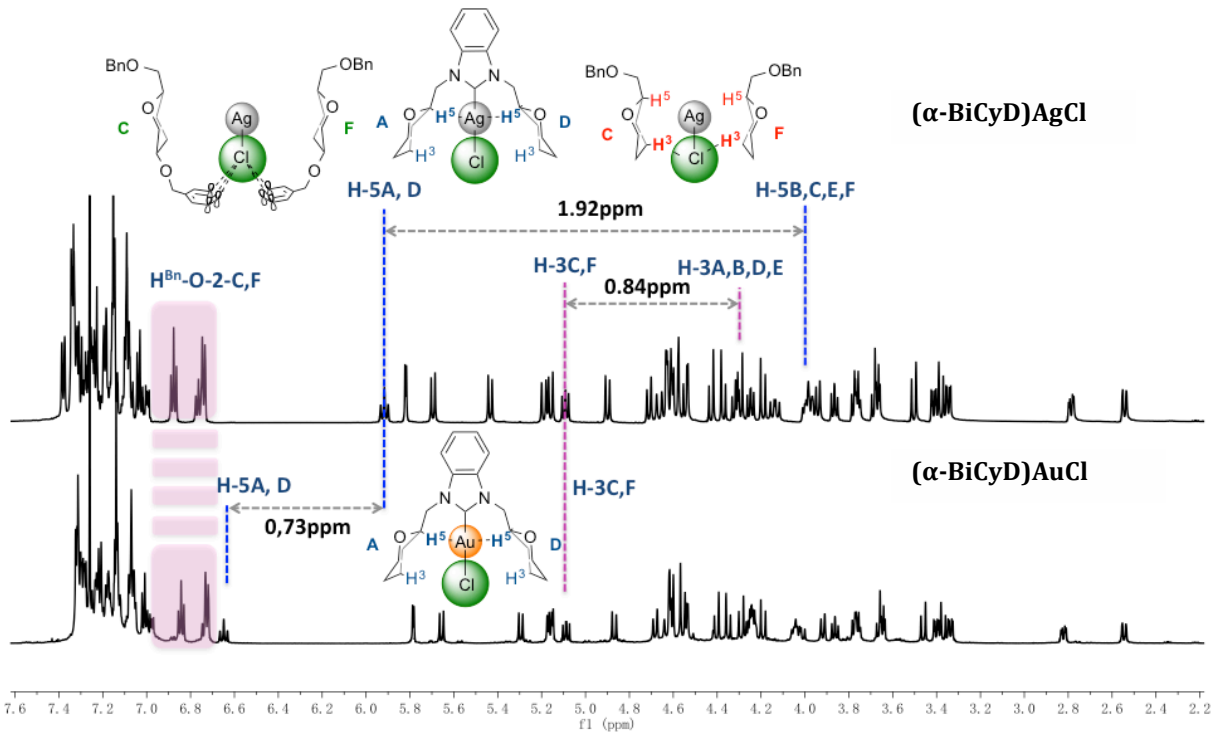

Figure S9. Stacked ^{1}H NMR spectra of **(α-BiCyD)Ag** and **Au** complexes ($CDCl_3$, 600MHz, 300K)

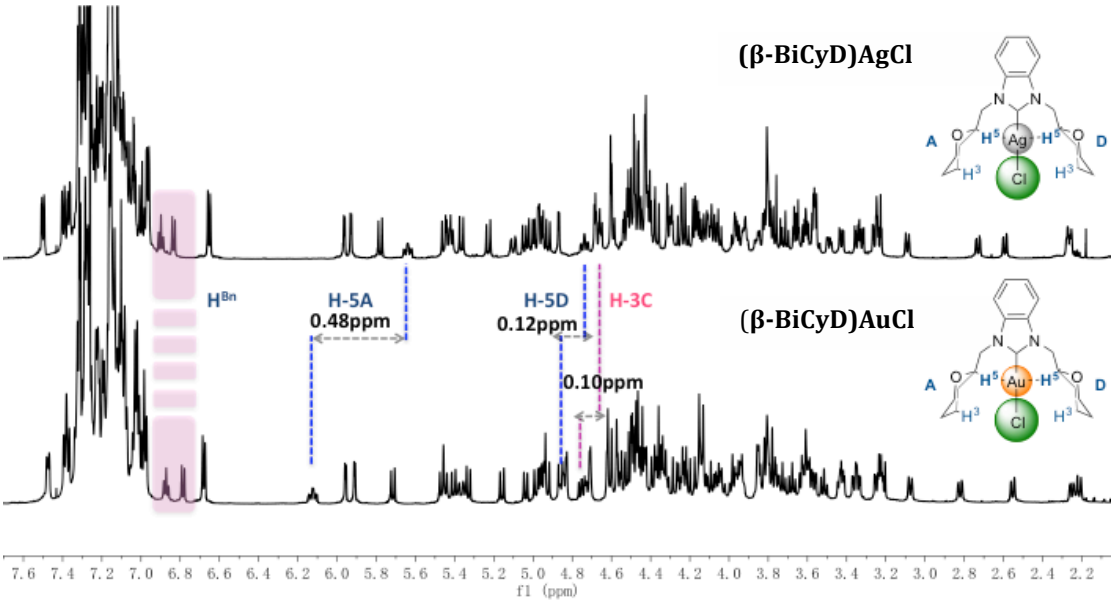

Figure S10. Stacked ^{1}H NMR spectra of **(β-BiCyD)Ag** and **Au** complexes ($CDCl_3$, 600MHz, 300K)

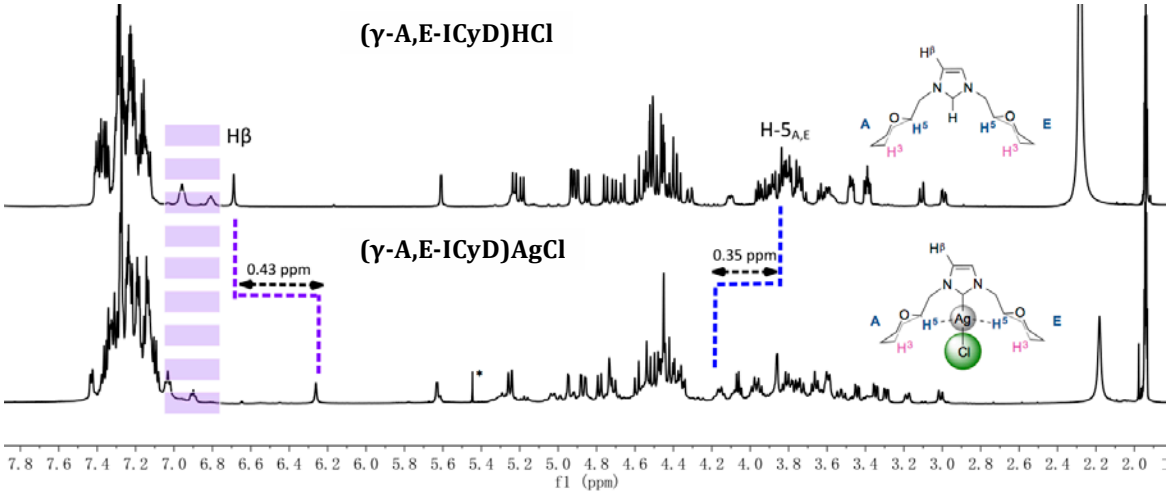

Figure S11. Stacked ^{1}H NMR spectra of **(γ-A,E-ICyD)HCl** and its **Ag** complex (CD_3CN, 600MHz, 300K)

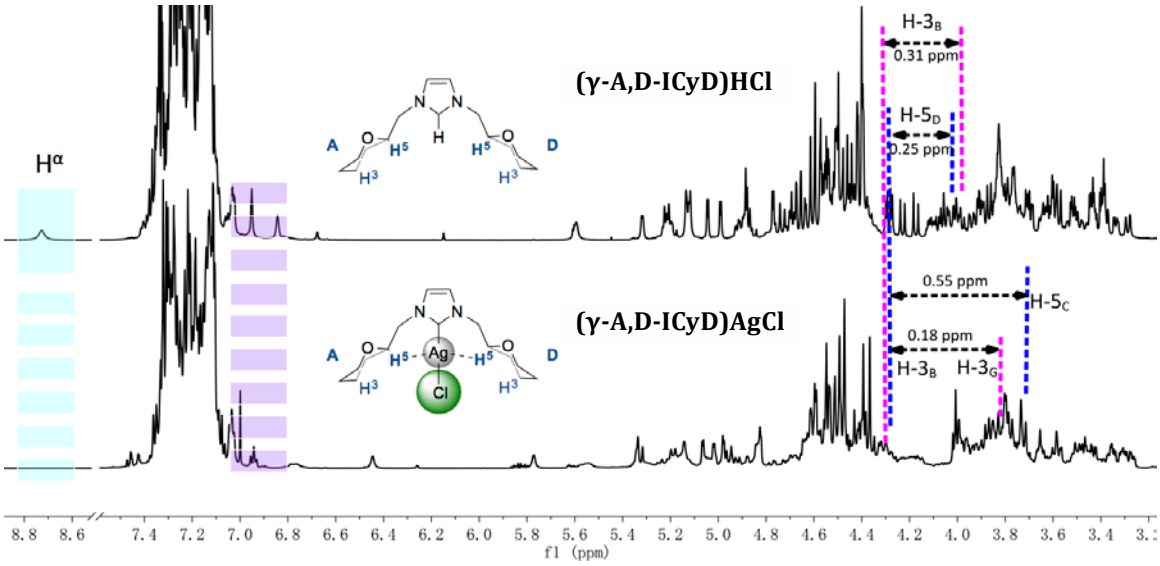

Figure S12. Stacked ^{1}H NMR spectra of **(γ-A,D-ICyD)HCl** and its **Ag** complex (CD_3CN, 600MHz, 300K)

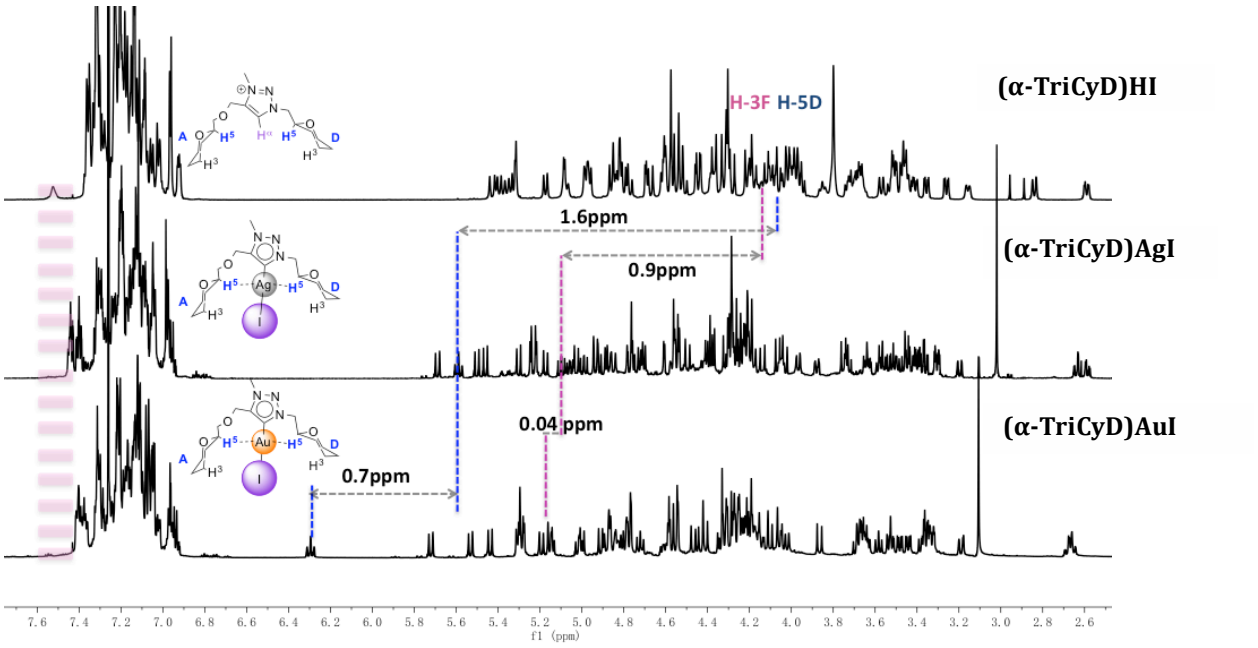

Figure S13. Stacked ^{1}H NMR spectra of **(α-TriCyD)HI** and its **Ag**, **Au** complexes ($CDCl_3$, 600MHz, 300K)

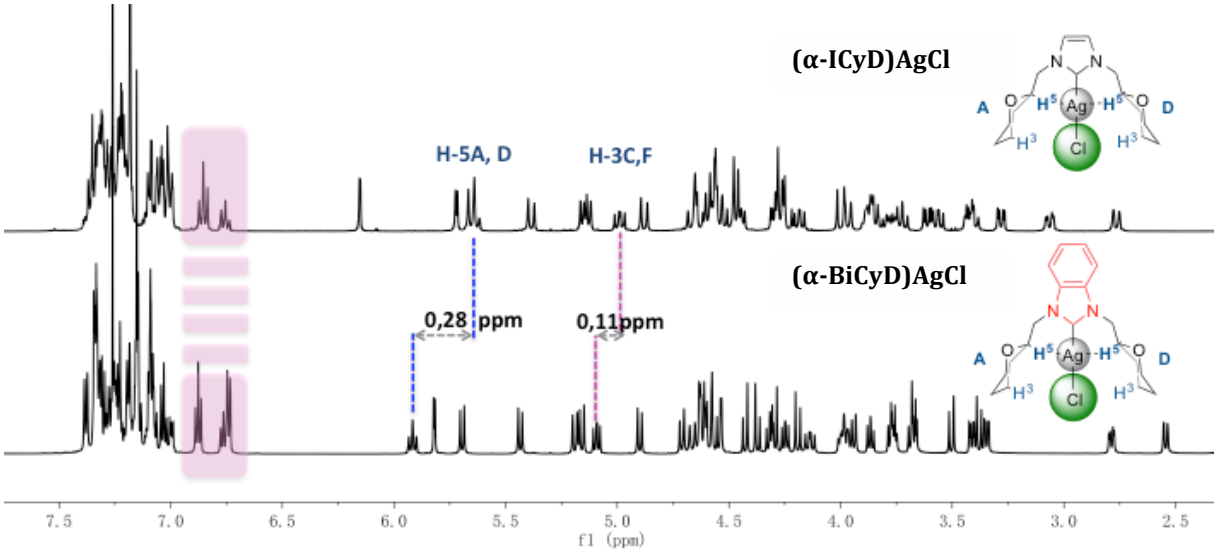

Figure S14. Stacked ^{1}H NMR spectra of **(α-ICyD)AgCl** and **(α-BiCyD)AgCl** ($CDCl_3$, 600MHz, 300K)

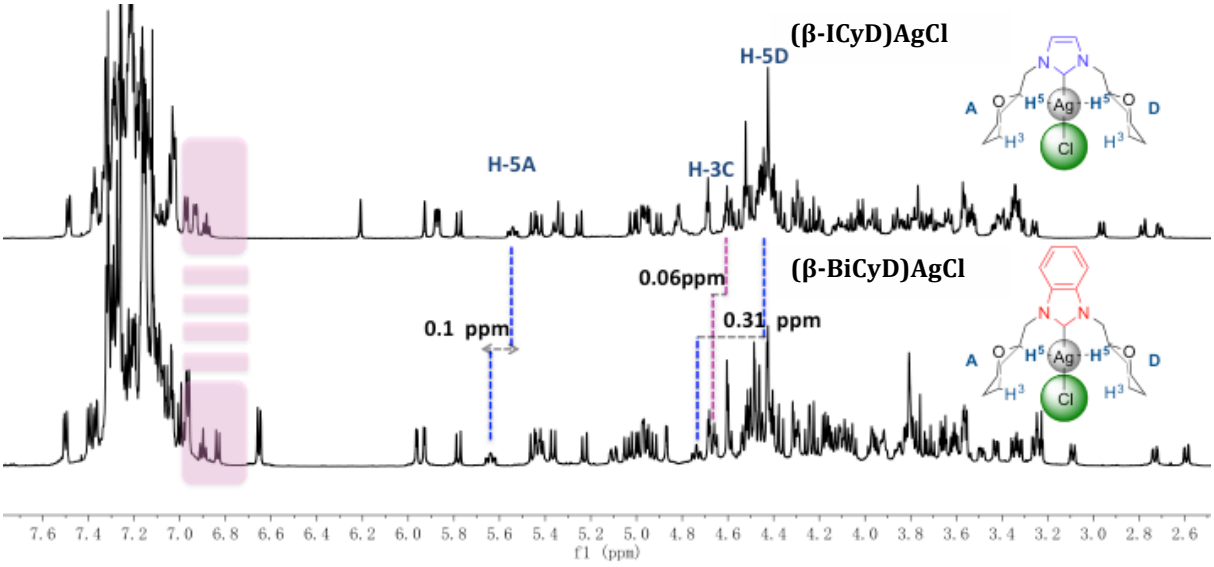

Figure S15. Stacked ^{1}H NMR spectra of **(β-ICyD)AgCl** and **(β-BiCyD)AgCl** ($CDCl_3$, 600MHz, 300K)

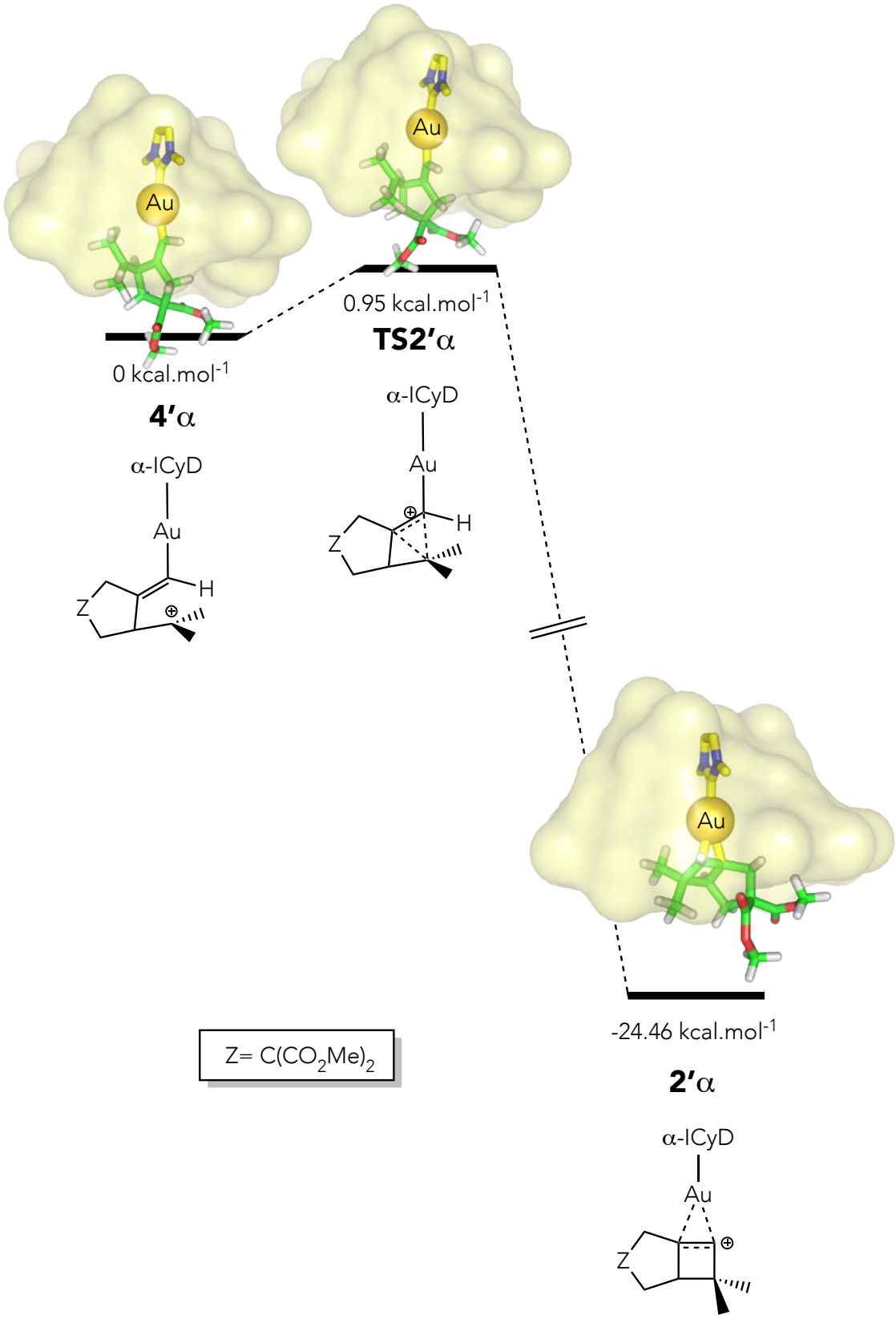

Figure S16. DFT calculation for the proposed mechanism of the Gold-catalyzed regioselective cycloisomerisation of enyne **1** using **α-ICyD**

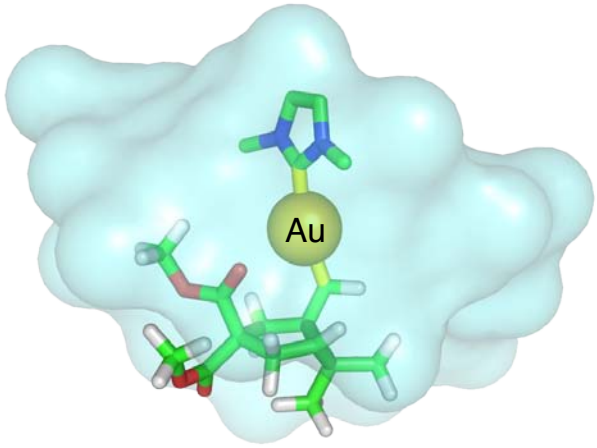

4β

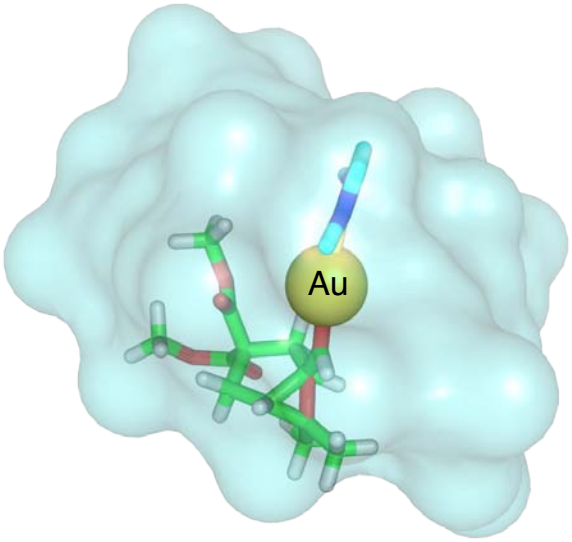

A

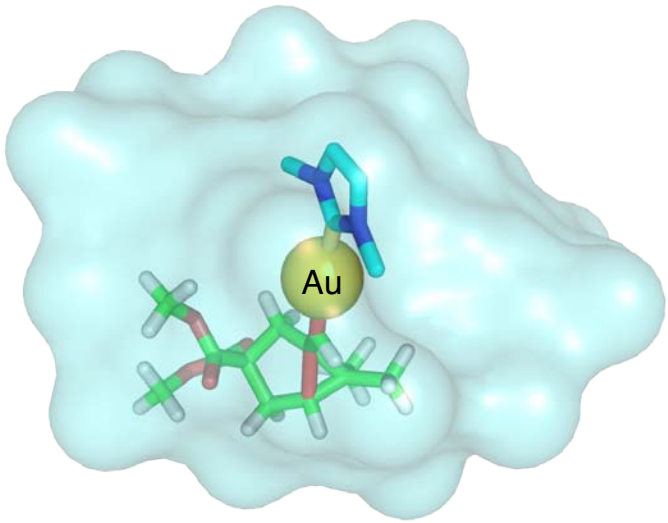

B

Figure S17. DFT calculation for the two conformers, obtained under constraint, leading to the products of the gold-catalyzed cycloisomerisation of enyne **1** using **β-ICyD.**

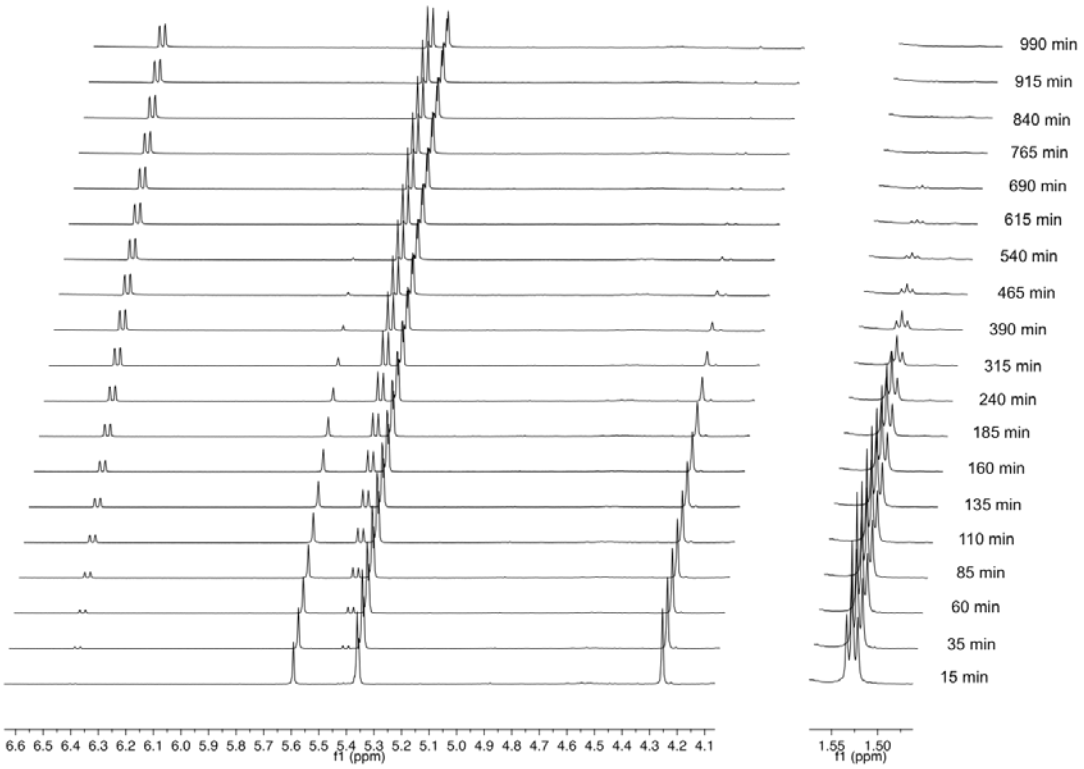

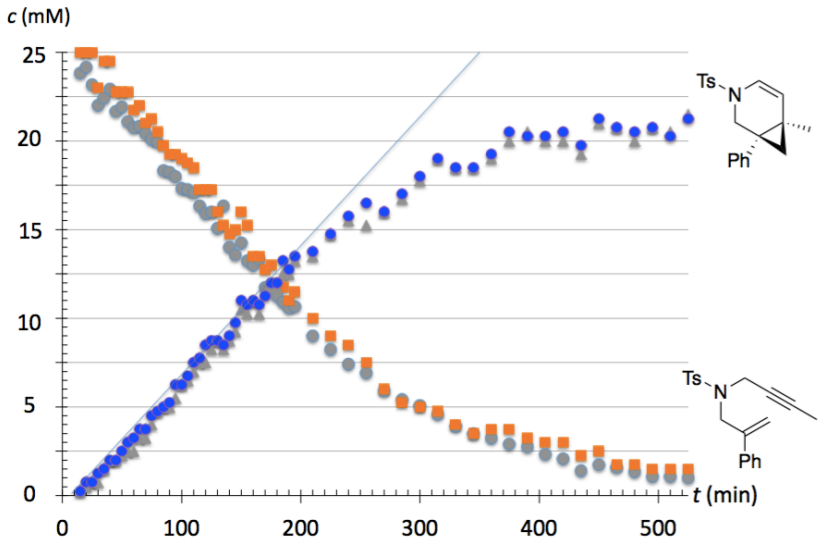

Figure S18. Cycloisomerization catalyzed by **β-ICyDAuCl** at 300K in CD_2Cl_2: a) Stacking of ^1H NMR spectra at different reaction times; b) Plot of the concentration as a function of time. The concentrations were determined by integration of different signals of the enyne and of the cyclized product. The internal reference was used for calibration. The slope at c = 0 for the cyclized product (blue line) gives an initial rate r_0 of ca. 1.2 10^{-6} mol L^{-1} s^{-1}.

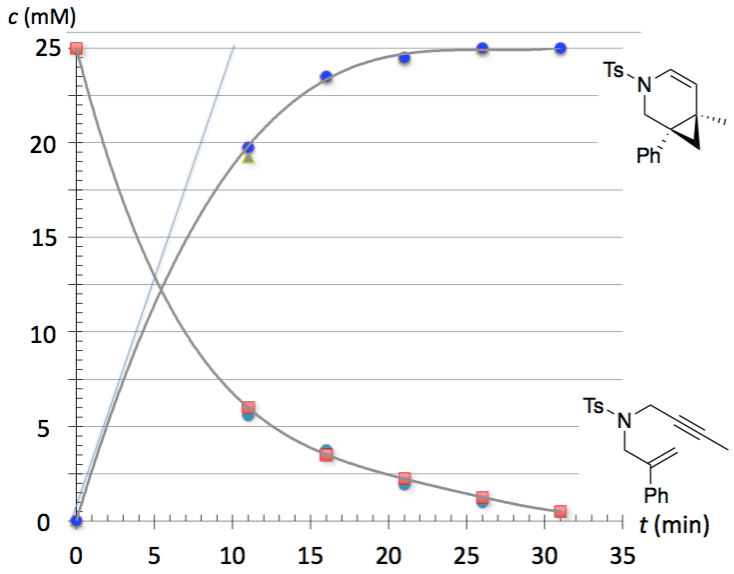

Figure S19. Cycloisomerization catalyzed by **(IPr)AuCl** at 300K in CD_2Cl_2. Plot of the concentrations as a function of time. The slope at c = 0 for the cyclized product (blue line) gives an initial rate r_0 of ca. 41.6 10^{-6} mol L^{-1} s^{-1}.

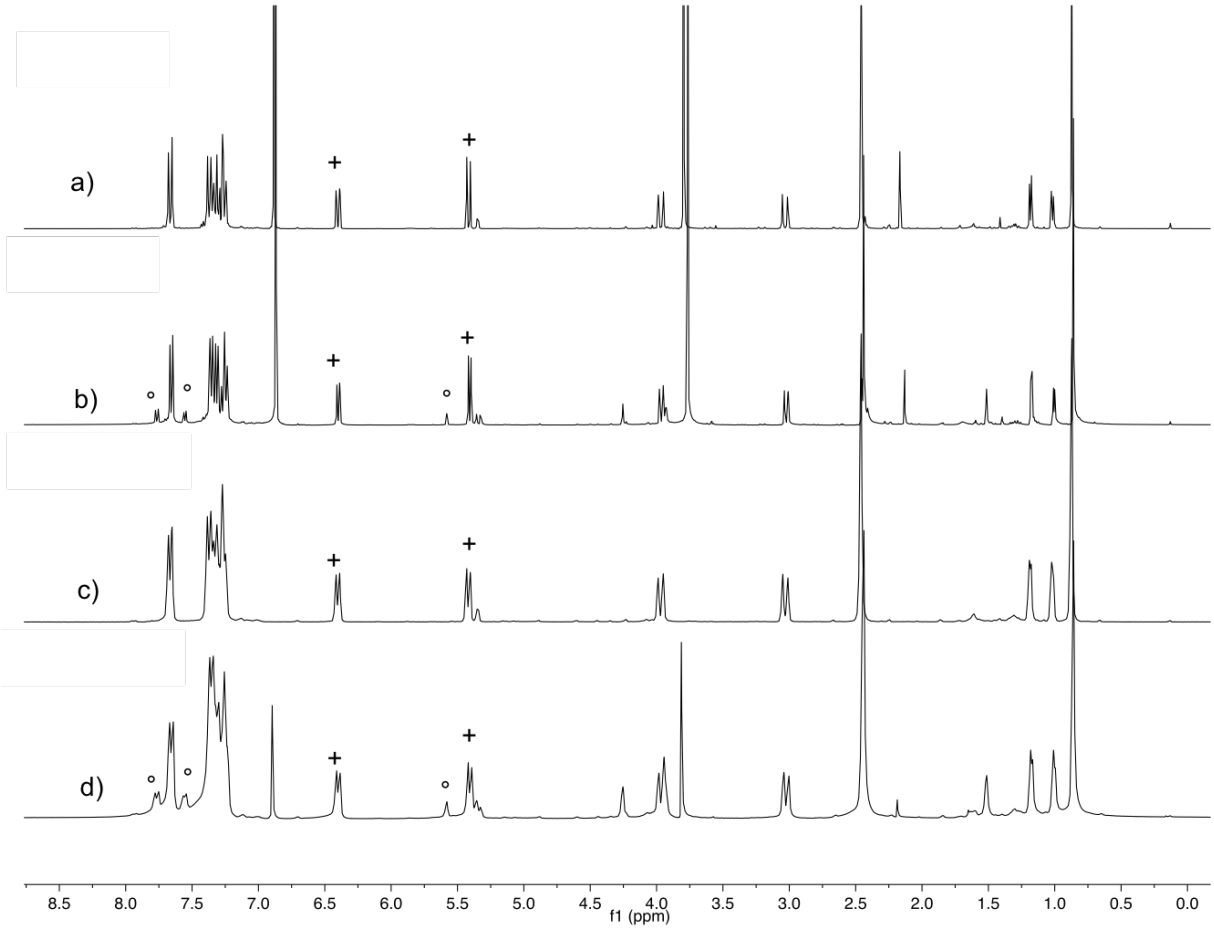

Figure S20. ^1H NMR spectra (300K, 400 MHz) in CD_2Cl_2– a) **(β-ICyD)AuCl**-catalyzed reaction with 10 equiv. of enyne **6** ; b) **(β-ICyD)AuCl**-catalyzed reaction with 20 equiv. of

enyne **6** ; c) **iPrAuCl**-catalyzed reaction with 10 equiv. of enyne **6**; **iPrAuCl**-catalyzed reaction with 20 equiv. of enyne **6**; protons annotated (+) belong to the cycloisomerisation product and (°) to the unreacted enyne **6**.

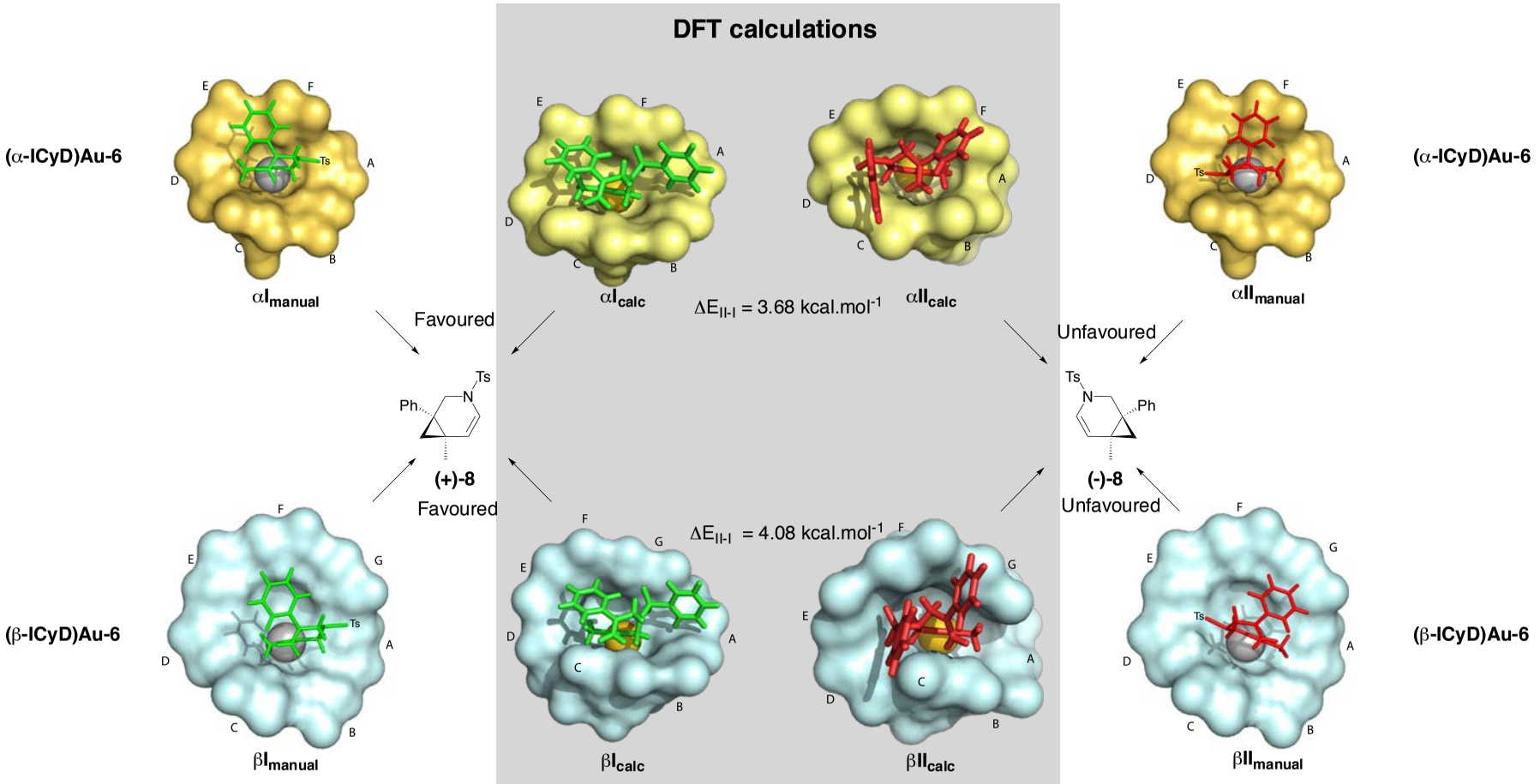

Figure S21. Comparison between static and DFT calculated models

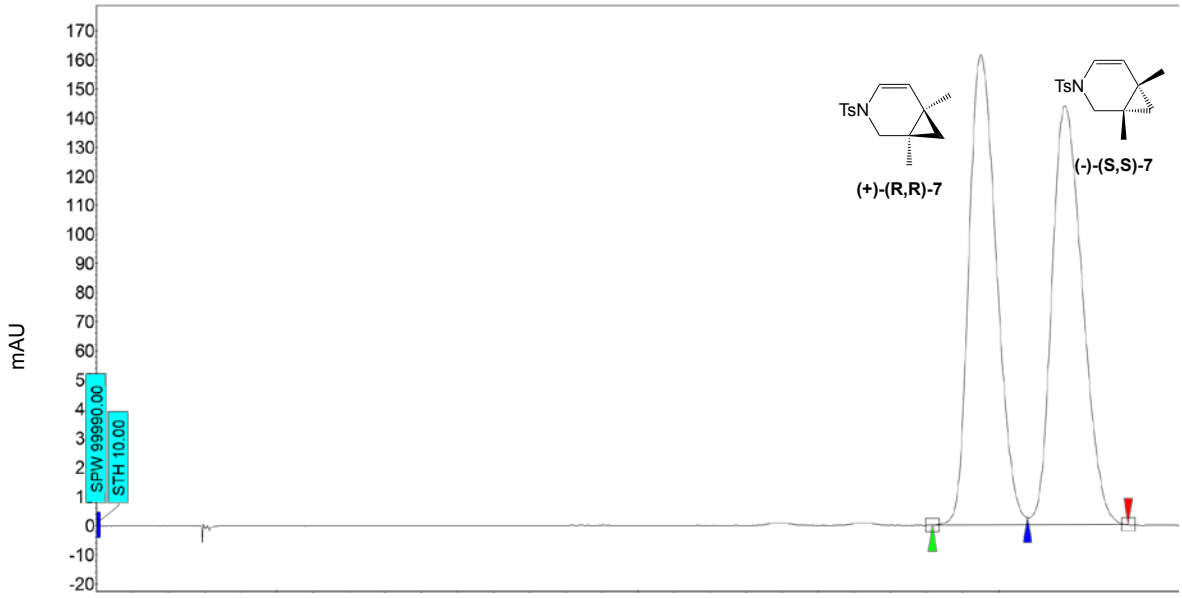

Min

Index	Time [Min]	Area [%]
1	4.90	50.189
2	5.37	49.811
Total		100.000

Figure S22. IPrAuCl-catalyzed cycloisomerization of enyne **5** - Chromatogram recorded on a CO_2 supercritical fluid chromatography (SFC) using AD-H column, pressure: 100 Bars, with a debit of 5 mL/min and 4 % MeOH as eluent at λ = 254 nm.

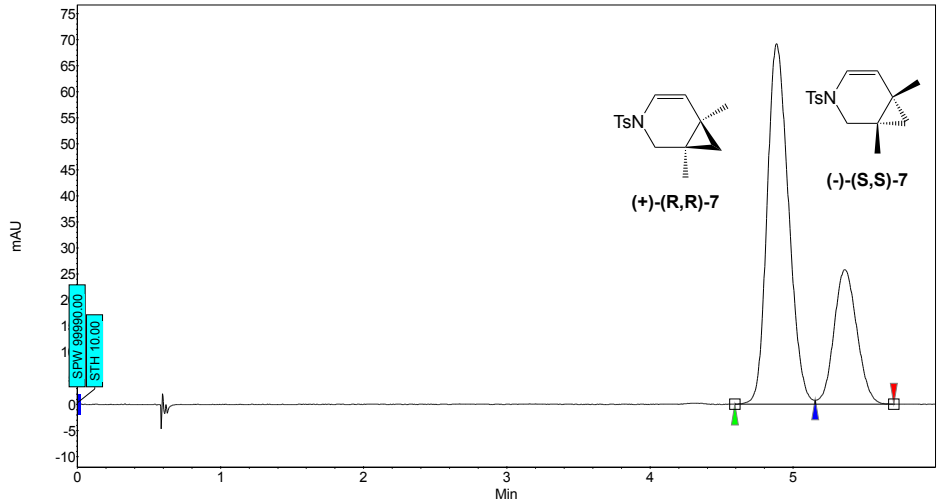

Index	Name	Time	Height	Area	Area	Selectivity	Res. HW
		[Min]	[µV]	[µV.Min]	[%]		
1	UNKNOWN	4.88	69.2	12.0	71.435	0.00	0.00
2	UNKNOWN	5.36	25.8	4.8	28.565	1.10	1.67
Total			95.0	16.8	100.000		

Figure S23. (α-ICyD)AuCl-catalyzed cycloisomerization of **5** - Chromatogram recorded on a CO_2 supercritical fluid chromatography (SFC) using AD-H column, pressure: 100 Bars, with a debit of 5 mL/min and 4 % MeOH as eluent at λ = 254 nm.

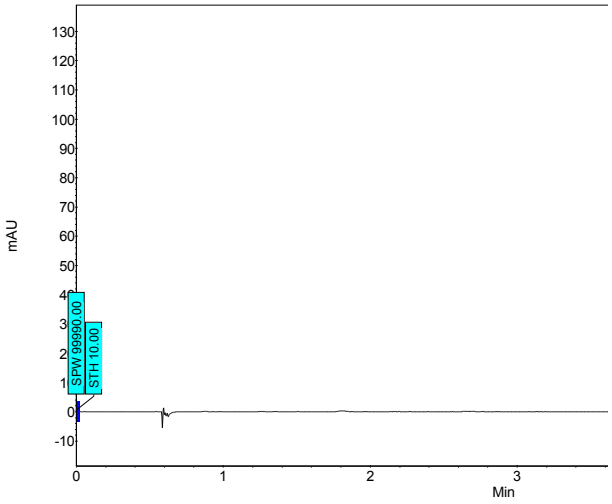

Index	Name	Time	Height	Area	Area	Selectivity	Res. HW
		[Min]	[µV]	[µV.Min]	[%]		
1	UNKNOWN	4.84	125.8	22.3	79.490	0.00	0.00
2	UNKNOWN	5.30	30.8	5.7	20.510	1.09	1.59
Total			156.5	28.0	100.000		

(+)-(R,R)-7

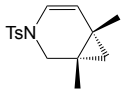

(-)-(S,S)-7

Figure S24. (β-ICyD)AuCl-catalyzed cycloisomerization of **5 -** Chromatogram recorded on a CO_2 supercritical fluid chromatography (SFC) using AD-H column, pressure: 100 Bars, with a debit of 5 mL/min and 4 % MeOH as eluent at λ = 254 nm.

Chiral HPLC report

Sample name: JM-426
Column: Chiralpak AD-H

Temperature: 25 degres
Mobile phase: Heptane/isopropanol (95/5), 1 mL/min

(-)-(S,S)-7 (+)-(R,R)-7

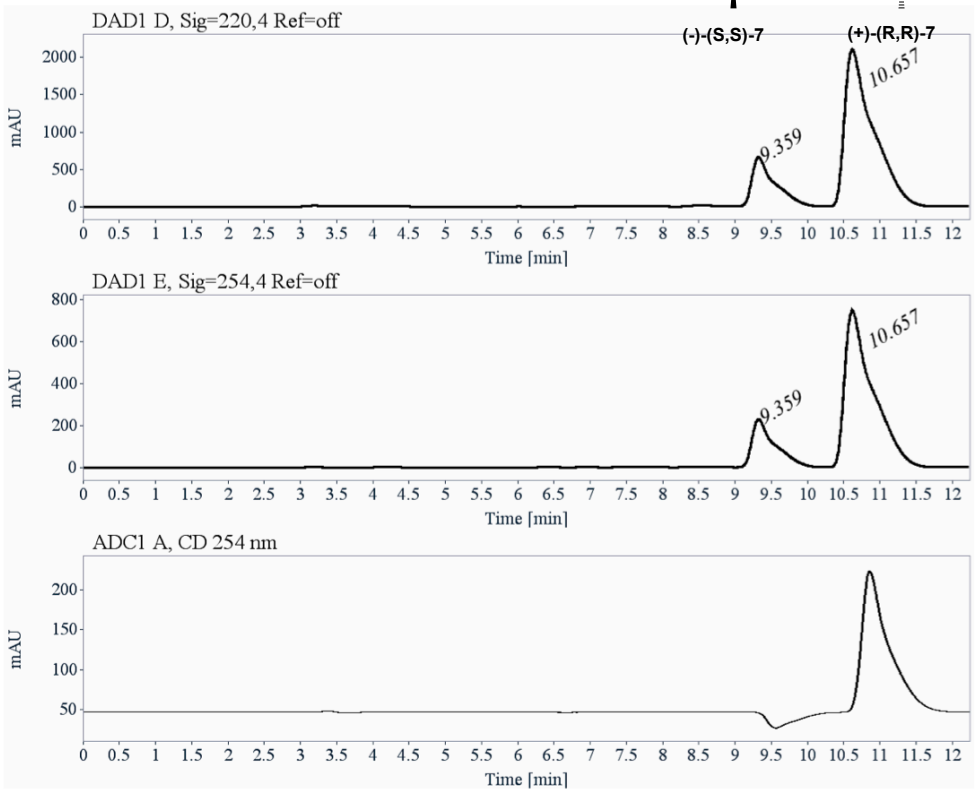

Signal: DAD1 D, Sig=220,4 Ref=off

RT [min]	Area	Area%	Capacity Factor	Enantioselectivity	Resolution (USP)
9.36	14423	19.98	2.17		
10.66	57768	80.02	2.61	1.20	2.46
Sum	72191	100.00			

Signal: DAD1 E, Sig=254,4 Ref=off

RT [min]	Area	Area%	Capacity Factor	Enantioselectivity	Resolution (USP)
9.36	5023	19.88	2.17		
10.66	20247	80.12	2.61	1.20	2.49
Sum	25270	100.00			

Plateforme de chromatographie chirale - Aix Marseille Université

Figure S25. (β-ICyD)AuCl-catalyzed cycloisomerization of **5** - Chromatogram recorded using AD-H column, with a debit of 1 mL/min and heptane/iPrOH (95:5) as eluent at λ = 254 nm and 220 nm.

Column: Chiralpak AZ-H

Temperature: 25 degres

Mobile phase: Heptane/isopropanol (95/5), 1 mL/min

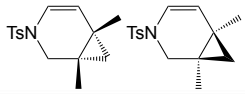

(-)-(S,S)-7 (+)-(R,R)-7

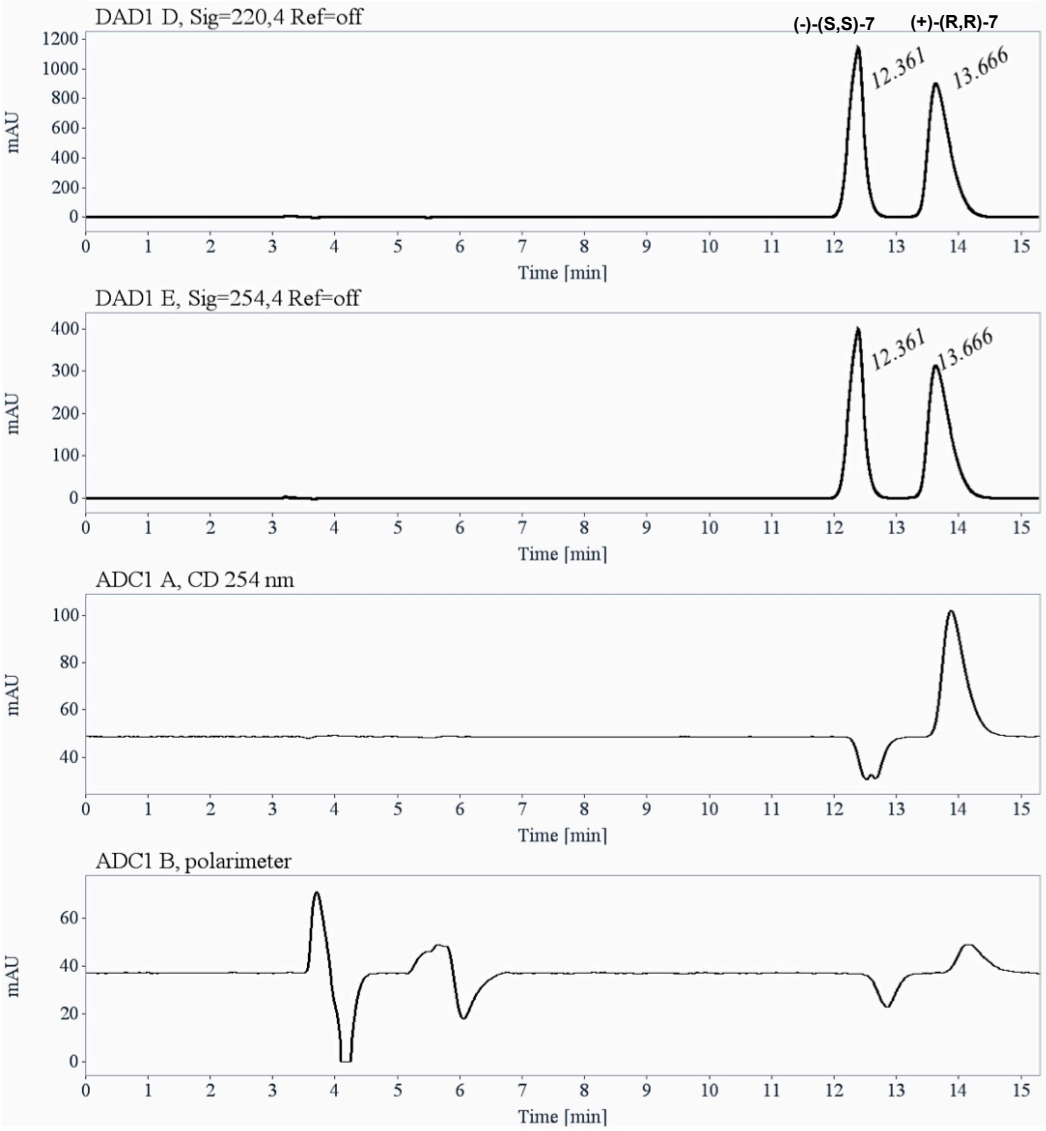

Signal: DAD1 D, Sig=220,4 Ref=off

RT [min]	Area	Area%	Capacity Factor	Enantioselectivity	Resolution (USP)
12.36	19265	46.49	3.19		
13.67	22171	53.51	3.63	1.14	2.40
Sum	41436	100.00			

Signal: DAD1 E, Sig=254,4 Ref=off

RT [min]	Area	Area%	Capacity Factor	Enantioselectivity	Resolution (USP)
12.36	6716	46.54	3.19		
13.67	7713	53.46	3.63	1.14	2.40
Sum	14429	100.00			

Figure S26. (γ-A,D-ICyD)AuCl-catalyzed cycloisomerization of **5** - Chromatogram recorded using AZ-H column, with a debit of 1 mL/min and heptane/iPrOH (95:5) as eluent at λ = 254 nm and 220 nm.

Column: Chiralpak AD-H

Temperature: 25 degres

Mobile phase: Heptane/isopropanol (95/5), 1 mL/min

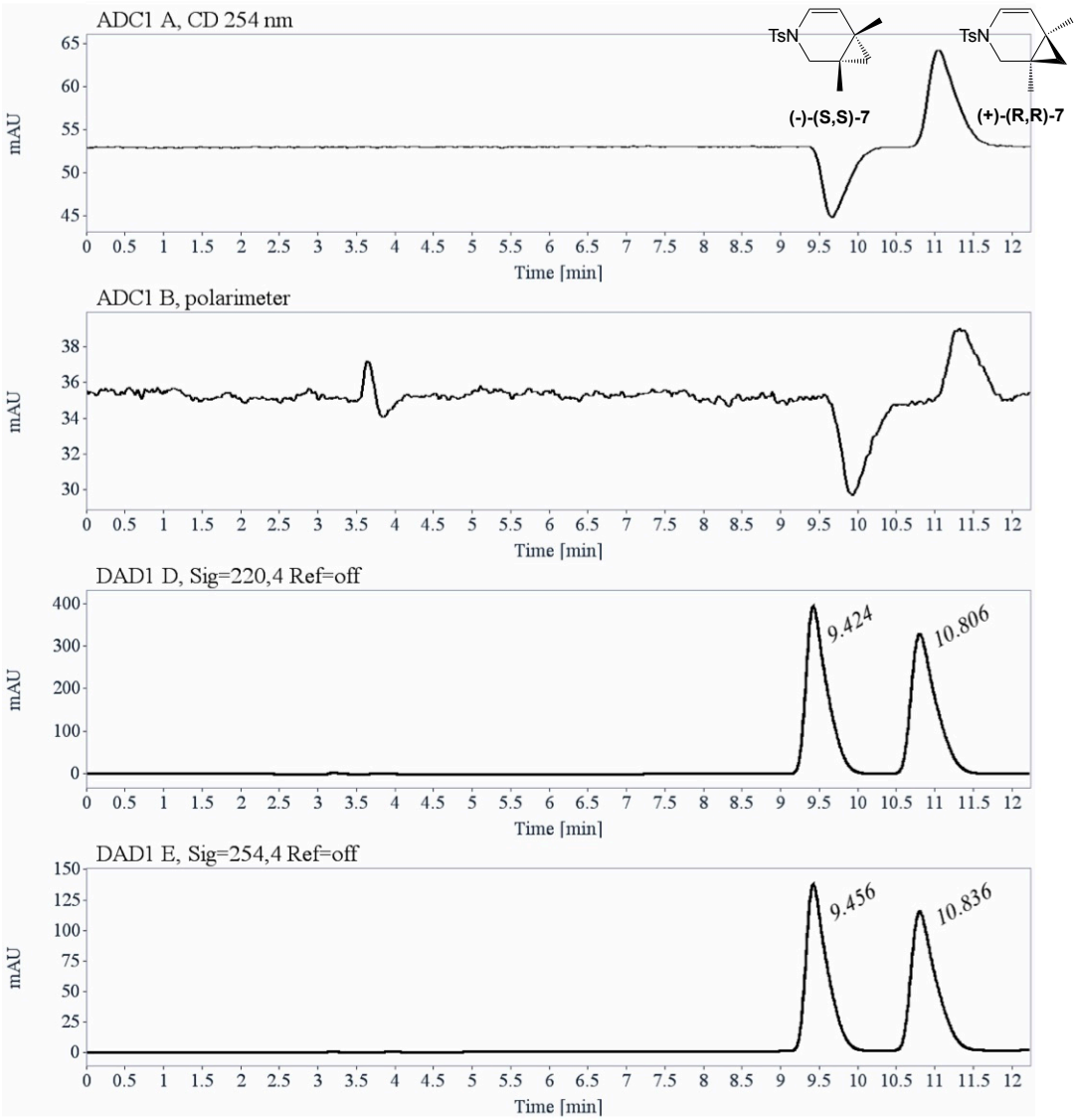

Signal: DAD1 D, Sig=220,4 Ref=off

RT [min]	Area	Area%	Capacity Factor	Enantioselectivity	Resolution (USP)
9.42	7423	50.37	2.19		
10.81	7313	49.63	2.66	1.21	2.60
Sum	14737	100.00			

Signal: DAD1 E, Sig=254,4 Ref=off

RT [min]	Area	Area%	Capacity Factor	Enantioselectivity	Resolution (USP)
9.46	2579	50.40	2.21		
10.84	2538	49.60	2.67	1.21	2.60
Sum	5118	100.00			

Figure S27. (γ-A,E-ICyD)AuCl-catalyzed cycloisomerization of **5** - Chromatogram recorded using AD-H column, with a debit of 1 mL/min and heptane/iPrOH (95:5) as eluent at λ = 254 nm and 220 nm.

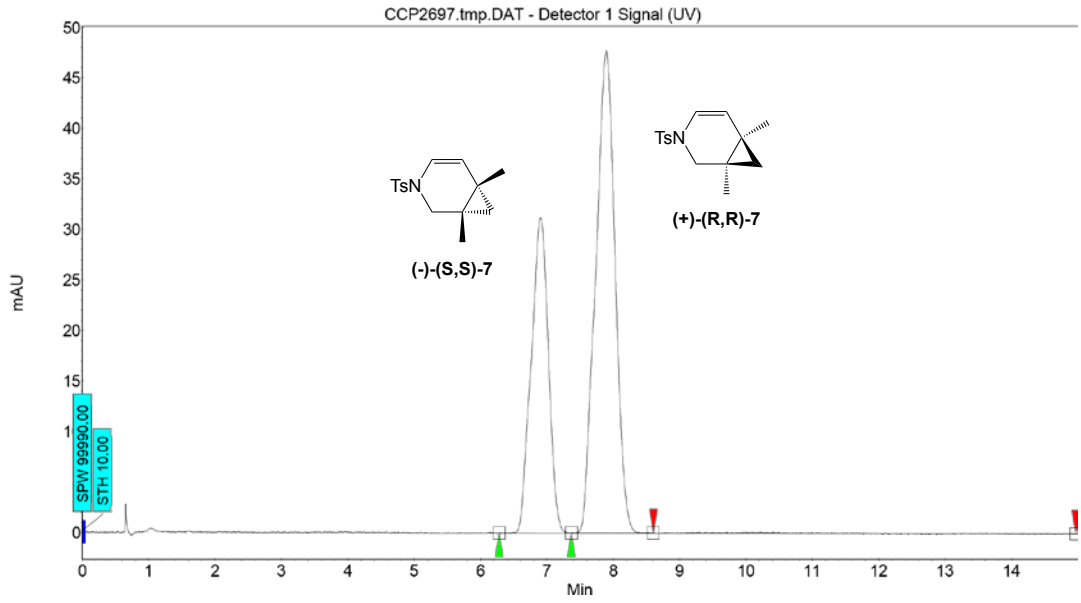

Index	Time [Min]	Area [%]
1	6.91	37.451
2	7.89	62.549
Total		100.000

Figure S28. (α-BiCyD)AuCl-catalyzed cycloisomerization of **5** – Chromatogram recorded on a CO_2 SFC using AD-H column, pressure: 100 Bars, with a debit of 5 mL/min and 4 % iPrOH as eluent at λ = 220 nm

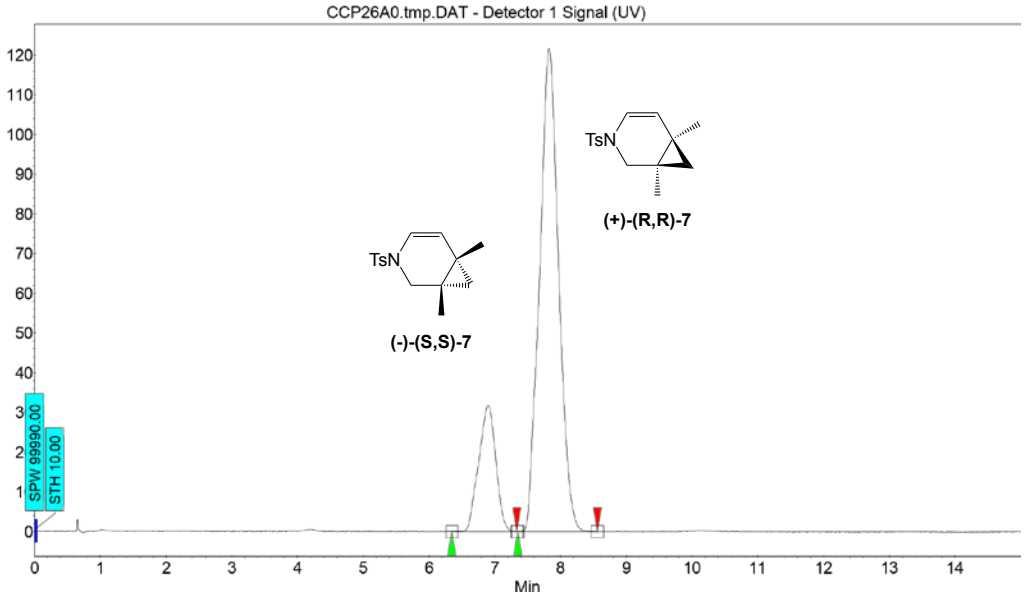

Index	Time [Min]	Area [%]
1	6.90	18.973
2	7.83	81.027
Total		100.000

Figure S29. (β-BiCyD)AuCl-catalyzed cycloisomerization of **5** - Chromatogram recorded on a CO_2 SFC using AD-H column, pressure: 100 Bars, with a debit of 5 mL/min and 4 % iPrOH as eluent at λ = 220 nm.

HPLC:

Column: Chiralpak AZ-H

Temperature: 25 degres

Mobile phase: Heptane/isopropanol (95/5), 1 mL/min

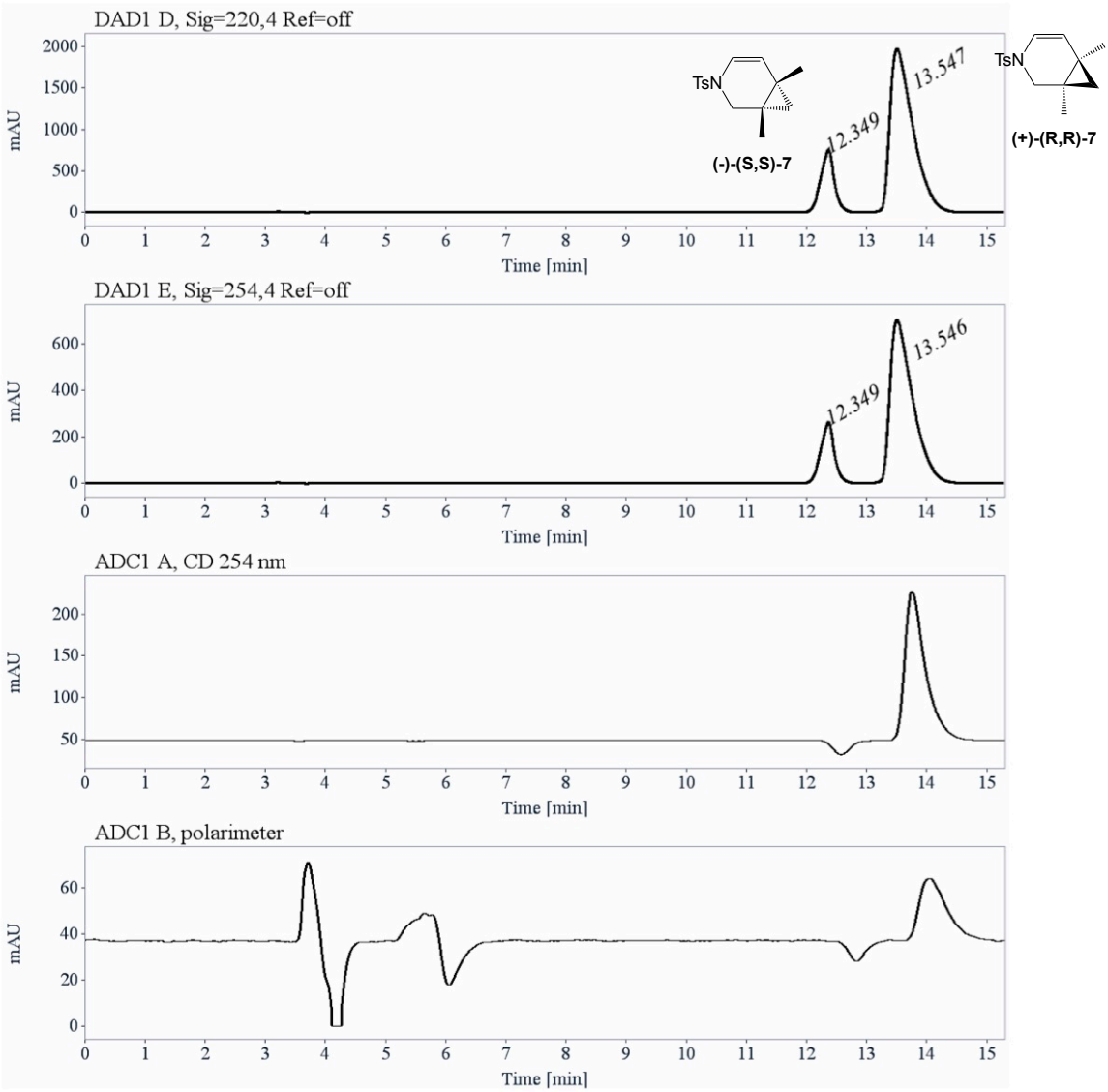

Figure S30. (β-BiCyD)AuCl-catalyzed cycloisomerization of **5** - Chromatogram recorded using AZ-H column, with a debit of 1 mL/min and heptan/iPrOH (95:5) as eluent at λ = 220 nm an 254 nm.

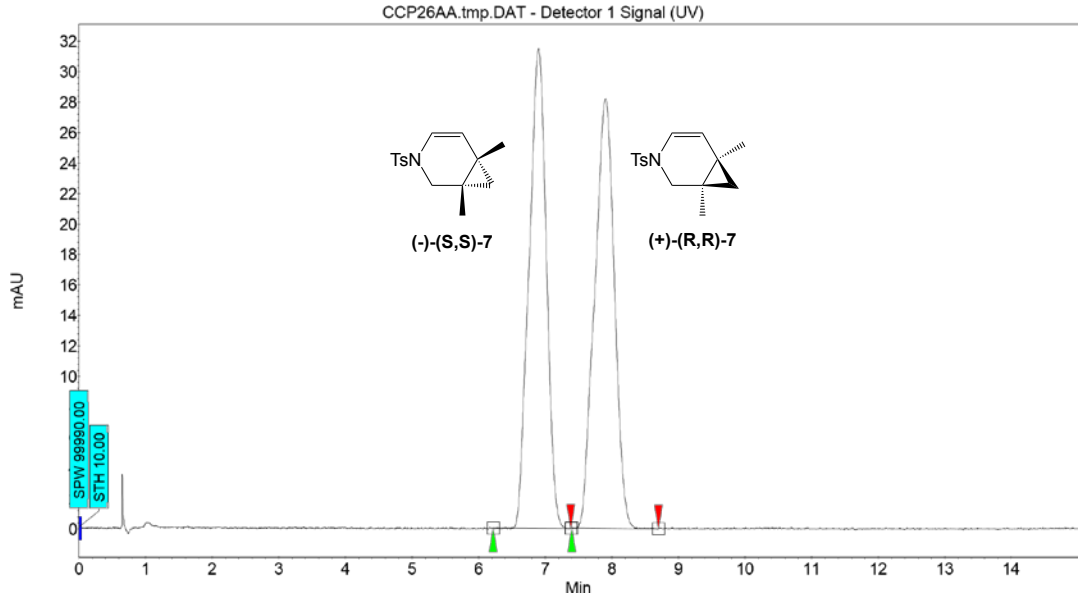

Index	Time [Min]	Area [%]
1	6.90	49.479
2	7.91	50.521
Total		100.000

Figure S31. (α-TriCyD)AuCl-catalyzed cycloisomerization of 5 - Chromatogram recorded on a CO_2 SFC using AD-H column, pressure: 100 Bars, with a debit of 5 mL/min and 4 % iPrOH as eluent at λ = 220 nm.

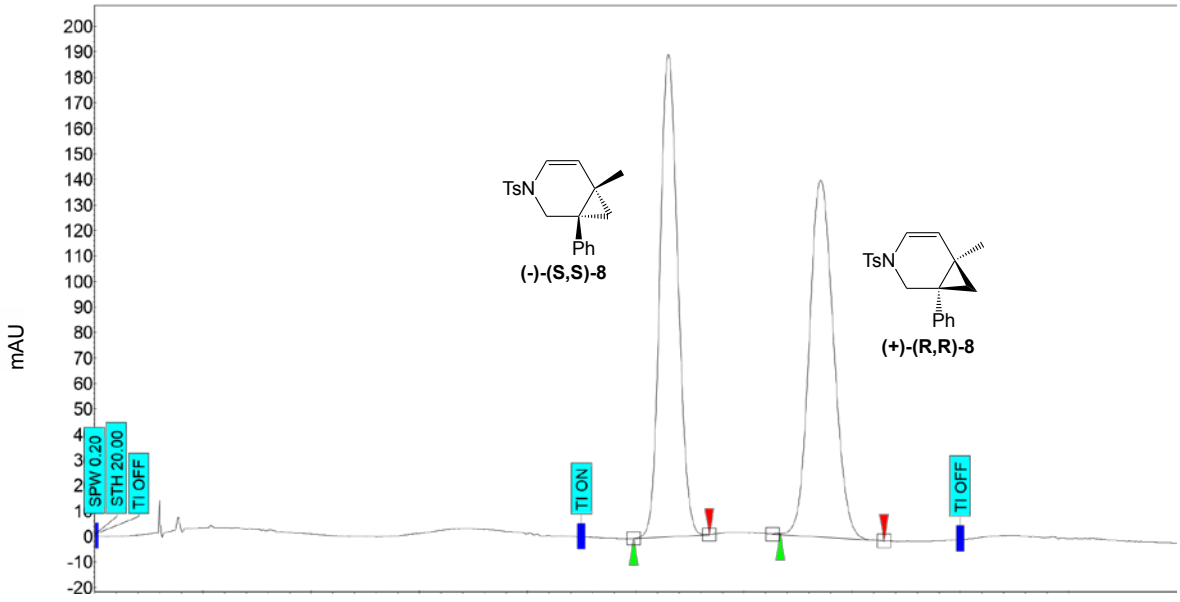

Index	Time [Min]	Area [%]
1	5.30	50.060
2	6.71	49.940
Total		100.000

Figure S32. IPrAuCl-catalyzed cycloisomerization of **6** - Chromatogram recorded on a CO_2 SFC using AD-H column, pressure: 100 Bars, with a debit of 5 mL/min and 8 % MeOH as eluent at λ = 220 nm.

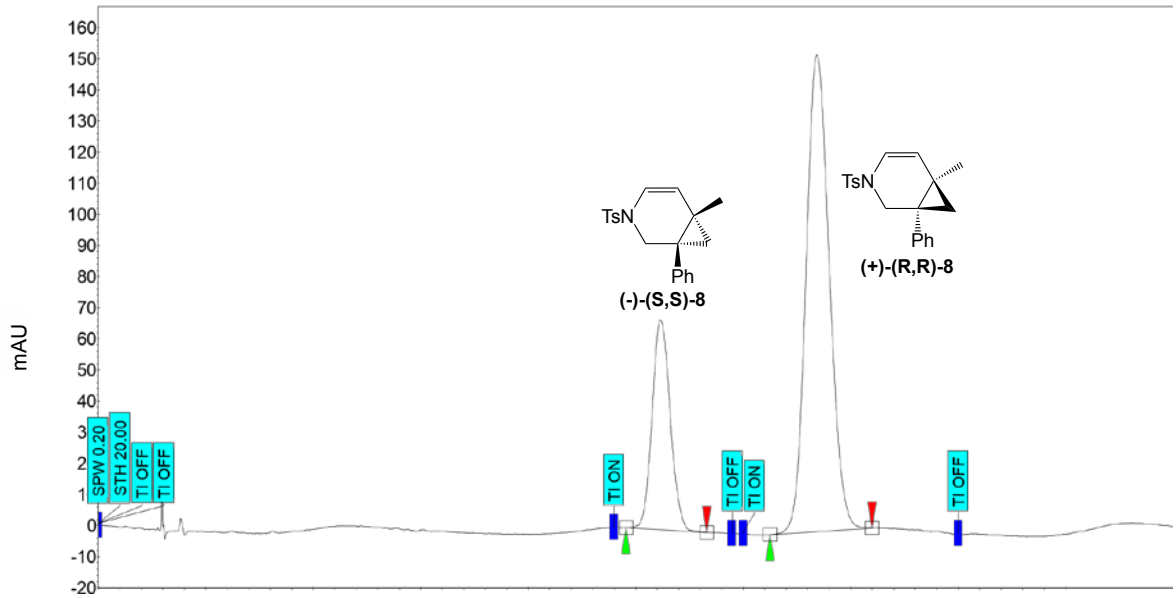

Index	Time [Min]	Area [%]
1	5.23	25.520
2	6.69	74.480
Total		100.000

Figure S33. (α-ICyD)AuCl-catalyzed cycloisomerization of **6** - Chromatogram recorded on a CO_2 SFC using AD-H column, pressure: 100 Bars, with a debit of 5 mL/min and 8 % MeOH as eluent at λ = 220 nm.

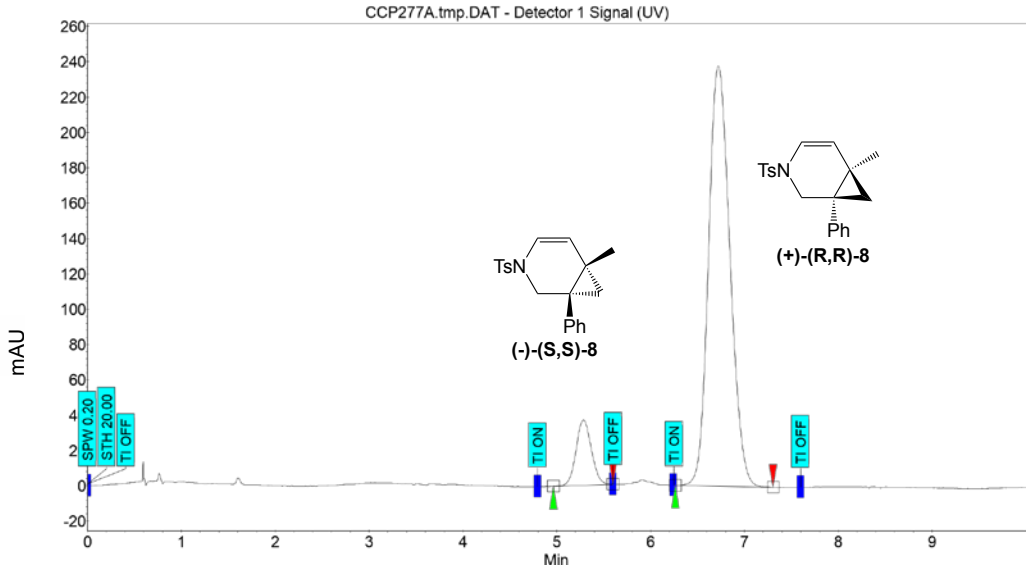

Index	Time [Min]	Area [%]
1	5.29	10.027
2	6.72	89.973
Total		100.000

Figure S34. (β-ICyD)AuCl-catalyzed cycloisomerization of **6** - Chromatogram recorded on a CO_2 SFC using AD-H column, pressure: 100 Bars, with a debit of 5 mL/min and 8 % MeOH as eluent at λ = 220 nm.

Column: Chiralpak AS-H

Temperature: 25 degres

Mobile phase: Heptane/isopropanol (95/5), 1 mL/min

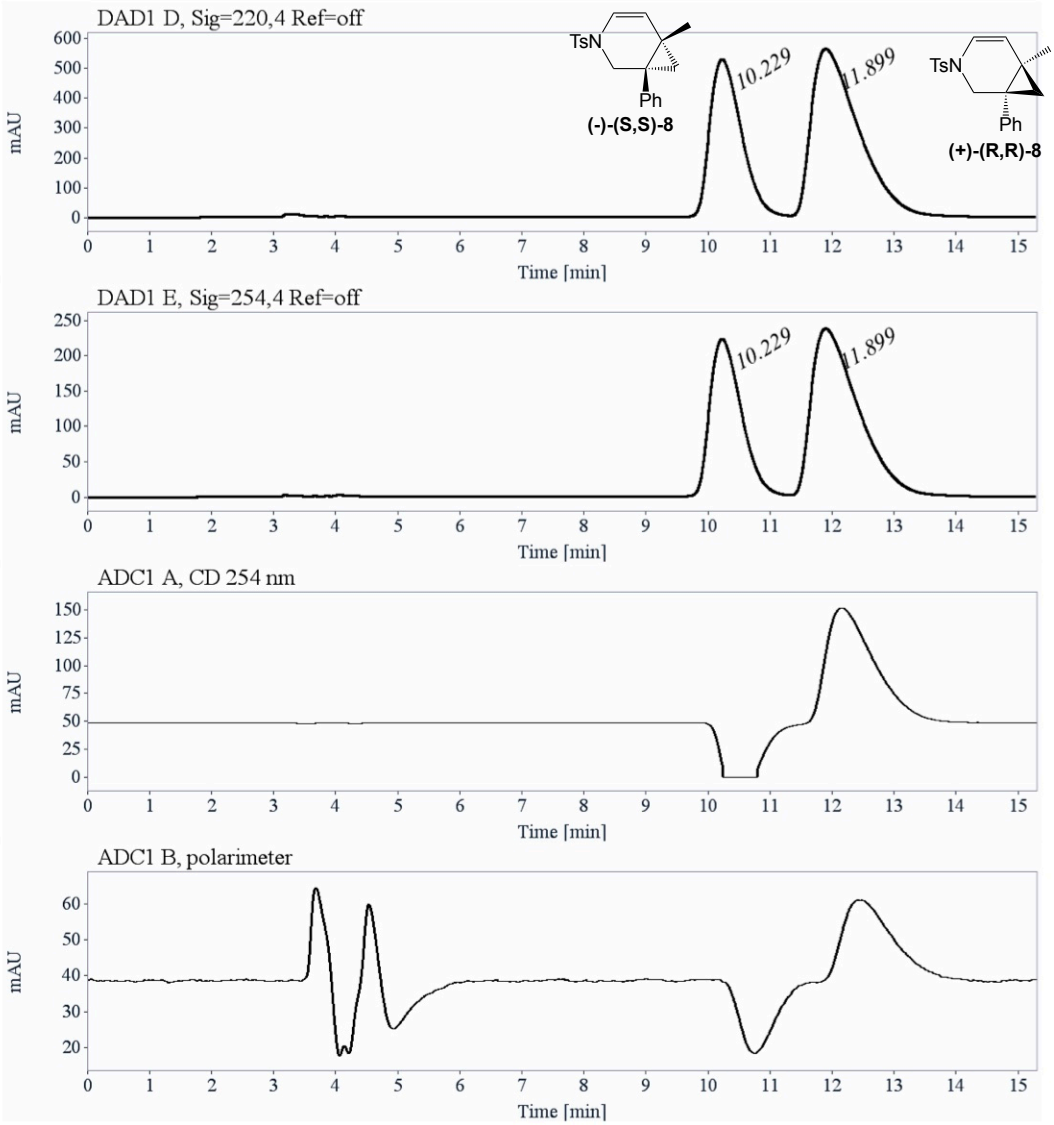

Signal: DAD1 D, Sig=220,4 Ref=off

RT [min]	Area	Area%	Capacity Factor	Enantioselectivity	Resolution (USP)
10.23	18687	38.69	2.47		
11.90	29606	61.31	3.03	1.23	1.44
Sum	48293	100.00			

Signal: DAD1 E, Sig=254,4 Ref=off

RT [min]	Area	Area%	Capacity Factor	Enantioselectivity	Resolution (USP)
10.23	7857	38.68	2.47		
11.90	12458	61.32	3.03	1.23	1.44
Sum	20315	100.00			

Figure S35. (γ-A,D-ICyD)AuCl-catalyzed cycloisomerization of **6** - Chromatogram recorded using AS-H column, with a debit of 1 mL/min and heptane/iPrOH (95:5) as eluent at λ = 220 nm and 254 nm.

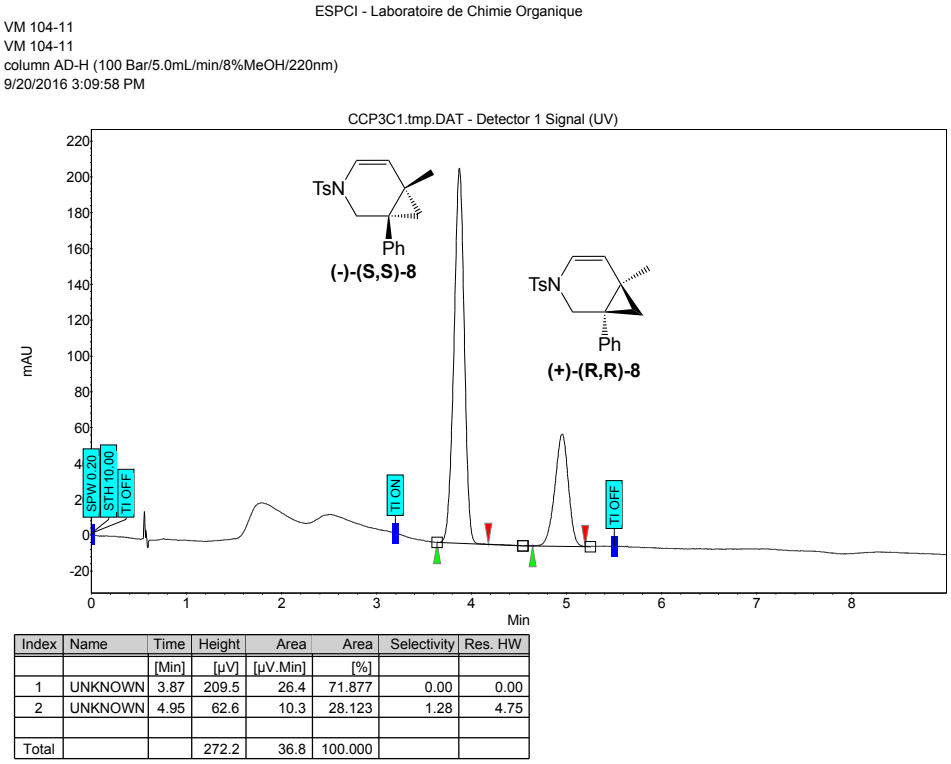

Index	Name	Time	Height	Area	Area	Selectivity	Res. HW
		[Min]	[µV]	[µV.Min]	[%]		
1	UNKNOWN	3.87	209.5	26.4	71.877	0.00	0.00
2	UNKNOWN	4.95	62.6	10.3	28.123	1.28	4.75
Total			272.2	36.8	100.000		

Figure S36. (γ-A,D-ICyD)AuCl-catalyzed cycloisomerization of **6** - Chromatogram recorded on a CO_2 SFC using AD-H column, pressure: 100 Bars, with a debit of 5 mL/min and 8 % MeOH as eluent at λ = 220 nm.

Column: Chiralpak AS-H

Temperature: 25 degres

Mobile phase: Heptane/isopropanol (95/5), 1 mL/min

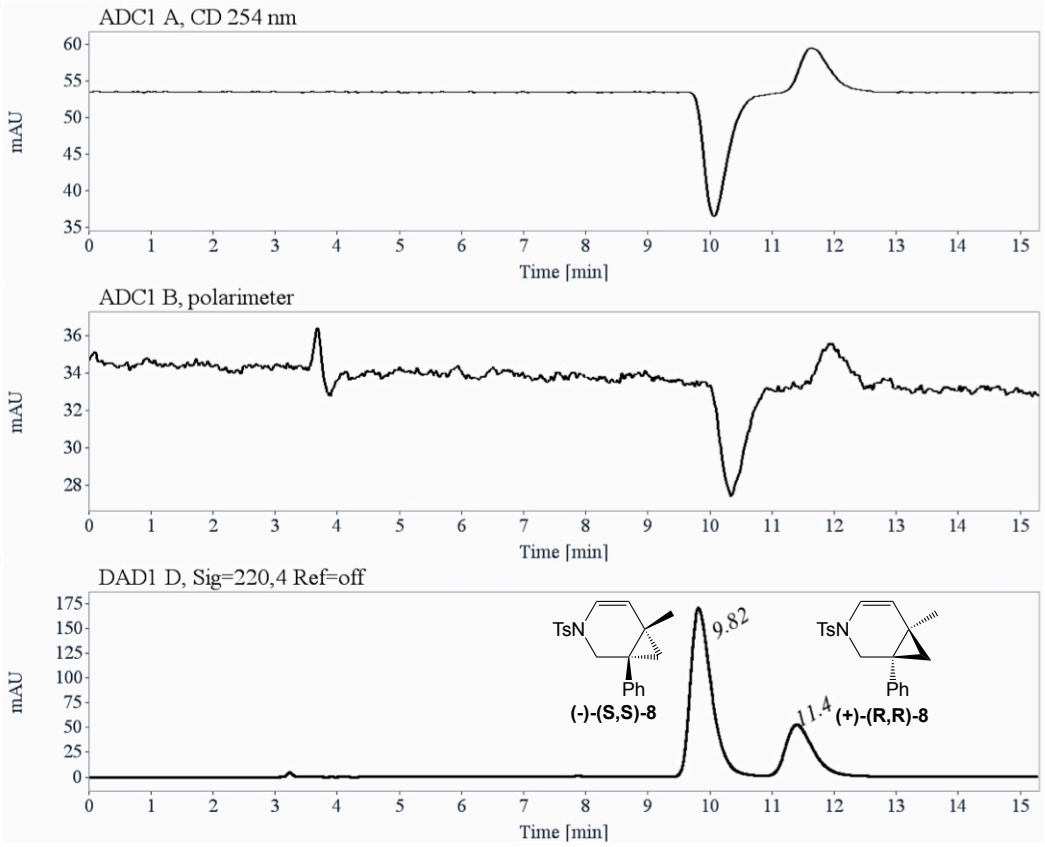

Signal: DAD1 D, Sig=220,4 Ref=off

RT [min]	Area	Area%	Capacity Factor	Enantioselectivity	Resolution (USP)
9.82	4033	70.90	2.33		
11.40	1656	29.10	2.86	1.23	2.24
Sum	5689	100.00			

Figure S37. (γ-A,D-ICyD)AuCl-catalyzed cycloisomerization of **6** - Chromatogram recorded using AS-H column, with a debit of 1 mL/min and heptane/iPrOH (95:5) as eluent at λ = 220 nm and 254 nm.

Supplemental schemes

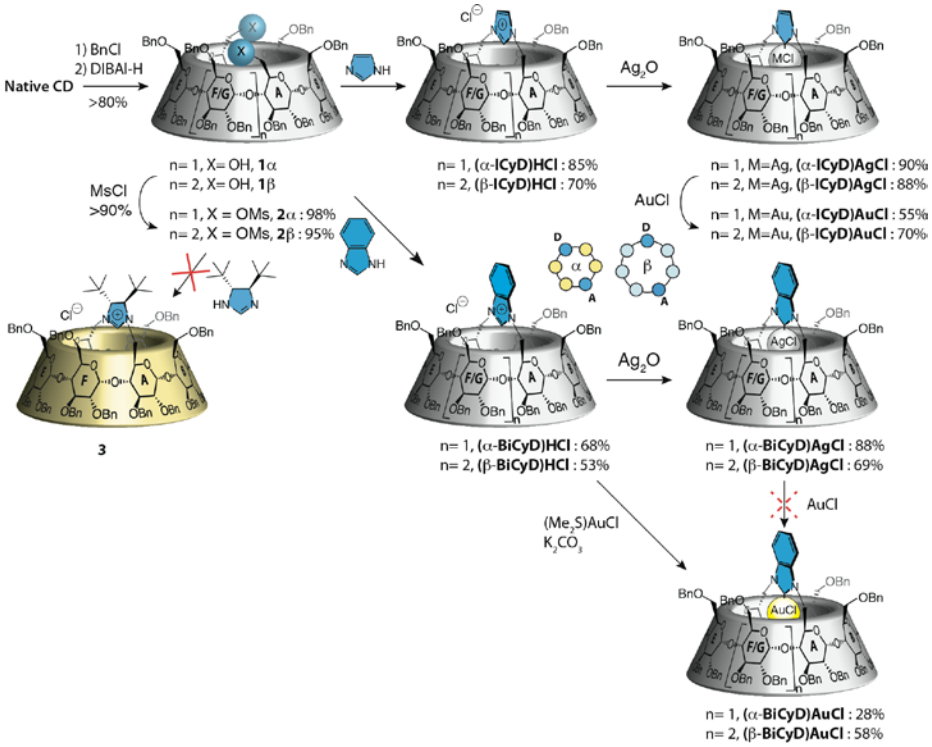

Scheme S1. Synthesis of α- and β-**ICyD** and α- and β-**BiCyD** silver and gold complexes.

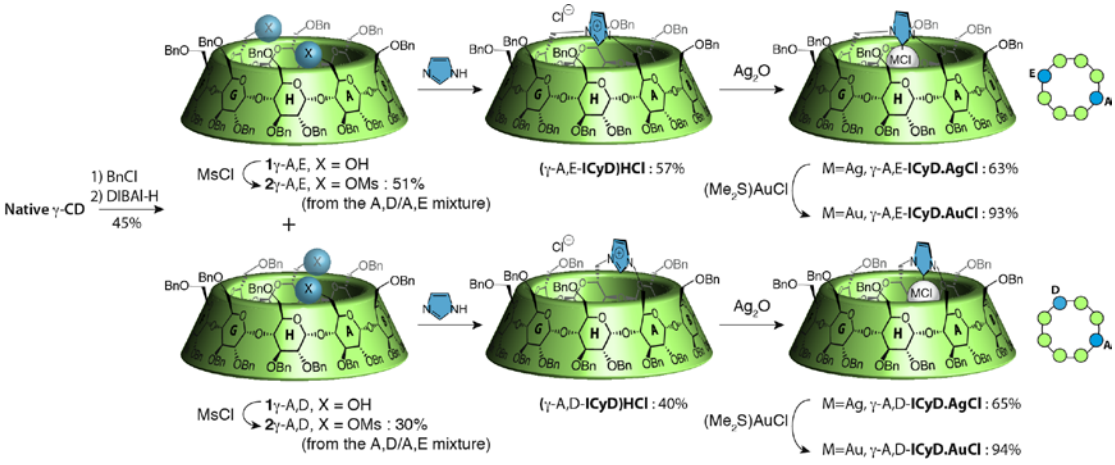

Scheme S2. Synthesis of γ-A,E- and γ-A,D-**ICyD** silver and gold complexes.

All syntheses of NHC-capped CDs started from perbenzylated α, and β-CD diols **1α**, **1β** obtained using perbenzylation of a,β-CDs followed by in-house DIBAL-H-mediated bis-debenzylation procedure (Scheme S1).[1,2] Both diols were bis-mesylated to afford CDs **2α** and **2β** in >90% yields.[3] In the case of γ-CD, the DIBAL-H deprotection affords a mixture of A,D

and A,E diols **1γ-A,D** and **1γ-A,E** (Scheme S2),[4] which were separated after mesylation to give pure A,D and A,E regioisomers **2γ-A,D** (30%) and **2γ-A,E** (51%). Treatment of **2α**, **2β**, **2γ-A,E** and **2γ-A,D** with imidazole gave the imidazolium-bridged CD chloride salts **(α-ICyD)HCl**,[5] **(β-ICyD)HCl**, **(γ-**A,E-**ICyD)HCl** and **(γ-**A,D-**ICyD)HCl** in 85%, 70%, 57% and 40% yield respectively. Noteworthy, the yield decreases with the increase of the size of the CD, but the capping is still preferred over the corresponding bis-imidazole formation.[6] In order to study the influence of the variation of electronic effects on the NHC, two other NHC precursors were used: a benzimidazole and a saturated di-tert-butyl-imidazoline. α-, and β-CD derived benzimidazolium-bridged CDs, coined **(α-BiCyD)HCl** and **(β-BiCyD)HCl**, were obtained through reaction of benzimidazole with bis-mesylated α- and β-CDs **2a**, **2b**, in 68%, 53% yield respectively. However, probably due to the steric hindrance of tert-butyl groups, reaction of di-tert-butyl-imidazoline with bis-mesylated α-CD **2a** did not yield a bridged compound. All the obtained bridged imidazoliums were submitted to the action of Ag_2O in CH_3CN to prepare the corresponding silver-NHC complexes in good yields. Gold complexes **(α-ICyD)AuCl**, **(β-ICyD)AuCl** were obtained from the corresponding silver complexes by transmetallation using AuCl in 55% and 70% yields respectively. (Scheme S1) **(γ-A,E-ICyD)AuCl** and **(γ-A,D-ICyD)AuCl** were obtained using $(Me_2S)AuCl$ in 93% and 94% yield respectively. (Scheme S2) Transmetallation of **(α-BiCyD)AgCl** and **(β-BiCyD)AgCl** with AuCl in CH_3CN consistently gave inseparable mixtures of starting silver complexes and aimed gold complexes. A direct method to give gold complexes[7,8] was then considered. With an excess of $(Me_2S)AuCl$ or AuCl and K_2CO_3 at 50°C, benzimidazolium compounds **(α-BiCyD)HCl** and **(β-BiCyD)HCl** gave the corresponding gold complexes **(α-BiCyD)AuCl** and **(β-BiCyD)AuCl** in 28%, 58% yield respectively. (Scheme S1)

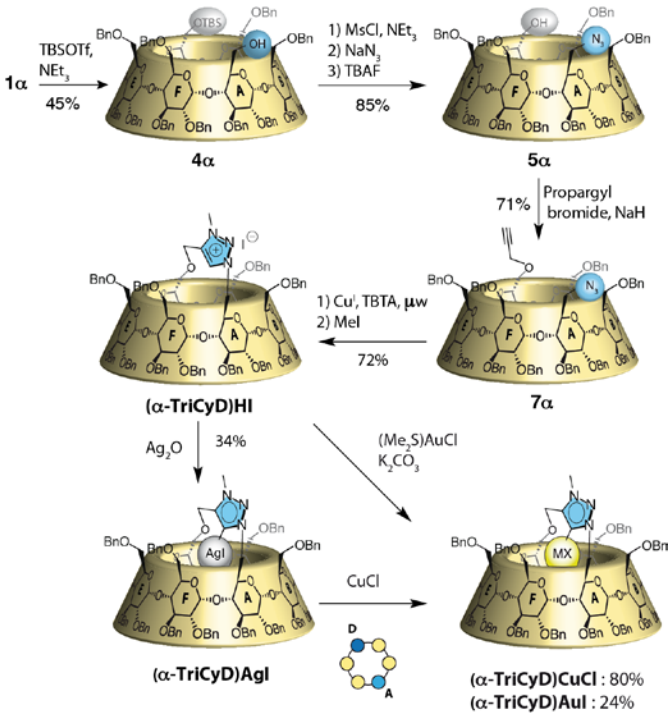

Scheme S3. Synthesis of α- and β-TriCyD silver and gold complexes

The so-called abnormal[9] or mesoionic carbenes (MICs)[10,11] have complementary electronic

properties to the NHCs. In particular they are stronger electron donors. For their synthesis we investigated an intramolecular copper(I)-catalyzed alkyne-azide cycloaddition (CuAAC).[12] We therefore needed to synthesize CDs functionalized on one side with an alkyne and on the diametrically opposed sugar with an azide. In recent years a few practical hetero-poly-functionalisation reactions have emerged based either on sulfonate displacement [13] or DIBAL-H deprotection[2,14,15] or both,[16] which makes this synthesis conceivable. For α-CD, we started our synthesis using a route developed by Hanessian.[17] α-CD diol **1a** was treated with only 0.5 eq. of tert-butyldimethylsilyl trifluoromethanesulfonate (TBSOTf) to generate the mono-OTBS substituted derivative **4a** in 45% yield within 2h. The remaining free single hydroxyl group in **4a** was subjected to mesylation, then, the product was treated with NaN_3 to afford the corresponding monoazide compound in 94% yield. Subsequent TBS group cleavage with TBAF gave the azidoalcohol α-CD derivative **5a**.[17] The hydroxyl group was further propargylated to give **7a**. Under the classical CuAAC conditions, an intramolecular cycloaddition product was obtained, which was methylated using iodomethane to afford the triazolium-capped α-CD that we called **(α-TriCyD)HI** in 72% yield over two steps. Upon treatment with Ag_2O **(α-TriCyD)AgI** was obtained in 34% yield. It is worth mentioning that probably due to the large amount of iodide when we methylated the capped triazole ring, we obtained the AgI complex rather than the AgCl complex. As in the case of **BiCyD** derivatives the transmetallation of **α-(TriCyD)AgI** with AuCl proved unsatisfactory, whereas the cupration was successful (80%). We therefore also used direct auration of the triazolium **(α-TriCyD)HI** using an excess of $(Me_2S)AuCl$ and K_2CO_3 at 50°C, to give **(α-TriCyD)AuI** in 24% yield. (Scheme S3) The synthesis of **β-TriCyD** was also attempted in a similar fashion, but in spite of several attempts using various conditions, it was impossible to isolate the desired **(β-TriCyD)AgI**.

It is worth mentioning that all metal complexes are stable under air and on silica gel, which highly facilitates their handling and purification, and is certainly due to their wrapping inside the cavity of the CD.

Supplemental table

Table S1. H-5 and H-3 chemical shifts for α,β,γ-ICyD, α,β-BiCyD and α-TriCyD silver complexes.

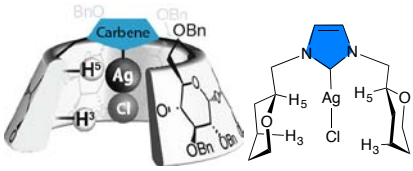

Compound	Sugar unit	A	B	C	D	E	F	G	H
(α-ICyD)AgCl[a]	**H-5**	5.64	3.88	3.89	5.64	3.88	3.89		
	H-3	4.18	4.29	4.98	4.18	4.29	4.98		
(α-BiCyD)AgCl[a]	**H-5**	5.92	3.98	4.00	5.92	3.98	4.00		
	H-3	4.27	4.32	5.09	4.27	4.32	5.09		
(α-TriCyD)AgI [a]	**H-5**	5.05	4.58	4.42	5.59	3.87	4.05		
	H-3	4.29	4.76	4.99	4.20	4.29	5.10		
(β-ICyD)AgCl[a]	**H-5**	5.54	3.97	3.78	4.44	3.25	3.57	3.67	
	H-3	4.06	4.51	4.60	3.95	4.24	4.10	4.20	
(β-BiCyD)AgCl[a]	**H-5**	5.64	3.92	3.93	4.74	3.09	3.57	3.85	
	H-3	4.08	4.48	4.66	4.05	4.22	4.13	4.30	
(γ-AE-ICyD)AgCl[b]	**H-5**	4.30	3.62	3.81	3.52	4.30	3.62	3.81	3.52
	H-3	3.95	3.90	4.10	4.11	3.95	3.90	4.10	4.11
(γ-AD-ICyD)AgCl[b]	**H-5**	4.30	4.01-3.58	4.01-3.58	4.27	4.01-3.58	4.01-3.58	4.01-3.58	4.20
	H-3	3.88	4.30	4.23	3.98	3.87	3.80	3.82	3.96

[a] in $CDCl_3$; [b] in CD_3CN

The chemical shifts of the H-3s and H-5s of all the synthesized complexes are reported in table S1. A general trend appears: H-5s belonging to glucose units linked to the carbene metal complex are the most deshielded, while their H-3s are among the less deshielded. For the H-3s, a general trend can be drawn: for derivatives where diametrically opposed sugars are linked: **(α-ICyD)AgCl, (α-BiCyD)AgCl, (α-TriCyD)AgI** and **(γ-AE-ICyD)AgCl** the H-3s on the clockwise (view from the primary rim) sugars are the most deshielded, i.e. sugars C and F for the α-CDs, and D and G for γ-CD. For the unsymmetrical CDs: **(β-ICyD)AgCl, (β-BiCyD)AgCl** and **(γ-AD-ICyD)AgCl**, the H-3s on sugars B and C, delineating the shortest route linking both sugars of the bridge, are the most deshielded. Now in more details, benzimidazolylidene complexes **BiCyDs** display H-5s, which are more deshielded than the imidazole-derived **ICyDs**. The deshielding of the H-5s on **γ-**CDs is notably less important than

for their a and b counterparts.

In addition to the previous shifts, in both **(α-ICyD)AgCl** and **(α-BiCyD)AgCl** the para and meta protons of the benzyl groups linked to the O-$2^{C,F}$ atoms undergo an upfield shift which was previously attributed to a halogen-π interaction. [18] This additional interaction materializes the enlargement of the second coordination sphere brought by the benzyl groups on the CD scaffold. These interactions highly stabilize the AgCl complex.[5] In the case of **(β-ICyD)AgCl** and **(β-BiCyD)AgCl**, three different benzyl groups are involved in such an interaction, hence demonstrating the asymmetry of this extended cavity and second coordination sphere compared to the **(α-ICyD)AgCl**. Notably, no shielding of benzyl protons is apparent for both **γ-ICyDs**, probably due to distance.

Table S2. Cartesian Coordinates of **4'α** related to **Figure S16**

Table S3. Cartesian Coordinates of **TS2'α** related to **Figure S16**

Table S4. Cartesian Coordinates of **2'α** related to **Figure S16**

Table S5. Cartesian Coordinates of **4β** related to **Figure S17**

Table S6. Cartesian Coordinates of conformer **A** related to **Figure S17**

Table S7. Cartesian Coordinates of conformer **B** related to **Figure S17**

Table S8. Cartesian Coordinates of $\alpha\mathbf{I}_{\mathbf{calc}}$ related to **Figure S21**

Table S9. Cartesian Coordinates of $\alpha\mathbf{II}_{\mathbf{calc}}$ related to **Figure S21**

Table S10. Cartesian Coordinates of $\beta\mathbf{I}_{\mathbf{calc}}$ related to **Figure S21**

Table S11. Cartesian Coordinates of $\beta\mathbf{II}_{\mathbf{calc}}$ related to **Figure S21**

Supplemental Experimental Procedures

General Informations

Dichloromethane was freshly distilled from P_2O_5, THF from sodium/benzophenone. DMF was dried over molecular sieves. Reactants were purchased from commercial sources and used without further purification. HRMS were recorded on a Bruker micrOTOF spectrometer, using Agilent ESI-L Low Concentration Tuning-Mix as reference. Optical rotations were measured on a Perkin–Elmer 341 digital polarimeter or a Jasco P-2000 polarimeter with a path length of 1 dm. NMR spectra were recorded on a Bruker Avance II 600 MHz or Brüker AM-400 MHz using residual solvent signal as internal reference. Assignments were aided by COSY, HSQC, NOESY, TOCSY and HMBC experiments.

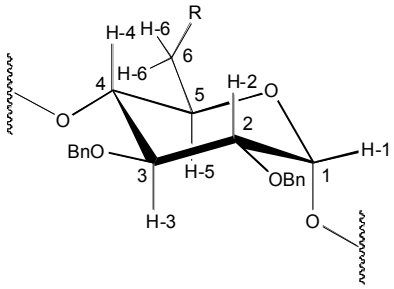

6A,6D-di-O-methylsulfonyl-2A-F,3A-F,6B,6C,6E,6F-Hexadeca-O-benzyl-α-cyclodextrin (2α)

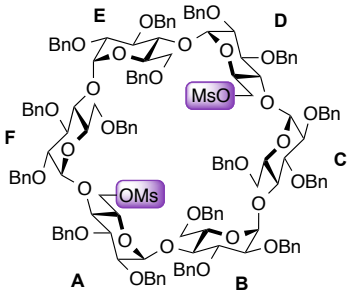

Triethylamine (230 µl, 1.66 mmol) followed by methanesulfonyl chloride (128 µl, 1.66 mmol) were added dropwise to a solution of diol **1α** (1 g, 414 µmol) in dichloromethane (20 ml). The mixture was stirred at r.t. and the reaction followed by TLC. After 1 h 30, the mixture was quenched with satd. aqueous $NaHCO_3$ (10 ml). The layers were separated and the organic layer was washed with H_2O (10 ml). The aqueous layer was then extracted with dichloromethane (2 x 10 ml) and the combined organic layers were dried with $MgSO_4$ and concentrated in vacuo. The residue was purified by silica gel chromatography (Cyclohexane/Ethyl Acetate, 3:1) to afford compound **2α** (1.06 g, 98%) as white foam.

The structure of the product was confirmed by comparison with the NMR spectra of the literature. [19]

6^{A},6^{D}-di-O-methylsulfonyl-2^{A-G},3^{A-G},6^{B},6^{C},6^{E},6^{F},6^{G}-Nonadeca-O-benzyl-β-cyclodextrin (2β)

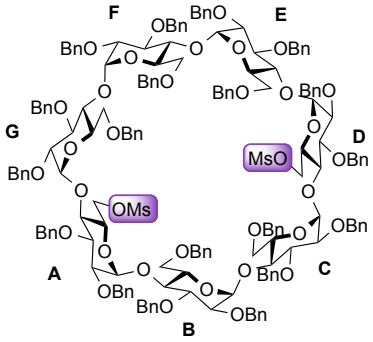

To a solution of **1β** (1.0 g, 0.35 mmol) in anhydrous CH_2Cl_2 (5 ml), triethylamine (0.2 ml, 140 ml) and methanesulfonyl chloride (110 µL, 140 mmol) were added at 0˚C. The reaction mixture was stirred at R.T. for 2h under nitrogen, and then water (5 ml) was added slowly, the layers were separated and the aqueous layer was extracted with DCM 3 times. The combined organic layers were dried over $MgSO_4$, filtered and concentrated. Silica gel chromatography of the residue (Cy/EtOAc 4:1) afforded compound **2β** (950 mg, 95%) as white foam.

The structure of the product was confirmed by comparison with the NMR spectra of the literature.[5]

6^{A},6^{E}-di-O-methylsulfonyl-2^{A-G},3^{A-G},6^{B},6^{C},6^{D},6^{F},6^{G},6^{H}-Docosa-O-benzyl-γ-cyclodextrin (2γ-A,E) and 6^{A},6^{D}-di-O-methylsulfonyl-2^{A-G},3^{A-G},6^{B},6^{C},6^{E},6^{F},6^{G},6^{H}-Docosa-O-benzyl-γ-cyclodextrin (2γ-A,D)

To a solution of the mixture of **1γ-A,D** and **1γ-A,E** (2 g, 0.611mmol) in anhydrous CH_2Cl_2 (40 mL), triethylamine (200 µL, 2.444 mmol) and methanesulfonyl chloride (340 µL, 0.46 mmol) were added at 0 ^{o}C. The reaction mixture was stirred at R.T. for 2h under nitrogen, and then water was added slowly, the layers were separated and the aqueous layer was extracted with DCM 3 times. The combined organic layers were dried over $MgSO_4$, filtered and concentrated. Silica gel chromatography of the residue (Cy/Et_2O 3.5:1) afforded **2γ-A,E** (1,07 g, 51% yield) in a first fraction followed by the second fraction containing **2γ-A,D** (0.589 mg, 30% yield) as a white foam.

6^{A},6^{E}-di-O-methylsulfonyl-2^{A-G},3^{A-G},6^{B},6^{C},6^{D},6^{F},6^{G},6^{H}-Docosa-O-benzyl-γ-cyclodextrin (2γ-A,E)

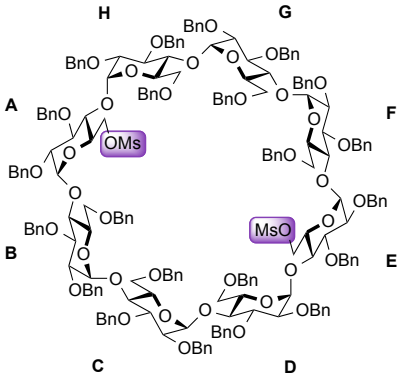

^{1}H NMR (600 MHz, $CDCl_3$): 7.43-6.98 (m, 110H, 110 x H-Ar), 5.59 (d, $^{3}J_{1,2}$ = 3.9 Hz, 2H, 2 x H-1), 5.50 (d, $^{2}J_{Ph\text{-}C\underline{H}H}$ = 10.7 Hz, 2H, 2 x CHPh), 5.47 (d, $^{2}J_{Ph\text{-}C\underline{H}H}$ = 10.4 Hz, 2H, 2 x CHPh), 5.27 (d, $^{2}J_{Ph\text{-}C\underline{H}H}$ = 10.7 Hz, 2H, 2 x CHPh), 5.07 (d, $^{3}J_{1,2}$ = 3.3 Hz, 2H, 2 x H-1), 5.03 (d, $^{3}J_{1,2}$ = 3.1 Hz, 2H, 2 x H-1), 4.92 (d, $^{3}J_{1,2}$ = 3.4 Hz, 2H, 2 x H-1), 4.88-4.86 (m, 6H, 6 x CHPh), 4.80 (d, $^{2}J_{Ph\text{-}C\underline{H}H}$ = 10.5 Hz, 2H, 2 x CHPh), 4.69 (d, $^{2}J_{Ph\text{-}C\underline{H}H}$ = 12.2 Hz, 2H, 2 x CHPh), 4.64-4.56 (m, 4H, 4 x CHPh), 4.55-4.33 (m, 28H, 4 x H-6, 2 x H-5, 22 x CHPh), 4.26 (d, $^{2}J_{Ph\text{-}C\underline{H}H}$ = 12.9 Hz, 2H, 2 x CHPh), 4.19-3.80 (m, 28H, 8 x H-3, 8 x H-4, 4 x H-5, 8 x H-6), 3.72-3.71 (m, 2H, 2 x H-5), 3.64-3.56 (m, 6H, 2 x H-2, 4 x H-6), 3.50 (dd, 2H, $^{3}J_{1,2}$ = 9.4Hz, $^{3}J_{2,3}$ = 3.5 Hz, 2 x H-2), 3.45-3.43 (m, 4H, 4 x H-2), 2.56 (s, 6H, 2 x $C\underline{H}_3$);

^{13}C NMR (151 MHz, $CDCl_3$): 139.89(2C), 139.72(2C), 139.59(2C), 138.97(2C), 138.71(4C), 138.56(2C), 138.50(2C), 138.46(2C), 138.00(4C) (22x C-Ar-quat.), 128.44-126.88 (110x C-Ar-tert.), 100.49(2C), 98.78(2C), 98.04(2C), 95.71(2C) (8 x C-1), 81.81(2C), 81.66(2C), 81.25(2C), 81.07(2C), 80.88(4C), 80.13(4C) (8 x C-3, 8 x C-4), 79.07(2C), 78.85(2C), 78.04(2C), 77.38 (2C) (8 x C-2), 76.91(2C), 76.54(2C), 76.40(2C), 74.21(2C), 73.98(2C), 73.43(2C), 73.37(4C), 72.73(2C), 72.70(2C), 72.50(2C) (22 x Ph-$C\underline{H}_2$), 71.80(2C), 71.33(4C)(6 x C-5), 69.67(2C), 69.36(2C), 69.30(2C)(6 x C-6), 68.61(2C)(2 x C-5), 67.65(2C) (2 x C-6), 36.60(2 x C-$C\underline{H}_3$);

$[\alpha]_D^{25}$ = +39.1 ($CHCl_3$, c = 1.0)

R_f = 0.4 (Cy/Et_2O 1:1)

HRMS (ESI) : calculated for $C_{204}H_{216}O_{44}S_2Na$ $[M+Na]^+$ 3456.3998, found 3456.3979, err. 0.6 ppm

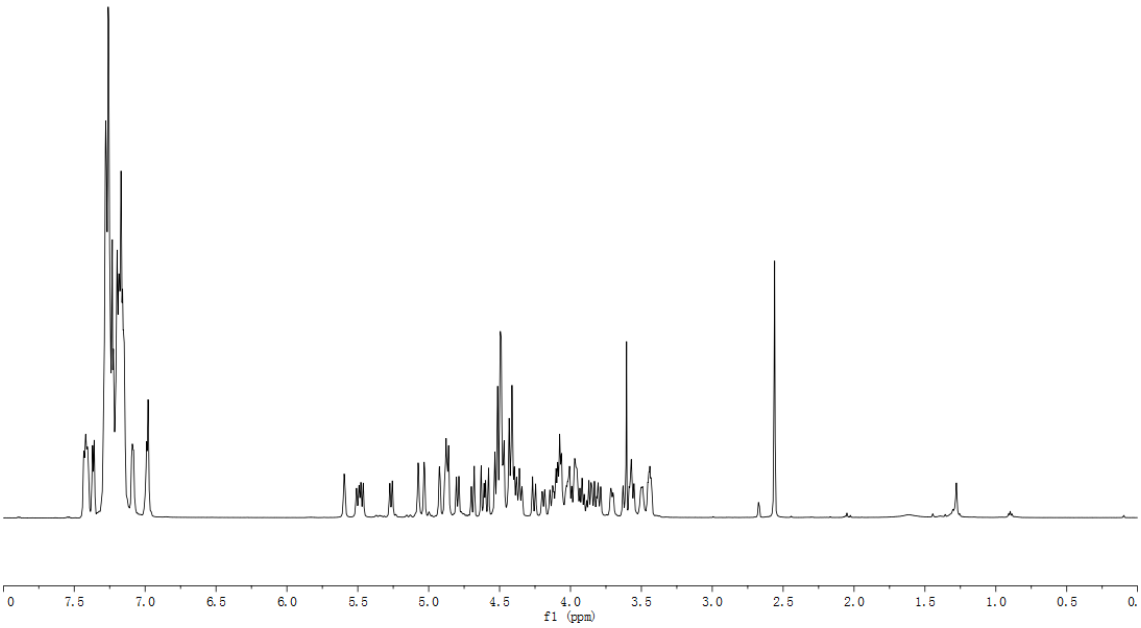

^{1}H NMR of **2γ-A,E** ($CDCl_3$, 600 MHz, 300 K)

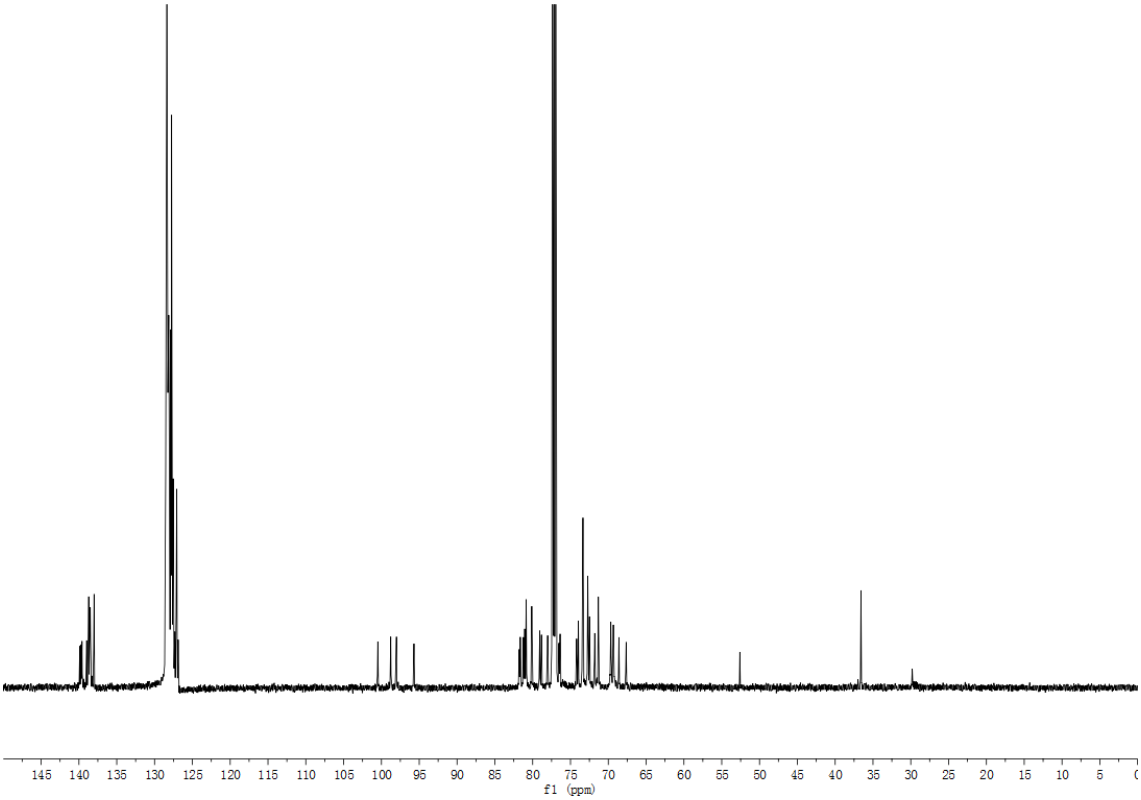

^{13}C NMR of **2γ-A,E** ($CDCl_3$, 151 MHz, 300 K)

6^{A},6^{D}-di-O-methylsulfonyl-2^{A-G},3^{A-G},6^{B},6^{C},6^{E},6^{F},6^{G},6^{H}-Docosa-O-benzyl-γ-cyclodextrin (2γ -A,D)

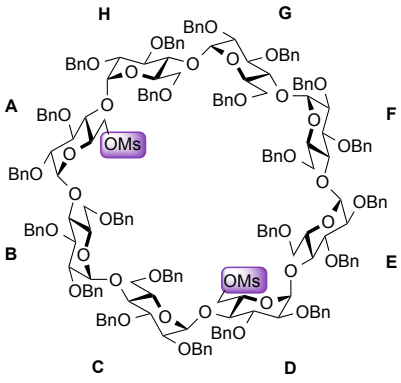

^{1}H NMR (600 MHz, $CDCl_3$): 7.35-7.08 (m, 110H, 110 x H-Ar), 5.39 (d, $^{3}J_{1,2}$ = 3.9 Hz, 1H, H-1), 5.36-5.32 (m, 2H, H-1, CHPh), 5.28-5.25 (m, 3H, 3 x CHPh), 5.17 (d, $^{3}J_{1,2}$ = 3.5 Hz, 1H, H-1), 5.14 (d, $^{3}J_{1,2}$ = 3.6 Hz, 1H, H-1), 5.11-5.01(m, 7H, 4 x H-1, 3 x CHPh) 4.85-4.73 (m, 9H, 9 x CHPh), 4.63 (d, $^{2}J_{Ph\text{-}C\underline{H}H}$ = 12.1 Hz, 1H, CHPh), 4.57-4.38 (m, 30H, 27 x CHPh, 3 x H-6), 4.26 (dd, $^{2}J_{6a,6b}$ = 10.8 Hz, $^{3}J_{5,6b}$ = 5.1 Hz, 1H, H-6), 4.10-3.68 (m, 30H, 6 x H-6, 8 x H-3, 8 x H-4, 8 x H-5), 3.58-3.47 (m, 12H, 6x H-2, 6 x H-6), 3.42 (dd, $^{3}J_{1,2}$ = 9.7Hz, $^{3}J_{2,3}$ = 3.4 Hz, 1H, H-2), 3.39 (dd, $^{3}J_{1,2}$ = 9.6Hz, $^{3}J_{2,3}$ = 3.4 Hz, 1H, H-2), 2.69 (s, 3H, $C\underline{H}_3$), 2.68 (s, 3H, $C\underline{H}_3$);

^{13}C NMR (151 MHz, $CDCl_3$): 139.55, 139.52, 139.50, 139.35, 139.33, 139.18, 138.95, 138.84, 138.60, 138.57, 138.40, 138.39, 138.38, 138.32, 138.28, 138.28, 138.26, 138.24, 138.20, 138.19, 138.17, 137.95 (22x C-Ar-quat.), 128.52-126.95 (110x C-Ar-tert.), 99.35, 99.01, 98.96, 98.63, 98.31, 98.14, 97.80, 97.77(8 x C-1), 81.25, 81.18, 81.08(2C), 81.03(2C), 80.86, 80.77, 80.33, 80.19, 79.78, 79.45, 79.21, 79.17(2C), 79.10(2C), 79.03(2C), 78.90(2C), 78.54, 78.13, 77.36 (8 x C-3, 8 x C-4, 8 x C-2), 76.37, 76.07, 76.04, 76.00, 75.81, 75.64, 75.16, 75.00, 73.52, 73.42, 73.40(2C), 73.37, 73.32, 73.27(2C), 73.16, 73.01, 72.87(2C), 72.80, 72.77(22 x Ph-$C\underline{H}_2$), 72.12, 71.77, 71.57, 71.52, 71.47(2C) (6 x C-5), 69.84 (C-6), 69.51(C-5), 69.41(C-6), 69.35(C-5), 69.30, 69.20, 69.11, 69.06, 68.94(2C) (6 x C-6), 37.00($C\underline{H}_3$), 36.92($C\underline{H}_3$) ;

$[\alpha]_D^{20}$ = +41.0 ($CHCl_3$, c = 1.0);

R_f = 0.33 (CyH/Et_2O 1:1)

HRMS (ESI) : calculated for $C_{204}H_{216}O_{44}S_2Na$ $[M+Na]^+$ 3456.3998, found 3456.4178, err. -5.2 ppm

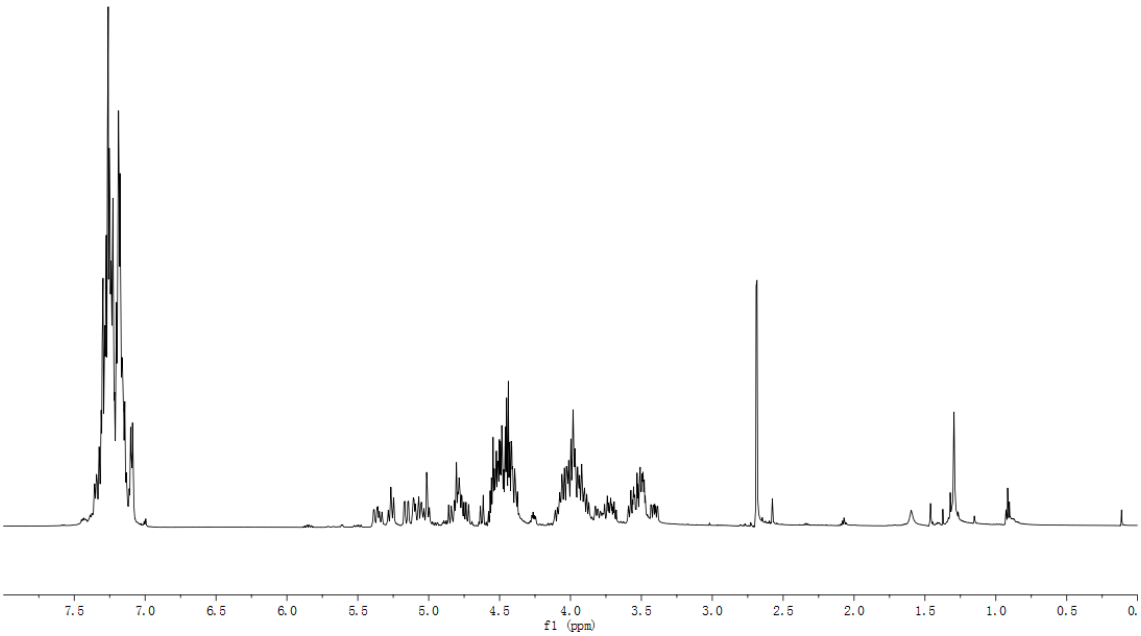

^{1}H NMR of **2γ-A,D** ($CDCl_3$, 600 MHz, 300 K)

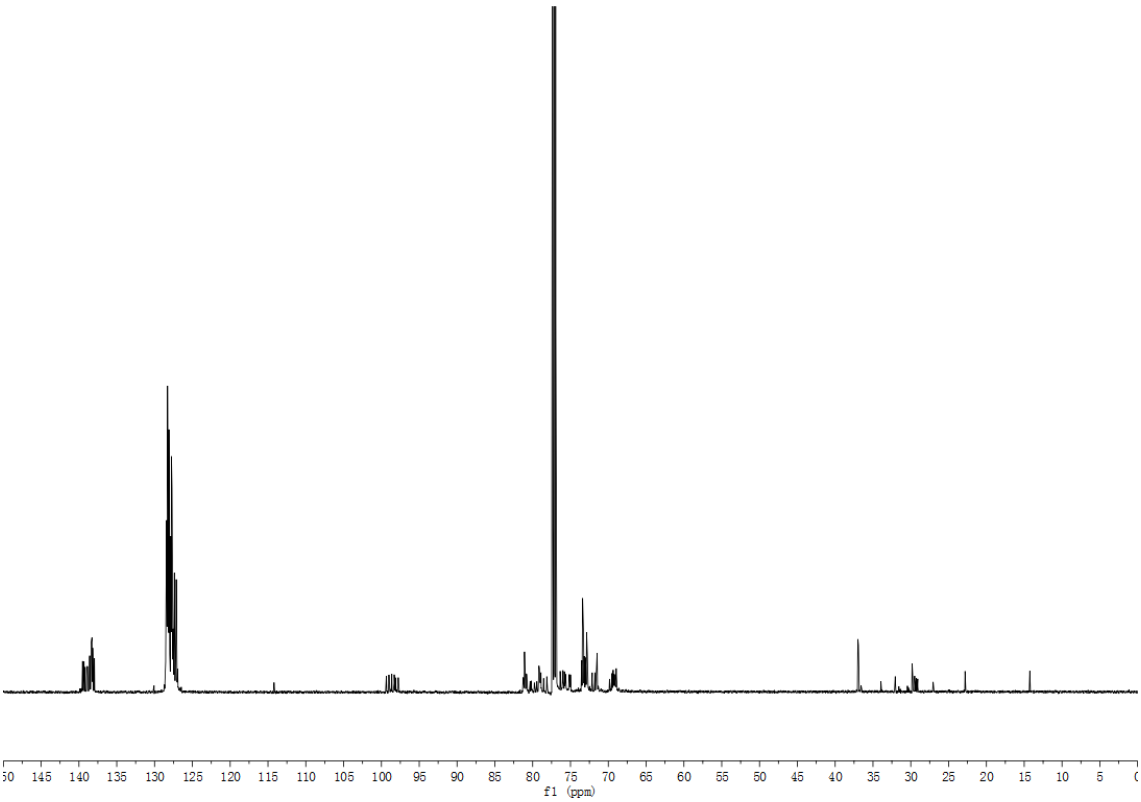

^{13}C NMR of **2γ-A,D** ($CDCl_3$, 151 MHz, 300 K)

(α-ICyD)HCl

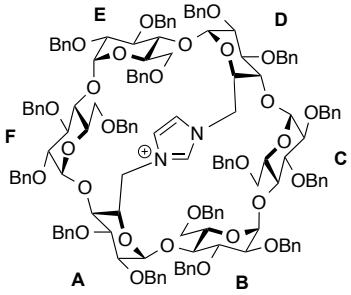

In a round-bottom flask under nitrogen, **2α** (1.13 g, 440 µmol) and imidazole (600 mg, 8.8 mmol) were dissolved in DMF (20 ml). The mixture was heated at 120 °C overnight and the reaction followed by TLC. After cooling down to r.t., the solvent was evaporated and the residue dissolved in 20 ml of dichloromethane and washed with 20 ml of aq. HCl (1M). The aqueous layer was extracted with dichloromethane (3 x 20 ml) and the combined organic layers were dried over $MgSO_4$ and concentrated to dryness. The residue was purified on silica gel chromatography (DCM/MeOH 100:1 then 100:5 then 100:10) to afford **(α-ICyD)HCl** (931 mg, 85 %) as a white foam.

The structure of the product was confirmed by comparison with the NMR spectra of the literature.[5]

^{1}H NMR (CD_3CN, 600 MHz, 300 K): δ 9.09 (s, 1H, N-CH=N), 7.43-7.06 (m, 70H, 70 x H-Ar), 6.97-6.95 (m, 4H, 4 x H-Ar), 6.89-6.84 (m, 8H, 6 x H-Ar, 2 x N-C<u>H</u>=C<u>H</u>-N), 5.66 (d, $^3J_{1,2}$ = 3.8 Hz, 2H, 2 x H-1C,F), 5.39 (d, $^2J_{Ph\text{-}C\underline{H}H}$ = 10.7 Hz, 2H, 2 x CHPh), 5.08 (d, $^2J_{Ph\text{-}C\underline{H}H}$ = 10.4 Hz, 2H, 2 x CHPh), 4.85 (d, $^2J_{Ph\text{-}C\underline{H}H}$ = 11.5 Hz, 2H, 2 x CHPh), 4.82 (d, $^3J_{1,2}$ = 3.4 Hz, 2H, 2 x H-1B,E), 4.79 (d, $^3J_{1,2}$ = 3.1 Hz, 2H, 2 x H-1A,D), 4.77 (d, $^2J_{Ph\text{-}C\underline{H}H}$ = 10.7 Hz, 2H, 2 x CHPh), 4.70 (d, $^2J_{Ph\text{-}C\underline{H}H}$ = 11.2 Hz, 2H, 2 x CHPh), 4.65-4.61 (m, 4H, 4 x CHPh), 4.56 (d, $^2J_{Ph\text{-}C\underline{H}H}$ = 12.3 Hz, 2H, 2 x CHPh), 4.54-4.45 (m, 10H, 8 x CHPh, 2 x H-6aA,D), 4.42 (d, $^2J_{Ph\text{-}C\underline{H}H}$ = 12.2 Hz, 2H, 2 x CHPh), 4.40-4.36 (m, 4H, 2 x CHPh, 2 x H-5A,D), 4.29 (d, $^2J_{Ph\text{-}C\underline{H}H}$ = 12.2 Hz, 2H, 2 x CHPh), 4.15 (dd, $^3J_{2,3}$ = 10.1 Hz, $^3J_{3,4}$ = 7.9 Hz, 2H, 2 x H-3C,F), 4.11 (d, $^2J_{Ph\text{-}C\underline{H}H}$ = 12.2 Hz, 2H, 2 x CHPh), 4.03-3.94 (m, 8H, 2 x H-3A,D, 2 x H-4C,F, 2 x H-6bA,D, 2 x H-6aC,F), 3.90 (bd, $^2J_{6a,6b}$ = 10.4 Hz, 2H, 2 x H-6bC,F), 3.88 (dd, $^3J_{2,3}$ = 9.7 Hz, $^3J_{3,4}$ = 8.7 Hz, 2H, 2 x H-3B,E), 3.73 (dd, $^3J_{4,5}$ = 9.8 Hz, $^3J_{3,4}$ = 7.8 Hz, 2H, 2 x H-4A,D), 3.73-3.70 (m, 2H, 2 x H-5C,F), 3.69 (dd, $^3J_{4,5}$ = 9.7 Hz, $^3J_{3,4}$ = 8.6 Hz, 2H, 2 x H-4B,E), 3.57 (dd, $^3J_{2,3}$ = 10.1 Hz, $^3J_{1,2}$ = 3.7 Hz, 2H, 2 x H-2C,F), 3.53 (bdd, $^3J_{4,5}$ = 9.9 Hz, $^3J_{5,6}$ = 4.8 Hz, 2H, 2 x H-5B,E), 3.46 (dd, $^3J_{2,3}$ = 9.8 Hz, $^3J_{1,2}$ = 3.0 Hz, 2H, 2 x H-2A,D), 3.38 (dd, $^3J_{2,3}$ = 9.9 Hz, $^3J_{1,2}$ = 3.3 Hz, 2H, 2 x H-2B,E), 3.25 (dd, $^2J_{6a,6b}$ = 10.8 Hz, $^3J_{5,6a}$ = 1.5 Hz, 2H, 2 x H-6aB,E), 3.11 (dd, $^2J_{6a,6b}$ = 10.8 Hz, $^3J_{5,6b}$ = 5.3 Hz, 2H, 2 x H-6bB,E) ppm.

^{13}C NMR (CD_3CN, 151 MHz, 300 K): δ 140.17 (2C), 139.98 (2C), 139.85 (2C), 139.64 (2C), 139.50 (2C), 139.15 (2C), 139.03 (2C), 138.89 (2C) (16 x C-Ar-quat.), 133.52 (N=CH-N), 129.50-127.72 (80 x C-Ar-tert.), 125.29 (2 x N-C<u>H</u>=C<u>H</u>-N), 98.99 (2 x C-1C,F), 98.63 (2 x C-1A,D), 98.10 (2 x C-1B,E), 82.34 (2 x C-4B,E, 2 x C-4C,F), 81.82 (2 x C-3A,D), 81.36 (2 x C-3B,E, 2 x C-3C,F), 80.47 (2 x C-2A,D), 80.19 (2 x C-2B,E), 78.27 (2 x C-2C,F), 77.27 (2 x Ph-<u>C</u>H$_2$) , 77.11 (2 x C-4A,D), 76.52 (2C), 74.85 (2C), 74.61 (2C) (6 x Ph-<u>C</u>H$_2$), 74.43 (2 x C-5C,F), 74.11 (2C), 73.98 (2C), 73.79 (2C), 73.19 (2C) (8 x Ph-<u>C</u>H$_2$), 73.03 (2 x C-5B,E), 71.27 (2 x C-5A,D), 71.24 (2 x C-6C,F), 69.23 (2 x C-6B,E), 53.91 (2 x C-6A,D) ppm.

R_f = 0.35 (CH_2Cl_2/MeOH 90:10)

HRMS (ESI) : calculated for $C_{151}H_{157}N_2O_{28}^+$ $[M]^+$ 2446.0917, found 2446.0831.

(β-ICyD)HCl

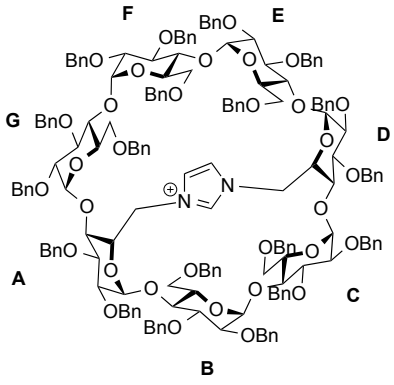

A mixture of compound **2β** (300 mg, 0.1 mmol) and imidazole (136 mg, 2 mmol) was dissolved in anhydrous DMF under a N_2 atmosphere. The reaction mixture was stirred at 120°C overnight. Then HCl solution (1 M) was added and the aqueous layer was extracted with DCM 3 times. The combined organic layers were dried over $MgSO_4$ filtered, and concentrated *in vacuo*. Silica gel chromatography of the residue (DCM/MeOH 95:5) afforded the perbenzylated imidazolium compound **(β-ICyD)HCl** (240 mg, 70 %).

^{1}H NMR (CD_3CN, 600 MHz): δ 7.36-6.84 (m, 97H, 95 × H-Ar, 2 × N-C<u>H</u>=C), 5.79 (bd, ^2J = 3.92 Hz, 2H, 2 × H-1), 5.38 (d, $^2J_{Ph\text{-}C\underline{H}H}$ = 11.33 Hz, 1H, CHPh), 5.27 (d, $^2J_{Ph\text{-}C\underline{H}H}$ = 11.17 Hz, 1H, CHPh), 5.19 (d, $^2J_{Ph\text{-}C\underline{H}H}$ = 10.50 Hz, 1H, CHPh), 5.06 (d, $^2J_{Ph\text{-}C\underline{H}H}$ = 10.63 Hz, 1H, CHPh), 4.98 (d, $^3J_{1,2}$ = 3.25 Hz, 1H, H-1), 4.89 (d, $^3J_{1,2}$ =3.88 Hz, 1H, H-1), 4.82-4.80 (m, 3H, CHPh, 2 × H-1), 4.76-4.70 (m, 5H, 4 × CHPh, H-1), 4.66(d, $^2J_{Ph\text{-}C\underline{H}H}$ = 10.92 Hz, 1H, CHPh), 4.61-4.30 (m, 31H, H-5, H-3, 2 × H-6, 27 × CHPh), 4.12-4.06 (m, 4H, 2× H-6, H-3, CHPh), 4.00-3.48(m, 28H, 6 × H-6, 4 × H-2, 5 × H-3, 7 × H-4, 6 × H-5), 3.43-3.38 (m, 2H, H-6, H-2), 3.31 (t, $^3J_{1,2}$ = $^3J_{2,3}$ = 2.36 Hz, 1H, H-2), 3.29 (t, $^3J_{1,2}$ = $^3J_{2,3}$ = 2.83, 1H, H-2), 3.20 (d, $^2J_{6a,6b}$ = 11.25 Hz, 1H, H-6), 3.10 (d, $^2J_{6a,6b}$ = 10.65 Hz, 1H, H-6), 2.84 (dd, $^2J_{6a,6b}$ = 10.65 Hz, $^3J_{5,6b}$ = 4.81 Hz, 1H, H-6) ppm.

^{13}C NMR (CD_3CN, 151MHz): δ140.69, 140.58, 140.56, 140.30, 140.08, 139.81, 139.73, 139.68, 139.65, 139.63 (2C), 139.56, 139.48, 139.26, 139.21, 138.98 (3C), 138.82 (19 × C-Ar-quat.), 129.53-128.05 (m, 95 × C-Ar-tert.), 124.98, 124.56 (2 × N-C<u>H</u>=C<u>H</u>-N), 100.56, 100.13, 99.28, 98.35, 97.28, 97.16, 96.68(7 × C-1), 83.00 (C-4), 82.56, 82.52(2 × C-3), 82.03, 81.91(2 × C-4), 81.57, 81.54, 81.43(3 × C-3), 81.14, 81.12, 81.11, 81.05(C-4, 2 × C-2, C-3), 80.50, 80.42, 80.28 (2C) (C-4, 2 × C-2, C-3), 79.94 (C-2), 78.72 (C-2), 78.31 (C-2), 77.22, 77.18, 76.80, 76.48, 76.10, 76.09, 75.16, 75.14, 75.02 (9 × Ph-<u>C</u>H$_2$), 74.19 (C-4), 74.15, 74.09, 73.99 (3 × Ph-<u>C</u>H$_2$), 74.05 (C-5), 73.94, 73.91 (2 × Ph-<u>C</u>H$_2$), 73.88 (C-4), 73.85, 73.83, 73.72, 73.49 (4 × Ph-<u>C</u>H$_2$), 73.35 (C-5), 73.19 (Ph-<u>C</u>H$_2$), 72.77, 72.73 (2C) (3 × C-5), 72.06 (C-5), 70.54, 70.46, 70.26 (3 × C-6), 70.23 (C-5), 69.12 (C-6), 68.85 (C-6), 53.28 (C-6), 52.86 (C-6) ppm.

$[\alpha]_D^{20}$= +49.5 ($CHCl_3$, *c* = 0.1)

R_f = 0.31 (DCM/MeOH 95:5)

HRMS (ESI) : calculated for $C_{178}H_{185}N_2NaO_{33}^{2+}$ $[M+Na]^{2+}$ 1450.6373, found 1450.6434 err. 4.2 ppm

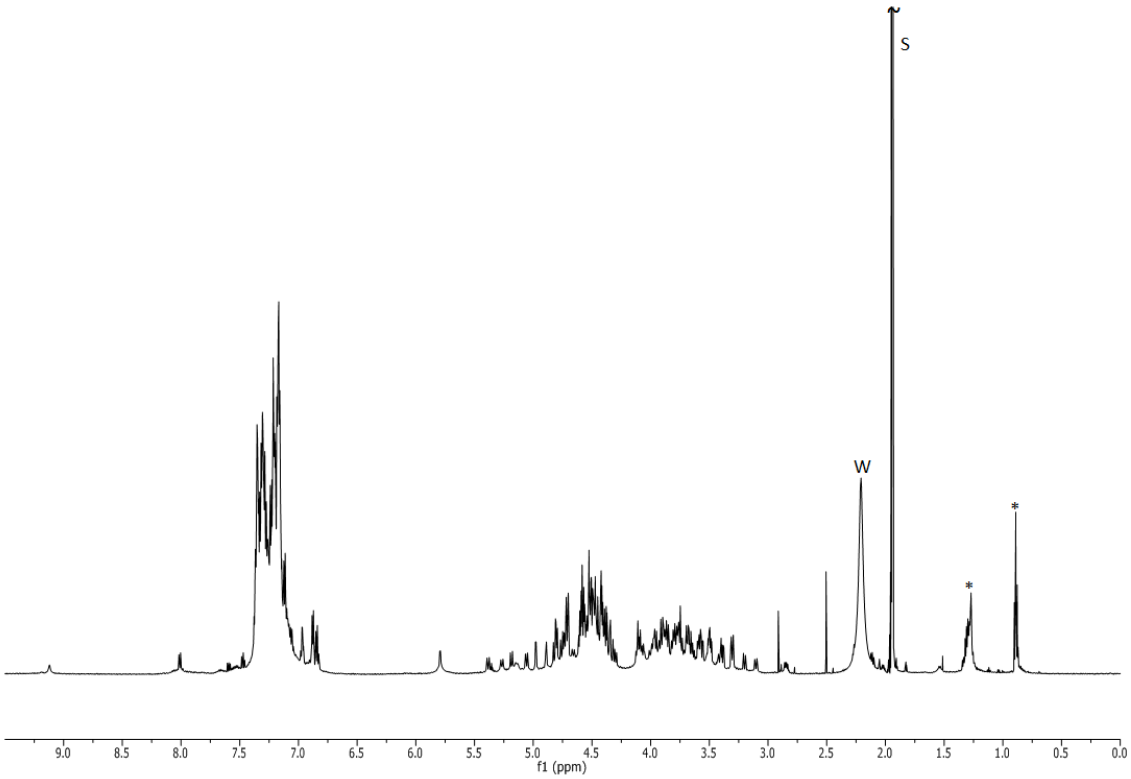

^{1}H NMR of **(β-ICyD)HCl** (CD_3CN, 600 MHz, 300 K – w= water, s= solvent, *=grease)

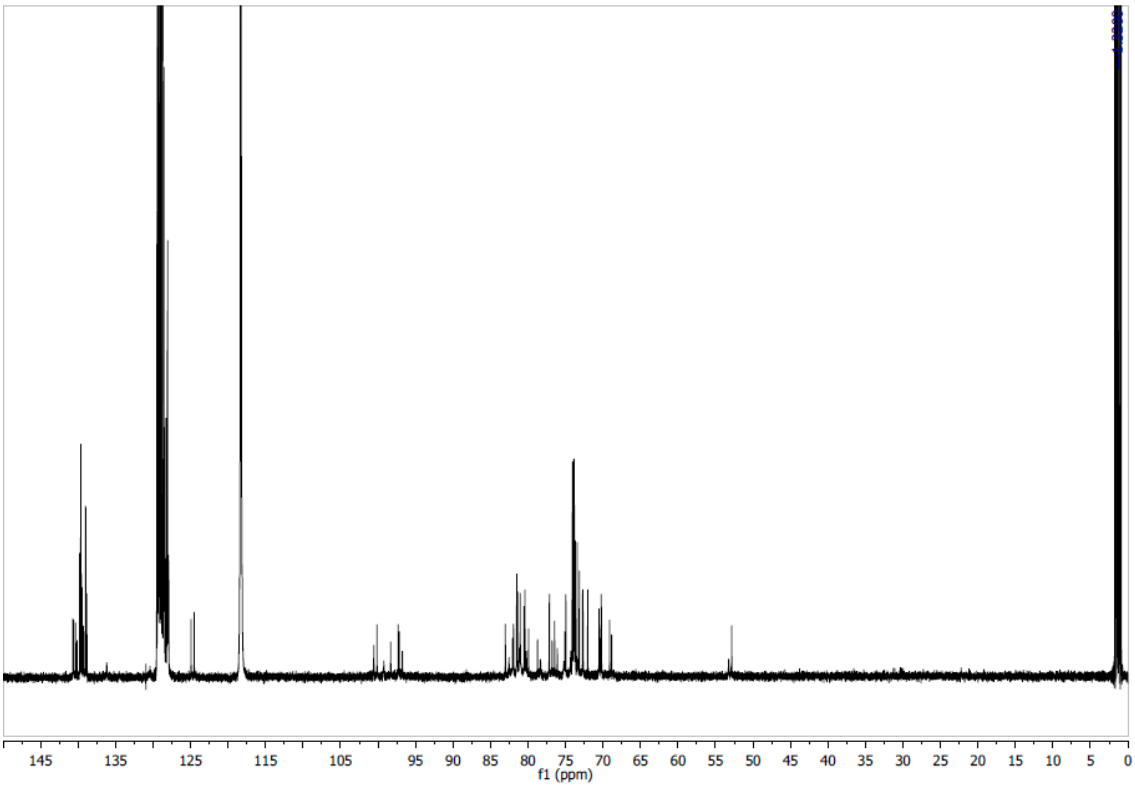

^{13}C NMR of **(β-ICyD)HCl** (CD_3CN, 151 MHz, 300 K)

(γ-A,E-ICyD)HCl

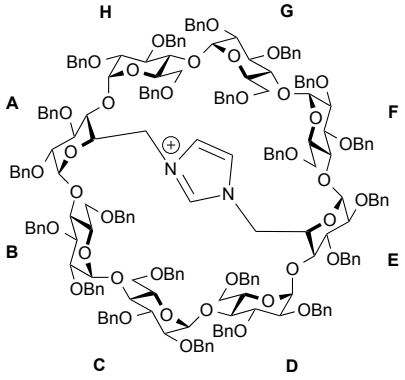

A mixture of compound **2γ-A,E** (43 mg, 0.012 mmol) and imidazole (26 mg, 0.38 mmol) was dissolved in anhydrous DMF under a N_2 atmosphere. The reaction mixture was stirred at 120°C overnight. Then HCl solution (1 M) was added and the aqueous layer was extracted with DCM 3 times. The combined organic layers were dried over $MgSO_4$ filtered, and concentrated in *vacuo*. Silica gel chromatography of the residue (DCM/MeOH 95:5) afforded the perbenzylated imidazolium bridged **(γ-A,E-ICyD)HCl** (24 mg, 58 %).

^{1}H NMR (600 MHz, CD_3CN): 7.41-7.12 (m, 104H, 104 x H-Ar), 6.96 (t, *J* = 7.6 Hz, 4H, 4 x H-Ar), 6.81(t, *J* = 7.4 Hz,2H, 2 x H-Ar), 6.69 (s, 2H, 2 x H-imidazolium), 5.61 (d, $^3J_{1,2}$ = 3.5 Hz, 2H, 2 x H-1D,H), 5.23 (d, $^2J_{Ph\text{-}C\underline{H}H}$ = 10.7 Hz, 2H, 2 x CHPh), 5.19 (d, $^2J_{Ph\text{-}C\underline{H}H}$ = 10.0 Hz, 2H, 2 x CHPh), 4.93 (d, $^3J_{1,2}$ = 3.0 Hz, 2H, 2 x H-1A,E), 4.92 (d, $^3J_{1,2}$ = 3.5 Hz, 2H, 2 x H-1C,G), 4.90 (d, $^3J_{1,2}$ = 3.3 Hz, 2H, 2 x H-1B,F), 4.85 (d, $^2J_{Ph\text{-}C\underline{H}H}$ = 10.9 Hz, 2H, 2 x CHPh), 4.75 (d, $^2J_{Ph\text{-}C\underline{H}H}$ = 10.7 Hz, 2H, 2 x CHPh), 4.71 (d, $^2J_{Ph\text{-}C\underline{H}H}$ = 11.1 Hz, 2H, 2 x CHPh), 4.66 (d, $^2J_{Ph\text{-}C\underline{H}H}$ = 11.3 Hz, 2H, 2 x CHPh), 4.59-4.37 (m, 32H, 32 x CHPh), 4.31 (dd, $^2J_{6a,6b}$ = 13.8 Hz, $^3J_{5,6b}$ = 2.4 Hz, 2H, 2 × H-6bA,E), 4.10 (dd, $^2J_{6a,6b}$ = 11.3 Hz, $^3J_{5,6b}$ = 4.7 Hz, 2H, 2 × H-6aH,D), 3.97-3.72 (m, 26H, H-6aC, H-6aG, H-6bD, H-6bH, H-6bC, H-6bG, H-6aA, H-6aE, 4 x H-5A,E,D,H, 8 x H-3A,B,C,D,E,F,G,H, 6 x H-4B,C,D,F,G,H), 3.64-3.58 (m, 6H, 2 x H-4A,E, 2 x H-5C,G, 2 x H-2D,H), 3.48-3.47 (m, 4H, 2 x H-2A,E, 2 x H-5B,F), 3.39 (ddd, 4H, 4 x H-2B,C,F,G), 3.11 (dd, $^2J_{6a,6b}$ = 11.2 Hz, $^3J_{5,6b}$ = 1.6 Hz, 2H, 2 × H-6aB,F), 3.11 (dd, $^2J_{6a,6b}$ = 11.0 Hz, $^3J_{5,6b}$ = 3.0 Hz, 2H, 2 × H-6bB,F).

^{13}C NMR (151 MHz, CD_3CN): 140.34(2C), 140.31(2C), 140.18(2C), 139.59(2C), 139.57(4C), 139.56(2C), 139.44(2C), 139.42(2C), 139.01(2C), 138.87(2C), (22x C-Ar-quat.), 129.50-128.05 (110x C-Ar-tert.), 125.08 (2 x N-C=C-N), 99.64(2C), 99.42(2C), 99.05(2C), 94.60(2C) (8 x C-1A,B,C,D,E,F,G,H), 82.38(2 x C-4C,G), 81.79(2 x C-3C,G), 81.28(2 x C-3A,E), 81.22(2 x C-3B,F), 81.02(2C), 80.77(4C)(6 x C-4A,B,D,E,F,H), 80.56(4C)(2 x C-3D,H, 2 x C-2A,E), 80.33(2C), 80.19(2C)(4 x C-2B,C,F,G), 78.27(2 x C-2D,H), 77.46(2C), 77.12(2C), 76.16(2C), 74.76(2C), 73.99(2C), 73.97(2C), 73.93(2C), 73.81 (2C), 73.51(2C), 73.41(2C), 73.22(2C)(22 x Ph-$\underline{C}H_2$), 72.74(2 x C-5D,H), 72.36(2C), 72.31(2C)(4 x C-5A,B,E,F), 71.20(2 x C-5C,G), 70.66(2 x C-6C,G), 70.26(2 x C-6D,H), 69.01(2 x C-6B,F), 52.10(2 x C-6A,E); **$[\alpha]_D^{20}$** = + 35.1 ($CHCl_3$, c = 1.0)

R_f = 0.29 (DCM/MeOH 95:5)

HRMS (ESI) : calculated for $C_{205}H_{213}O_{38}N_2$ $[M]^+$ 3310.4791, found 3310.4963, err. -5.2 ppm

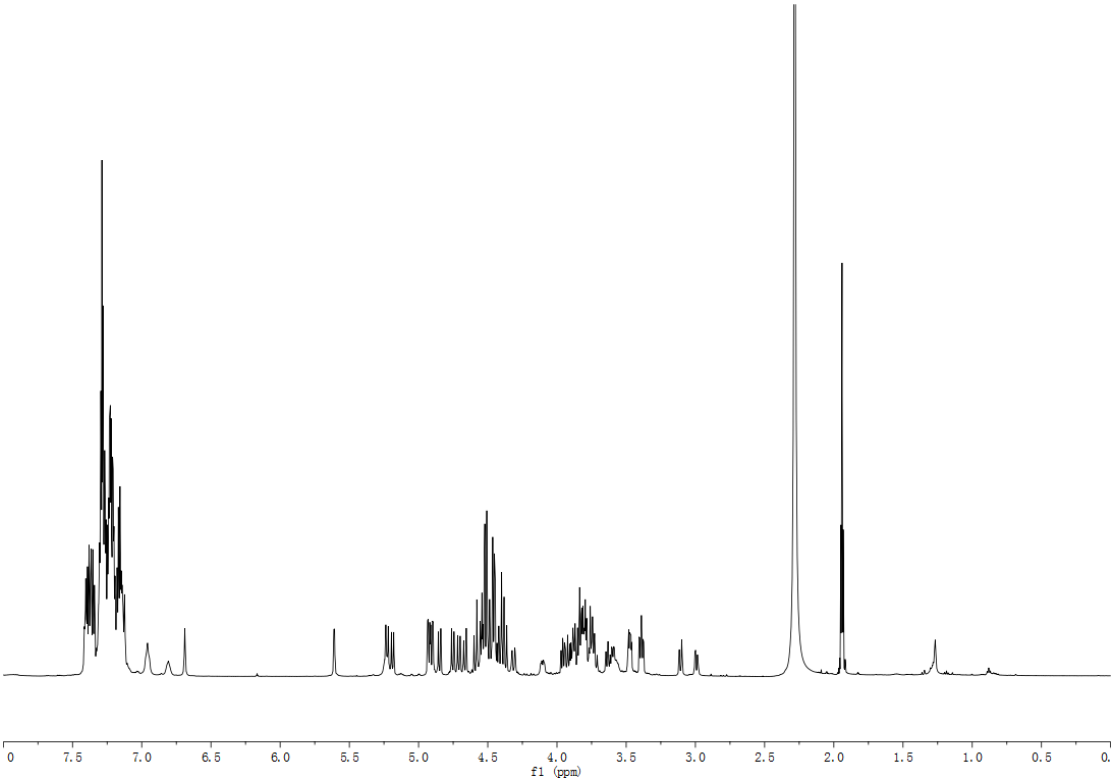

^{1}H NMR of **(γ-A,E-ICyD)HCl** (CD_3CN, 600 MHz, 300K)

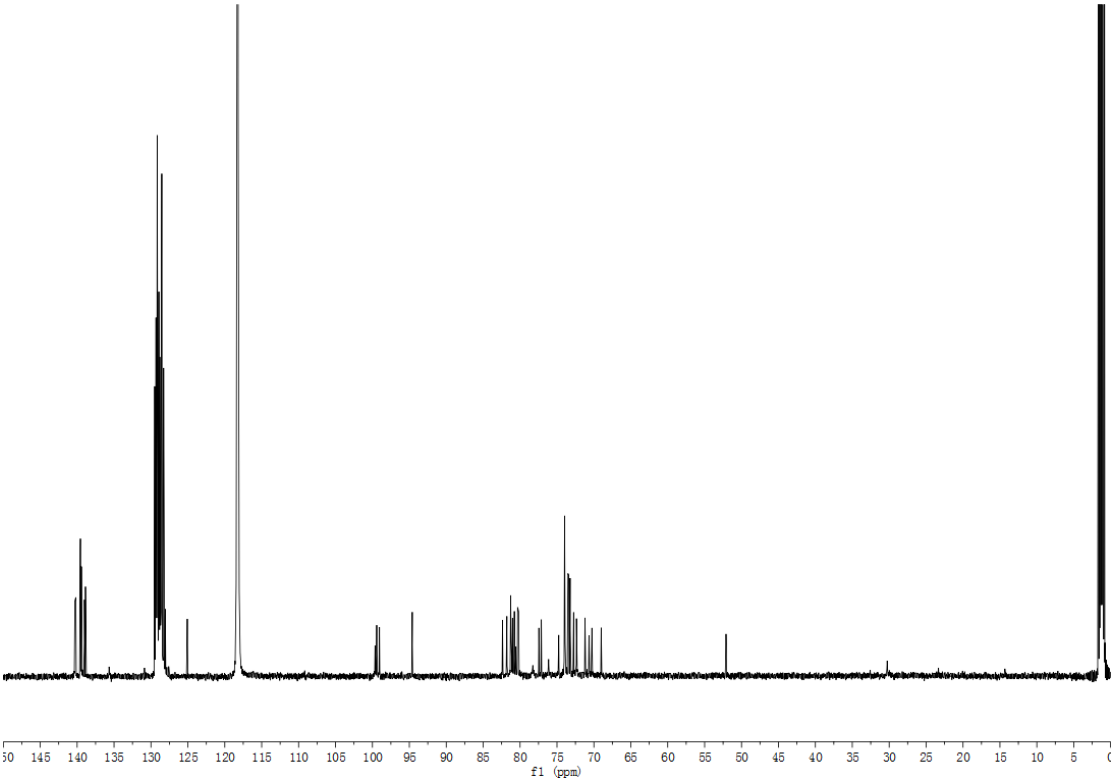

^{13}C NMR of **(γ-A,E-ICyD)HCl** (CD_3CN, 151 MHz, 300 K)

(γ-A,D-ICyD)HCl

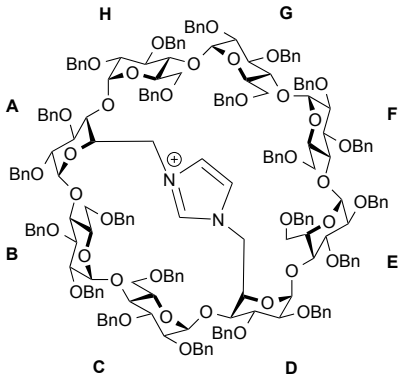

A mixture of compound **2γ-A,D** (34 mg, 0.01 mmol) and imidazole (60 mg, 0.9 mmol) was dissolved in anhydrous DMF under a N_2 atmosphere. The reaction mixture was stirred at 120°C overnight. Then HCl solution (1 M) was added and the aqueous layer was extracted with DCM 3 times. The combined organic layers were dried over $MgSO_4$ filtered, and concentrated in *vacuo*. Silica gel chromatography of the residue (DCM/MeOH 95:5) afforded the 6A,6D imidazolium bridged **(γ-A,D-ICyD)HCl** (13.4 mg, 40 %).

^{1}H NMR (600 MHz, CD_3CN): 8.73 (s, 1H, N-C<u>H</u>=N), 7.41-7.09 (m, 110H, 110 x H-Ar), 6.95 (s, 1H, H-Im), 6.84 (s, 1H, H-Im), 5.60 (d, $^3J_{1,2}$ = 3.9 Hz, 1H, H-1C), 5.32 (d, $^3J_{1,2}$ = 3.8 Hz, 1H, H-1H), 5.25-5.18 (m, 2H, 2 x CHPh), 5.14-5.12 (m, 3H, 2 x H-1D,G, CHPh), 5.04 (d, $^3J_{1,2}$ = 3.5 Hz, 1H, H-1E), 4.99 (d, $^3J_{1,2}$ = 3.5 Hz, 1H, H-1F), 4.94-4.83 (m, 3H, H-1B, 2 x CHPh), 4.77 (d, $^3J_{1,2}$ = 3.4 Hz, 1H, H-1A), 4.76-4.37 (m, 38H, H-6aA, H-6aD, H-5A, 35 x CHPh), 4.30-4.27 (m, 2H, 2 x CHPh), 4.23 (d, $^2J_{\text{Ph-C}\underline{\text{H}}\text{H}}$ = 11.2 Hz, 1H, CHPh), 4.17 (d, $^2J_{\text{Ph-C}\underline{\text{H}}\text{H}}$ = 11.6 Hz, 1H, CHPh), 4.13-3.48 (m, 37H, 8 x H-3A,B,C,D,E,F,G,H, 8 x H-4 A,B,C,D,E,F,G,H, 7 x H-5 B,C,D,E,F,G,H, 2 x H-2A,H, H-6bA, H-6aC, H-6bC, H-6bD, H-6aE, H-6bE, H-6aF, H-6bF, H-6aG, H-6bG, H-6aH, H-6bH), 3.45-3.42 (m, 3H, 3 x H-2C,D,G), 3.40-3.38 (m, 2H, 2 x H-2B,E), 3.34 (dd, $^3J_{1,2}$ =9.4 Hz, $^3J_{2,3}$ = 3.6 Hz, 1H, H-2F), 3.28 (br d, 1H, H-6aB), 3.03 (dd, $^2J_{6a,6b}$ = 10.5 Hz, $^3J_{5,6b}$ = 6.3Hz, 1H, H-6bB);

^{13}C NMR (151 MHz, CD_3CN): 140.44, 140.42, 140.38, 140.35, 139.62, 139.59, 139.57, 139.52, 139.47, 139.42, 139.36, 139.35, 139.29, 139.28, 139.21, 139.18, 139.09, 139.07, 139.04, 138.90, 138.89, 138.88(22x C-Ar-quat.), 129.52-127.61 (110x C-Ar-tert.), 125.05, 124.48(C-Im), 99.82, 99.39, 98.62, 98.35(2C), 98.08, 97.45, 95.49(8 x C-1), 81.90, 81.83, 81.46, 81.23(2C), 81.05, 80.87, 80.78, 80.70(2C), 80.68(2C),80.40, 80.39, 80.24, 80.22, 80.13, 80.00, 79.91, 79.84, 79.62(7 x C-3A,B,C,D,E,F,G, 8 x C-4A,B,C,D,E,F,G,H, 6 x C-2A,B,C,E,F,G,) 78.95(C-3H), 78.10(C-2D), 77.48, 77.15, 77.05(3 x Ph-<u>C</u>H_2), 76.61 (C-2H), 76.40, 76.10, 76.02, 75.94, 75.71, 74.78, 74.20(2C), (8 x Ph-<u>C</u>H_2), 74.06 (C-5), 73.96, 73.91(2C), 73.84(3C) (6 x Ph-<u>C</u>H_2), 73.72 (C-5), 73.70, 73.51, 73.44(3 x Ph-<u>C</u>H_2), 73.27(C-5), 73.23, 73.01(2 x Ph-<u>C</u>H_2), 72.69, 72.66, 72.61(3 x C-5), 71.16(C-5D), 70.95(C-6), 70.49(C-5A), 70.26, 70.11, 69.98, 69.47, 69.43(5 x C-6), 53.40(C-6D), 52.63(C-6A);

$[\alpha]_D^{20}$ = + 38.5 ($CHCl_3$, c = 1.0)

R_f = 0.29 (DCM/MeOH 95:5)

HRMS (ESI): calculated for $C_{205}H_{213}O_{38}N_2$ $[M]^+$ 3310.4791, found 3310.4647, err. 4.3 ppm

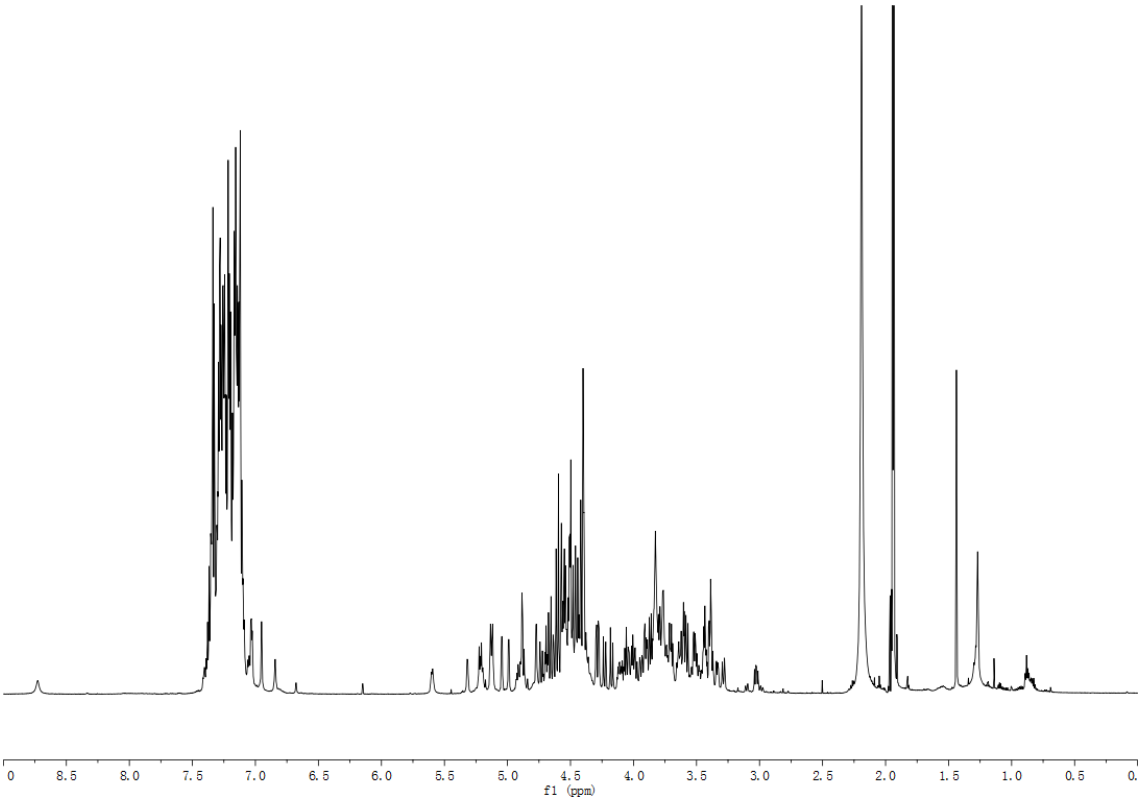

^{1}H NMR of **(γ-A,D-ICyD)HCl** (CD_3CN, 600 MHz, 300 K)

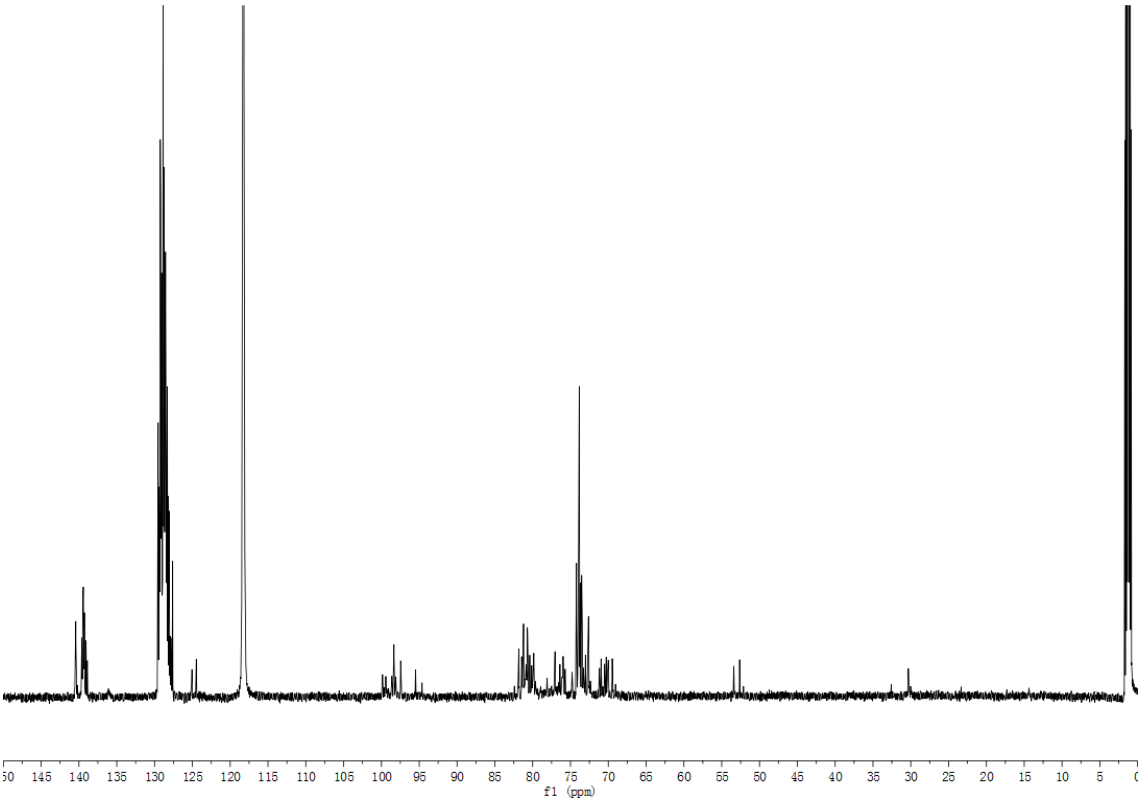

^{13}C NMR of **(γ-A,D-ICyD)HCl** (CD_3CN, 151 MHz, 300 K)

(α-ICyD)AgCl

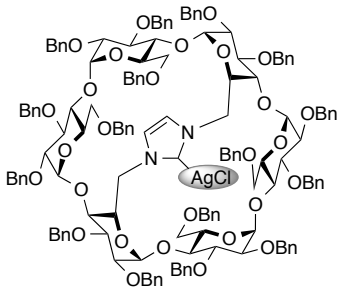

In a round-bottom flask under nitrogen, imidazolium **(α-ICyD)HCl** (570 mg, 230 µmol) and silver oxide (532 mg, 2.30 mmol) were dissolved in 29 ml of acetonitrile. The black suspension was vigorously stirred at R.T. overnight, then filtrated on celite, rinsed with acetonitrile and concentrated *in vacuo*. The residue was purified on silica gel chromatography (Cyclohexane/AcOEt 4:1 then 3:1) to afford complex **(α-ICyD)AgCl** (536 mg, 90 %) as a white foam.

The structure of the product was confirmed by comparison with the NMR spectra of the literature.[5]

^{1}H NMR : ($CDCl_3$, 600 MHz, 300 K): δ 7.38-6.97 (m, 74H, 74 x H-Ar), 6.84 (t, $^{3}J_{o,m}$ = $^{3}J_{m,p}$ = 7.7 Hz, 4H, 4 x H-*m*-Ar), 6.74 (t, $^{3}J_{m,p}$ = 7.4 Hz, 2H, 2 x H-*p*-Ar), 6.14 (bs, 2H, 2 x N-CH=CH-N), 5.71 (d, $^{3}J_{1,2}$ = 3.7 Hz, 2H, 2 x H-1C,F), 5.65-5.60 (m, 4H, 2 x CHPh, 2 x H-5A,D), 5.37 (d, $^{2}J_{Ph\text{-}CHH}$ = 10.8 Hz, 2H, 2 x CHPh), 5.15-5.11 (m, 4H, 4 x CHPh), 4.98 (dd, $^{3}J_{2,3}$ = 10.2 Hz, $^{3}J_{3,4}$ = 7.7 Hz, 2H, 2 x H-3C,F), 4.87 (d, $^{2}J_{Ph\text{-}CHH}$ = 11.3 Hz, 2H, 2 x CHPh), 4.65 (d, $^{2}J_{Ph\text{-}CHH}$ = 11.5 Hz, 2H, 2 x CHPh), 4.63 (d, $^{3}J_{1,2}$ = 3.5 Hz, 2H, 2 x H-1B,E), 4.60-4.42 (m, 16H, 12 x CHPh, 2 x H-1A,D, 2 x H-6aA,D), 4.29-4.25 (m, 6H, 4 x CHPh, 2 x H-3B,E), 4.22 (d, $^{2}J_{Ph\text{-}CHH}$ = 12.7 Hz, 2H, 2 x CHPh), 4.16 (dd, $^{3}J_{2,3}$ = 9.7 Hz, $^{3}J_{3,4}$ = 7.7 Hz, 2H, 2 x H-3A,D), 3.98 (d, $^{2}J_{Ph\text{-}CHH}$ = 12.2 Hz, 2H, 2 x CHPh), 3.95 (d, $^{2}J_{6a,6b}$ = 10.3 Hz, 2H, 2 x H-6aC,F), 3.88-3.80 (m, 6H, 2 x H-4C,F, 2 x H-5B,E, 2 x H-5C,F), 3.76 (dd, $^{2}J_{6a,6b}$ = 10.5 Hz, $^{3}J_{5,6b}$ = 5.2 Hz, 2H, 2 x H-6bC,F), 3.71 (t, $^{3}J_{3,4}$ = $^{3}J_{4,5}$ = 9.2 Hz, 2H, 2 x H-4B,E), 3.60 (dd, $^{3}J_{2,3}$ = 10.2 Hz, $^{3}J_{1,2}$ = 3.8 Hz, 2H, 2 x H-2C,F), 3.55 (dd, $^{3}J_{4,5}$ = 10.1 Hz, $^{3}J_{3,4}$ = 7.7 Hz, 2H, 2 x H-4A,D), 3.42-3.37 (m, 4H, 2 x H-2B,E, 2 x H-6bA,D), 3.27 (dd, $^{3}J_{2,3}$ = 9.8 Hz, $^{3}J_{1,2}$ = 3.0 Hz, 2H, 2 x H-2A,D), 3.04 (dd, $^{2}J_{6a,6b}$ = 10.9, $^{3}J_{5,6a}$ = 3.3 Hz, 2H, 2 x H-6aB,E), 2.76 (dd, $^{3}J_{6a,6b}$ = 11.0 Hz, $^{3}J_{5,6b}$ = 1.7 Hz, 2H, 2 x H-6bB,E) ppm.

^{13}C NMR ($CDCl_3$, 151 MHz, 300 K): δ 176.56 (C-Ag), 140.27 (2C), 139.92 (2C), 139.60 (2C), 139.10 (2C), 139.03 (2C), 138.81 (2C), 138.33 (2C), 138.01 (2C) (16 x C-Ar$^{quat.}$), 128.72-126.71 (80 x C-Ar$^{tert.}$), 122.11 (d, $^{3}J_{C,Ag}$ = 6.7 Hz, 2 x N-CH=CH=N), 98.66 (2 x C-1C,F), 98.09 (2C), 98.06 (2C) (2 x C-1A,D, 2 x C-1B,E), 82.60 (2 x C-4C,F), 81.51 (2 x C-3A,D), 81.36 (2 x C-4B,E), 80.26 (2 x C-3B,E), 80.12 (2 x C-2A,D), 79.64 (2 x C-3C,F), 79.11 (2 x C-2B,E), 79.98 (2 x C-2C,F), 76.76 (2 x C-4A,D), 76.64 (2C), 76.39 (2C), 74.16 (2C) (6 x Ph-CH_2), 73.78 (2 x C-5C,F), 73.47 (2C), 73.31 (2C), 73.23 (2C), 72.80 (2C), 72.35 (2C) (10 x Ph-CH_2), 71.92 (2 x C-5B,E), 71.14 (2 x C-6C,F), 70.80 (2 x C-5A,D), 67.82 (2 x C-6B,E), 54.36 (2 x C-6A,D) ppm.

Note : the chemical shift of the carbene carbon was deduced from cross-correlation but could not be observed directly due to coupling with ^{107}Ag and ^{109}Ag.

R_f = 0.21 (Cyclohexane/Ethyl Acetate 4:1)

HRMS (ESI) : calculated for $C_{151}H_{156}AgClN_2Na_2O_{28}^{2+}$ $[M+2Na]^{2+}$ 1316.4684, found 1316.4674.

(β-ICyD)AgCl

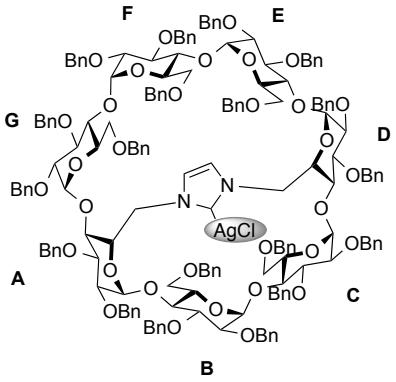

A mixture of perbenzylated imidazolium **(β-ICyD)HCl** (2.25 g, 0.77 mmol) and silver oxide (1.8 g, 7.7mmol) was dissolved in anhydrous acetonitrile (50 ml) under a N_2 atmosphere. The reaction mixture was stirred at r.t. overnight. Then the silver oxide was filtered on a celite pad and the residue was washed with acetonitrile, and the solvents were evaporated. Silica gel chromatography of the residue (CyH/ EtOAc: 4:1) gave the silver complex **(β-ICyD)AgCl** (2.0 g, 85 %).

^{1}H NMR ($CDCl_3$, 600 MHz): δ 7.48-6.88 (m, 95H, 95 × H-Ar), 6.21 (s, 1H, N-C<u>H</u>=C), 5.93 (s, 1H, N-C<u>H</u>=C), 5.88 (d, $^3J_{1,2}$ = 3.61 Hz, 1H, H-1G), 5.86 (d, $^3J_{1,2}$ = 3.61 Hz, 1H, H-1C), 5.78 (d, $^2J_{\text{Ph-C}\underline{\text{H}}\text{H}}$ = 11.78 Hz, 1H, CHPh), 5.54 (m, 1H, H-5A), 5.45 (d, $^2J_{\text{Ph-C}\underline{\text{H}}\text{H}}$ = 10,82 Hz, 1H, CHPh), 5.42 (d, $^2J_{\text{Ph-C}\underline{\text{H}}\text{H}}$ = 11.18 Hz, 1H, CHPh), 5.35-5.33 (m, 2H, 2 × CHPh), 5.25 (d, $^2J_{\text{Ph-C}\underline{\text{H}}\text{H}}$ = 12.38 Hz, 1H, CHPh), 5.02 (d, $^2J_{\text{Ph-C}\underline{\text{H}}\text{H}}$ = 11.31 Hz, 1H, CHPh), 5.00 (d, $^2J_{\text{Ph-C}\underline{\text{H}}\text{H}}$ = 5.66 Hz, 1H, CHPh), 4.98-4.94 (m, 3H, 3 × CHPh), 4.83 (d, $^2J_{6a,6b}$ = 5.42 Hz, 1H, H-6aD), 4.82 (d, $^3J_{1,2}$ = 3.57 Hz, 1H, H-1D), 4.69 (m, 2H, 2 × H-1E,F), 4.60 (m, 2H, H-1A, H-3C), 4.58 (d, $^3J_{1,2}$ = 3.04 Hz, 1H, H-1B), 4.56 (d, $^2J_{\text{Ph-C}\underline{\text{H}}\text{H}}$ = 11.79 Hz, 1H, CHPh), 4.51-4.38 (m, 23H, H-3B, H-6bA, H-5D, 20 ×CHPh), 4.36 (d, $^2J_{\text{Ph-C}\underline{\text{H}}\text{H}}$ = 10.48 Hz, 1H, CHPh), 4.31 (d, $^2J_{\text{Ph-C}\underline{\text{H}}\text{H}}$ = 3.87 Hz, 1H, CHPh), 4.29 (d, $^2J_{\text{Ph-C}\underline{\text{H}}\text{H}}$ = 2.80 Hz, 1H, CHPh), 4.27 (d, $^2J_{\text{Ph-C}\underline{\text{H}}\text{H}}$ = 2.56 Hz, 1H, CHPh), 4.25-4.20 (m, 3H, 2 × H-3E,G, CHPh), 4.14-3.94 (m, 7H, H-6aG, H-5B, H-4C, 3 × H-3A,D,F, CHPh), 3.87-3.63 (m, 11H, H-6aF, H-6bF, H-6aC, H-6bC, H-6bG, 4 × H-4G,E,B,A, 2 × H-5C,G), 3.57-3.51 (m, 5H, 2 × H-2C,G, 2 × H-4F,D, H-5F), 3.43-3.37 (m, 3H, H-6aA, H-6bD, H-6aE), 3.35-3.30 (m, 5H, 5 × H-2E,F,D,B,A), 3.25(m, 1H, H-5E), 2.96(d, $^2J_{6a,6b}$ = 10.78 Hz, 1H, H-6bE), 2.78 (d, $^2J_{6a,6b}$ = 10.72 Hz, 1H, H-6aB), 2.71(dd, $^2J_{6a,6b}$ = 10.95 Hz, $^3J_{5,6b}$ = 3.10 Hz, 1H, H-6bB);

^{13}C NMR ($CDCl_3$, 151 MHz): δ140.58, 140.21, 140.10, 140.05, 139.57, 139.18, 139.04, 138.98, 138.91, 138.79, 138.72(2C), 138.60, 138.58, 138.52, 138.26, 138.19, 138.08, 137.68, (19 × C-Ar.quat.), 128.57-126.56 (m, 95 × C-Ar-tert.), 122.71, 121.26 (2 × N-<u>C</u>H=<u>C</u>H-N), 100.91, 99.69, 98.61, 98.23, 97.52, 97.27, 96.96(7 × C-1A,B,C,D,E,F,G), 83.32 (C-4F), 82.26 (C-3A), 82.07, 81.94 (2 × C-4C,G), 81.29 (C-3D), 80.73, 80.46 (2 × C-4B,E), 80.44 (C-2B), 80.25 (C-3F), 80.17 (C-2A), 80.14, 79.97, 79.89, 79.54 (4 × C-3B,C,E,G), 78.89, 78.66, 77.99, 77.89, 77.39 (5 × C-2C,D,E,F,G), 76.94 (Ph-<u>C</u>H$_2$), 76.85 (Ph-<u>C</u>H$_2$), 76.39 (2 × Ph-<u>C</u>H$_2$), 76.20 (Ph-<u>C</u>H$_2$), 74.37 (C-4A), 74.36 (Ph-<u>C</u>H$_2$), 74.28 (Ph-<u>C</u>H$_2$), 73.86 (C-5C), 73.81, 73.73, 73.57, 73.49, 73.44(5 × Ph-<u>C</u>H$_2$), 73.43 (C-4D), 73.28 (Ph-<u>C</u>H$_2$), 73.19 (C-5G), 73.18, 73.07, 72.98, 72.76, 72.70 (5 × Ph-<u>C</u>H$_2$), 72.36 (C-5F), 72.33 (Ph-<u>C</u>H$_2$), 71.89, 71.86, 71.55 (3 × C-5B,D,E), 70.56 (C-6C), 70.50 (C-5A), 70.34, 69.94, 68.21, 67.63, 55.63, 53.29 (6 × C-6A,B,D,E,F,G)

$[\alpha]_D^{20}$= +46.8 ($CHCl_3$, *c* = 0.1)

R_f = 0.21 (CyH/AcOEt 4:1)

HMRS (ESI) calculated for $C_{178}H_{184}AgN_2O_{33}^+$ $[M\text{-}Cl]^+$ 2984.1827, found 2984.1777 err. 1.7 ppm

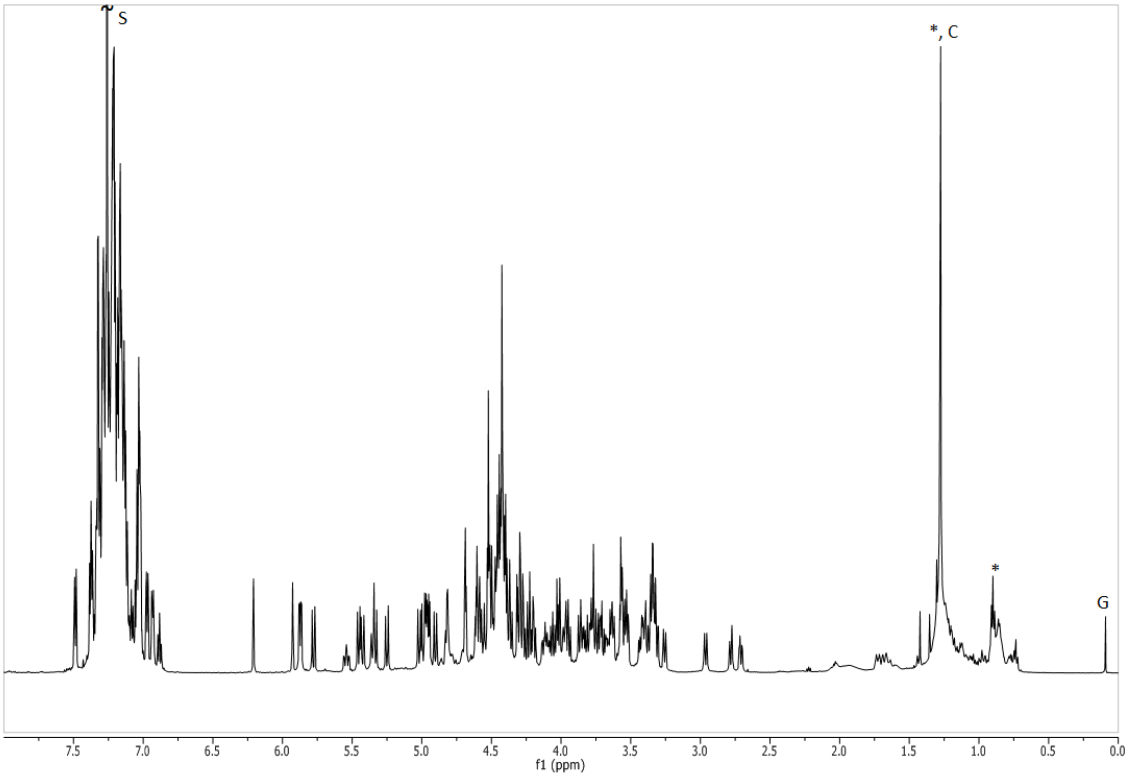

^{1}H NMR of **(β-ICyD)AgCl** ($CDCl_3$, 600 MHz, 300 K, s= solvent, G= grease, c= Cy)

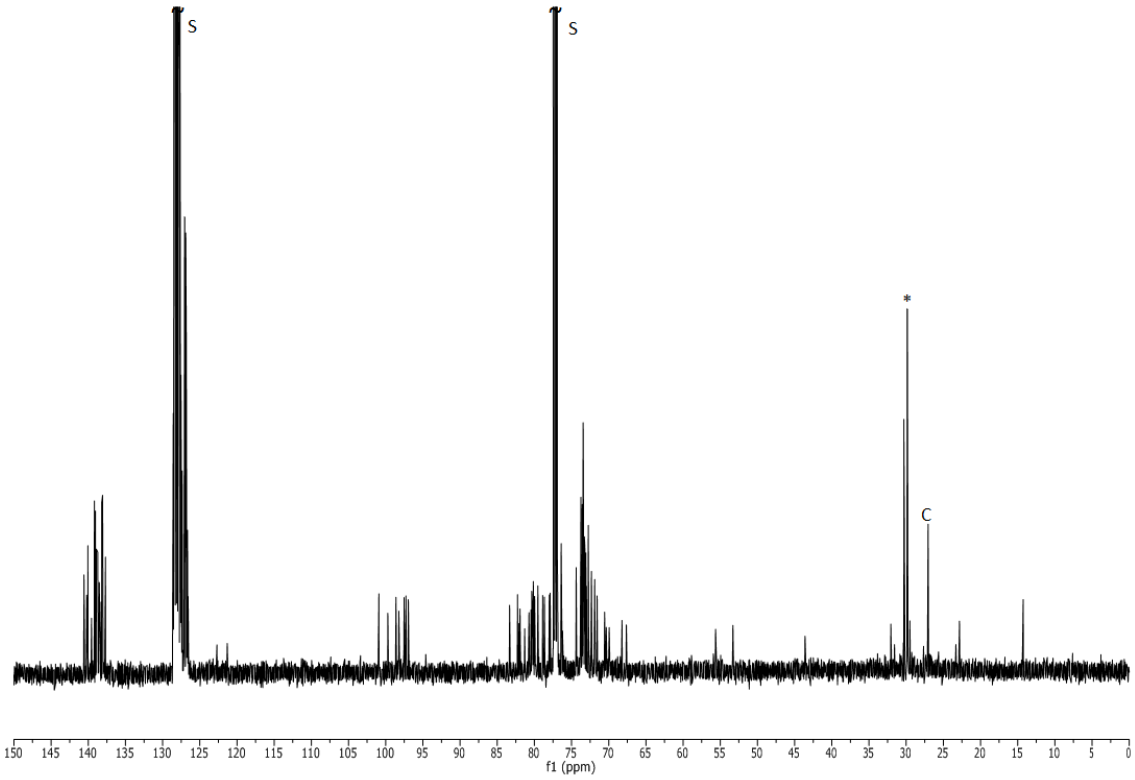

^{13}C NMR of **(β-ICyD)AgCl** ($CDCl_3$, 151 MHz, 300 K)

(γ-A,E-ICyD)AgCl

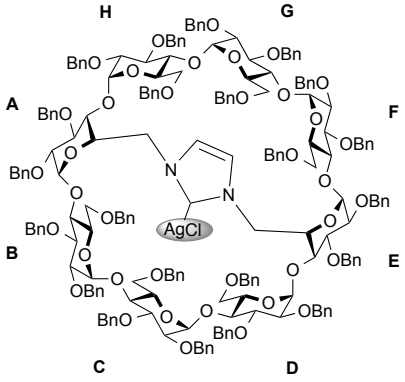

A mixture of perbenzylated imidazolium **(γ-A,E-ICyD)HCl** (142 mg, 0.042 mmol) and silver(Ⅰ) oxide (100 mg, 0.42 mmol) was dissolved in anhydrous acetonitrile under a N_2 atmosphere. The reaction mixture was stirred at r.t. overnight. Then the silver oxide was filtered on a celite pad and the residue was washed with acetonitrile, and the solvents were evaporated. Silica gel chromatography of the residue (CyH/ EtOAc: 4:1) gave the silver complex **(γ-A,E-ICyD)AgCl** as white foam (92 mg, 63 %).

^{1}H NMR (600 MHz, CD_3CN): 7.43-7.08 (m, 104H, 104 x H-Ar), 7.03 (t, 4H, 4 x H-Ar), 6.90(t, 2H, 2 x H-Ar), 6.26(s, 2H, 2 x H-Im), 5.63 (d, $^3J_{1,2}$ = 3.6 Hz, 2H, 2 x H-1D,H), 5.25-5.24 (m, 4H, 4 x CHPh), 4.95(d, $^3J_{1,2}$ = 3.2 Hz, 2H, 2 x H-1A,E), 4.88 (d, $^3J_{1,2}$ = 3.3 Hz, 2H, 2 x H-1B,F), 4.86 (d, $^3J_{1,2}$ = 3.5 Hz, 2H, 2 x H-1C,G), 3.47 (d, $^2J_{\text{Ph-C}\underline{\text{H}}\text{H}}$ = 10.8 Hz, 2H, 2 x CHPh), 4.73-4.71 (m, 4H, 4 x CHPh), 4.59-4.34 (m, 36H, 34 x CHPh, H-6aA, H-6aE), 4.18-4.16 (m, 4H, 2 x H-3C, G, 2 x H-5A,E), 4.09-4.07 (m, 4H, 2 x H-3D,H, H-6bD, H-6bH), 3.99-3.95 (m, 4H, 4 x H-3A,B,E,F), 3.87-3.53 (m, 24H, 6 x H-5B,C,D,F,G,H, 8 x H-4A,B,C,D,E,F,G,H, 2 x H-2D,H, H-6bA, H-6bE, H-6aC, H-6aG, H-6bC, H-6bG, H-6aD, H-6aH), 3.44 (dd, $^3J_{1,2}$ =9.7 Hz, $^3J_{2,3}$ = 3.0 Hz, 2H, 2 x H-2A,E), 3.35 (dd, $^3J_{1,2}$ =9.9 Hz, $^3J_{2,3}$ = 3.3 Hz, 2H, 2 x H-2B,F), 3.29 (dd, $^3J_{1,2}$ =10.0 Hz, $^3J_{2,3}$ = 3.4 Hz, 2H, 2 x H-2C,G), 3.18 (br d, ^2J= 11.1 Hz, 2H, H-6aB, H-6aF), 3.01 (d, ^2J= 11.2 Hz, 2H, H-6bB, H-6bF);

^{13}C NMR (151 MHz, CD_3CN): 141.23(2C), 141.08(2C), 140.64(2C), 139.93(2C), 139.84(2C), 139.74(2C), 139.71(2C), 139.70(2C), 139.68(2C), 139.35(2C), 139.22(2C) (22x C-Ar-quat.),129.46-127.71 (110x C-Ar-tert.), 99.95(2C), 99.31(2C), 98.82(2C), 94.93(2C) (8 x C-1), 82.69 (2C), 82.05 (2C)(4 x C-4A,C,E,G), 81.95(2C)(2 x C-4D,H), 81.88(2C)(2 x C-3A,E), 81.34(4C)(2 x C-3C,G, 2 x C-2A,E), 81.19(2C), 81.00(2C)(2 x C-3B,F, 2 x C-4B,F), 80.65(4C)(2 x C-3D,H, 2 x C-2B,F), 80.19(2C)(2 x C-2C,G), 78.04 (2C) (2 x C-2D,H), 77.32(2C), 76.99(2C), 74.82(2C), 73.92(2C), 73.90(2C), 73.84(2C), 73.78(2C), 73.68(2C) (16 x Ph-$\underline{\text{C}}\text{H}_2$), 73.58 (2C)(2 x C-5A,E), 73.43(2C), 73.30(2C), 73.20(2C) (6 x Ph-$\underline{\text{C}}\text{H}_2$), 72.93(2C)(2 x C-5C,G), 72.39(2C) (2 x C-5B,F), 71.41(2C)(2 x C-5D,H), 70.96(2C), 70.79(2C)(4 x C-6C,D,G,H), 69.33(2C) (2 x C-6B,F), 54.27(2C)(2 x C-6A,E);

C-Ag cannot be observed.

$[\alpha]_D^{20}$ = +31.3 ($CHCl_3$, c = 1.0)

R_f = 0.43 (CyH/EtOAc 3:1)

HRMS (ESI): calculated for $C_{205}H_{212}O_{38}N_2Ag$ $[M]^+$ 3416.3764, found 3416.3886, err. -3.6 ppm.

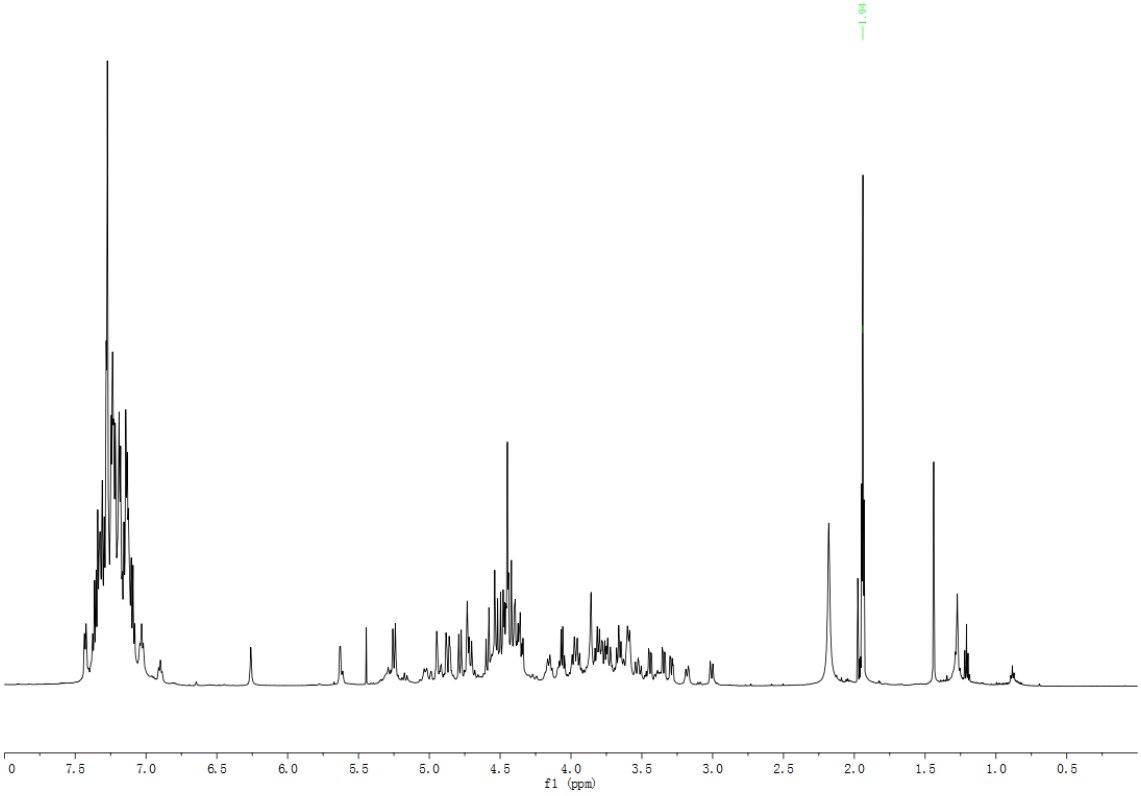

^{1}H NMR of **(γ-A,E-ICyD)AgCl** (CD_3CN, 600 MHz, 300 K)

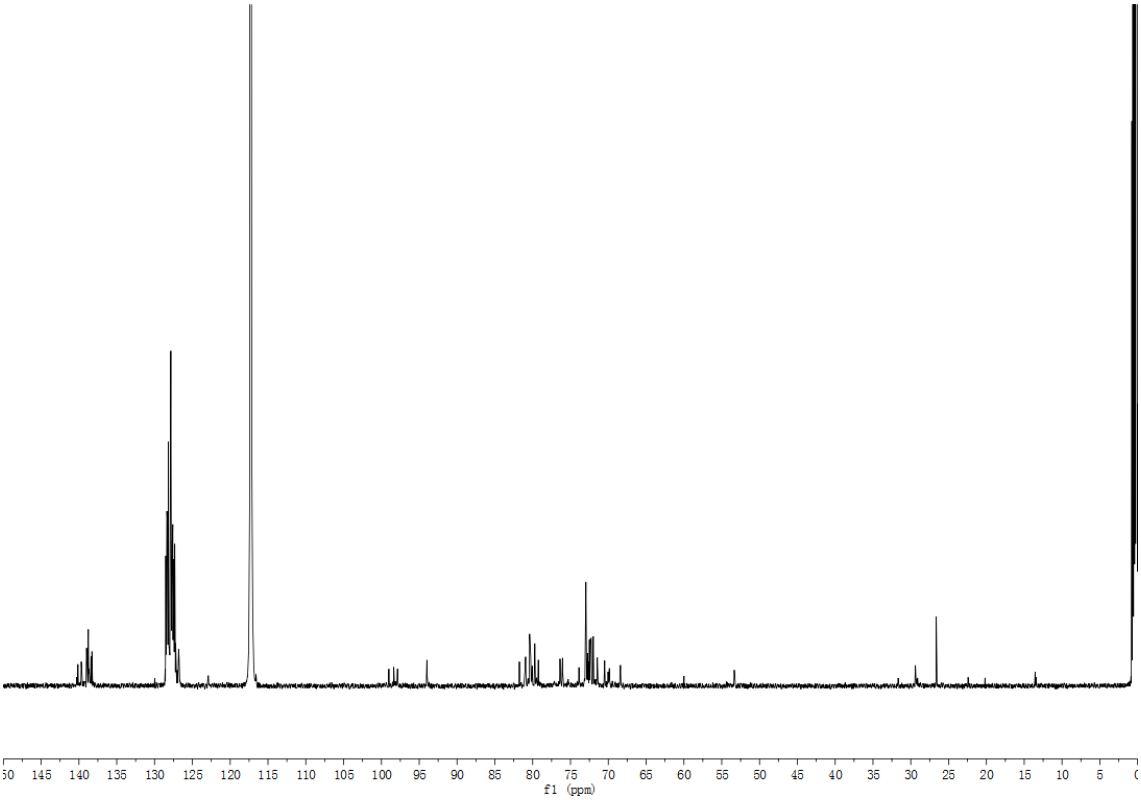

^{13}C NMR of **(γ-A,E-ICyD)AgCl** (CD_3CN, 151 MHz, 300 K)

(γ-A,D-ICyD)AgCl

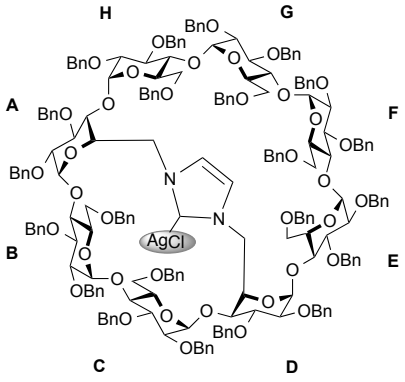

A mixture of perbenzylated imidazolium **(γ-A,D-ICyD)HCl** (26 mg, 0.007 mmol) and silver(Ⅰ) oxide (36 mg, 0.155 mmol) was dissolved in anhydrous acetonitrile under a N_2 atmosphere. The reaction mixture was stirred at r.t. overnight. Then the silver oxide was filtered on a celite pad and the residue was washed with acetonitrile, and the solvents were evaporated. Silica gel chromatography of the residue (CyH/EtOAc: 4:1) gave the silver complex **(γ-A,D-ICyD)AgCl** as white foam (17 mg, 65 %).

^{1}H NMR (600 MHz, CD_3CN): 7.46-6.94 (m, 112H, 110 x H-Ar, 2 x H-Im), 5.77 (d, $^3J_{1,2}$ = 3.38 Hz, 1H, H-1C), 5.38-5.36 (m, 2H, H-1H, CHPh), 5.18-5.14 (m, 2H, CHPh, H-1D), 5.06 (d, $^3J_{1,2}$ = 3.5 Hz, 1H, H-1G), 5.02 (d, $^3J_{1,2}$ = 3.7 Hz, 1H, H-1E), 4.98 (d, $^3J_{1,2}$ = 3.6 Hz, 1H, H-1F), 4.96 (d, $^2J_{\text{Ph-C}\underline{\text{H}}\text{H}}$ = 11.7 Hz, 1H, CHPh), 4.84-4.82 (m, 3H, CHPh, 2 x H-1A,B), 4.69-4.20 (m, 47H, H-6aA, H-6aD, 3 x H-5 A,D,H, 2 x H-3 B,C, 40 x CHPh), 4.01-3.58 (m, 29H, H-2H, 8 x H-4 A,B,C,D,E,F,G,H, 6 x H-3 A,D,E,F,G,H, 5 x H-5 B,C,E,F,G, H-6bA, H-6bD, H-6aC, H-6bC, H-6aF, H-6aG, H-6bG, H-aH, H-6bH), 3.52-3.43(m, 5H, H-6bF, H-6bE, 3 x H-2A,D,G), 3.36-3.35 (m, 2H, 2 x H-2C,E), 3.32-3.26 (m, 3H, 2 x H-2B,F, H-6aE), 3.05(br d, 1H, H-6aB), 2.90(br d, 1H, H-6bB);

^{13}C NMR (151 MHz, CD_3CN): 140.90, 140.77, 140.71(2C), 140.21, 139.82, 139.78, 139.71, 139.70, 139.67, 139.64, 139.63, 139.61, 139.54, 139.49, 139.45, 139.44, 139.38, 139.31, 139.23, 139.17, 138.14 (22x C-Ar-quat.), 129.42-127.62 (110x C-Ar-tert.), 124.86, 118.72(C-Im), 100.59, 99.12, 99.11, 97.79, 97.75(2C), 97.47, 96.16 (8 x C-1), 83.03(C-3H), 81.96(2C), 81.36(4C), 81.00(4C), 80.73(2C), 80.47(3C)(5 x C-3A,B,C,E,G, 4 x C-4B, D,E,F, 6 x C-2A,B,C,D,E,F,G), 79.64(2C, C-4C, C-2F), 79.09(C-3D), 78.65(C-2C), 78.29(C-3F), 77.35(Ph-$\underline{\text{C}}\text{H}_2$), 76.52(2C, 2 x C-4G,H), 76.46(Ph-$\underline{\text{C}}\text{H}_2$), 75.87 (Ph-$\underline{\text{C}}\text{H}_2$), 75.65(Ph-$\underline{\text{C}}\text{H}_2$), 75.52(C-4A), 74.93, 74.25, 74.23, 74.15, 74.08, 74.02, 73.81(2C), 73.78(2C), 73.77(3C), 73.74, 73.69(2C), 73.64, 73.55(18 x Ph-$\underline{\text{C}}\text{H}_2$), 73.50(2C, 2 x C-5), 73.46, 73.36, 73.26, 72.92, 72.69, 72.39, 72.31, 72.18(5 x C-5), 71.19, 70.75, 70.39, 69.90, 69.40, 68.90(6 x C-6B,C,E,F,G,H), 56.74(C-6D), 53.48(C-6A);

$[\alpha]_D^{20}$ = +38.5 ($CHCl_3$, c = 1.0)

R_f = 0.43 (CyH/EtOAc 3:1)

HRMS (ESI): calculated for $C_{205}H_{212}O_{38}N_2AgCl$ $[M+Na]^+$ 3474.3350, found 3474.3150, err. 5.7 ppm

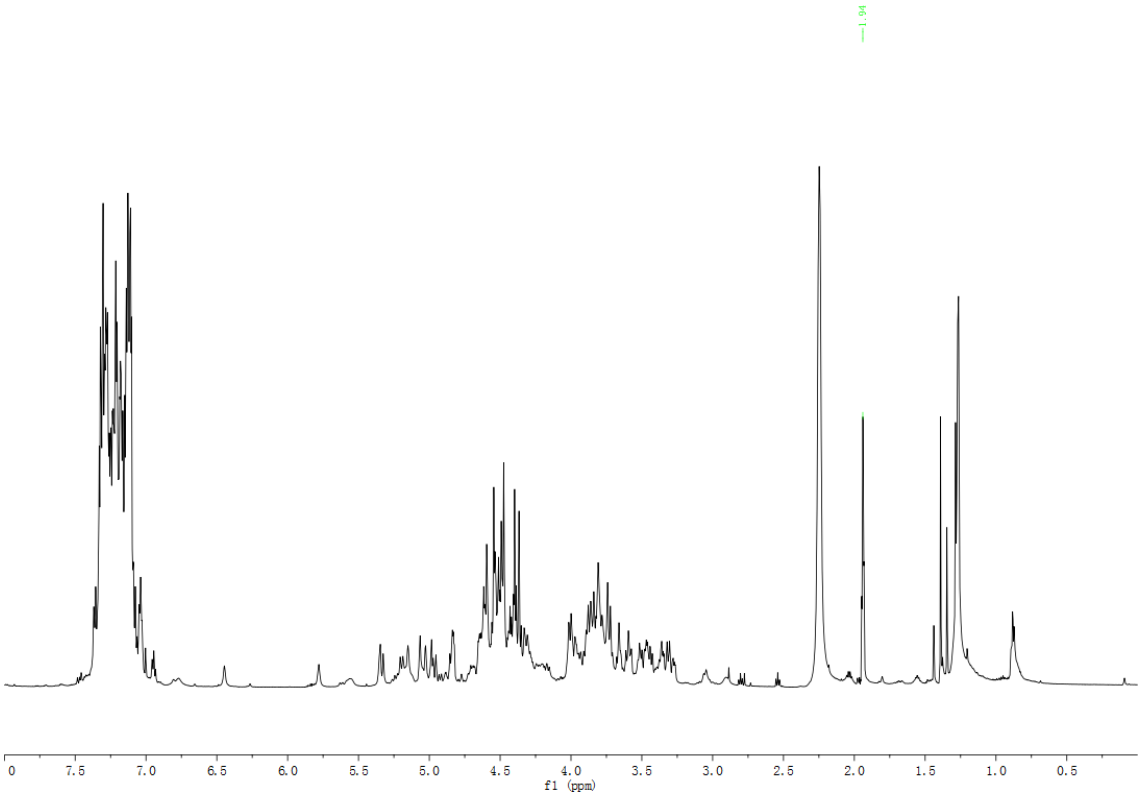

^{1}H NMR of **(γ-A,D-ICyD)AgCl** (CD_3CN, 600 MHz, 300 K)

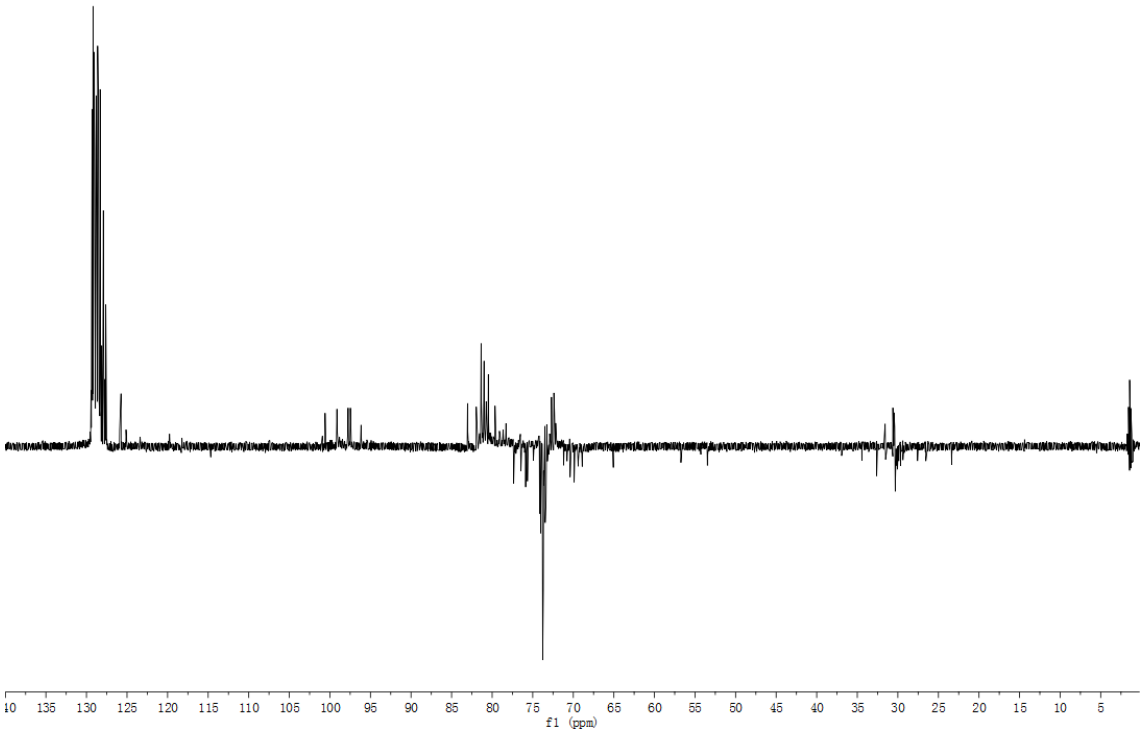

^{13}C-dept NMR of **(γ-A,D-ICyD)AgCl** (CD_3CN, 151 MHz, 300 K)

(α-ICyD)CuCl

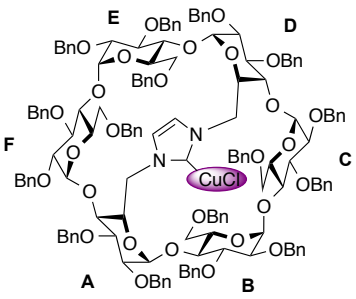

Method A: Under argon, **(α-ICyD)HCl** (625 mg, 252 µmol) and copper(I) oxide (35 mg, 246 mmol) were dissolved in 6 ml of 1,4-dioxane previously degassed by bubbling argon for 15 minutes. The mixture was heated at 100 °C overnight, cooled down to R. T., filtered on Celite, the cake washed with CH_2Cl_2 and the solvent evaporated *in vacuo*. The residue was purified on silica gel chromatography (Cyclohexane/Ethyl Acetate 7:3) to afford copper complex **(α-ICyD)CuCl** (512 mg, 80 %) as a white foam.

Method B: Copper(I) chloride (excess) and silver complex **(α-ICyD)AgCl** (50 mg, 19.3 µmol) were stirred in dichloromethane (2 ml) under argon. After 72 h the suspension was filtrated on Celite®, washed with dichloromethane and concentrated to afford the copper complex **(α-ICyD)CuCl** (50 mg, quant.).

The structure of the product was confirmed by comparison with the NMR spectra of the literature. [5]

^{1}H NMR ($CDCl_3$, 600 MHz, 300 K) : δ 7.39-6.97 (m, 74H, 74 x H-Ar), 6.82 (t, $^3J_{o,m}$ = $^3J_{m,p}$ = 7.7 Hz, 4H, 4 x H-*o*-Ar), 6.69 (t, $^3J_{m,p}$ = 7.4 Hz, 2H, 2 x H-*p*-Ar), 6.16 (s, 2H, 2 x N-CH=CH-N), 5.79-5.74 (m, 4H, 2 x H-1C,F, 2 x H-5A,D), 5.63 (d, $^2J_{Ph\text{-}CHH}$ = 10.4 Hz, 2H, 2 x CHPh), 5.23 (d, $^2J_{Ph\text{-}CHH}$ = 10.5 Hz, 2H, 2 x CHPh), 5.16-5.11 (m, 4H, 4 x CHPh), 5.07 (dd, $^3J_{2,3}$ = 10.3 Hz, $^3J_{3,4}$ = 7.9 Hz, 2H, 2 x H-3C,F), 4.85 (d, $^2J_{Ph\text{-}CHH}$ = 11.3 Hz, 2H, 2 x CHPh), 4.69 (d, $^3J_{1,2}$ = 3.5 Hz, 2H, 2 x H-1B,E), 4.68-4.57 (m, 8H, 8 x CHPh), 4.56 (d, $^3J_{2,3}$ = 3.0 Hz, 2H, 2 x H-1A,D), 4.55-4.45(m, 8H, 6 x CHPh, 2 x H-6aA,D), 4.30-4.24 (m, 6H, 4 x CHPh, 2 x H-3B,E), 4.23 (d, $^3J_{1,2}$ = 12.7 Hz, 2H, 2 x CHPh), 4.20 (dd, $^3J_{2,3}$ = 9.8 Hz, $^3J_{3,4}$ = 7.7 Hz, 2H, 2 x H-3A,D), 4.02-3.87 (m, 10H, 2 x CHPh, 2 x H-4C,F, 2 x H-5B,E, 2 x H-5C,F, 2 x H-6aC,F), 3.83 (dd, $^2J_{6a,6b}$ = 10.5 Hz, $^3J_{5,6b}$ = 4.9 Hz, 2H, 2 x H-6bC,F), 3.73 (t, $^3J_{3,4}$ = $^3J_{4,5}$ = 9.2 Hz, 2H, 2 x H-4B,E), 3.61 (dd, $^3J_{2,3}$ = 10.3 Hz, $^3J_{1,2}$ = 3.7 Hz, 2H, 2 x H-2C,F), 3.56 (dd, $^3J_{4,5}$ = 10.0 Hz, $^3J_{3,4}$ = 7.7 Hz, 2H, 2 x H-4A,D), 3.45 (dd, $^3J_{2,3}$ = 9.9 Hz, $^3J_{1,2}$ = 3.4 Hz, 2H, 2 x H-2B,E), 3.39 (dd, $^2J_{6a,6b}$ = 14.0 Hz, $^3J_{5,6b}$ = 10.1 Hz, 2H, 2 x H-6bA,D), 3.28 (dd, $^3J_{2,3}$ = 9.8 Hz, $^3J_{1,2}$ = 3.0 Hz, 2H, 2 x H-2A,D), 3.05 (dd, $^2J_{6a,6b}$ = 10.9 Hz, $^3J_{5,6a}$ = 3.3 Hz, 2H, 2 x H-6aB,E), 2.76 (dd, $^2J_{6a,6b}$ = 11.0 Hz, $^3J_{5,6b}$ = 1.7 Hz, 2H, 2 x H-6bB,E) ppm.

^{13}C NMR ($CDCl_3$, 151 MHz, 300 K) : δ 173.52 (C-Cu), 140.01 (2C), 139.91 (2C), 139.59 (2C), 139.18 (2C), 139.08 (2C), 138.82 (2C), 138.36 (2C), 138.06 (2C) (16 x C-Ar-quat.), 128.91-126.62 (80 x C-Ar-tert.), 121.56 (2 x N-CH=CH-N), 98.42 (2 x C-1C,F), 98.09 (2 x C-1A,D), 97.71 (2 x C-1B,E), 82.23 (2 x C-4C,F), 81.54 (2 x C-3A,D), 81.43 (2 x C-4B,E), 80.24 (2C), 80.13 (2C) (2 x C-2A,D, 2 x C-3B,E), 79.66 (2 x C-3C,F), 79.25 (2 x C-2B,E), 77.01 (2 x C-2C,F), 76.65 (2 x C-4A,D), 76.54 (2C), 76.45 (2C), 74.13 (2C) (6 x Ph-CH_2), 73.67 (2 x C-5C,F), 73.45 (2C), 73.28 (2C), 73.24 (2C), 72.59 (2C), 72.31 (2C) (10 x Ph-CH_2), 71.85 (2 x C-5B,E), 71.50 (2 x C-5A,D), 71.05 (2 x C-6C,F), 67.91 (2 x C-6B,E), 54.15 (2 x C-6A,D) ppm.

R_f = 0.21 (Cyclohexane/Ethyl Acetate 4:1)

HRMS (ESI) : calculated for $C_{151}H_{156}CuN_2O_{28}^+$ $[M\text{-}Cl]^+$ 2508.0135, found 2508.0152.

(β-ICyD)CuCl

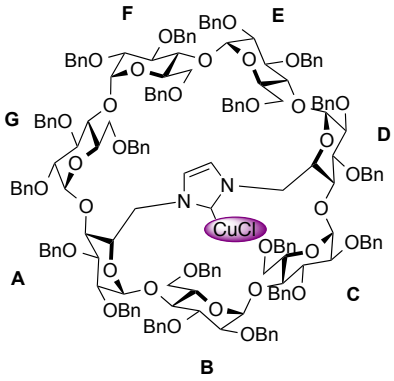

Method A: Under argon, **(β-ICyD)HCl** (2.8 g, 0.96 mmol) and copper(I) oxide (414 mg, 2.88 mmol) were dissolved in 20 ml of 1,4-dioxane previously degassed by bubbling argon for 15 minutes. The mixture was heated in a Schlenker reactor at 120 °C overnight, cooled down to r. t., filtered on celite, the cake washed with CH_2Cl_2 and the solvent evaporated *in vacuo*. The residue was purified on silica gel chromatography (Cyclohexane/Ethyl Acetate 4:1) to afford copper complex **(β-ICyD)CuCl** (2.3 mg, 80 %) as a white foam.

Method B: Copper(I) chloride (571mg, 6.1mmol) and silver complex **(β-ICyD)AgCl** (2.02g, 0.762mmol) were stirred in dichloromethane (20ml) under argon. The mixture was stirred at R.T overnight, the suspension was filtrated on celite, washed with dichloromethane. The residue was purified on silica gel chromatography (Cyclohexane/ Ethyl acetate 3:1) to afford copper complex **(β-ICyD)CuCl** (1.92g, 97%) as a white foam.

^{1}H NMR ($CDCl_3$, 600MHz): δ 7.47-6.88 (m, 95H, 95 × H-Ar), 6.15 (s, 1H, N-CH=C), 5.91-5.90 (m, 2H, N-CH=C, H-1G), 5.87 (d, $^3J_{1,2}$ = 3.07 Hz, 1H, H-1C), 5.76-5.74 (m, 2H, CHPh, H-5A), 5.45 (d, $^2J_{Ph\text{-}CHH}$ = 10,02 Hz, 1H, CHPh), 5.40-5.38 (m, 2H, 2 × CHPh), 5.26--5.24 (m, 2H, 2 × CHPh), 4.99 (d, $^2J_{Ph\text{-}CHH}$ = 11.02 Hz, 1H, CHPh), 4.94-4.89 (m, 6H, 5 × CHPh, H-6aD), 4.80 (d, $^3J_{1,2}$ = 3.53 Hz, 1H, H-1D), 4.72-4.68 (m, 3H, 2 × H-1E,F, H-3C), 4.64 (d, $^3J_{1,2}$ = 4.00 Hz, 1H, H-1B), 4.60-4.59(m, 2H, H-1A, H-3B), 4.57-4.03 (m, 35H, 2 × H-5D,B, 4 × H-3E,G,F,A, H-4C, H-6aA, H-6aG, 26 ×CHPh), 3.94 (dd, $^2J_{3,4}$ = 8.85 Hz, $^3J_{2,3}$ = 8.85 Hz, 1H, H-3D), 3.90-3.52(m, 16H, 2 × H-2C,G, 6 × H-4E,G,B,A,D,F, 3 × H-5C,G,F, H-6bC, H-6bF, H-6bG, H-6aC, H-6aF), 3.43 (br d, 1H, H-6bE), 3.37-3.30(m, 7H, 5 × H-2B,F,E,D,A, H-6bD, H-6bA), 3.25(br d, 1H, H-5E), 2.99(br d, 1H, H-6aE), 2.79-2.73(m, 2H, H-6aB, H-6bB);

^{13}C NMR ($CDCl_3$, 151MHz): δ 176.23(Cu-C), 140.48, 140.22, 140.12, 140.02, 139.55, 139.16, 139.05, 138.99, 138.87, 138.85, 138.79, 138.77, 138.61, 138.59, 138.51, 138.27, 138.24, 138.09, 137.74 (19 × C-Ar.quat.), 128.57-126.50 (m, 95 × C-Ar-tert.), 122.12, 120.87 (2 × N-CH=CH-N), 101.03, 99.51, 98.58, 97.94, 97.42, 97.31, 96.83(7 × C-1A,B,C,D,E,F,G), 83.47(C-4F), 82.22(C-4C), 82.06(C-4G), 81.66(C-3A), 81.41(C-3D), 80.68(C-4E), 80.57(C-4B), 80.38(C-2A), 80.27(C-3F), 80.19, 80.02(2 × C-3E,G), 79.93(C-3B), 79.89(C-3C), 79.38, 78.99, 78.82, 78.04(4 × C-2D,E,F,B), 77.96(C-2C), 77.47(C-2G), 76.96, 76.79, 76.41, 76.39, 76.19, 74.41(6 × Ph-CH_2), 74.33 (C-4A), 74.25(Ph-CH_2), 73.74, 73.73(2 × Ph-CH_2), 73.70(C-5C), 73.54, 73.49, 73.44, 73.29(4 × Ph-CH_2), 73.27(C-4D), 73.11(C-5G), 73.07, 72.97, 72.75, 72.72, 72.69(5 × Ph-CH_2), 72.35(C-5F), 72.34 (Ph-CH_2), 72.05, 71.84, 71.51(3 × C-5D,E,B), 70.89(C-5A), 70.52, 70.43, 69.81(3 × C-6C,F,G), 68.27(C-6E), 67.71(C-6B), 55.14(C-6D), 53.01(C-6A).

$[\alpha]_D^{20}$ = 48.0 ($CHCl_3$, c = 1)

R_f = 0.21 (CyH / AcOEt 4:1)

HRMS(ESI) calcd. $[C_{178}H_{184}N_2O_{33}CuCl + Na]^+$: 2998.1658, found 2998.1513 err. 4.8 ppm

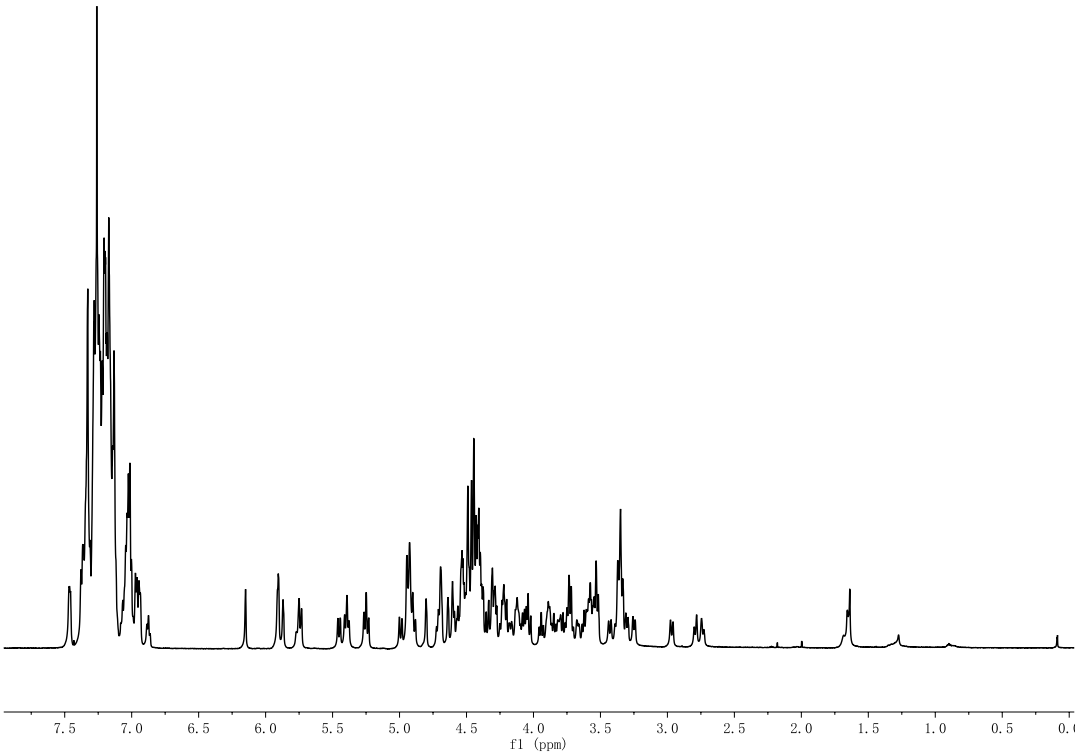

^{1}H NMR of **(β-ICyD)CuCl** ($CDCl_3$, 600 MHz, 300 K)

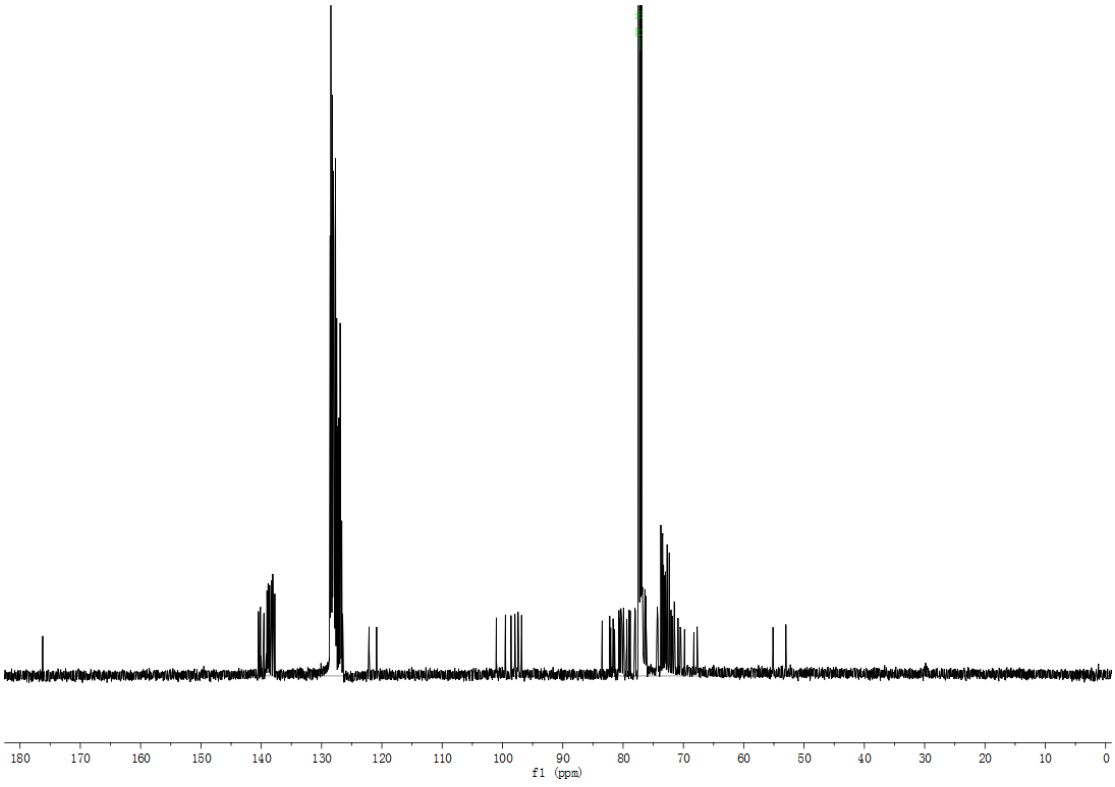

^{13}C NMR of **(β-ICyD)CuCl** ($CDCl_3$, 151 MHz, 300 K)

(α-ICyD)AuCl

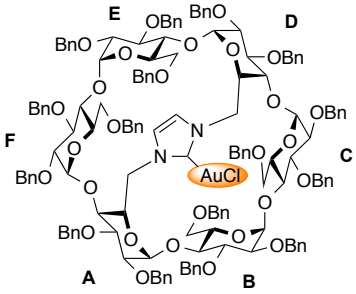

In a flame-dried two-neck flask under argon, silver complex **(α-ICyD)AgCl** (1 g, 0.385 mmol) and gold(I) chloride (897 mg, 3.85 mmol) were dissolved in 50 ml of acetonitrile previously degased by three “freeze-pump-thaw” cycles. The reaction was protected from light and stirred overnight at r.t. Mass spectrometry then indicated the reaction was incomplete and gold(I) chloride (100 mg, 0.43 mmol) was added. The reaction was maintained for 8 h, then filtrated on Celite, rinsed abundently with CH_2Cl_2 and concentrated *in vacuo*. The residue was purified on silica gel chromatography (Cyclohexane/Ethyl Acetate 4:1) to afford the gold complex **(α-ICyD)AuCl** (567 mg, 55 %).

The structure of the product was confirmed by comparison with the NMR spectra of the literature. [5]

^{1}H NMR ($CDCl_3$, 600 MHz, 300 K) : δ 7.41-6.97 (m, 74H, 74 x H-Ar), 6.83 (t, $^3J_{o,m}$ = $^3J_{m,p}$ = 7.7 Hz, 4H, 4 x H-*o*-Ar), 6.73 (t, ^3J = 7.4 Hz, 2H, 2 x H-*p*-Ar), 6.38 (t, $^3J_{4,5}$ = $^3J_{5,6}$ = 10.1 Hz, 2H, 2 x H-5A,D), 6.09 (s, 2H, 2 x N-CH=CH-N), 5.71 (d, $^3J_{1,2}$ = 3.8 Hz, 2H, 2 x H-1C,F), 5.63 (d, $^2J_{Ph\text{-}CHH}$ = 10.6 Hz, 2H, 2 x CHPh), 5.27 (d, $^2J_{Ph\text{-}CHH}$ = 10.7 Hz, 2H, 2 x CHPh), 5.17-5.11 (m, 4H, 4 x CHPh), 5.02 (dd, $^3J_{2,3}$ = 10.2 Hz, $^3J_{3,4}$ = 7.9 Hz, 2H, 2 x H-3C,F), 4.86 (d, $^2J_{Ph\text{-}CHH}$ = 11.2 Hz, 2H, 2 x CHPh), 4.68-4.40 (m, 20H, 14 x CHPh, 2 x H-1A,D, 2 x H-1B,E, 2 x H-6aA,D), 4.32-4.23 (m, 6H, 6 x CHPh), 4.24 (t, $^3J_{2,3}$ = $^3J_{3,4}$ = 9.4 Hz, 2H, 2 x H-3B,E), 4.18 (dd, $^3J_{2,3}$ = 9.7 Hz, $^3J_{3,4}$ = 7.6 Hz, 2H, 2 x H-3A,D), 4.14 (bd, $^3J_{4,5}$ = 9.7 Hz, 2H, 2 x H-5B,E), 4.01 (d, $^2J_{Ph\text{-}CHH}$ = 12.2 Hz, 2H, 2 x CHPh), 3.98-3.93 (m, 4H, 2 x H-5C,F, 2 x H-6aC,F), 3.85 (dd, $^3J_{4,5}$ = 9.4 Hz, $^3J_{3,4}$ = 8.0 Hz, 2H, 2 x H-4C,F), 3.79 (dd, $^2J_{6a,6b}$ = 10.6 Hz, $^3J_{5,6b}$ = 5.4 Hz, 2H, 2 x H-6bC,F), 3.72 (t, $^3J_{3,4}$ = $^3J_{4,5}$ = 9.3 Hz, 2H, 2 x H-4B,E), 3.61 (dd, $^3J_{2,3}$ = 10.2 Hz, $^3J_{1,2}$ = 3.8 Hz, 2H, 2 x H-2C,F), 3.57 (dd, $^3J_{4,5}$ = 10.1 Hz, $^3J_{3,4}$ = 7.6 Hz, 2H, 2 x H-4A,D), 3.43 (dd, $^3J_{2,3}$ = 9.9 Hz, $^3J_{1,2}$ = 3.5 Hz, 2H, 2 x H-2B,E), 3.33-3.26 (m, 4H, 2 x H-2A,D, 2 x H-6bA,D), 3.10 (dd, $^2J_{6a,6b}$ = 10.8 Hz, $^3J_{5,6a}$ = 3.3 Hz, 2H, 2 x H-6aB,E), 2.76 (bd, $^2J_{6a,6b}$ = 10.8 Hz, 2H, 2 x H-6bB,E) ppm.

^{13}C NMR ($CDCl_3$, 151 MHz, 300 K) : δ 169.73 (C-Au), 140.17 (2C), 139.83 (2C), 139.59 (2C), 139.15 (2C), 139.10 (2C), 138.84 (2C), 138.36 (2C), 138.07 (2C) (16 x C-Ar-quat.), 128.73-126.67 (80 x C-Ar-tert.), 121.52 (2 x N-CH=CH-N), 98.53 (2 x C-1C,F), 98.03 (2C), 97.99 (2C) (2 x C-1A,D, 2 x C-1B,E), 82.59 (2 x C-4C,F), 81.82 (2 x C-3A,D), 81.43 (2 x C-4B,E), 80.36 (2C), 80.25 (2C) (2 x C-2A,D, 2 x C-3B,E), 79.53 (2 x C-3C,F), 79.14 (2 x C-2B,E), 77.12 (2 x C-2C,F), 76.96 (2 x C-4A,D), 76.65 (2C), 76.40 (2C), 74.22 (2C) (6 x Ph-CH_2), 73.73 (2 x C-5C,F), 73.47 (2C), 73.29 (2C), 73.21 (2C), 72.65 (2C), 72.33 (2C) (10 x Ph-CH_2), 71.53 (2 x C-5B,E), 71.12 (2 x C-6C,F), 69.90 (2 x C-5A,D), 67.92 (2 x C-6B,E), 54.32 (2 x C-6A,D) ppm.

R_f = 0.21 (Cyclohexane/Ethyl Acetate 4:1)

HRMS (ESI) : calculated for $C_{151}H_{156}AuClN_2NaO_{28}^+$ $[M+Na]^+$ 2700.0091, found 2700.0089.

(β-ICyD)AuCl

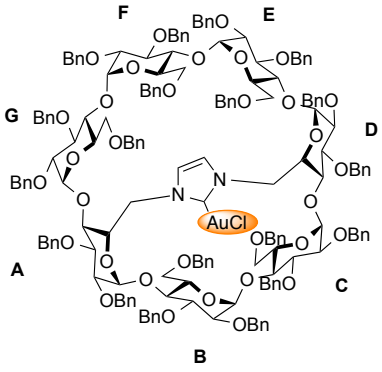

In a flame-dried two-neck flask under argon, silver complex **(β-ICyD)AgCl** (455 mg, 0.15 mmol) and gold(I) chloride (349 mg, 1.5 mmol) were dissolved in 20 ml of acetonitrile previously degassed by three 〝freeze-pump-thaw〞 cycles. The reaction was protected from light and stirred overnight at r.t. It was then filtrated on Celite, rinsed abundantly with DCM and concentrated *in vacuo.* The residue was purified on silica gel chromatography (CyH/AcOEt 4:1) to afford the gold complex **(β-ICyD)AuCl** (327 mg, 70 %).

^{1}H NMR ($CDCl_3$, 400 MHz): δ 7.46-6.89 (m, 95H, 95 × H-Ar), 6.15 (s, 1H, N-CH=C), 6.06 (m, 1H, H-5A), 5.88-5.86 (m, 3H, N-CH=C, 2 × H-1C,G), 5.73 (d, $^{2}J_{Ph\text{-}CHH}$ = 11.79 Hz, 1H, CHPh), 5.48 (d, $^{2}J_{Ph\text{-}CHH}$ = 11.22 Hz, 1H, CHPh), 5.42 (d, $^{2}J_{Ph\text{-}CHH}$ = 6.15 Hz, 1H, CHPh), 5.39 (d, $^{2}J_{Ph\text{-}CHH}$ = 5.42 Hz, 1H, CHPh), 5.30 (d, $^{2}J_{Ph\text{-}CHH}$ = 12.69 Hz, 1H, CHPh), 5.21 (d, $^{2}J_{Ph\text{-}CHH}$ = 12.20 Hz, 1H, CHPh), 5.08 (d, $^{2}J_{6a,6b}$ = 13.01 Hz, 1H, H-6aD), 5.01-4.90 (m, 6H, 6 × CHPh), 4.79 (bd, 1H, H-1D), 4.74-4.69 (m, 3H, H-3C, 2 × H-1E,F), 4.64-4.60 (m, 3H, 2 × H-1A,B, CHPh), 4.58-4.12 (m, 31H, 2 × H-5D,B, 3 × H-3B,E,G, H-6bA, H-6aG, 24 × CHPh), 4.06-3.98 (m, 5H, 3 × H-3A,D,F, H-4C, CHPh), 3.92-3.52 (m, 16H, H-6bG, H-6aC, H-6aF, H-6bF, H-6bC, 2 × H-2C,G, 6 × H-4G,F,B,A,E,D, 3 × H-5C,F,G), 3.44 (d, $^{2}J_{6a,6b}$ =9.40 Hz, 1H, H-6aE), 3.39-3.26 (m, 8H, 5 × H-2A,B,D,E,F, H-5E, H-6bD, H-6aA), 2.96 (d, 1H, H-6bE), 2.79-2.72 (m, 2H, 2 × H-6B) ppm.

^{13}C NMR ($CDCl_3$, 100 MHz): δ 171.42 (C-Au), 140.52, 140.19, 140.08, 140.04, 139.62, 139.13, 139.06, 138.93, 138.90, 138.81, 138.79(2C), 138.63, 138.61, 138.52, 138.27, 138.21, 138.14, 137.76 (19 × C-Ar.quat.), 128.55-126.57 (m, 95 × C-Ar-tert.), 122.00, 120.85 (2 × N-CH=CH-N), 100.91, 99.52, 98.78, 98.12, 97.55, 97.24, 96.71 (7 × C-1A,B,C,D,E,F,G), 83.32 (C-4F), 82.42 (C-3A), 82.09, 81.99 (2 × C-4C,G), 81.29 (C-3D), 80.88 (C-4E), 80.43, 80.20, 80.15, 80.07, 80.00, 79.85, 79.28 (C-2A, 5 × C-3F,B,E,G,C, C-4B), 78.97, 78.74, 78.09, 77.82, 77.48, 77.36 (6 × C-2B,C,D,F,E,G), 76.94 (Ph-CH_2), 76.67 (Ph-CH_2), 76.42 (Ph-CH_2), 76.29 (Ph-CH_2), 74.49 (Ph-CH_2), 74.31 (Ph-CH_2), 74.14 (C-4A), 73.77 (C-4D), 73.71, 73.56 (2C), 73.51, 73.46 (5 × Ph-CH_2), 73.42(C-5C), 73.34, 73.31 (2 × Ph-CH_2), 73.11 (C-5G), 72.99 ,72.96 ,72.90, 72.71 (2C), 72.40 (6 × Ph-CH_2), 72.31 (C-5F), 71.46, 71.40, 71.35 (3 × H-5D,B,E), 70.59, 70.38 (2 × C-6C,F), 69.92 (C-5A), 69.85, 68.32, 67.74, 55.16, 53.20 (6 × C-6A,B,D,E,G) ppm.

$[\alpha]_D^{20}$ = +43.2 ($CHCl_3$, *c* = 1)

R_f = 0.21(CyH / AcOEt 4:1)

HRMS(ESI) calculated for $C_{178}H_{184}AuClN_2NaO_{33}^{+}$ $[M+Na]^{+}$ 3132.2028, found 3132.2134 err. 3.4 ppm

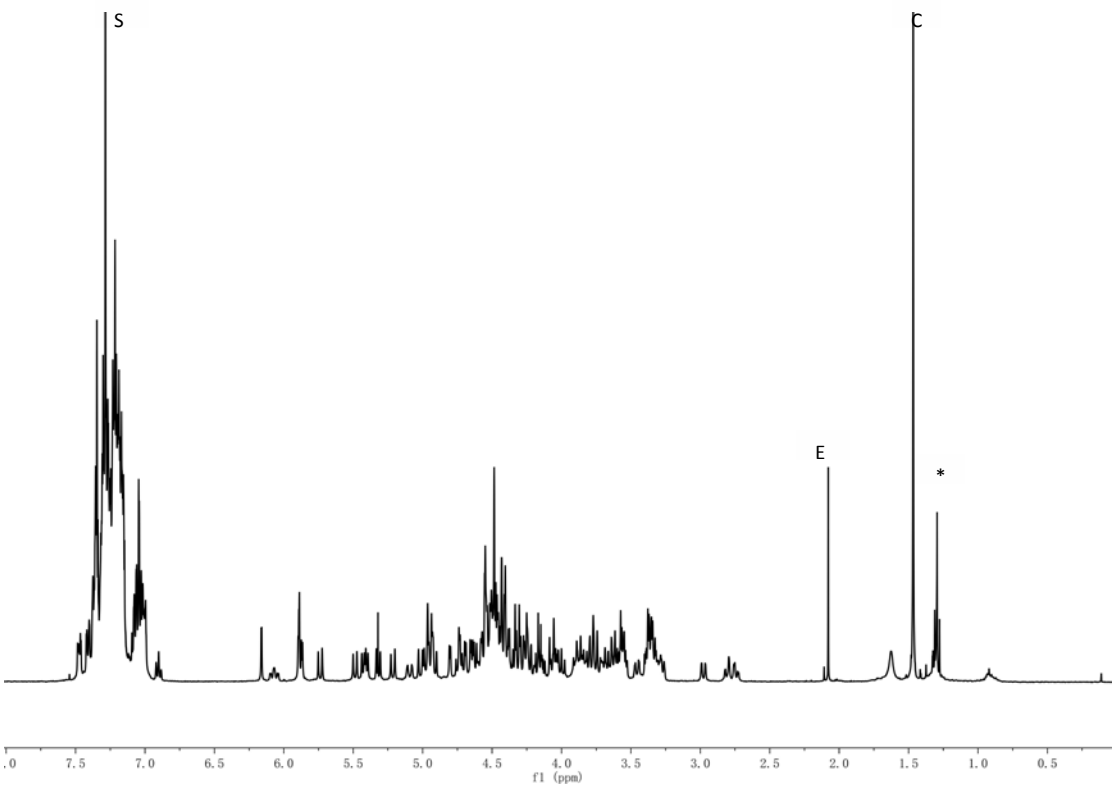

^{1}H NMR of **(β-ICyD)AuCl** ($CDCl_3$, 400 MHz, 300K, S=solvent, E= EtOAc, C= Cy, *: grease)

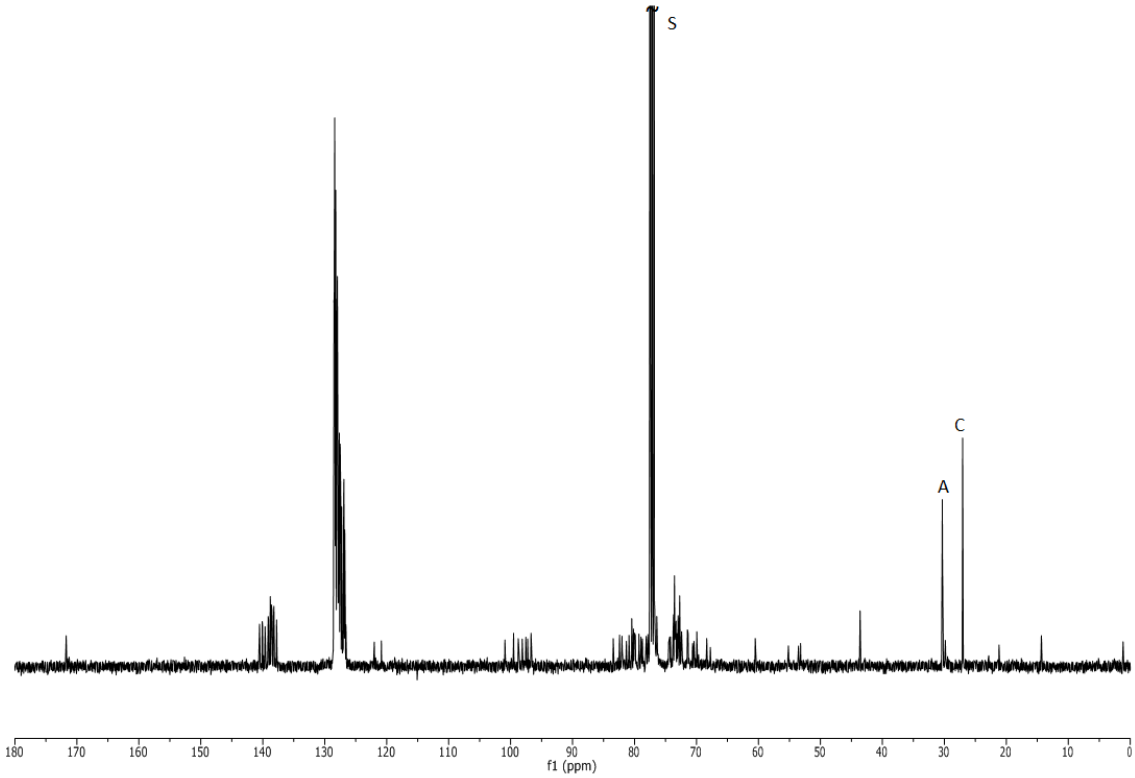

^{13}C NMR of **(β-ICyD)AuCl** ($CDCl_3$, 100 MHz, 300 K)

(γ-A,D-ICyD)AuCl

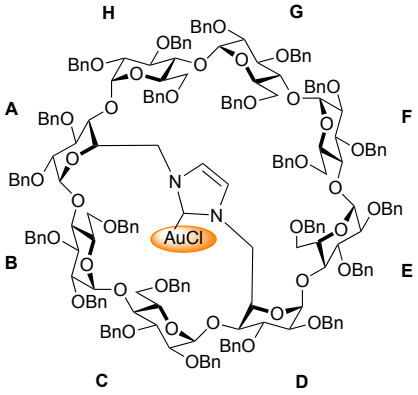

A mixture of perbenzylated imidazolium **(γ-A,D-ICyD)AgCl** (118 mg, 61 mmol, 1 eq) and $Au(Me_2S)Cl$ (13 mg, 61 mmol, 1eq) were dissolved in anhydrous CH_2Cl_2, under nitrogen atmosphere. The reaction was stirred overnight at room temperature for 20 hours. Then, the reaction was filtered on a celite pad and the residue was washed several times with CH_2Cl_2. Then, the reaction mixture was purified in silica gel chromatography (Cyclohexane: Ethyl acetate 2:1) giving the gold complex **(γ-A,D-ICyD)AuCl** as a white foam (114 mg, 94% yield).

^{1}H NMR: (CD_3CN, 600MHz): d 7.40-6.85 (m, 112H, 110 x H-Ar, 2 x H-Im), 5.77 (d, *J* = 2.80 Hz, 1H, H-1), 5.33-5,18 (m, 3H, 1 x H-1, 2 x CHPh), 5.15-5.06 (m, 3H, 2 x H-1, 1 x CHPh), 5,04-5,00 (m, 2H, 1 x H-1, 1 x CHPh), 4,93 (d, *J* = 3,43 Hz, 1H, 1 x H-1), 4,85 (d, *J* = 3.45Hz, 2H, 2 x H-1), 4,75 (d, *J* = 11.2Hz, 1H, 1 x CHPh), 4,72-4,28 (m, 42H, 1 x H-3, 1 x H-5, 2 x H-6, 38 x CHPh), 4,23-4,16 (m, 4H, 2 x H-5, 1 x H3, 1 x CHPh), 4.07-3.65 (25H, 6 x H-3, 6 x H-4, 5 x H-5, 8 x H-6), 3.63-3.40 (m, 8H, 4 x H-2, 2 x H-4, 2 x H-6) 3.38-3.22 (m, 6H, 4 x H-2, 2 x H-6), 3.06 (d, *J* = 11.0Hz, 1H, 1 x H-6), 2.92 (d, *J* = 10.8 Hz, 1H, 1xH-6);

^{13}C NMR: (CD_3CN, 151MHz): d 171.1 (C-Au), 141.5, 141.0, 140.9, 140.8, 140.7, 140.0, 139.8, 139.7, 139.6, 139.5, 139.4, 139.3, 139.3 (22 x C-Ar-quat.), 129.5, 129.4, 129.3, 129.2, 129.1, 129.0, 128.9, 128.8, 128.7, 128.6, 128.5, 128.4, 128.3, 128.2, 128.2, 128.1, 128.0, 127.8, 128.6 (110 x C-Ar, 2 x C-Im), 100.7 (C-1), 99.0 (3 x C-1), 97.7 (3 x C-1), 96.2 (C-1), 83.1 (C-3), 82.0 (C-2), 81.6, 81.5 (3 x C-3, 2 x C-4), 81.2, 81.1 (1 x C-2, 2 x C-3, 1 x C-4), 80.7 (1 x C-2, 1 x C-3, 1 x C-4), 80.5 (2 x C-2), 79.9 (C-2, C-4), 79.1 (C-3), 78.7(C-2), 77.7 (C-4), 77.4 (C-4), 76.7, 76.1, 76.0, 75.9, 75.1, 74.1, 73.8, 73.7, 73.6 (21 x Ph-$\underline{C}H_2$), 75.6 (C-2), 73.5 (C-4), 73.3 (Ph-$\underline{C}H_2$), 73.3 (C-5), 72.8 (C-5), 72.7 (C-5), 72.6 (2 x C-5), 72.4 (C-5), 71.7 (C-5), 71.6 (C-5), 71.2 (C-6), 70.9 (C-6), 70.5 (C-6), 70.0 (C-6), 69.6 (C-6), 69.1 (C-6), 56.0 (C-6), 53.5 (C-6).

HRMS: $[C_{205}H_{212}N_2O_{38}AuClNa_2]^{2+}$: calcd. 1794.6956, found 1794.6957 err. 0.05ppm

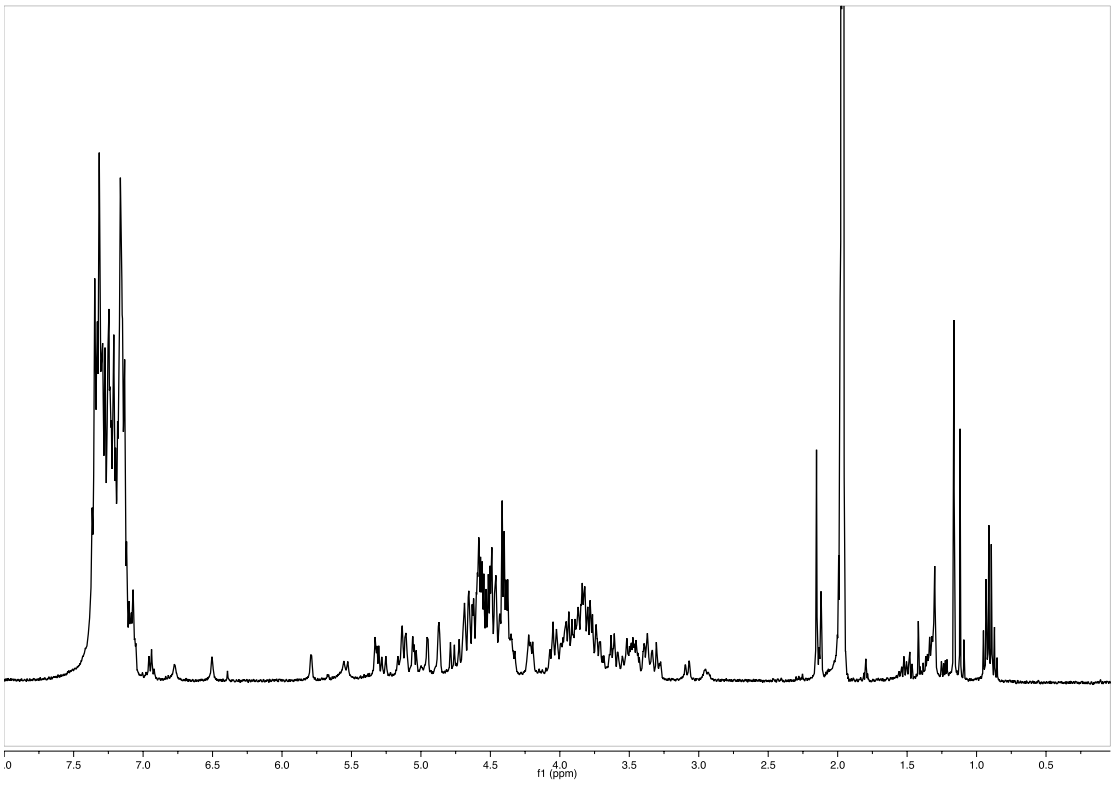

^{1}H NMR of **(γ-A,D-ICyD)AuCl** (CD_3CN, 600 MHz, 300 K)

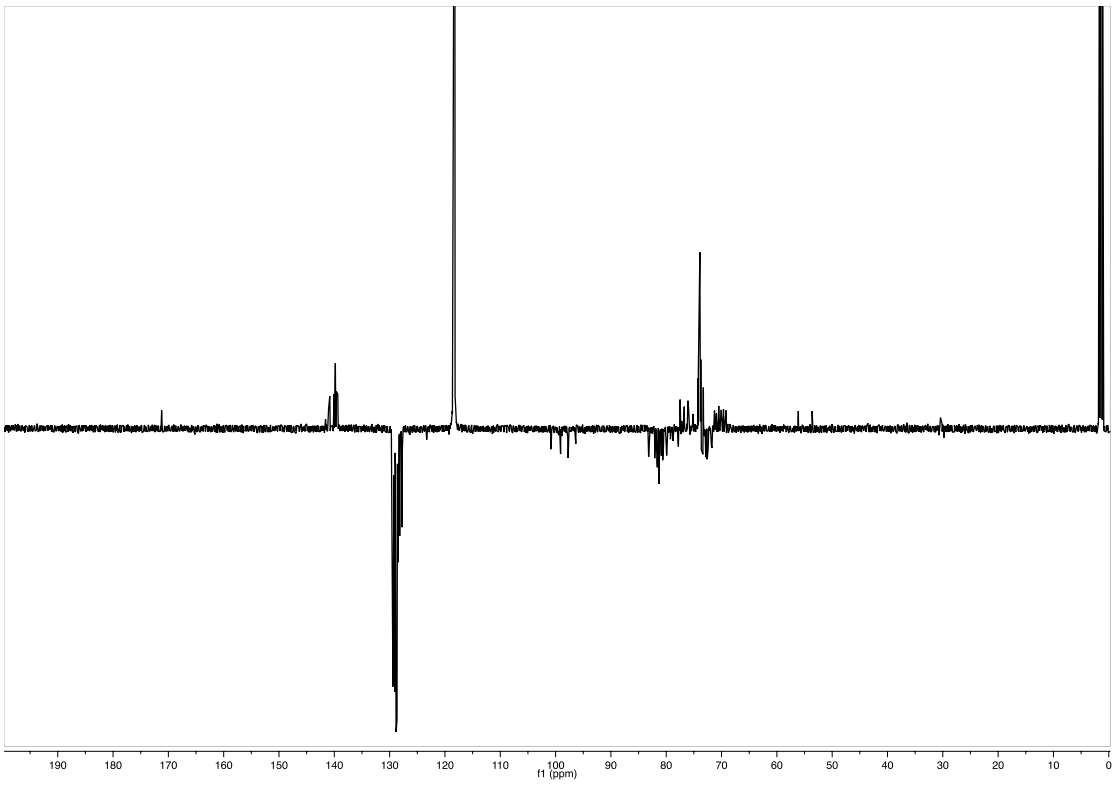

^{13}C JMod NMR of **(γ-A,D-ICyD).AuCl** (CD_3CN, 151 MHz, 300 K)

(γ-A,E-ICyD)AuCl

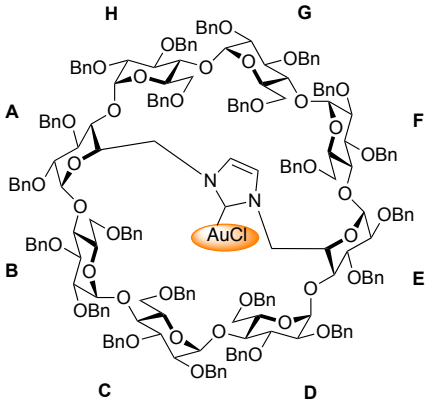

A mixture of perbenzylated imidazolium **(γ-A,E-ICyD)AgCl** (150 mg, 61 mmol) and Au(Me_2S)Cl (13 mg, 61 mmol) were disolved in anhydrous CH_2Cl_2, under nitrogen atmosphere. The reaction was stirred overnight at room temperature for 20 hours. Then, the reaction was filtered on a celite pad and the residue was washed several times with CH_2Cl_2. Then, the reaction mixture was purified in silica gel chromatography (Cyclohexane: Ethyl acetate 2:1) giving the gold complex **(γ-A,E-ICyD)AgCl** as a white foam (143mg, 93% yield).

^{1}H NMR (CD_3CN, 400MHz): d 7.43-7.06 (m, 104H, 104 x H-Ar), 6.93 (t, 4H, $^3J_{o,m} = {}^3J_{m,p}$ = 7.6 Hz, 4 x H-*m*-Ar), 6.79 (t, 2H, $^3J_{m,p}$ = 7.41 Hz, 2 x H-*p*-Ar), 6.36 (s, 2H, 2 x N-CH=CHN), 5.64 (d, $^3J_{1,2}$ = 3.6 Hz, 2H, 2 x H-1D,H), 5,39 (d, ^2J = 11.3Hz, 2H, 2 x CHPh), 5.27 (d, ^2J=11.7Hz, 2H, 2 x CHPh), 5.21 (d, ^2J = 11.1Hz, 2H, 2 x CHPh), 6.06 (d, ^2J = 11.3 Hz, 2H, 2 x CHPh), 4.92 (d, $^3J_{1,2}$ = 3.6Hz, 2H, 2 x H-1A,E), 4,87 (d, $^3J_{1,2}$ = 3.6Hz, 2H, 2 x H1-B,F), 4.83 (d, $^3J_{1,2}$ = 3.6Hz, 2H, 2 x H1-C,G), 4.80-4,27 (m, 40H, 2 x H-5A,E, 2 x H-6A,E, 36x CHPh), 4.22-4.05 (m, 6H, 2 x H-6D,H, 2 x H-3C,G, 2 x H-3D,H), 3.98-3.76 (m, 14H, 2 x H-3A,E, 2 x H-3B,F, 2 x H-4B,F, 2 x H-5C,G, 4 x H-6C,G, 2 x H-4D,H), 3.74-3.59 (m, 6H, 2 x H-5B,F, 2 x H-4C,G, 2 x H-6D,H), 3.57-3,48 (m, 4H, 2 x H-5D,H, 2 x H-4A,E), 3,47-3,40 (m, 6H, 2 x H-6A,E, 2 x H-2A,E, 2 x H-2D,H), 3,34 (dd, 2H, $^3J_{2,3}$ = 9.6 Hz, $^3J_{2,1}$ = 3,3 Hz, 2 x H-2B,F), 3.31-3.20 (m, 4H, 2 x H-2C,G, 2 x H-6B,F), 3.05 (d, 1H, ^2J=11.2 Hz, 2 x H-6B,F);

^{13}C NMR (CD_3CN, 100MHz): d 172.2 (C-Au), 141.4 (2C), 141.0 (2C), 140.8 (2C), 140.9 (2C), 140.7 (2C), 139.9 (2C), 139.8 (2C), 139.77 (2C), 139.7 (2C), 139.3 (2C), 139.2(2C) (22 x C-Ar-quat.), 129.5, 129.4, 129.3, 129.2, 129.1, 129.0, 129.0, 128.9, 128.8, 128.7, 128.6, 128.6, 128.5, 128.4, 128.2, 128.1, 127.9, 127.8, 127.6 (110 x C-Ar-tert), 99.7 (2 x C-1C,G), 99.2 (2 x C-1B,F), 98.7 (2 x C-1A,E), 94.9 (2 x C-1D,H), 82.7 (2 x C-4C,G), 82.4 (2 x C-4D,H), 82.1(2 x C-3A,E), 81.8 (2 x C-3D,H), 81.5 (2 x C-3B,F), 81.2 (4C, 2 x C-4B,F, 2 x C-3C,G), 80.9 (2 x C-2A,E), 80.6 (2 x C-2B,F), 80.31 (2 x C-2C,G), 79.3 (2 x Ph-$\underline{C}H_2$), 79,0 (2 x Ph-$\underline{C}H_2$), 78.9 (2 x C-2D,H), 78.9 (2 x Ph-$\underline{C}H_2$), 78.7 (2 x Ph-$\underline{C}H_2$), 78.6 (2 x Ph-$\underline{C}H_2$), 78.3 (2 x Ph-$\underline{C}H_2$), 77.6 (2 x Ph-$\underline{C}H_2$), 77.0 (2 x Ph-$\underline{C}H_2$), 76.9 (2 x Ph-$\underline{C}H_2$), 74.8 (2 x Ph-$\underline{C}H_2$), 74.0 (6 x Ph-$\underline{C}H_2$), 73.9 (6 x Ph-$\underline{C}H_2$), 73.7 (2 x Ph-$\underline{C}H_2$), 73.5 (2 x Ph-$\underline{C}H_2$), 73.4 (2 x Ph-$\underline{C}H_2$), 73.3 (2 x Ph-$\underline{C}H_2$), 73.3 (2 x C-4A,E), 73.2(2 x Ph-$\underline{C}H_2$), 73.0 (2 x C-5C,G), 72.4 (2 x C-5B,F), 72.3 (2 x C-5A,E), 71.9 (2 x C-5D,H), 71.1 (2 x C-6C,G), 70.9 (2 x C-6D,H), 69.4 (2 x C-6B,F), 54.2 (2 x C-6A,E)

HRMS (ESI): $[C_{205}H_{212}N_2O_{38}AuClNa_2]^{2+}$: calcd: 1794.6956 found: 1794.6959 err. 0.16ppm

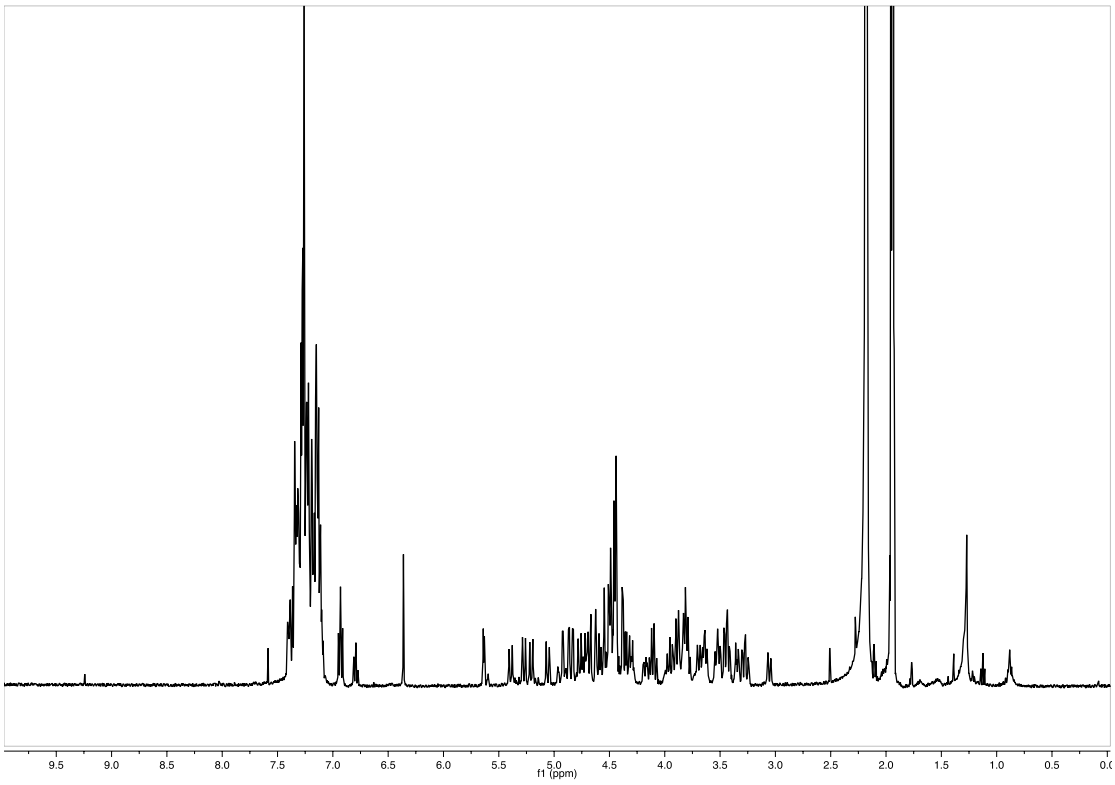

^{1}H NMR of **(γ-A,E-ICyD)AuCl** (CD_3CN, 400 MHz, 300 K)

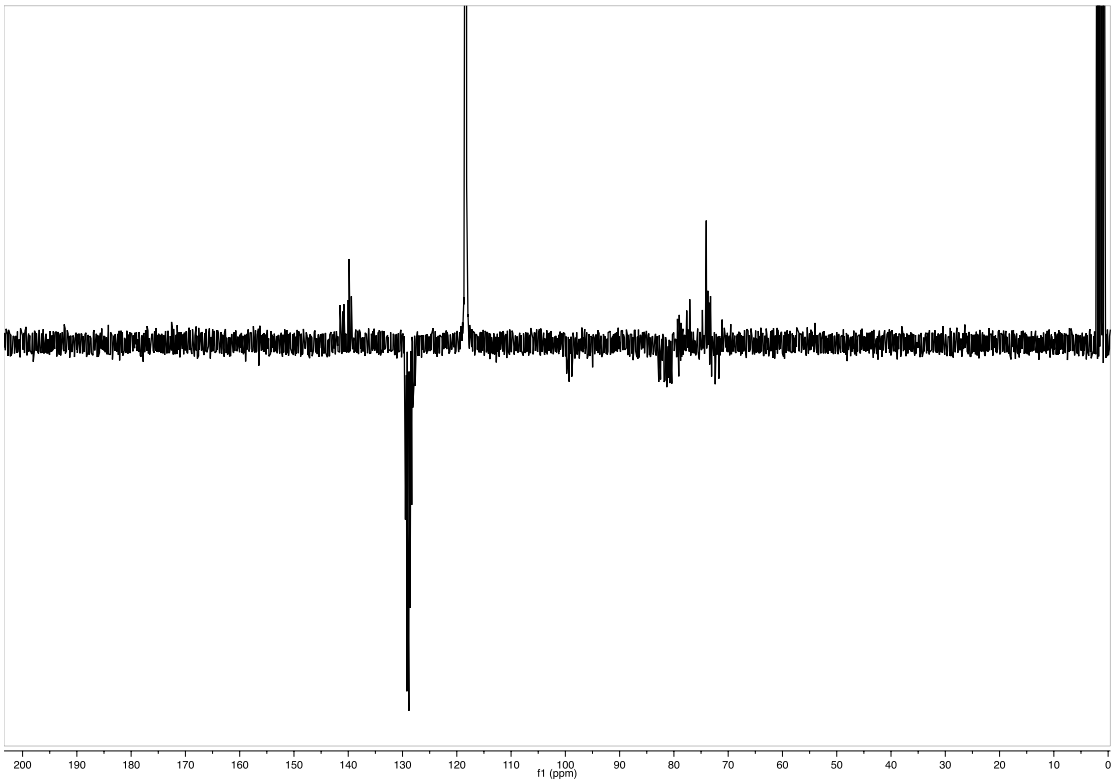

^{13}C JMod NMR of **(γ-A,E-ICyD).AuCl** (CD_3CN, 100 MHz, 300 K)

(α-BiCyD)HCl

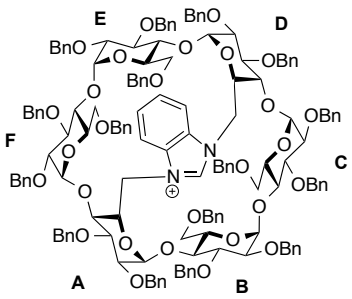

A mixture of compound **2α** (3.7 g, 1.44 mmol, 1eq.) and benzimidazole (3.4 g, 28.8 mmol, 20eq.) was dissolved in anhydrous DMF under N_2 atmosphere. The reaction mixture was stirred at 120°C overnight, and followed by TLC. Then adding another 20 equiv. benzimidazole (3.4 g, 28.8 mmol) and the reaction was stirred for 12 h. Then HCl solution (1 M) was added, the aqueous layer was extracted with DCM 3 times. The combined organic layers were dried over $MgSO_4$ filtered, and concentrated under vacuum. Silica gel chromatography of the residue (DCM/MeOH 95:5) afforded the perbenzylated benzimidazolium compound **(α-BiCyD)HCl** (2.5 mg, 68 %). This compound cannot be well defined due to a rotation conformation, and broad signals were observed by ^{1}H NMR in CD_3CN.

^{1}H NMR (CD_3CN, 400 MHz): δ 9.84 (s, 1H, N-C<u>H</u>-N), 7.40-6.88(m, 84H, 80 × H-Ar, 4 x H-BzIm), 5.73-2.80 (m, 74H, 6 × H-1, 6 × H-2, 6 × H-3, 6 × H-4, 6 × H-5, 12 × H-6, 32 ×CHPh) ppm.

^{13}C NMR (CD_3CN, 100 MHz): δ 139.44 (2C), 139.24 (2C), 139.11 (2C), 138.94 (2C), 138.71 (2C), 138.37 (2C), 138.10 (2C), 138.07 (2C) (16×C-Ar-quat.), 132.45 (2 × N-<u>C</u>=<u>C</u>-N), 129.08-127.14 (80 × C-Ar-tert.), 111.05 (4C, Ar-BzIm), 98.30 (2 × C-1), 98.08 (2 × C-1), 97.55 (2 × C-1), 81.84 (2C), 81.57 (2C), 81.10 (2C), 81.03 (2C), 80.49 (2C), 80.42 (2C), 80.03 (2C), 79.42 (2C), 77.61 (2C), 77.09 (2C), 76.46 (2C), 75.74 (2C), 74.18 (2C), 74.00 (2C), 73.77 (2C), 73.70 (2C), 73.56 (2C), 73.20 (2C), 72.83 (2C), 72.24 (2C), 70.85 (2C), 70.41 (2C), 68.21 (2C) (6 × C-2, 6 × C-3, 6 × C-4, 6 × C-5, 6 × C-6, 16 ×Ph-<u>C</u>H_2) ppm.

$[\alpha]_D^{20}$= +54.4 ($CHCl_3$, *c* = 1)

R_f = 0.21 (DCM/MeOH 95:5)

HRMS (ESI) calculated for $C_{155}H_{159}N_2O_{28}^+$ $[M]^+$ 2496.1074, found 2496.1039 err. 1.4 ppm

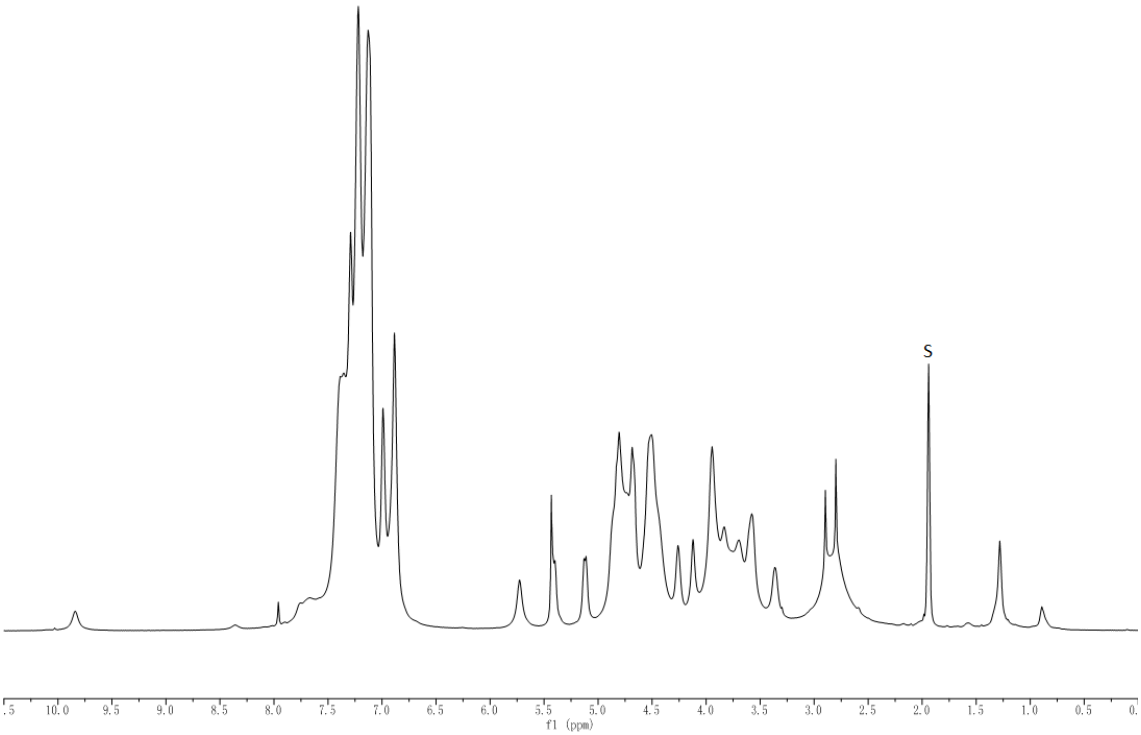

^{1}H NMR of **(α-BiCyD)HCl** (CD_3CN, 600 MHz, 300 K)

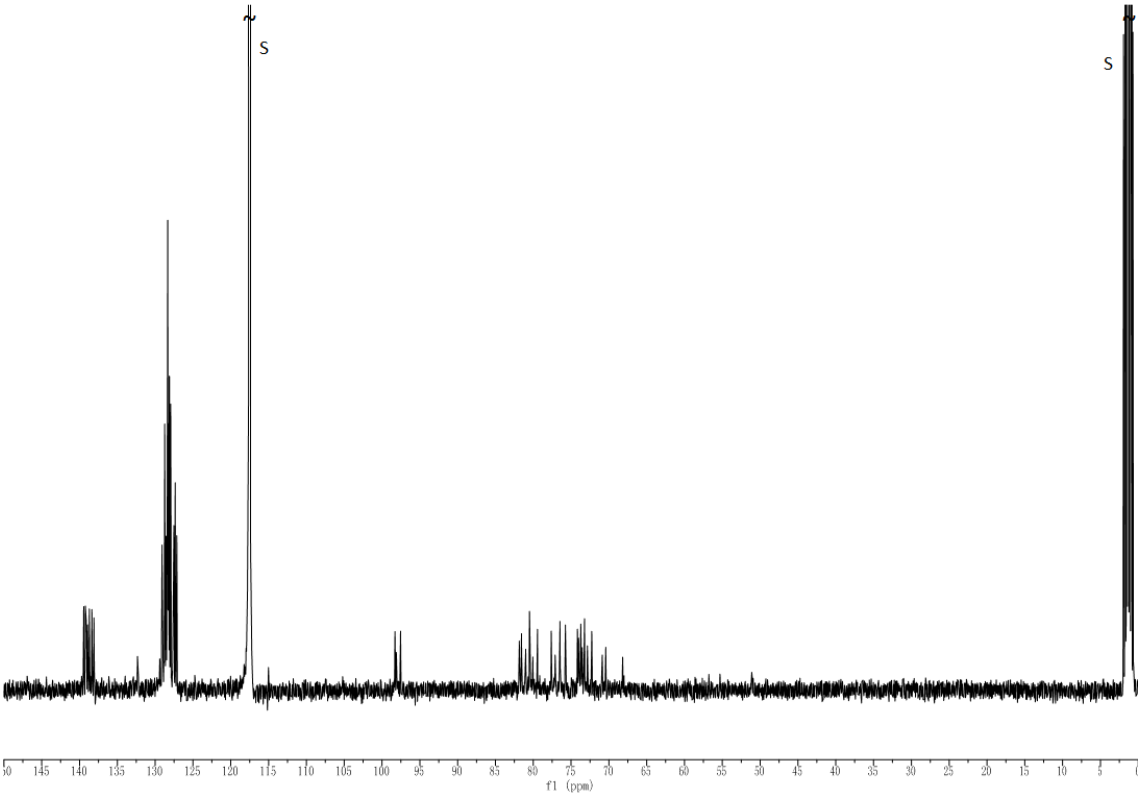

^{13}C NMR of **(α-BiCyD)HCl** (CD_3CN, 151 MHz, 300 K)

(β-BiCyD)HCl

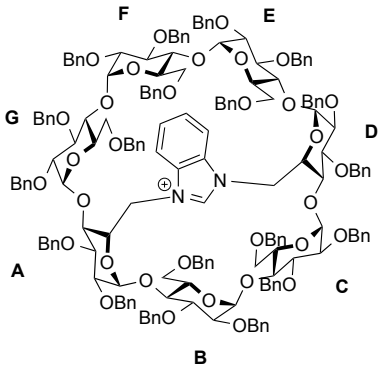

In a round-bottom flask under nitrogen, **2β** (2.8 g, 0.093 mmol) and benzimidazole (4.4 g, 0.04 mmol) were dissolved in DMF (20 mL). The mixture was heated at 120 °C overnight and the reaction followed by TLC. After cooling down to r.t., the solvent was evaporated and the residue dissolved in 20 ml of dichloromethane and washed with 20 ml of aq. HCl (1M). The aqueous layer was extracted with dichloromethane (3 x 20 ml) and the combined organic layers were dried over $MgSO_4$ and concentrated to dryness. The residue was purified on silica gel chromatography (DCM/MeOH 100:1 then 100:5 then 100:10) to afford **(β-BiCyD)HCl** (1.45 g, 53 %) as a white foam.

^{1}H NMR (CD_3CN, 400MHz): δ 7.65 (br d, 1H, H-Benzimidazole), 7.50 (d, ^2J = 8.4, 1H, H-Benzimidazole), 7.38-6.81(m, 97H, 95 × H-Ar, 2 × H-Benzimidazole), 5.86 (ws, 2H, 2 × H-1), 5.43 (d, 1H, $^2J_{Ph\text{-}CHH}$=11.6Hz, CHPh), 5.34 (br d, 1H, $^2J_{Ph\text{-}CHH}$=11.5Hz, CHPh), 5.22-5.17 (m, 2H, 2 × CHPh), 5.09 (br d, 1H, $^2J_{Ph\text{-}CHH}$=11.5Hz, CHPh), 5.00(s, 1H, H-1), 4.94-4.90 (m, 3H, H-1, CHPh, H-6), 4.85-4.26 (m, 40H, 3 × H-1, 3 × H-6, 2 × H-5, 32 × CHPh), 4.15-3.42 (m, 29H, 6 × H-6, 5 × H-5, 7 × H-4, 7 × H-3, 4 × H-2), 3.36 (dd, $^3J_{2,3}$=9.9Hz, $^3J_{1,2}$=3.6Hz, 1H, H-2), 3.28 (dd, $^3J_{2,3}$=9.6Hz, $^3J_{1,2}$=3.0Hz, 1H, H-2), 3.24 (dd, $^3J_{2,3}$=8.5Hz, $^3J_{1,2}$=2.5Hz, 1H, H-2), 2.79-2.72 (m, 2H, 2 × H-6), 2.41-2.34 (m, 2H, 2 × H-6);

^{13}C NMR (CD_3CN, 100MHz): δ 140.74, 140.73, 140.40, 140.20, 139.81, 139.69, 139.67, 139.61, 139.57, 139.34, 139.31, 138.96, 138.91, 138.89, 138.86, 138.84, 138.77, 138.71(2C) (19×C-At.quat.), 133.30, 133.02 (2×N-C=C-N benzimidazole), 129.42-127.86 (m, 95 × C-Ar-tert.), 123.14 (2C) , 115.39, 113.98. (4×C-benzimidazole), 100.47, 100.14, 99.16, 98.25, 97.38, 97.18, 96.92 (7×C-1), 83.01, 83.00, 82.28, 81.81, 81.79, 81.46, 81.40, 81.38, 81.31(2C), 81.21, 81.18(2C), 81.02, 80.97, 80.57, 80.54, 80.39(2C), 79.93, 78.90(7×C-2, 7×C-3, 7×C-4), 77.15, 77.12, 76.84, 76.52, 76.20, 75.28, 75.04, 74.98 (8 × Ph-$\underline{C}H_2$) , 74.16, 74.14 (2×C-5), 73.96, 73.90, 73.83, 73.80, 73.69, 73.60, 73.56, 73.50, 73.41, 73.28, 73.10(11 × Ph-$\underline{C}H_2$), 72.99, 72.53, 72.52, 71.97, 71.19 (5×C-5), 70.88, 70.46, 70.21, 68.63, 68.02, 50.78, 49.35(7×C-6);

$[\alpha]_D^{20}$ = +56.3 ($CHCl_3$, *c* = 0.5)

R_f = 0.35 (DCM/MeOH : 95:5)

HRMS(ESI) calculated for $C_{182}H_{187}N_2O_{33}^+$ $[M]^+$ 2928.3011, found 2928.3003, err. 0.3 ppm

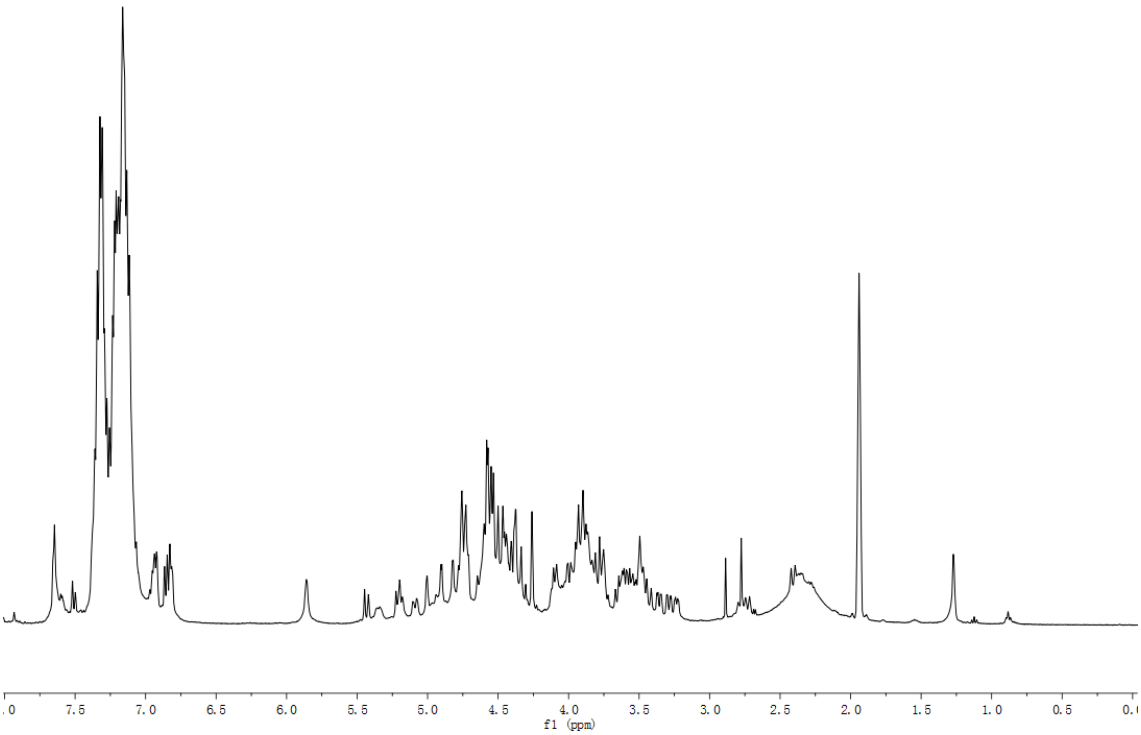

^{1}H NMR of **(β-BiCyD)HCl** (CD_3CN, 400 MHz, 300 K)

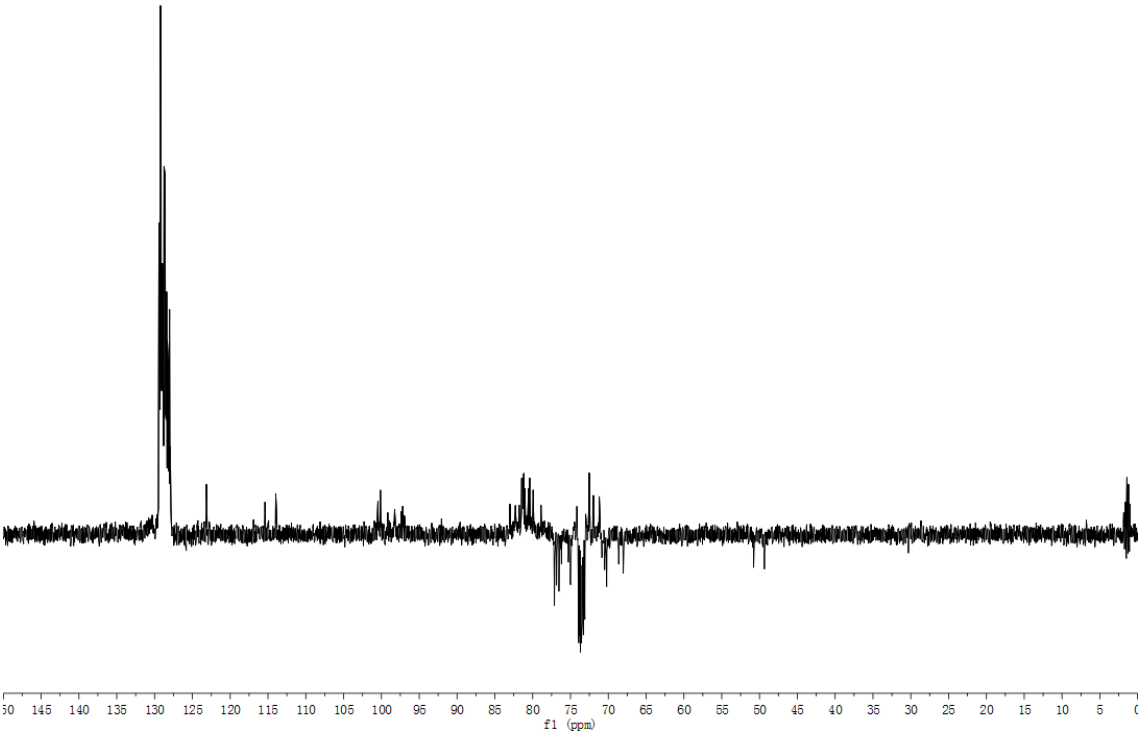

^{13}C Dept NMR of **(β-BiCyD)HCl** (CD_3CN, 100 MHz, 300 K)

(α-BiCyD)AgCl

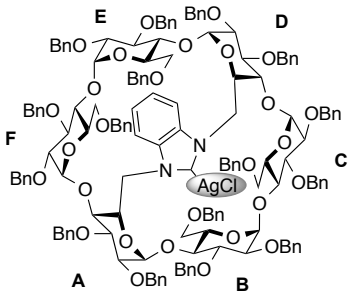

A mixture of perbenzylated benzimidazolium **(α-BiCyD)HCl** (45 mg, 18 µmol) and silver(I) oxide (42 mg, 180 µmol) was dissolved in anhydrous CH_3CN under a N_2 atmosphere. The reaction mixture was stirred at r.t. overnight. Then the silver oxide was filtered on a celite pad and the residue was washed with CH_3CN, and the solvents were evaporated. Silica gel chromatography of the residue (cyclohexane/ EtOAc 4:1) gave the silver complex **(α-BiCyD)AgCl** (42 mg, 88 %).

^{1}H NMR ($CDCl_3$, 600 MHz): δ 7.48-7.10 (m, 74H, 70 × H-Ar, 4H-BzIm), 6.98 (t, $^3J_{o,m} = {}^3J_{m,p}$ = 7.74 Hz, 4H, 4 × H-Ar), 6.86 (m, 6H, 6 × H-Ar), 6.02 (t, $^3J_{4,5} = {}^3J_{5,6}$ = 10.6 Hz, 2H, 2 × H-5A, D), 5.92 (d, $^3J_{1,2}$ = 3.76 Hz, 2H, 2 × H-1C, F), 5.80 (d, $^2J_{Ph\text{-}C\underline{H}H}$ = 10.84 Hz, 2H, 2 × CHPh), 5.53 (d, $^2J_{Ph\text{-}C\underline{H}H}$ = 10,70 Hz, 2H, 2 × CHPh), 5.29 (d, $^2J_{Ph\text{-}C\underline{H}H}$ = 11.42 Hz, 2H, 2 × CHPh), 5.26 (d, $^2J_{Ph\text{-}C\underline{H}H}$ = 11.16Hz, 2H, 2 × CHPh), 5.19 (dd, $^3J_{2,3}$ = 7.90, $^3J_{3,4}$ = 8.04, 2H, 2×H-3C,F), 5.00 (d, $^2J_{Ph\text{-}C\underline{H}H}$ = 11.33 Hz, 2H, 2 × CHPh), 4.81 (d, $^2J_{Ph\text{-}C\underline{H}H}$ = 10.90Hz, 2H, 2 × CHPh), 4.77 (d, $^2J_{6a,6b}$ = 13.96 Hz, 2H, 2 × H-6aA,D), 4.73 (m, 4H, 2 × H-1B,E, 2 × CHPh), 4.72-4.66 (m, 6H, 6 × CHPh), 4.64 (d, $^3J_{1,2}$ = 3.01 Hz, 2H, 2 × H-1A,D), 4.53 (d, $^2J_{Ph\text{-}C\underline{H}H}$ = 12.02 Hz, 2H, 2 × CHPh), 4.48 (d, $^2J_{Ph\text{-}C\underline{H}H}$ = 11.81 Hz, 2H, 2 × CHPh), 4.43-4.40 (m, 4H, 2 × H-3B,E, 2 × CHPh), 4.36 (dd, $^3J_{2,3}$ = 7.26 Hz, $^3J_{3,4}$ = 7.76 Hz, 2H, 2 × H-3A,D), 4.30(d, $^2J_{Ph\text{-}C\underline{H}H}$ = 12.83 Hz, 2H, 2 × CHPh), 4.24 (dd, $^2J_{6a,6b}$ = 10.25 Hz, $^3J_{5,6b}$ = 3.65 Hz, 2H, 2 × H-6bA,D), 4.11-4.04 (m, 6H, 4 × H-5B,E,C,F, 2 × H-6aC,F), 3.97 (t, $^3J_{3,4} = {}^3J_{4,5}$ = 8.59 Hz, 2H, 2 × H-4C,F), 3.89-3.85 (m, 4H, 2 × H-4A,D, 2 × H-6bC,F), 3.79-3.76 (m, 4H, 2 × H-4B,E, 2 × H-2C,F), 3.61 (d, $^2J_{Ph\text{-}C\underline{H}H}$ = 12.18 Hz, 2H, 2 × CHPh), 3.52 (dd, $^3J_{1,2}$ =3.40 Hz, $^3J_{2,3}$ = 9.74 Hz, 2H, 2 × H-2B,E), 3.49 (d, $^2J_{Ph\text{-}C\underline{H}H}$ = 11.97 Hz, 2H, 2 × CHPh), 3.45 (dd, $^3J_{1,2}$ = 3.05 Hz, $^3J_{2,3}$ = 9.90 Hz, 2H, 2 × H-2A,D), 2.89 (dd, $^2J_{6a,6b}$ = 10.67 Hz, $^3J_{5,6b}$ = 3.77 Hz, 2H, 2 × H-6aB,E), 2.65 (d, $^2J_{6a,6b}$ = 10.04 Hz, 2H, 2 × H-6bB,E)

^{13}C NMR ($CDCl_3$, 151 MHz): δ 185.40 (C-Ag), 140.25 (2C), 139.91 (2C), 139.54 (2C), 139.05 (2C), 139.02 (2C), 138.78 (2C), 138.22 (2C), 137.81 (2C) (16 × C-Ar-quat.), 134.61 (2 × N-$\underline{C}$=$\underline{C}$-N, $J_{C,Ag}$ = 7.0), 128.75-126.74 (80 × C-Ar-tert.), 124.45, 111.06 (4C, Ar-BzIm), 98.71 (2 × C-1C,F), 98.25 (2 × C-1A,D), 97.94 (2 × C-1B,E), 82.63 (2 × C-4C,F), 81.58 (4C) (2 × C-3A,D, 2 × C-4B,E), 80.31 (2 × C-3B,E), 80.15 (2 × C-2A,D), 79.74 (2 × C-3C,F), 79.16 (2 × C-2B,E), 77.03, 76.96 (2 × C-4A,D, 2 × C-2C,F), 76.65 (2 × Ph-$\underline{C}H_2$), 76.43 (2 × Ph-$\underline{C}H_2$), 74.23 (2 × Ph-$\underline{C}H_2$), 73.73 (2 × C-5C,F), 73.33 (2 × Ph-$\underline{C}H_2$), 73.24 (2 × Ph-$\underline{C}H_2$), 72.86 (2 × Ph-$\underline{C}H_2$), 72.57 (2 × Ph-$\underline{C}H_2$), 72.20 (2 × Ph-$\underline{C}H_2$), 71.69 (2 × C-5B,E), 71.15 (2 × C-6C,F), 70.97 (2 × C-5A,D), 67.80 (2 × C-6B,E), 49.98 (2 × C-6A,D)

$[\alpha]_D^{20}$ = +39.0 ($CHCl_3$, *c* = 0.1)

R_f = 0.28 (CyH/AcOEt 4:1)

HRMS(ESI) calculated for $C_{155}H_{158}AgClN_2Na_2O_{28}^{2+}$ $[M+Na]^{2+}$ 1341.4763, found 1341.4811. err. 3.6 ppm

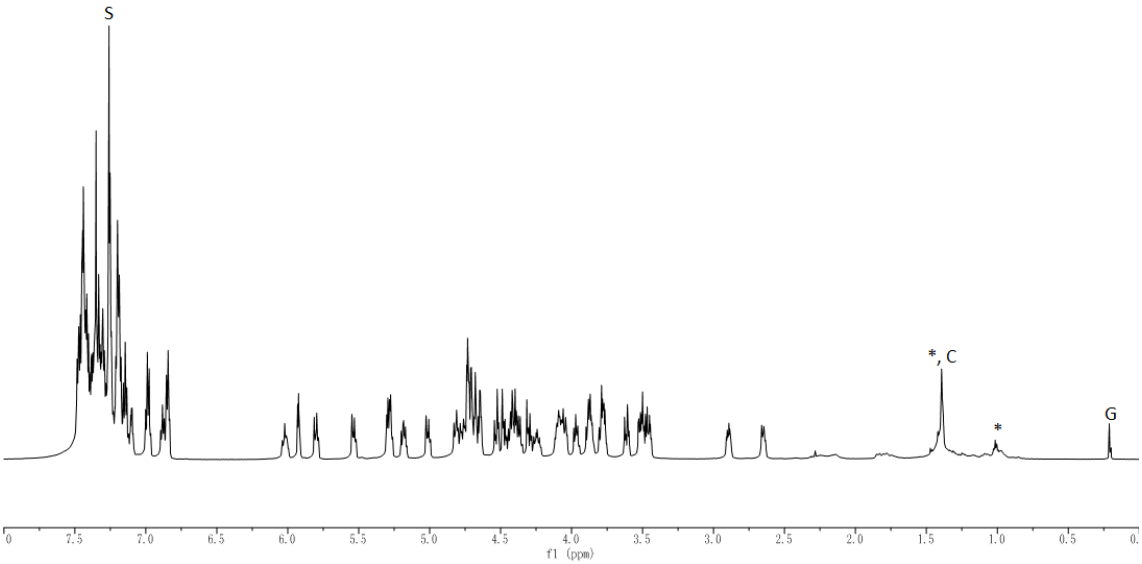

^{1}H NMR of **(α-BiCyD)AgCl** ($CDCl_3$, 600 MHz, 300 K)

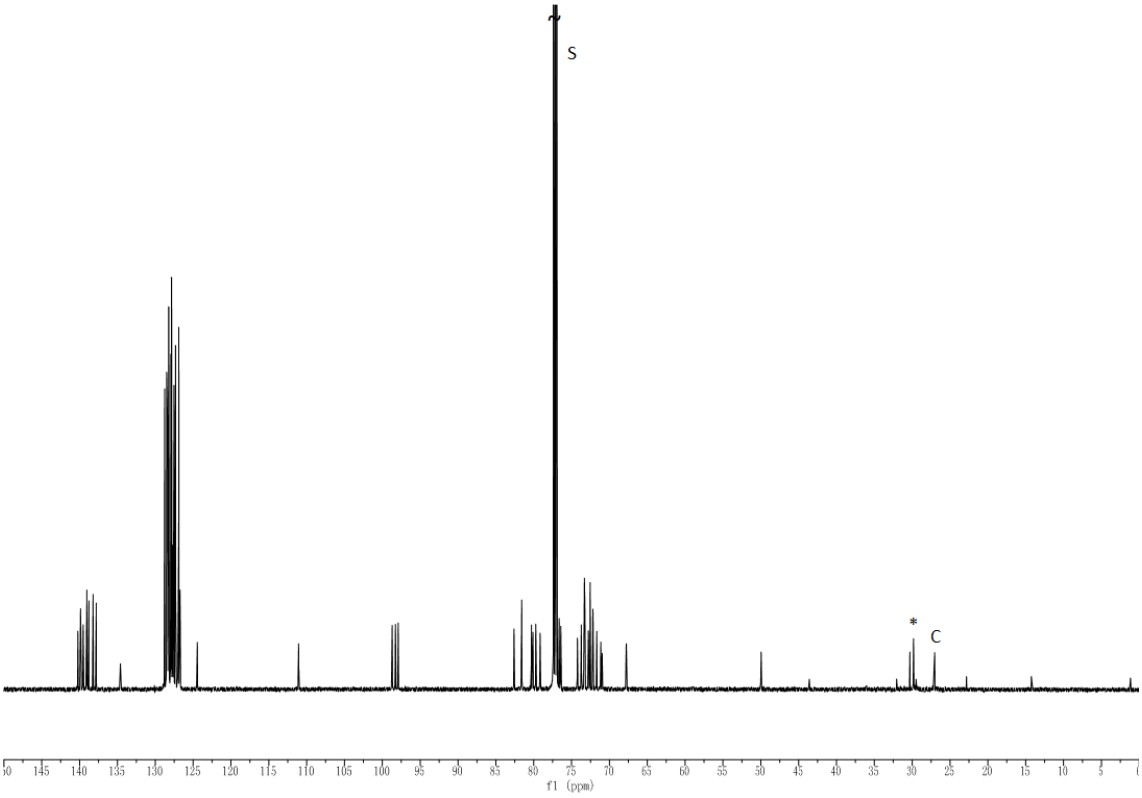

^{13}C NMR of **(α-BiCyD)AgCl** ($CDCl_3$, 151 MHz, 300 K)

(β-BiCyD)AgCl

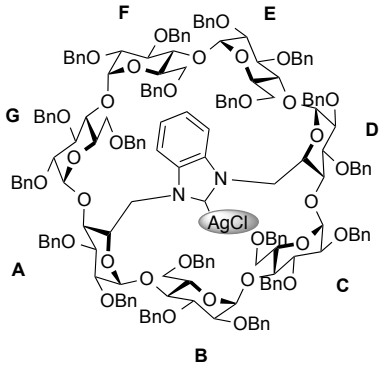

A mixture of compound **(β-BiCyD)HCl** (1 g, 0.34mmol, 1 eq.) and silver(I) oxide (1.2 g, 5.06 mol, 15 eq) was dissolved in anhydrous CH_3CN under a N_2 atmosphere. The reaction mixture was stirred at r.t. overnight. Then the silver oxide was filtered on a celite pad and the residue was washed with CH_3CN, and the solvents were evaporated. Silica gel chromatography of the residue (cyclohexane/ EtOAc: 4:1) gave **(β-BiCyD)AgCl** as a white foam (711 mg, 69%).

^{1}H NMR ($CDCl_3$, 600MHz): δ 7.50-6.65 (m, 99H, 95×H-Ar, 4H-Benzimidazole), 5.96 (d, 1H, $^3J_{1,2}$ = 3.71 Hz, H-1G), 5.93 (d, 1H, $^3J_{1,2}$=3.46Hz, H-1C), 5.78 (d, 1H, $^2J_{Ph\text{-}C\underline{H}H}$=11.16Hz, CHPh), 5.64(m, 1H, H-5A), 5.45-5.41(m, 3H, 3 × CHPh), 5.36(d, 1H, $^2J_{Ph\text{-}C\underline{H}H}$ =11.24Hz, CHPh), 5.23(d, 1H, $^2J_{Ph\text{-}C\underline{H}H}$ =11.81Hz, CHPh), 5.10(d, 1H, $^2J_{6a,6b}$=13.43Hz, H-6aD), 5.04-4.92(m, 6H, 6 × CHPh), 4.87(d, 1H, $^3J_{1,2}$=3.20Hz, H-1D), 4.74(m, 1H, H-5D), 4.68-4.65(m, 3H, H-1F, H-3C, H-6bA), 4.60-4.58(m, 3H, 2×H-1B,E, CHPh), 4.53-4.36(m, 14H, H-1A, H-3B, 12 × CHPh), 4.31-4.29 (m, 3H, H-3G, 2 × CHPh), 4.25-4.04 (m, 14H, 4×H-3E,F,A,D, H-6aA, H-6bD, H-6aG, 7 × CHPh), 3.97-3.90 (m, 4H, 2 × H-5B,C H-4C, H-6bG), 3.85-3.54(m, 16H, 6 × H-4A,B,D,E,F,G, 2 × H-2C,G, 2 × H-5F,G, H-6aC, H-6bC, H-baF, 3×CHPh), 3.48 (dd, 1H, $^2J_{6a,6b}$=11.31Hz, $^3J_{5,6b}$=5.03Hz, H-6bF), 3.43 (dd, 1H, $^3J_{2,3}$=10.05Hz, $^3J_{1,2}$=4.39Hz, H-2D), 3.36-3.31(m, 2H, 2×H-2B,F), 3.26-3.22 (m, 3H, 2×H-2A,E, CHPh), 3.09(bd, 1H, $^3J_{4,5}$=9.45, H-5E), 2.73(d, 1H, $^2J_{6a,6b}$ =10.80Hz, H-6aE), 2.59(d, 1H, $^2J_{6a,6b}$ =10.80Hz, H-6aB), 2.26(m, 2H, H-6bB, H-6bE)

^{13}C NMR ($CDCl_3$, 151MHz): δ 140.47, 140.10(2C), 139.99, 139.62, 139.09, 139.00, 138.94,138.91, 138.80, 138.70, 138.68, 138.63, 138.58, 138.52, 138.23, 138.10, 138.06, 137.34(19×C-Ar.quat.), 128.53-126.52 (m, 95×C-Ar-tert.), 135.14, 134.34 (2×N-$\underline{C}$=$\underline{C}$-N), 128.53-126.52 (m, 95×C-Ar-tert.), 124.34, 124.28, 112.32, 111.04 (4×C-benzimidazole), 100.73, 99.78, 98.60, 98.27, 97.54, 97.04, 96.93(7×C-1A,B,C,D,E,F,G), 83.10 (C-4F), 82.36 (C-4G), 82.18, 82.12 (C-4C, C-3A), 81.39 (C-3D), 80.72(C-4E), 80.52 (C-2A), 80.30, 80.19, 80.14(2C) (C-2D, C-4B, 2×C-3B,F), 79.99 (C-3G), 79.88(C-3E), 79.65(C-3C), 78.92, 78.57, 78.16, 77.87, 77.37 (5×H-2G,B,C,E,F), 77.00, 76.89, 76.48, 76.34 (2C) (5×Ph-$\underline{C}H_2$), 74.58 (C-4A), 74.47, 74.30 (2×Ph-$\underline{C}H_2$), 73.91 (C-4D), 73.79 (Ph-$\underline{C}H_2$) , 73.66 (C-5G), 73.44(C-5C), 73.33, 73.42 (2×Ph-$\underline{C}H_2$), 73.26, 73.09, 73.06, 72.75, 72.72, 72.68 (6×Ph-$\underline{C}H_2$), 72.62 (C-5D), 72.61, 72.58 (2×Ph-$\underline{C}H_2$), 72.23 (Ph-$\underline{C}H_2$), 72.14 (C-5F), 71.66 (2 × C-5E,B), 71.19 (C-5A), 70.97 (C-6C), 70.37 (C-6G), 69.70 (C-6F), 67.51 (C-6B), 67.30 (C-6E), 67.17 (C-6D), 49.03 (C-6A); C-Ag can not be observed.

$[\alpha]_D^{20}$= 56.9 ($CHCl_3$, c=0.5)

R_f = 0.28 (CyH/AcOEt 4:1)

HRMS(ESI) calculated for $C_{182}H_{186}AgN_2O_{33}^+$ $[M]^+$ 3034.1983, found 3034.2087, err. -3.4ppm

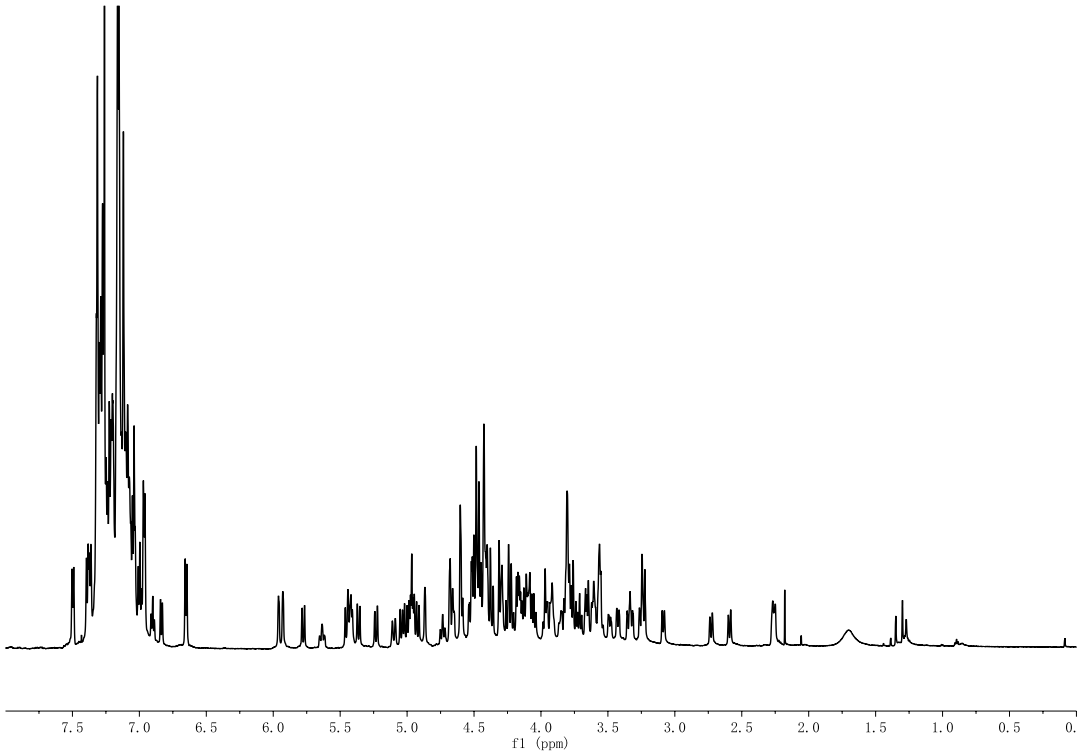

^{1}H NMR of **(β-BiCyD)AgCl** ($CDCl_3$, 600 MHz, 300 K)

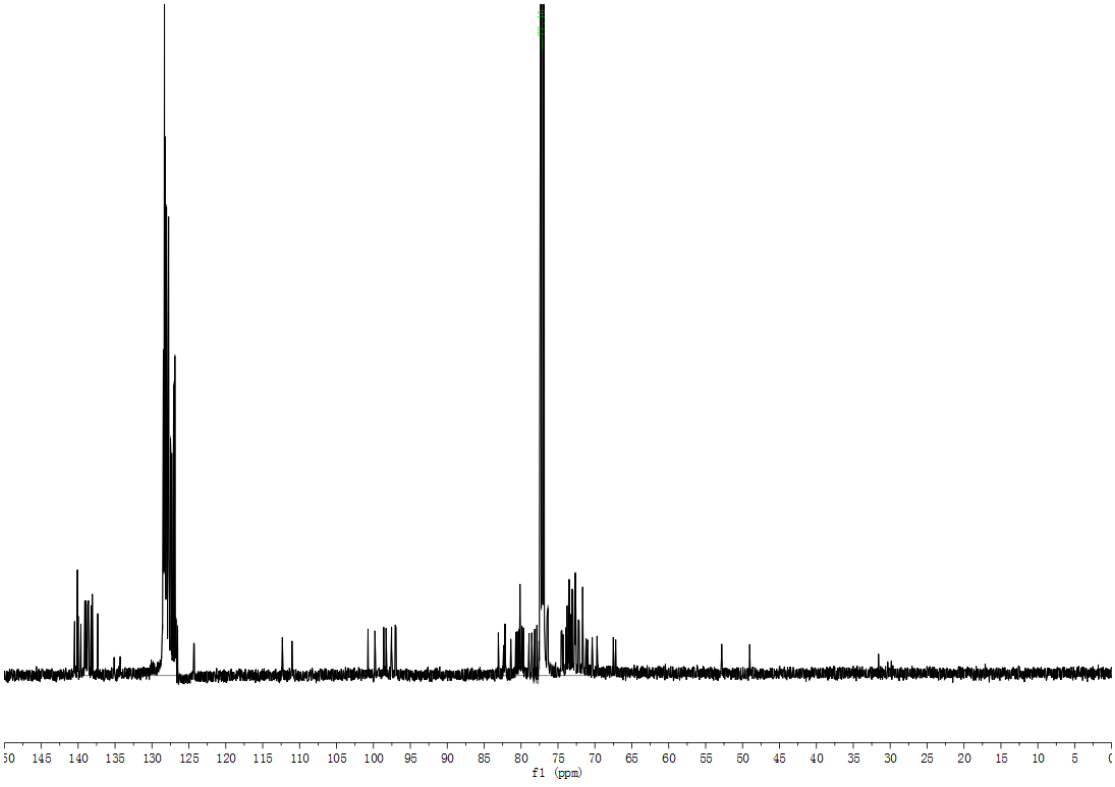

^{13}C NMR of **(β-BiCyD)AgCl** ($CDCl_3$, 151 MHz, 300 K)

(α-BiCyD)AuCl

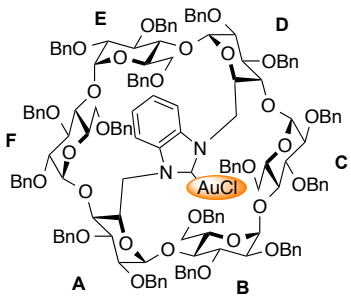

In a flame-dried two-neck flask under argon, a mixture of **(α-BiCyD)HCl** (100 mg, 39.5 µmol, 1 equiv.), chloro(dimethylsulfide) gold(I) (90 mg, 395 mmol, 10 equiv.) and potassium carbonate (55 mg, 395 mmol, 10 equiv.) was dissolved in in 2ml of acetonitrile previously degassed by three ”freeze-pump-thaw” cycles. The reaction mixture was stirred at 50°C overnight. Then the chloro(dimethylsulfide) gold(I) was filtered on a celite pad and the residue was washed with CH_3CN, and the solvents were evaporated. Silica gel chromatography of the residue (cyclohexane/ EtOAc: 5:1) gave the gold complex **(α-BiCyD)AuCl** as a white foam (30 mg, 28%).

^{1}H NMR ($CDCl_3$, 600MHz): δ 7.32-6.97 (m, 74H, 70 × H-Ar, 4H-BzIm), 6.84 (t, ^3J = 7.55 Hz, 4H, 4 × H-Ar), 6.73 (m, 6H, 6 × H-Ar), 6.65 (t, $^3J_{4,5}$ = $^3J_{5,6}$ = 10.4 Hz, 2H, 2 × H-5A, D), 5.78 (d, $^3J_{1,2}$ = 3.7 Hz, 2H, 2 × H-1C, F), 5.66 (d, $^2J_{\text{Ph-CHH}}$ = 10.8 Hz, 2H, 2 × CHPh), 5.30 (d, $^2J_{\text{Ph-CHH}}$ = 10,6 Hz, 2H, 2 × CHPh), 5.17 (d, $^2J_{\text{Ph-CHH}}$ = 11.2 Hz, 2H, 2 × CHPh), 5.15 (d, $^2J_{\text{Ph-CHH}}$ =11.2 Hz, 2H, 2 × CHPh), 5.09 (dd, $^3J_{2,3}$ = 7.6, $^3J_{3,4}$ = 8.3, 2H, 2×H-3C,F), 4.87 (d, $^2J_{\text{Ph-CHH}}$ = 11.5 Hz, 2H, 2 × CHPh), 4.68 (d, $^2J_{\text{Ph-CHH}}$ = 10.8Hz, 2H, 2 × CHPh), 4.63-4.53 (m, 14H, 2 × H-6aA,D, 2 × H-1B,E, 2 × H-1A,D, 8 × CHPh), 4.42-4.19 (m, 14H, 8 × CHPh, 2 × H-3B,E, 2 × H-3A,D, 2 × H-5B,E), 4.06-4.01 (m, 4H, 2 × H-5C,F, 2 × H-6aA,D), 3.92 (d, 2H, 2 × H-6bC,F), 3.86 (t, $^3J_{3,4}$ = $^3J_{4,5}$ =7.8 Hz, 2H, 2 × H-4C,F), 3.78-3.75 (m, 4H, 2 × H-4A,D, 2 × H-6aC,F), 3.67-3.64(m, 4H, 2 × H-4B,E, 2 × H-2C,F,), 3.45 (d, $^2J_{\text{Ph-CHH}}$ = 11.9 Hz, 2H, 2 × CHPh), 3.40 (dd, $^3J_{1,2}$ =3.7 Hz, $^3J_{2,3}$ = 9.6 Hz, 2H, 2 × H-2B,E), 3.37 (d, $^2J_{\text{Ph-CHH}}$ = 12.4 Hz, 2H, 2 × CHPh), 3.34 (dd, $^3J_{1,2}$ =2.9 Hz, $^3J_{2,3}$ = 9.8 Hz, 2H, 2 × H-2A,D), 2.92 (dd, $^2J_{6a,6b}$ = 10.5 Hz, $^3J_{5,6b}$ = 3.8 Hz, 2H, 2 × H-6aB,E), 2.54 (br d, 2H, 2 × H-6bB,E)

^{13}C NMR ($CDCl_3$, 151MHz): δ 177.97 (C-Au), 140.11 (2C), 139.89 (2C), 139.54 (2C), 139.16 (2C), 139.05 (2C), 138.80 (2C), 138.28 (2C), 137.86 (2C) (16 × C-Ar-quat.), 134.01 (2 × N-C=C-N), 128.78-126.70 (80 × C-Ar-tert.), 124.62, 110.98 (4C, Ar-BzIm), 98.59 (2 × C-1C,F), 98.28 (2 × C-1A,D), 97.82 (2 × C-1B,E), 82.57 (2 × C-4C,F), 81.91(2 × C-3A,D), 81.68(2 × C-4B,E), 80.45 (2 × C-3B,E), 80.26 (2 × C-2A,D), 79.66 (2 × C-3C,F), 79.19 (2 × C-2B,E), 77.36, 77.13 (2 × C-4A,D, 2 × C-2C,F), 76.68 (2 × Ph-CH_2), 75.47 (2 × Ph-CH_2), 74.30 (2 × Ph-CH_2), 73.69 (2 × C-5C,F), 73.30 (2 × Ph-CH_2), 73.23 (2 × Ph-CH_2), 72.69 (2 × Ph-CH_2), 72.56 (2 × Ph-CH_2), 72.18 (2 × Ph-CH_2), 71.35 (2 × C-5B,E), 71.11 (2 × C-6C,F), 70.10 (2 × C-5A,D), 67.91 (2 × C-6B,E), 49.75 (2 × C-6A,D)

$[\alpha]_D^{20}$= 56.6 ($CHCl_3$, c=1.0)

R_f = 0.28 (CyH/AcOEt 4:1)

HRMS(ESI) calculated for $C_{155}H_{158}AuClN_2O_{28}^+$ $[M+Na]^+$ 2750.0247, found 2750.0270, err. -0.8 ppm

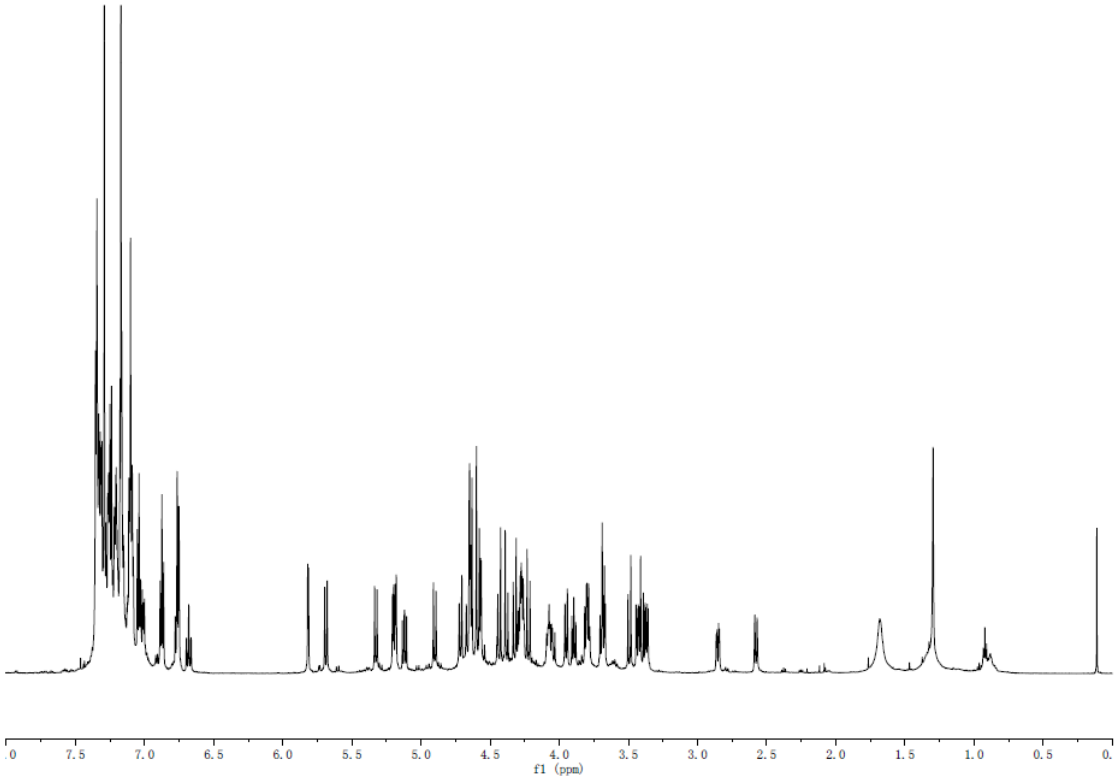

^{1}H NMR of **(α-BiCyD)AuCl** ($CDCl_3$, 600 MHz, 300 K)

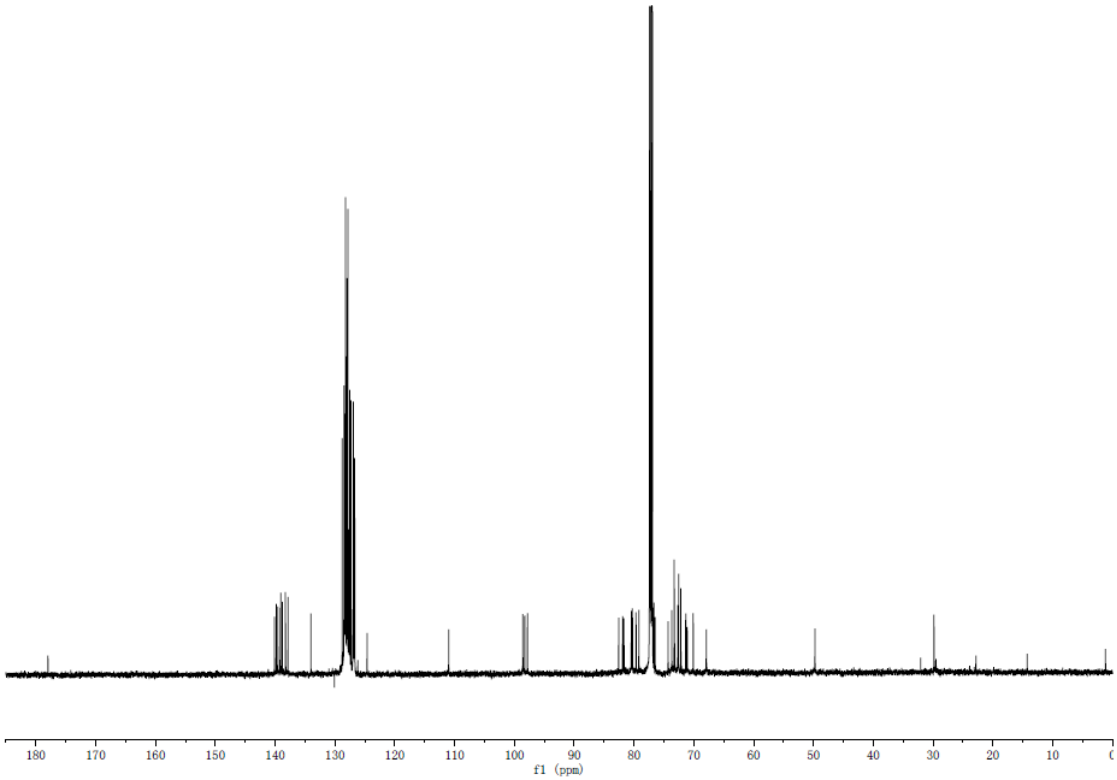

^{13}C NMR of **(α-BiCyD)AuCl** ($CDCl_3$, 151 MHz, 300 K)

(β-BiCyD)AuCl

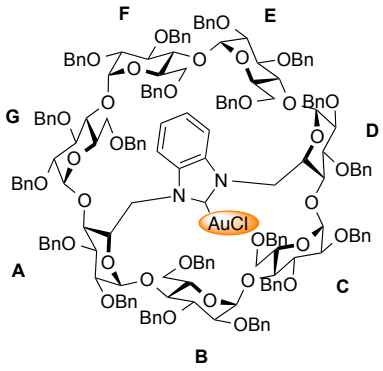

In a flame-dried two-neck flask under argon, a mixture of **(β-BiCyD)HCl** (300 mg, 0.102 mmol, 1 equiv.), chloro(dimethylsulfide) gold(I) (181 mg, 0.615 mmol, 6 equiv.) and potassium carbonate (170 mg, 1.23 mmol, 12 equiv.)was dissolved in in 5ml of acetonitrile previously degassed by three ”freeze-pump-thaw” cycles. The reaction mixture was stirred at 50˚C overnight. Then the chloro(dimethylsulfide) gold(I) was filtered on a celite pad and the residue was washed with CH_3CN, and the solvents were evaporated. Silica gel chromatography of the residue (cyclohexane/ EtOAc: 5:1) gave the gold complex **(β-BiCyD)AuCl** as a white foam.(190 mg, 58%).

^{1}H NMR ($CDCl_3$, 600MHz): δ 7.47-6.98(m, 95H, 92 × H-Ar, 3H-Benzimidazole), 6.87 (t, $^3J_{o,m}$=$^3J_{m,p}$ =7.17Hz, 1H, H-Ar), 6.79 (d, ^2J=7.89Hz, 1H, H- Benzimidazole), 6.68 (d, J=7.89Hz, 2H, 2×H-Ar), 6.12 (dt, $^3J_{4,5}$=$^3J_{5,6}$ =9.94, 1H, H-5A), 5.96 (d, $^3J_{1,2}$ = 3.55Hz, 1H, H-1G), 5.91 (d, $^3J_{1,2}$ = 3.80Hz, 1H, H-1C), 5.71 (d, $^2J_{\text{Ph-CHH}}$ = 11.20 Hz, 1H, CHPh) 5.46-5.33 (m, 4H, 3 × CHPh, H-6bD), 5.16 (d, $^2J_{\text{Ph-CHH}}$ = 12.05 Hz, 1H, CHPh), 5.04 (d, $^2J_{\text{Ph-CHH}}$ = 10.30 Hz, 1H, CHPh), 4.99-4.93 (m, 4H, 4 × CHPh), 4.87-4.83 (m, 3H, H-1D, H-5D, CHPh), 4.76-4.71 (m, 3H, H-1F, H-3C, H-6bA), 4.62-3.92 (m, 42H, 3 × H-1B,E,A, 6 × H-3A,B,D,E,F,G, 2 × H-5C, B, H-4C, H-6aG, H-6bG, H-6aA, H-6aD, 26 × CHPh), 3.85-3.56 (m, 12H, 5 × H-4G,A,D,E,B, 2 ×H-5F, G, 2 × H-2C,G, H-6aC,H-6bC, H-6aF), 3.51 (t, $^3J_{3,4}$ = 8.44 Hz $^3J_{4,5}$ = 9.50 Hz, 1H, H-4F), 3.44-3.42 (m, 2H, H-2D, H-6bF), 3.36-3.34 (m, 2H, 2 × H-B,F), 3.25-3.21(m, 3H, 2 × H-A,E, CHPh), 3.07 (d, $^3J_{4,5}$=10.02, 1H, H-5E), 2.82 (d, $^2J_{6a,6b}$ = 10.05 Hz, 1H, H-6aE), 2.56 (d, $^2J_{6a,6b}$ = 11.11 Hz, 1H, H-6aB), 2.25 (d, $^2J_{6a,6b}$ = 10.02 Hz, 1H, H-6bB), 2.21 (d, $^2J_{6a,6b}$ = 11.66 Hz, 1H, H-6bE);

^{13}C NMR ($CDCl_3$, 151MHz): δ 179.87 (C-Au), 140.38, 140.19, 140.30, 139.92, 139.68, 139.04, 139.02, 138.90, 138.87, 138.83, 138.79, 138.76, 138.66, 138.58, 138.56, 138.30, 138.12, 138.09, 137.43 (19×C-At.quat.), 134.45, 133.85 (2×N-C=C-N), 128.54-126.54(m, 95×C-Ar-tert.), 124.55, 124.45, 112.27, 111.08 (4×C-benzimidazole), 100.75, 99.49, 98.74, 98.10, 97.53, 97.02, 96.64(7×C-1A,B,C,D,E,F,G), 83.20(C-4F), 82.37, 82.31(C-3A, C-4G), 82.08(C-4C), 81.40 (C-3D), 80.87(C-4E), 80.55(C-2E), 80.26(2C), 80.11 (3×C-3F, B, G), 80.04(C-4B), 79.94(C-2D), 79.78(C-3E), 79.50(C-3C), 78.97(C-2F), 78.62(C-2B), 78.28(C-2A), 77.81(C-2C), 77.63(C-2G), 76.99, 76.78, 76.61, 76.50, 76.29, 74.59, 74.36(7×Ph-CH_2), 74.30(C-4A), 73.83(C-5C), 73.58(Ph-CH_2), 73.56(C-4D), 73.54(Ph-CH_2), 73.40(Ph-CH_2), 73.35(C-5G), 73.06(2C), 72.92, 72.75, 72.61(2C), 72.51(2C), 72.33(9×Ph-CH_2), 72.08, 72.06(2×C-5D,F), 71.61(C-5E), 71.24 (C-5B), 70.96(C-6C), 70.55(C-5A), 70.25(C-6G), 69.90(C-6F), 67.66(C-6B), 67.29(C-6E), 52.37(C-6D), 48.83(C-6A);

$[\alpha]_D^{20}$=77.5 ($CHCl_3$, c=1.0)

R_f = 0.31 (CyH/AcOEt 4:1)

HRMS(ESI) calculated for $C_{182}H_{186}AuClN_2O_{33}^+$ $[M+Na]^+$ 3182.2184, found 3182.2046, err. 4.4ppm

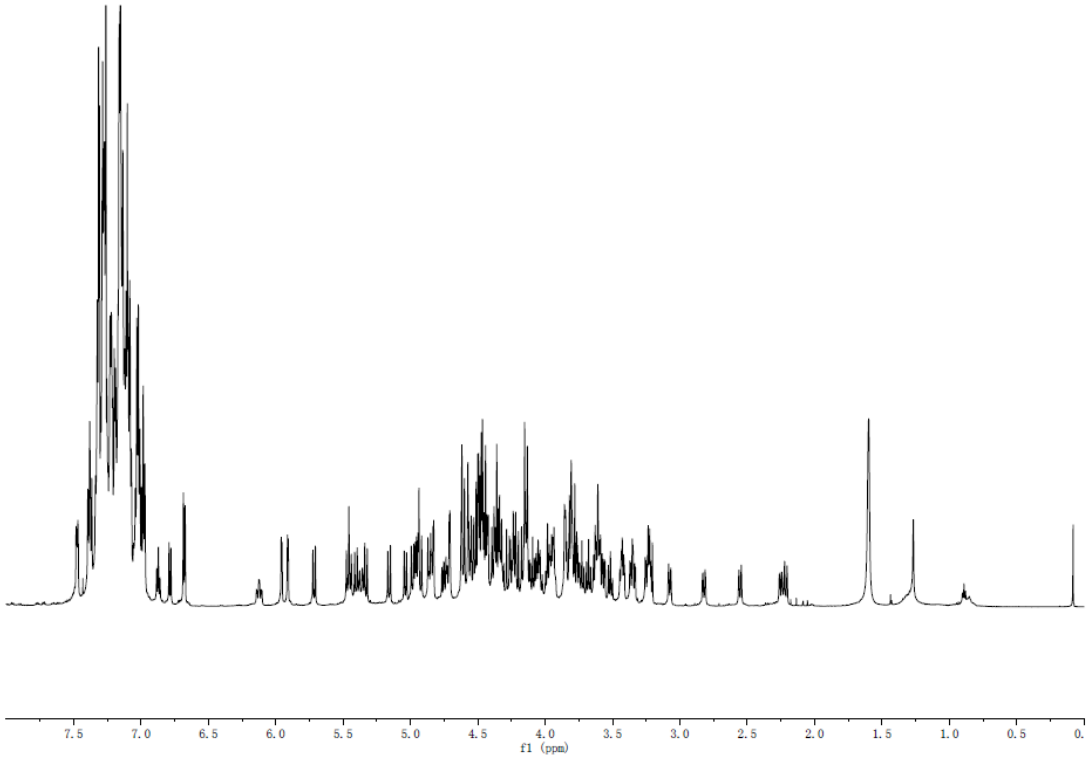

^{1}H NMR of **(β-BiCyD)AuCl** ($CDCl_3$, 600 MHz, 300 K)

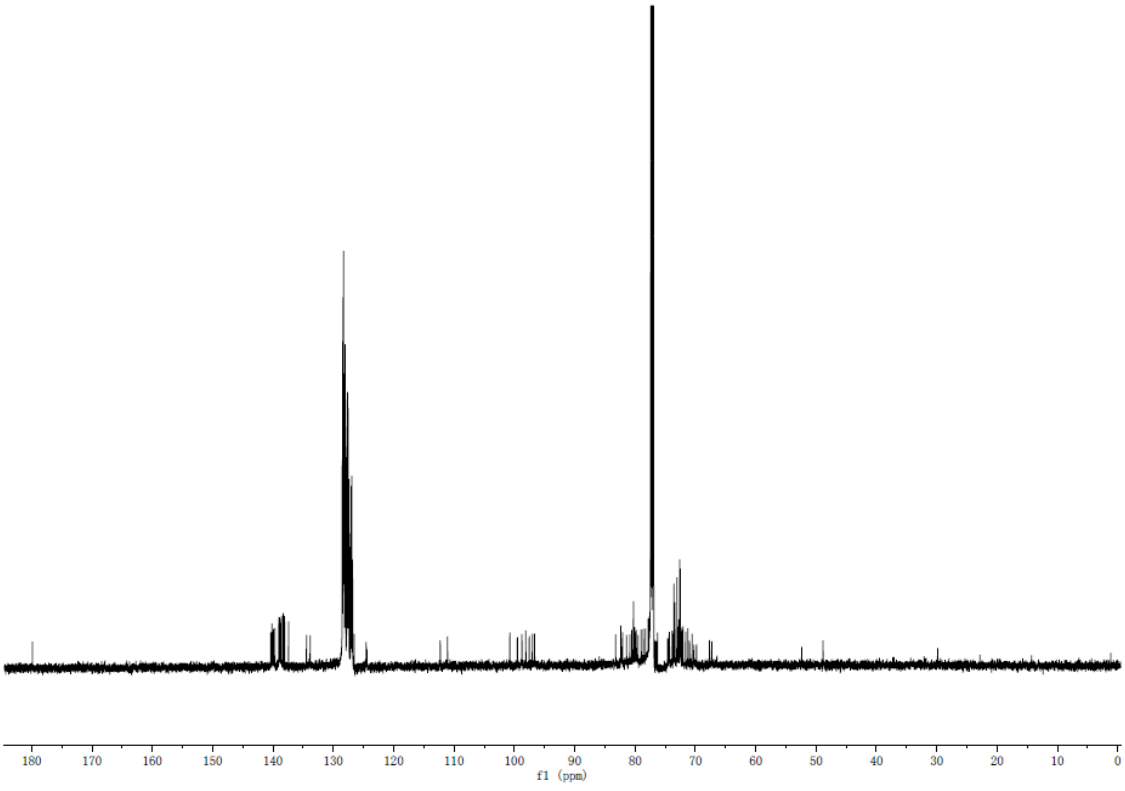

^{13}C NMR **(β-BiCyD)AuCl** ($CDCl_3$, 151 MHz, 300 K)

Compound 7α

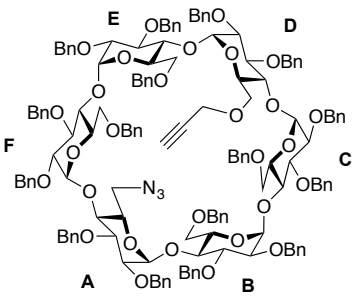

To a solution of **5α** (1.14 g, 0.468 mmol, 1 eq) in anhydrous DMF (15 mL) under nitrogen, NaH (60% in oil, 94 mg, 2.34 mmol, 5 eq.) was added in small portions. The reaction mixture was stirred for 1h, then propargyl bromide (80% in toluene, 270 µL, 2.34 mmol, 5 eq) was added dropwise at R.T. The reaction mixture was stirred at R.T overnight in the dark. The solvent was evaporated and the residue was dissolved in EtOAc. Water was added and the layers were separated. The aqueous layer was extracted with EtOAc 3 times and the combined organic layers were washed with brine, dried over $MgSO_4$, filtered and evaporated. The residue was purified by silica gel chromatography (CyH:EtOAc=3:1) to afford the compound **7α** (818 mg, 71%) as a white foam.

^{1}H NMR ($CDCl_3$, 400MHz): δ 7.33-7.10 (m, 80H, 80 × H-Ar), 5.24-5.04 (m, 7H, 3 × H-1, 4 × CHPh), 5.01-5.00 (m, 2H, 1 × CHPh, 1 × H-1), 4.98 (d, $^2J_{1,2}$ = 3.3Hz, 1H, H-1), 4.95 (d, $^2J_{1,2}$ = 3.3Hz, 1H, H-1), 4.89-4.81 (m, 11H, 11 × CHPh), 4.59-4.30 (m, 16H, 16 × CHPh), 4.16-3.39 (m, 32H, 12 × H-6, 6 × H-3, 6 × H-4, 6 × H-5, 2 × O-$\underline{CH_2}$-CCH), 2.24 (t, ^4J = 2.1Hz, 1H, O-CH_2-C$\underline{C}$H)

^{13}C NMR ($CDCl_3$, 100MHz): δ139.49, 139.44, 139.41, 139.39, 139.38, 139.27, 138.66, 138.63, 138.43, 138.40(2C), 138.24, 138.17, 138.15, 138.05, 138.02 (16 × C-Ar-quat.), 128.51-126.68 (80 × C-Ar-tert.), 98.90, 98.81, 98.78, 98.71, 98.63, 98.01(6 × C-1), 81.42, 81.27, 81.19, 81.08, 80.98, 80.94, 80.90, 80.81, 80.73, 80.58, 79.89, 79.80, 79.66, 79.32, 79.19, 78.22, 78.14, 76.90, 76.38 (19C, 6 × C-2, 6 × C-3, 6 × C-4, O-CH_2-$\underline{C}$CH), 76.33, 76.30, 76.06, 75.94, 74.59, 74.51 (6 × CHPh), 74.42 (O-CH_2-$\underline{C}\underline{C}$H), 73.57 (3C), 73.50 (2C), 73.32, 73.11 (2C), 72.60, 72.53 (10 × CHPh), 71.98 (2C), 71.90 (2C), 71.71, 70.62 (6 × C-5), 69.69, 69.64, 69.51, 69.22, 62.27 (5 × C-6), 58.52 (O-$\underline{C}H_2$-CCH), 52.19 (C-6).

$[\alpha]_D^{20}$ = +39 ($CHCl_3$, c=0.1)

R_f = 0.6 (CyH/AcOEt 3:1)

HRMS(ESI) $[C_{151}H_{157}N_3O_{29}\ Na\ ]^+$: calcd. 2499.0800, found 2499.1052, err. 6.8 ppm

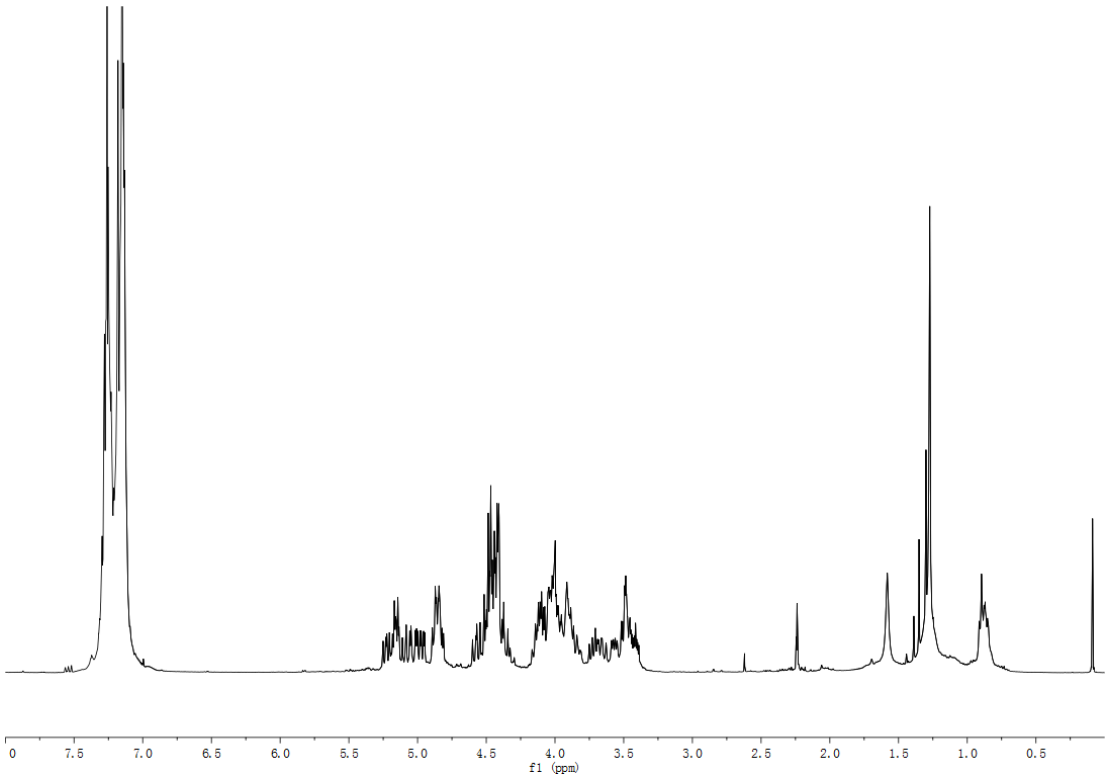

^{1}H NMR of Compound **7**α ($CDCl_3$, 400 MHz, 300 K)

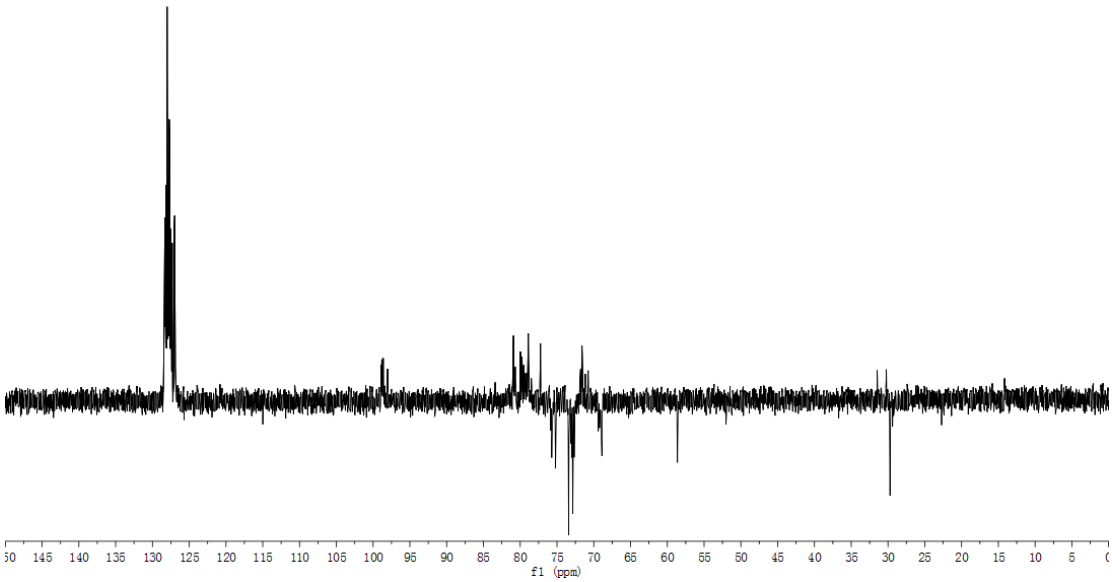

^{13}C dept NMR of Compound **7α** ($CDCl_3$, 100 MHz, 300 K)

Triazole-capped α-CD

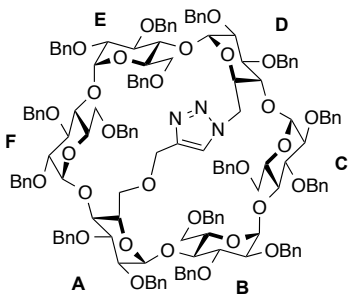

N,N-Diisopropylethylamine (340 µl, 1.64 mmol, 4 equiv.), Tris[(1-benzyl-1H-1,2,3-triazol-4-yl) methyl amine (87 mg, 0.164 mmol, 0.4 equiv.), and Tetrakis (acetonitrile) copper(I) hexafluorophosphate (61 mg, 0.164 mmol, 0.4 equiv.) were added to a solution of **7α** (1 g, 0.41 mmol, 1 equiv.) in anhydrous DMF (8 ml) at R.T under Ar in a microwave vial. The reaction mixture was heated at 100˚C under microwaves for 1h. Then the solvent was evaporated and the residue was purified by silica gel chromatography (CyH: EtOAc = 4:1) to give the compound **triazole-capped α-CD** as a white foam (725 mg, 72%).

^{1}H NMR ($CDCl_3$, 600MHz): δ 7.39-6.91 (m, 81H, 80 × H-Ar, H-triazole), 5.53-5.51 (m, 2H, 2 × CHPh), 5.34 (d, $^{2}J_{Ph\text{-}C\underline{H}H}$ = 11.1 Hz, 1H, CHPh), 5.31(d, $^{2}J_{1,2}$ = 3.5Hz, 1H, H-1F), 5.25-5.24 (m, 2H, CHPh, H-1C), 5.06-5.03 (m, 2H, 2 × CHPh), 4.92-4.86 (m, 6H, 5 × CHPh, H-6bD), 4.81(d, $^{2}J_{Ph\text{-}C\underline{H}H}$ = 10.6 Hz, 1H, CHPh), 4.76-4.75(m, 2H, 2 ×H-1A,D), 4.72(d, $^{2}J_{Ph\text{-}C\underline{H}H}$ = 12.0 Hz, 1H, CHPh), 4.66-4.65(m, 2H, CHPh, H-1B), 4.61(d, $^{2}J_{1,2}$ = 3.1Hz, 1H, H-1E), 4.55(d, ^{2}J = 12.0 Hz, 1H, 1 × O-C$\underline{H}_2$-C=C), 4.50-4.10 (m, 26H, 18 × CHPh, 1 × O-C$\underline{H}_2$-C=C, 2 × H-5A,D, 3 × H-3C,F,B, H-6aD, H-6aB), 4.04-3.91(m, 7H, 3 × H-3A,D,E, 2 × H-5B,C, H-6aA, H-6bC), 3.85-3.78(m, 6H, 3 × H-4E,F,B, H-5F, H-6aF, H-6bF), 3.72-3.68(m, 2H, H-4C, H-6aC), 3.55-3.31(m, 11H, 6 ×H-2A,B,C,D,E,F, 2 × H-4A,D, H-5E, H-6bA, H-6bB), 2.91(br d, ^{2}J =10.9, 1H, H-6aE), 2.81(dd, $^{2}J_{6a,6b}$ = 11.7 Hz, $^{3}J_{5,6b}$ = 3.5 Hz, 1H, H-6bE)

^{13}C NMR ($CDCl_3$, 151MHz): δ 148.27 (CH=$\underline{C}$-N), 139.88, 139.71, 139.58, 139.53, 139.49, 139.45, 138.83, 138.79, 138.54, 138.47, 138.25, 138.12, 138.00, 137.85, 137.68(2C) (16 × C-Ar-quat.), 128.59-126.15 (80 × C-Ar-tert.), 119.66 ($\underline{C}$H=C-N), 101.18, 100.93, 100.66, 100.56, 98.56(2C) (6×C-1A,B,C,D,E,F), 83.58(C-4C), 82.58 (C-4F), 82.64 (C-4D), 81.99 (C-4B), 81.66 (C-4E), 81.30, 80.97, 80.87(2C), 80.56(2C), 80.35 (6 × C-3A,B,C,D,E,F, C-4A), 80.01(C-2A), 79.32(C-2D), 78.76(C-2E), 78.41(C-2B), 78.01(C-2F), 77.36(C-2C), 76.76, 76.74, 76.27, 76.20, 74.45, 74.13, 73.53, 73.41, 73.38, 73.34(10× Ph-$\underline{C}H_2$), 73.23(C-6A), 73.19, 73.06, 72.98, 72.88(4× Ph-$\underline{C}H_2$), 72.87 (C-5C), 72.73 (C-5D), 72.57 (C-5A), 72.20 (Ph-$\underline{C}H_2$), 72.01 (C-5F), 71.88(C-5B), 71.82 (CHPh), 71.73(C-5E), 69.96 (C-6C), 69.43 (C-6F), 68.54(C-6B), 67.76 (C-6E), 65.83(CH_2-O-$\underline{C}$), 52.51(C-6D)ppm.

$[\alpha]_D^{20}$= 43.5 ($CHCl_3$, c=0.5)

R_f = 0.33 (CyH/AcOEt 3:1)

HRMS(ESI) calcd. $[C_{151}H_{157}N_3O_{29} + Na\ ]^+$: 2499.0795, found 2499.0890 err. -3.8 ppm

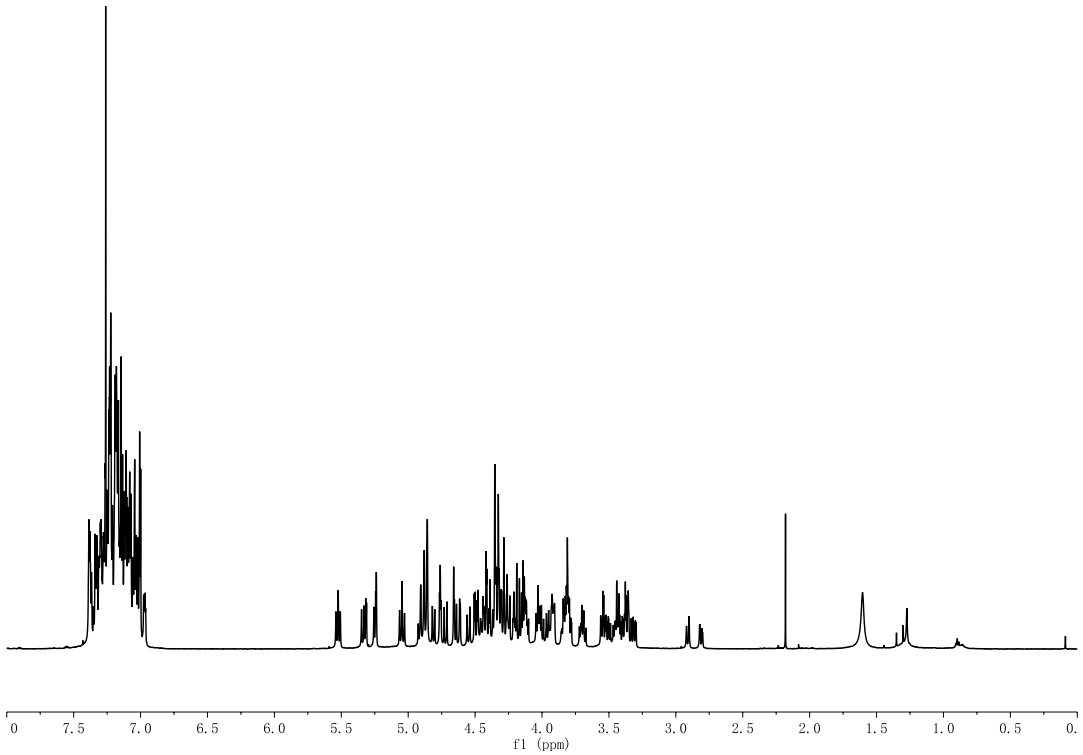

^{1}H NMR of **Triazole-capped α-CD** ($CDCl_3$, 600 MHz, 300 K)

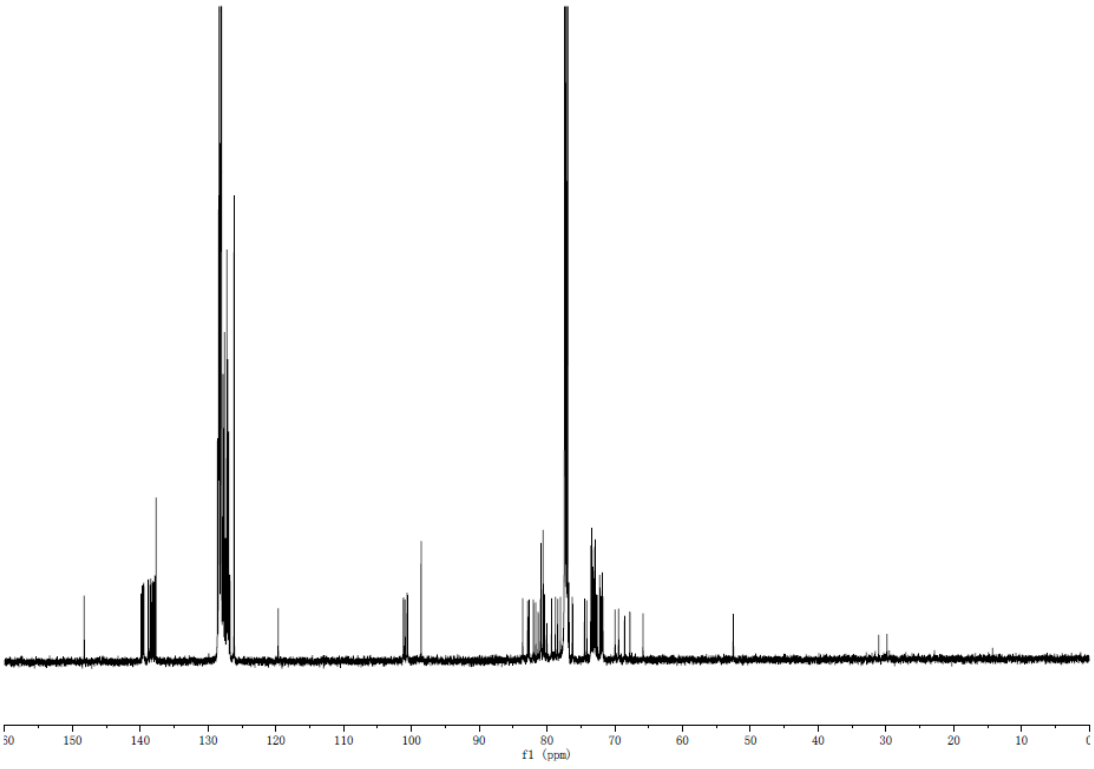

^{13}C NMR of **Triazole-capped α-CD** ($CDCl_3$, 151 MHz, 300 K)

(α-TriCyD)HI

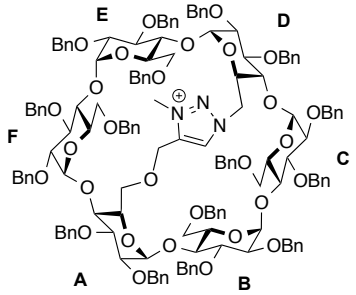

Triazole-capped α-CD obtained in the previous step (100mg, 0.04mmol) was added in Iodomethane (3ml) at 50°C under N_2 overnight. Then the solvent was evaporated and the residue was purified by silica gel chromatography (DCM: MeOH= 95:5) to give the compound **(α-TriCyD)HI** as a yellow foam (100mg, quant).

^{1}H NMR ($CDCl_3$, 600MHz): δ 7.53 (s, 1H, H-triazolium), 7.36-6.92 (m, 80H, 80 × H-Ar), 5.44-5.31 (m, 5H, 3 × CHPh, H-6aD, H-1F), 5.17 (d, $^2J_{Ph\text{-}C\underline{H}H}$ = 10.3 Hz, 1H, CHPh), 5.09-5.07 (m, 2H, H-1F, 1 × O$C\underline{H}_2$-N), 4.98-4.95 (m, 3H, 3 × CHPh), 4.86-4.76 (m, 6H, 5 × CHPh, H-1A), 4.69 (s, $^2J_{1,2}$ = 3.7Hz, 1H, H-1B), 4.67 (d, $^2J_{Ph\text{-}C\underline{H}H}$ = 11.7 Hz, 1H, CHPh), 4.62-4.60 (m, 3H, 2 × H-1D,E, O$C\underline{H}_2$-N), 4.58-4.51 (m, 6H, 6 × CHPh), 4.45-4.43 (m, 2H, 2 × CHPh), 4.39-4.28 (m, 9H, H-6aB, H-6bC, 7 × CHPh), 4.21-3.94 (m, 14H, H-6bD, H-6aF, H-6bA, 2 × CHPh, 2 × H-5A,D, 6 × H-3C,F,E,D,A,B, H-4B), 3.85(m, 1H, H-5C), 3.81-3.80 (m, 4H, H-5B, 3 × CH_3), 3.74-3.64 (m, 5H, H-6aA, H-6bF, 2 × H-4E,F, H-5F), 3.57-3.41 (m, 9H, H-6bB, H-6aC, 4 × H-2C,F,A,B, 3 × H-4A,D,C), 3.36 (dd, $^3J_{1,2}$ =2.4 Hz, $^3J_{2,3}$ = 3.2 Hz, 1H, H-2D), 3.27 (dd, $^3J_{1,2}$ =3.5 Hz, $^3J_{2,3}$ = 3.1 Hz, 1H, H-2E), 3.16 (br d, ^2J =9.8, 1H, H-5E), 2.84 (br d, ^2J =10.6, 1H, H-6aE), 2.59 (dd, $^2J_{6a,6b}$ = 11.1 Hz, $^3J_{5,6b}$ = 2.6 Hz, 1H, H-6bE);

^{13}C NMR ($CDCl_3$, 151MHz): δ 144.37 (CH=$\underline{C}$-N), 139.69, 139.37, 139.33, 139.22, 139.19, 139.15, 138.61, 138.58, 138.29, 138.10, 137.93, 137.77, 137.73, 137.66, 137.54, 136.81 (16 × C-Ar-quat.), 128.84-126.06 (80 × C-Ar-tert.), 125.66 ($\underline{C}$H=C-N), 101.86, 101.23, 100.48, 100.29, 99.01, 97.96 (6×C-1A,B,C,D,E,F), 83.68, 83.12, 82.92,81.68 (4×C-4D,F,E,C), 81.23(C-4B), 81.03(C-3A), 80.74(C-3B), 80.47 (C-3F), 80.41 (C-4A), 80.03 (C-3E), 79.96 (C-2A), 79.73 (2C)(2×C-3C,D), 78.88(C-2D), 78.63(C-2E), 78.01(C-2B), 77.87 (C-2C), 75.66 (Ph-$\underline{C}H_2$), 75.60 (C-2F), 75.55, 75.11, 75.94, 75.19, 75.14, 74.02 (2C)(7× Ph-$\underline{C}H_2$), 73.91 (C-6F), 73.47 (C-5C), 73.46, 73.43, 73.32, 73.20, 72.99, 72.77 (6× Ph-$\underline{C}H_2$), 72.70, 72.66 (2×C-5D,F), 72.56, 72.40 (2× Ph-$\underline{C}H_2$), 72.23(C-5E), 72.17(C-5A), 72.06 (C-5B), 71.24(C-6C), 70.02(C-6A), 67.99(C-6B), 66.92 (C-6E), 63.14(CH_2-O-$\underline{C}$), 56.12 (C-6D), 40.69 ($\underline{C}H_3$);

$[\alpha]_D^{20}$= 41.2 ($CHCl_3$, c=1)

R_f = 0.35 (DCM: MeOH= 95:5)

HRMS(ESI) calcd. $[C_{152}H_{160}N_3O_{29}]^+$: 2491.1132, found 2491.1098 err. 1.4 ppm

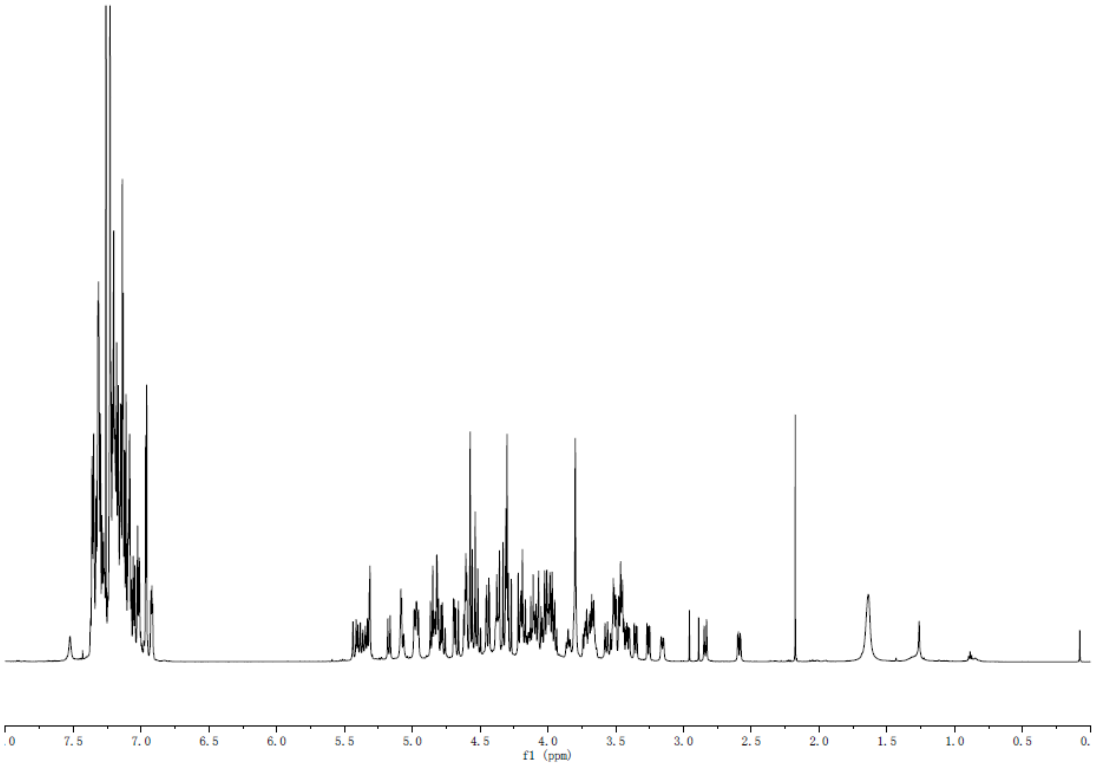

^{1}H NMR of **(α-TriCyD)HI** ($CDCl_3$, 600 MHz, 300 K)

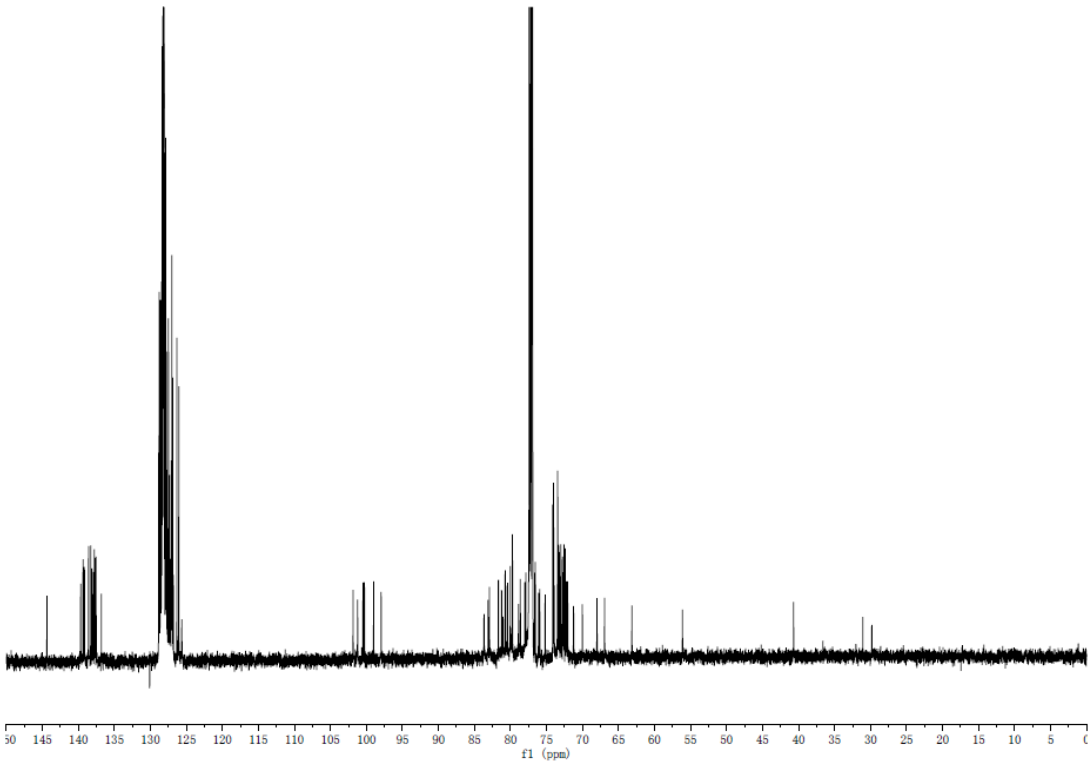

^{13}C NMR **of (α-TriCyD)HI** ($CDCl_3$, 151 MHz, 300 K)

(α-TriCyD)AgI

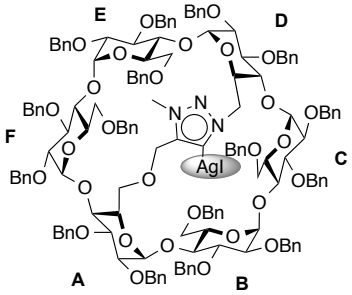

A mixture of perbenzylated deoxy triazolium **(α-TriCyD)HI** (200mg, 0.08 mmol, 1eq.) and silver(I) oxide (950 mg, 4mmol, 50eq.) was dissolved in anhydrous CH_3CN under a N_2 atmosphere. The reaction mixture was stirred at r.t. overnight. Then the silver oxide was filtered on a Celite pad and the residue was washed with CH_3CN, and the solvents were evaporated. Silica gel chromatography of the residue (cyclohexane/ EtOAc 4:1) gave the silver complex **(α-TriCyD)AgI** (75 mg, 34 %).

^{1}H NMR ($CDCl_3$, 600MHz): δ 7.45-6.94 (m, 80H, 80 × H-Ar), 5.69 (d, $^2J_{Ph\text{-}C\underline{H}H}$ = 11.3 Hz, 1H, CHPh), 5.59(t, $^3J_{4,5}$ = $^3J_{5,6}$ = 9.1 Hz, 1H, H-5D), 5.50 (d, $^2J_{Ph\text{-}C\underline{H}H}$ = 11.5 Hz, 1H, CHPh), 5.46 (d, $^2J_{Ph\text{-}C\underline{H}H}$ = 10.5 Hz, 1H, CHPh), 5.30 (d, $^2J_{Ph\text{-}C\underline{H}H}$ = 11.5 Hz, 1H, CHPh), 5.24 (d, $^3J_{1,2}$ = 3.2Hz, 1H, H-1F), 5.23 (d, $^2J_{Ph\text{-}C\underline{H}H}$ = 11.0 Hz, 1H, CHPh)5.22(d, $^3J_{1,2}$ = 3.2Hz, 1H, H-1C), 5.17 (d, $^2J_{Ph\text{-}C\underline{H}H}$ = 11.5 Hz, 1H, CHPh), 5.10 (dd, $^3J_{2,3}$=10.2 Hz, $^3J_{3,4}$ =8.6 Hz, 1H, H-3F), 5.05 (td, $^3J_{4,5}$ =10.3 Hz, $^3J_{5,6}$ = 7.1 Hz, 1H, H-5A), 5.03 (d, $^2J_{Ph\text{-}C\underline{H}H}$ = 11.4 Hz, 1H, CHPh), 4.99 (dd, $^3J_{2,3}$=10.2 Hz, $^3J_{3,4}$ =8.7 Hz, 1H, H-3C), 4.93-4.84 (m, 4H, 4 × CHPh, H-6aD), 4.79-4.74 (m, 3H, CHPh, H-1A, H-3B), 4.72 (d, $^2J_{Ph\text{-}C\underline{H}H}$ = 8.5 Hz, 1H, CHPh), 4.70 (d, $^2J_{Ph\text{-}C\underline{H}H}$ = 8.5 Hz, 1H, CHPh), 4.60 (d, $^3J_{1,2}$ = 3.2Hz, 1H, H-1D), 4.59-4.53 (m, 5H, 2 ×H-1B,E, H-5B, 2 × CHPh), 4.50 (d, $^2J_{Ph\text{-}C\underline{H}H}$ = 12.8 Hz, 1H, CHPh), 4.44-4.36 (3H, 2 × CHPh, H-5C), 4.31-4.13 (m, 19H, 3 ×H-3A,D,E, H-6bD, H-6aF, H-6aB, H-6aA, CH_2-O-C$\underline{H}$, 11 × CHPh), 4.06-4.02 (m, 3H, 2 × CHPh, H-5F), 3.97 (br d, ^2J =9.7, 1H, H-6aC), 3.87 (br d, ^2J =10.0, 1H, H-5E), 3.75-3.72 (m, 2H, H-4B, CH_2-O-C$\underline{H}$), 3.65-3.62 (m, 2H, H-4E, H-6bC), 3.58-3.36 (m, 10H, 4 × H-4C,D,F,A, H-6bF, H-6bA, 4 × H-2C,F,A,D), 3.31-3.29 (m, 2H, 2 × H-2B,E), 3.20 (br d, ^2J =11.6, 1H, H-6bB), 3.02 (s, 3H, CH_3), 2.64(br d, ^2J =9.6, 1H, H-6aE), 2.58 (dd, $^2J_{6a,6b}$ = 10.7 Hz, $^3J_{5,6b}$ = 2.5 Hz, 1H, H-6bE);

^{13}C NMR ($CDCl_3$, 151MHz): δ 146.76 (CH_2-C-N), 140.83, 140.78, 140.64, 140.61, 140.47, 140.17, 139.99, 139.40(2C), 139.09, 138.80, 138.85(2C), 138.51, 138.31(2C) (16 × C-Ar-quat.), 128.65-126.30 (80 × C-Ar-tert.), 101.34, 101.31, 100.98(2C), 100.81, 100.72 (6×C-1A,B,C,D,E,F), 84.70(C-4F), 84.13(C-4C), 82.68(C-4B), 81.96(C-4E), 81.75(C-4D), 81.16(C-3A), 80.99, 80.92(C-3D, C-4A), 80.64(C-2A), 80.35(C-2D), 79.98, 79.96(C-3B, C-3E), 79.19, 79.15, 79.11, 78.87(C-3F, C-3C, C-2B, C-2E), 77.74(C-2F), 77.44(C-2C), 76.77, 76.74, 76.40, 76.35, 74.59, 74.22, 73.78(7× Ph-$\underline{C}H_2$), 73.73(C-6A), 73.26, 73.07, 73.04, 73.01, 72.90, 72.81(6 × Ph-CH2), 72.77 (C-5A), 72.75 (C-5F), 72.73 (Ph-$\underline{C}H_2$), 72.63 (C-5C), 72.41 (Ph-$\underline{C}H_2$), 72.07 (Ph-$\underline{C}H_2$), 71.77 (C-5B), 71.75 (C-6F), 71.57 (C-5E), 71.41 (C-5D), 70.80 (C-6C), 69.45(C-6B), 68.24(C-6E), 62.50(CH2-O-C), 56.71(C-6D), 34.79 (CH_3)

$[\alpha]_D^{20}$=38.4 ($CHCl_3$, c=0.5)

R_f = 0.25 (CyH/AcOEt 3:1)

HRMS(ESI) calcd. $[C_{152}H_{159}AgIN_3O_{29} + Na]^+$: 2746.9047, found: 2746.9132, err. -3.1 ppm

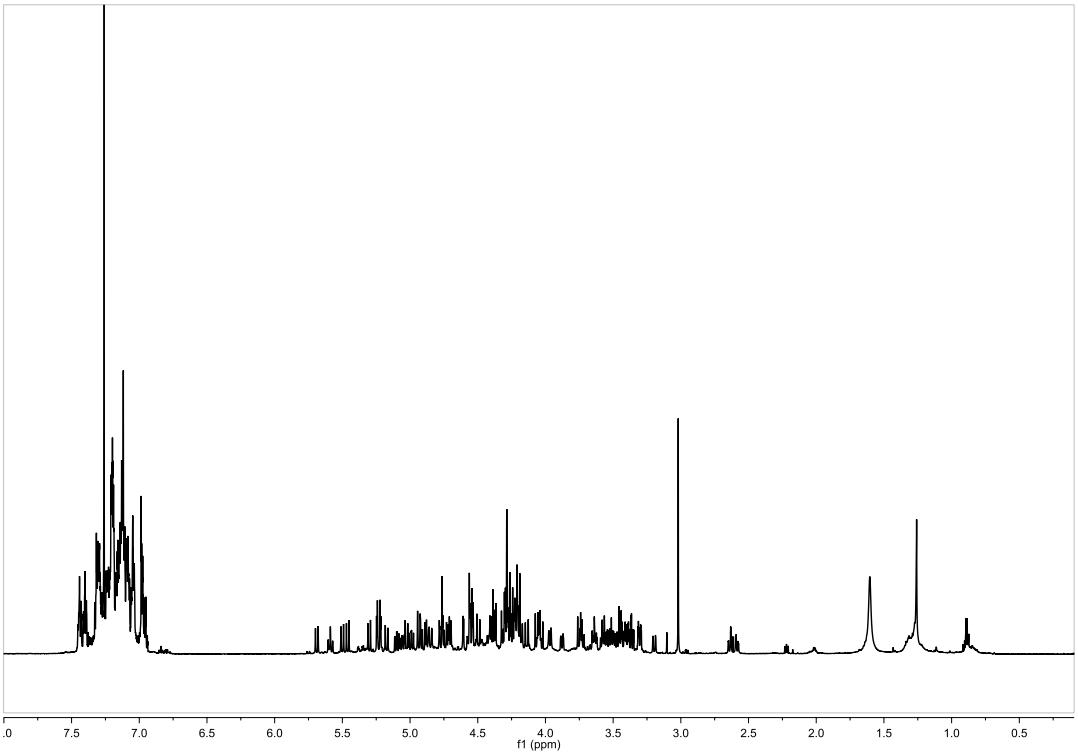

^{1}H NMR of **(α-TriCyD)AgI** ($CDCl_3$, 600 MHz, 300 K)

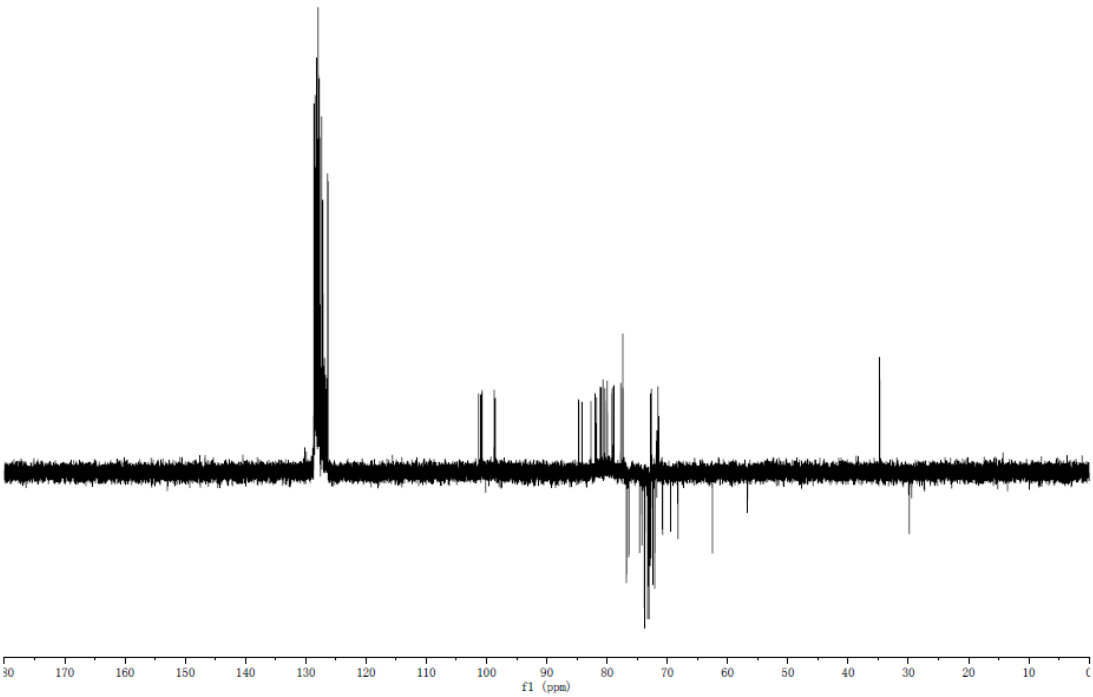

^{13}C dept NMR of **(α-TriCyD)AgI** ($CDCl_3$, 151 MHz, 300 K)

(α-TriCyD)AuI

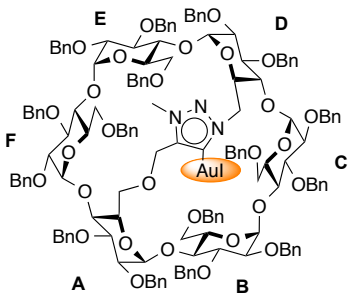

In a flame-dried two-neck flask under argon, a mixture of **(α-TriCyD)HI** (1 g, 0.402 mmol, 1 eq.), Chloro(dimethylsulfide) gold(I) (592 mg, 2.01 mmol, 5 eq) and potassium carbonate (834 mg, 6.03 mmol, 15 eq) was dissolved in 15ml of acetonitrile previously degassed by three ”freeze-pump-thaw” cycles. The reaction mixture was stirred at 60°C overnight. Then the Chloro(dimethylsulfide) gold(I) was filtered on a celite pad and the residue was washed with CH_3CN, and the solvents were evaporated. Silica gel chromatography of the residue (cyclohexane/ EtOAc: 3:1) gave the gold complex **(α-TriCyD)AuI** (270 mg, 24%) as a yellow foam.

^{1}H NMR ($CDCl_3$, 600MHz): δ 7.41-6.93 (m, 80H, 80 × H-Ar), 6.29(t, $^3J_{4,5}$ = $^3J_{5,6}$ = 9.4 Hz, 1H, H-5D), 5.72 (d, $^2J_{Ph\text{-}C\underline{H}H}$ = 10.4 Hz, 1H, CHPh), 5.53 (d, $^2J_{Ph\text{-}C\underline{H}H}$ = 11.0 Hz, 1H, CHPh), 5.44 (d, $^2J_{Ph\text{-}C\underline{H}H}$ = 11.0 Hz, 1H, CHPh), 5.31-5.28 (m, 4H, CHPh, 2 ×H-1C,F, H-5A), 5.19-5.14 (m, 3H, 2 × CHPh, H-3F), 5.03-4.99(m, 2H, CHPh, H-3C), 4.91-4.77(m, 9H, 5 × CHPh, H-5B, H-1A, H-6aD, H-6bA), 4.72(t, $^3J_{2,3}$ = $^3J_{3,4}$ = 9.5 Hz, 1H, H-3B), 4.61-4.54(m, 6H, 2 × CHPh, 3 ×H-1B,D,E, H-5C), 4.47-4.41(m, 3H, 3 × CHPh), 4.34-4.02(m, 26H, 15 × CHPh, 3 ×H-3A,E,D, 2 × H-5F,E, H-6bC, H-6bB, H-6aA, H-6bF, H-6bD, CH_2-O-C$\underline{H}$), 3.86(d, ^2J =12.9, CH_2-O-C$\underline{H}$), 3.70-3.63 (m, 4H, H-6aF, H-6aC, 2 × H-4E,B), 3.58 (t, $^3J_{4,5}$ = $^3J_{3,4}$ = 8.5 Hz, 1H, H-4C), 3.54-3.51(m, 2H, 2 × H-4F,D), 3.48 (dd, $^3J_{1,2}$ = 4.1Hz, $^3J_{2,3}$ = 3.9 Hz, 1H, H-2C), 3.44(dd, $^3J_{1,2}$ = 3.8Hz, $^3J_{2,3}$ = 3.6 Hz, 1H, H-2F), 3.39-3.32(m, 5H, H-4A, 2 ×H-2D,A,E,B), 3.18(br d, ^2J =11.9, 1H, H-6aB), 3.11(s, 3H, CH_3), 2.69-2.65(m, 2H, H-6aE, H-6bE)

^{13}C NMR ($CDCl_3$, 151MHz): δ 168.5 (C-Au), 145.03 (CH_2-C-N), 140.67, 140.59, 140.45, 140.41, 140.10, 139.89, 139.53, 139.34, 139.11, 138.98, 138.81, 138.74, 138.57, 138.52, 138.29, 138.27 (16 × C-Ar-quat.), 128.62-126.21 (80 × C-Ar-tert.), 100.94, 100.71, 100.50, 100.36, 98.85, 98.48(6×C-1A,B,C,D,E,F), 84.40 (C-4F), 84.01 (C-4C), 82.96 (C-4B), 81.91 (C-4E), 81.46 (C-4D), 81.13, 81.07, 81.01 (C-4A,C-3A, C-3D), 80.73, 80.44 (C-2A, C-2D), 80.17 (C-3B), 80.08 (C-3E), 79.39 (C-3F), 79.26 (C-3C), 79.18, 78.92 (C-2B, E), 77.87 (C-2F), 77.50 (C-2C), 76.75, 76.70, 76.44, 76.39(4× Ph-$\underline{C}H_2$), 74.72(C-6A), 74.49, 73.95, 73.79, 73.24, 73.13, 73.11, 72.99, 72.89, 72.80, 72.75 (10 × Ph-$\underline{C}H_2$), 72.53 (C-5F), 72.46 (C-5C), 72.38 (Ph-$\underline{C}H_2$), 72.36 (C-5A), 71.95 (Ph-$\underline{C}H_2$), 71.52(C-6C), 71.29(C-5E), 71.21(C-5B), 70.91(C-6F), 69.75(C-5D), 69.50(C-6B), 68.47(C-6E), 62.86(CH_2-O-$\underline{C}$), 56.60 (C-6D), 35.52 ($\underline{C}H_3$) ppm.

$[\alpha]_D^{20}$=39.8 ($CHCl_3$, c=0.1)

R_f = 0.25 (CyH/AcOEt 3:1)

HRMS(ESI) calcd. $[C_{152}H_{159}AuIN_3O_{29} + Na]^+$: 2836.9662, found: 2836.9560, err. 3.6 ppm

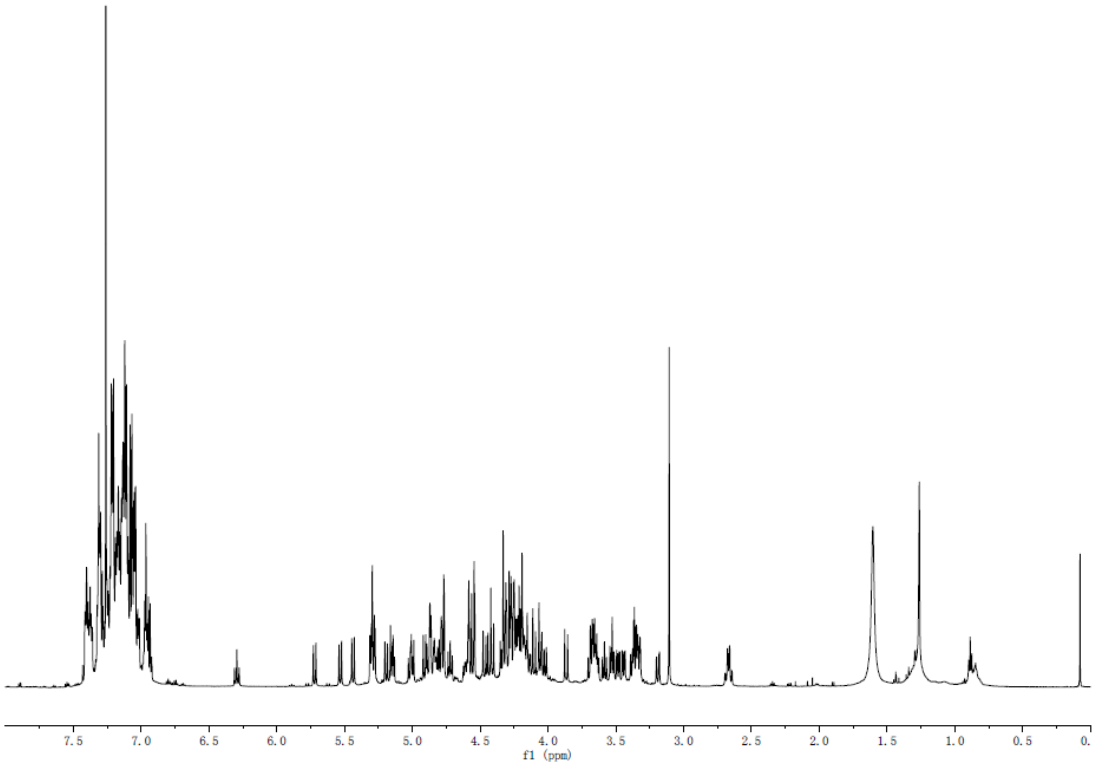

^{1}H NMR of **(α-TriCyD)AuI** ($CDCl_3$, 600 MHz, 300 K)

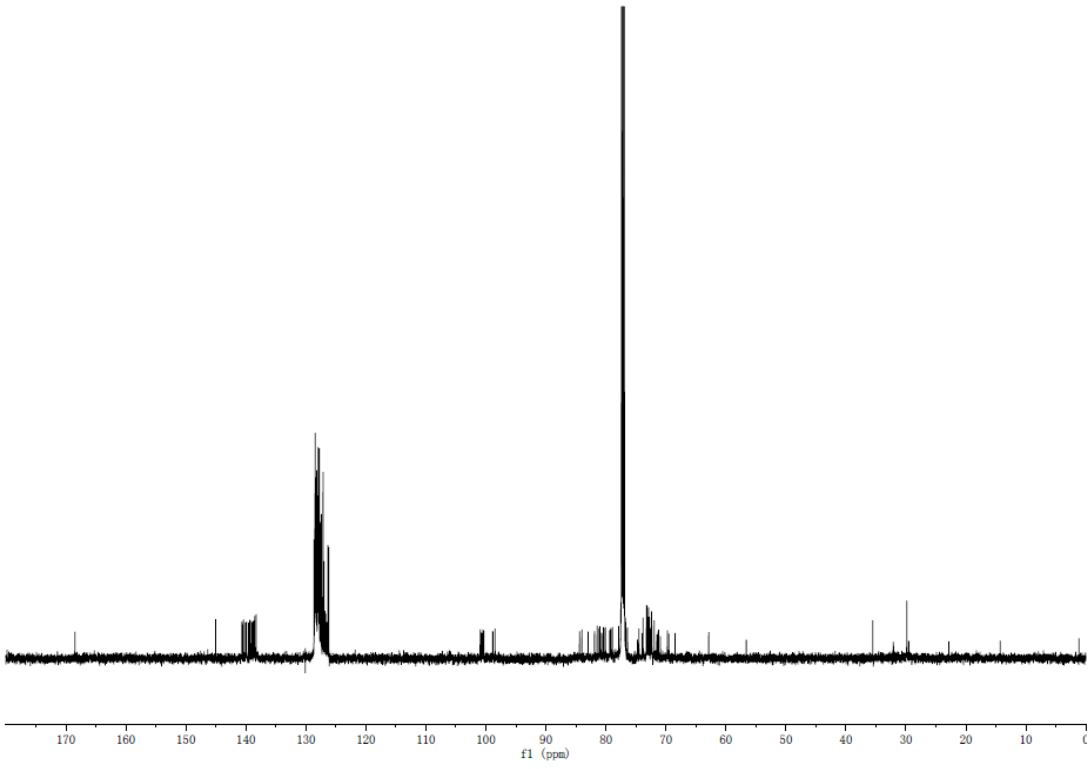

^{13}C NMR of **(α-TriCyD)AuI** ($CDCl_3$, 151 MHz, 300 K)

(α-TriCyD)CuCl

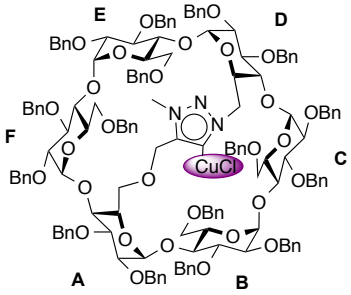

Copper(I) chloride (20 mg, 73.4 µmol) and silver complex compound **(α-TriCyD)AgI** (20 mg, 3.7 µmol) were stirred in dichloromethane (0.5 ml) under argon. The mixture was stirred at R.T overnight, the suspension was filtrated on celite®, washed with dichloromethane. The residue was purified on silica gel chromatography (Cyclohexane/ Ethyl acetate 3:1) to afford copper complex **(α-TriCyD)CuCl** as a white foam (80%).

^{1}H NMR ($CDCl_3$, 600 MHz): δ 7.44-6.77 (m, 80H, 80 × H-Ar), 5.66 (d, $^{2}J_{Ph\text{-}C\underline{H}H}$ = 11.0 Hz, 1H, CHPh), 5.58 (d, $^{2}J_{Ph\text{-}C\underline{H}H}$ = 11.0 Hz, 1H, CHPh), 5.51 (t, $^{3}J_{4,5} = {}^{3}J_{5,6}$ = 9.3 Hz, 1H, H-5D), 5.39-5.38 (m, 2H, 2 ×H-1C,F), 5.31 (d, $^{2}J_{Ph\text{-}C\underline{H}H}$ = 11.4 Hz, 1H, CHPh), 5.24 (d, $^{2}J_{Ph\text{-}C\underline{H}H}$ = 10.3 Hz, 1H, CHPh), 5.16 (d, $^{2}J_{Ph\text{-}C\underline{H}H}$ = 10.8 Hz, 1H, CHPh), 5.10-5.08 (m, 2H, CHPH, H-5A), 5.03(t, $^{3}J_{2,3} = {}^{3}J_{3,4}$ = 9.1 Hz, 1H, H-3C), 4.97 (t, $^{3}J_{2,3} = {}^{3}J_{3,4}$ = 9.1 Hz, 1H, H-3F), 4.88(d, $^{2}J_{Ph\text{-}C\underline{H}H}$ = 10.4 Hz, 1H, CHPh), 4.85-4.82 (m, 2H, 2 × CHPh), 4.78-4.67 (m, 8H, 3 × CHPh, H-5B, 3 ×H-1B,E,A, H-6bD), 4.59-4.42 (m, 11H, H-1D, H-3B, H-5C, 8× CHPh), 4.37-4.11 (m, 19H, CH_2-O-C$\underline{H}$, H-6bF, H-6aD, H-6bB, 3 ×H-3A,E,D, H-5F, 11 × CHPh), 4.08-4.06 (m, 2H, CHPh, H-6bA), 3.95-3.93 (m, 2H, H-5E, H-6bC), 3.86 (d, ^{2}J =13.0 Hz, CH_2-O-C$\underline{H}$,), 3.82 (dd, $^{2}J_{6a,6b}$ = 10.7 Hz, $^{3}J_{5,6b}$ = 5.0Hz, 1H, H-6aC), 3.74-3.68(m, 4H, H-6aF, 3 × H-4B,E,C), 3.59-3.57 (m, 3H, H-6aA, 2 × H-4F,D), 3.51 (dd, $^{3}J_{1,2}$ = 4.1Hz, $^{3}J_{2,3}$ = 3.5 Hz, 1H, H-2C), 3.48 (dd, $^{3}J_{1,2}$ = 3.8 Hz, $^{3}J_{2,3}$ = 3.4 Hz, 1H, H-2F), 3.43-3.40(m, 3H, 2 ×H-2B,E, H-4A), 3.34-3.33 (m, 2H, 2 ×H-2A,D), 3.26 (wd, 1H, H-6aB), 3.12(s, 3H, CH_3), 2.68-2.65 (m, 2H, H-6aE, H-6bE)

^{13}C NMR ($CDCl_3$, 151 MHz): δ 161.04 (C-Cu), 146.94 (CH_2-C-N), 140.43, 140.39(2C), 140.22, 139.95, 139.95, 139.39, 139.23, 138.97, 138.95, 138.72, 138.63, 138.54(2C), 138.33, 138.27(16 × C-Ar-quat.), 128.60-126.48 (80 × C-Ar-tert.), 100.42, 99.83, 99.72, 99.65, 98.36, 98.30 (6×C-1A,B,C,D,E,F), 83.74(C-4F), 83.18(C-4C), 82.46(C-4B), 81.63(C-4E), 81.47(C-3A), 81.05 (C-3D), 80.55, 80.47, 80.34, 80.25, 80.21(C-4D, C-2A, C-2D, C-3E, C-3B), 79.69, 79.63, 79.58, 79.49, 79.44(C-2B,C-2E, C-4A, C-3C, C-3F), 77.51, 77.35(C-2C, C-2F), 76.68, 76.65, 76.37, 76.29, 74.51(5× Ph-$\underline{C}H_2$), 74.40(C-6A), 74.04, 73.74, 73.52, 73.26, 73.15, 73.06, 72.98, 72.93, 72.82(9 × Ph-$\underline{C}H_2$), 72.67, 72.59 (C-5C, C-5F), 72.21(Ph-$\underline{C}H_2$), 72.05(C-5A), 71.82(Ph-$\underline{C}H_2$), 71.74(H-5D), 71.72(H-5E), 71.49(C-5B), 71.01(H-6F), 70.44(H-6C), 69.78(H-6B), 68.47(H-6E), 62.78 (CH_2-O-$\underline{C}$), 56.70(C-6D), 34.92 ($\underline{C}H_3$) ppm.

$[\alpha]_D^{20}$= 77.2°($CHCl_3$, c=0.1)

R_f = 0.25 (CyH/AcOEt 3:1)

HRMS(ESI) calcd. $[C_{152}H_{159}CuClN_3O_{29} + Na]^+$: 2610.9936, found 2611.0049, err. -4.3 ppm

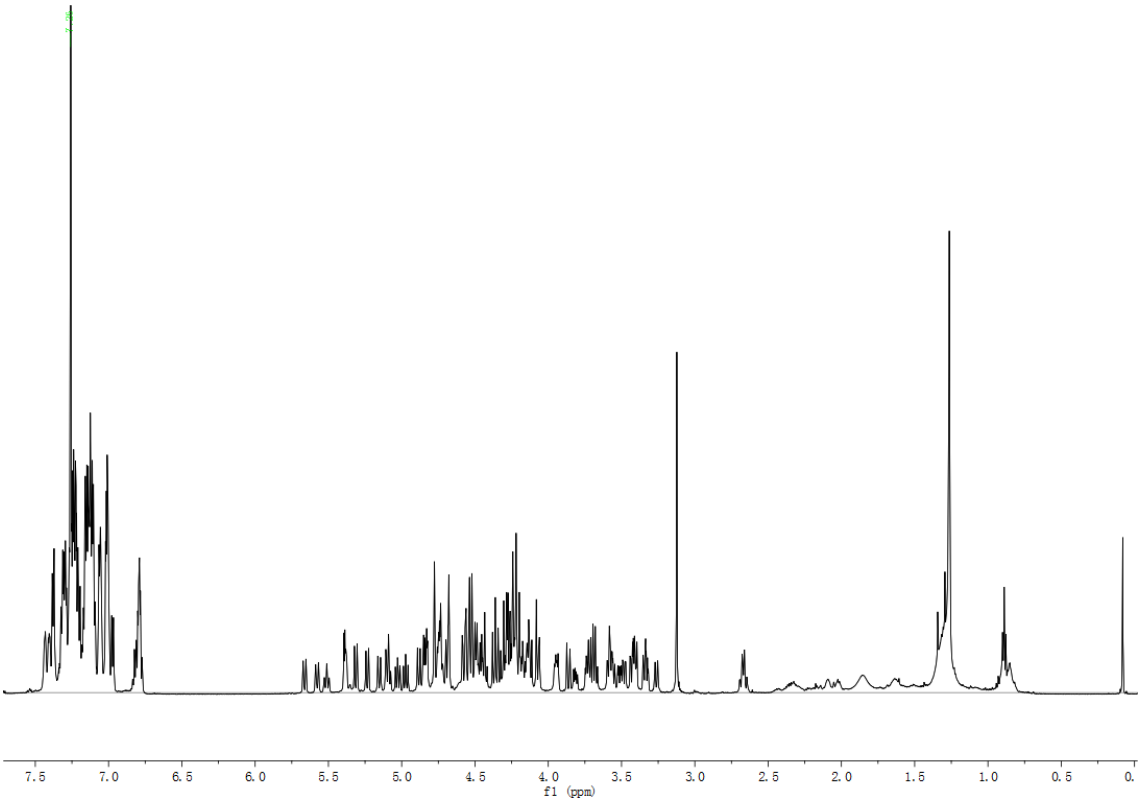

^{1}H NMR of **(α-TriCyD)CuCl** ($CDCl_3$, 600 MHz, 300 K)

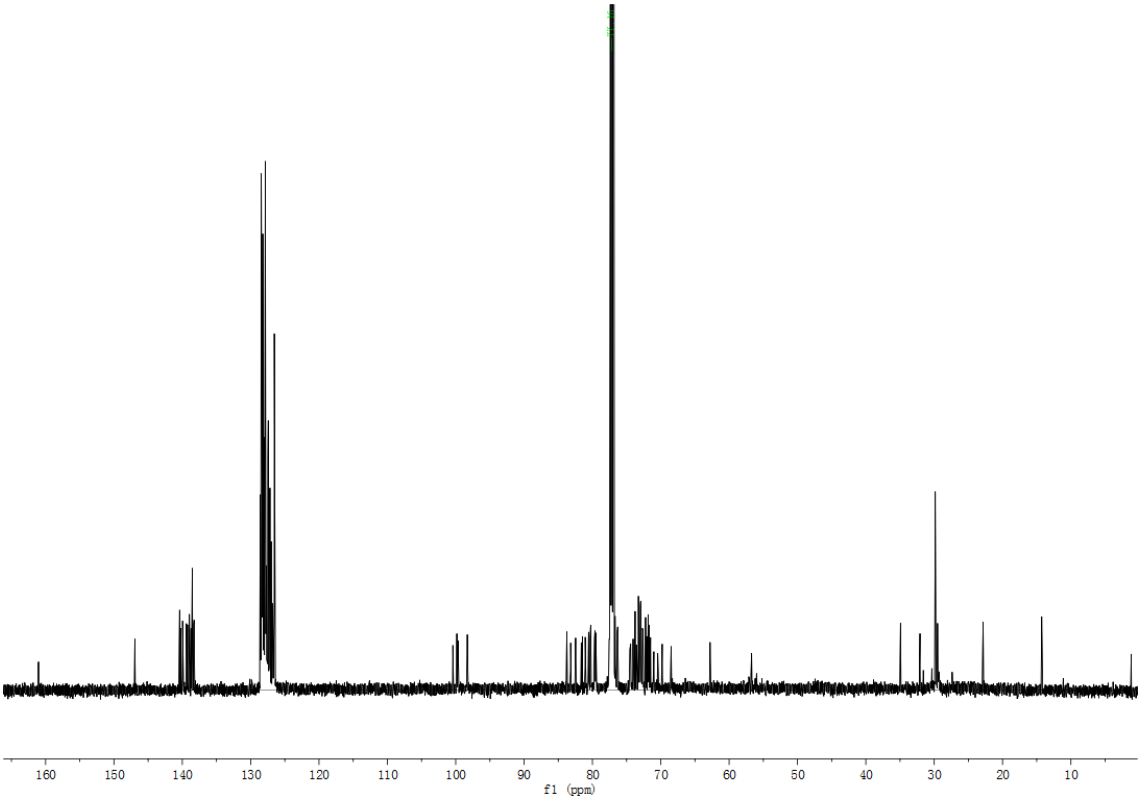

^{13}C NMR of **(α-TriCyD)CuCl** ($CDCl_3$, 151 MHz, 300 K)

NHC-capped CD-Gold(I) catalysis

1. Gold(I)-catalyzed cycloisomerization of enyne 1*: regioselectivity*

To a solution of gold(I) complex (0.02 equiv) in dry and degassed solvent was added $AgSbF_6$ (0.02 equiv). After 10 min stirring at room temperature, the precipitation of AgCl occurred (white solid). Then, a solution of 1,6-enyne (1 equiv) in dry and degassed dichloromethane was added (final concentration 0.025 M). The mixture was stirred and monitored by TLC. When the reaction was complete, the mixture was filtered over a short pad of silica and washed with ethyl acetate. The solution was concentrated under reduced pressure. Subsequent purification by flash-chromatography on silica gel, using pentane/EtOAc (98:2) as eluent, afforded the desired products.

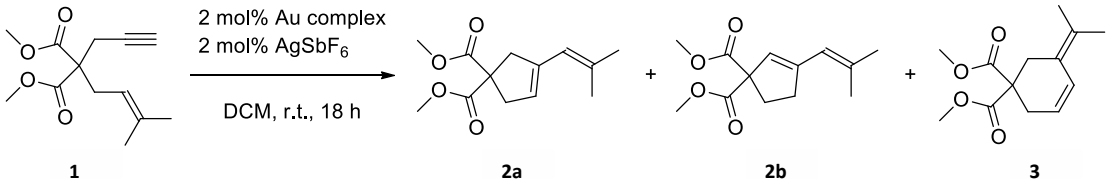

^{1}H NMR of 2a (400 MHz, $CDCl_3$) δ 5.88 5.68 (m, 1H), 5.40-5.33 (m, 1H), 3.72 (s, 6H), 3.21-3.14 (m, 2H), 3.06-2.99 (m, 2H), 1.80 (s, 3H), 1.76 (s, 3H). The spectral data correspond to those previously reported.[20]

^{1}H NMR of 2b (400 MHz, $CDCl_3$) δ 5.81-5.75 (m, 1H), 5.60-5.55 (m, 1H), 3.70 (s, 6H), 2.68-2.59 (m, 2H), 2.50-2.41 (m, 2H), 1.82 (s, 3H), 1.79 (s, 3H). The spectral data correspond to those previously reported.[21]

^{1}H NMR of 3 (400 MHz, $CDCl_3$) δ 6.42 (dt, *J* = 10.2, 2.0 Hz, 1H), 5.60 (dt, *J* = 10.4, 4.2 Hz, 1H), 3.69 (s, 6H), 2.86-2.78 (m, 2H), 2.69-2.62 (m, 2H), 1.77 (s, 3H), 1.76 (s, 3H). The spectral data correspond to those previously reported.[22]

Reactions with **(IPr)AuCl**, **(α-ICyD)AuCl**, and **(β-ICyD)AuCl** were published previously.[5]

Using **(γ-A,D-ICyD)AuCl** (14.9 mg, 0.004 mmol, 2 mol%), $AgSbF_6$ (1.47 mg, 0.004 mmol, 2 mol%) and dimethyl 2-(3-methylbut-2-enyl)-2-(prop-2-ynyl)malonate (**1**) (50 mg, 0.21 mmol), the reaction mixture was stirred at rt for 15 h. A mixture of **2a** and **2b** and **3** was obtained as a colorless oil in 80% yield. **2a** and **2b** in a 1:0.56 ratio (72%) and **3** (28%) *(see ^{1}H NMR spectrum of the mixture below).*

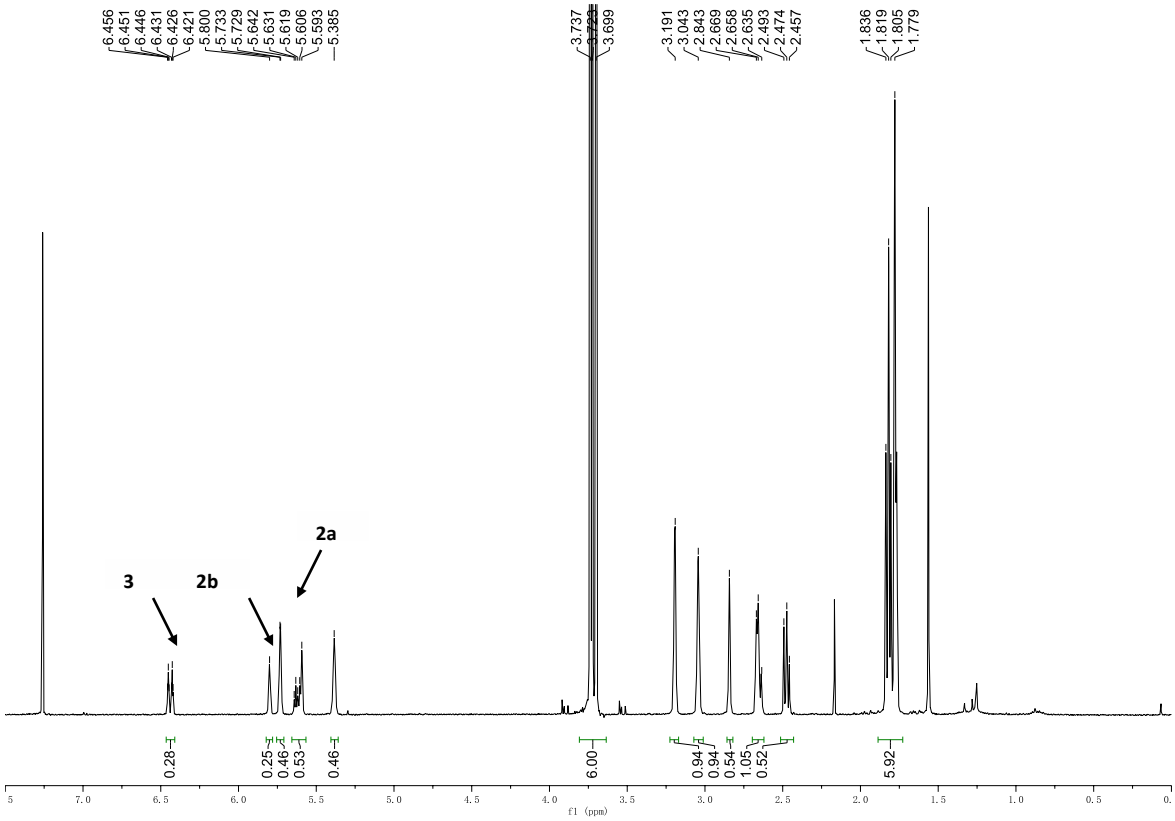

Using **(γ-A,E-ICyD)AuCl** (15 mg, 0.004 mmol, 2 mol%), $AgSbF_6$ (1.5 mg, 0.004 mmol, 2 mol%) and dimethyl 2-(3-methylbut-2-enyl)-2-(prop-2-ynyl)malonate (**1**) (50 mg, 0.21 mmol), the reaction mixture was stirred at rt for 15 h. A mixture of **2a** and **2b** and **3** was obtained as a colorless oil in 100% yield. **2a** and **2b** in a 1:0.14 ratio (55%) and **3** (45%) *(see ^{1}H NMR spectrum of the mixture below)*.

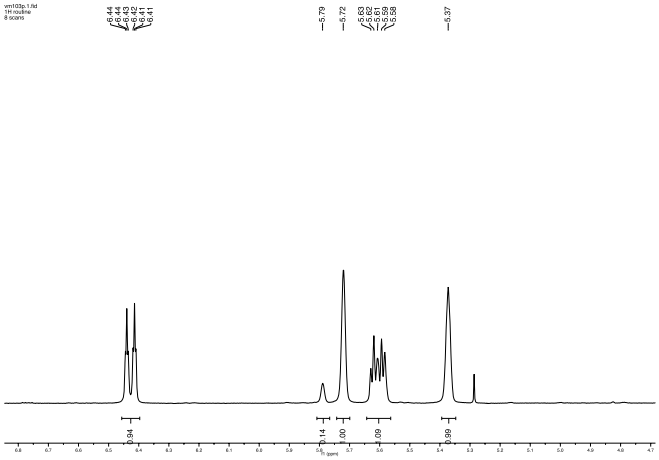

Using **(α-BiCyD)AuCl** (23 mg, 0.008 mmol, 2 mol%) and $AgSbF_6$ (2.2 mg, 0.008 mmol, 2 mol%) and dimethyl 2-(3-methylbut-2-enyl)-2-(prop-2-ynyl)malonate (**1**) (100 mg, 0.42 mmol). the reaction mixture was stirred at rt for 15 h. A mixture of **2a** and **2b** and **3** was obtained as a colorless oil in 87% yield. **2a** and **2b** in a 1:0.2 ratio (90%) and **3** (10%) *(see ^{1}H NMR*

spectrum of the mixture below).

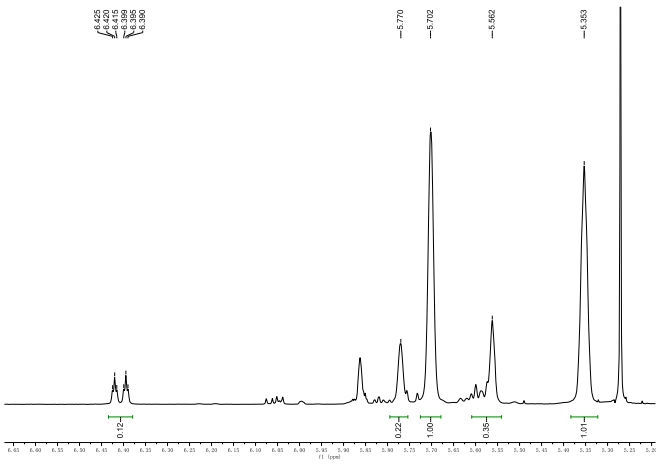

Using **(β-BiCyD)AuCl** (27 mg, 0.008 mmol, 2 mol%) and $AgSbF_6$ (2.2 mg, 0.008 mmol, 2 mol%) and dimethyl 2-(3-methylbut-2-enyl)-2-(prop-2-ynyl)malonate (**1**) (100 mg, 0.42 mmol). The reaction mixture was stirred at rt for 15 h. A mixture of **2a** and **2b** and **3** was obtained as a colorless oil in 88% yield. **2a** and **2b** in a 1:0.6 ratio (21%) and **3** (79%) *(see ^1H NMR spectrum of the mixture below)*.

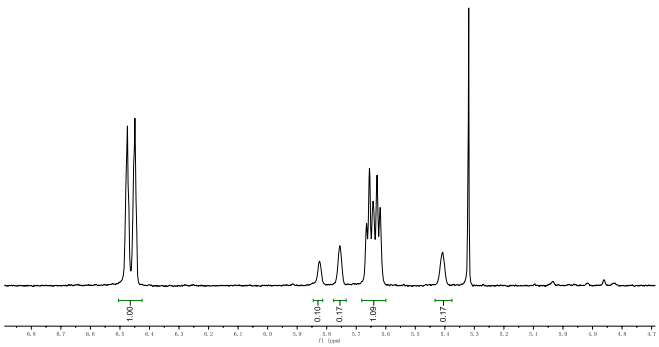

Using **(α-TriCyD)AuCl** (24 mg, 0.008 mmol, 2 mol%) and $AgSbF_6$ (2.2 mg, 0.008 mmol, 2 mol%) and dimethyl 2-(3-methylbut-2-enyl)-2-(prop-2-ynyl)malonate (**1**) (100 mg, 0.42 mmol), the reaction mixture was stirred at rt for 15 h. A mixture of **2a** and **2b** and **3** was obtained as a colorless oil in 78% yield. **2a** and **2b** in a 1:0.8 ratio (96%) and **3** (4%) *(see ^1H NMR spectrum of the mixture below)*.

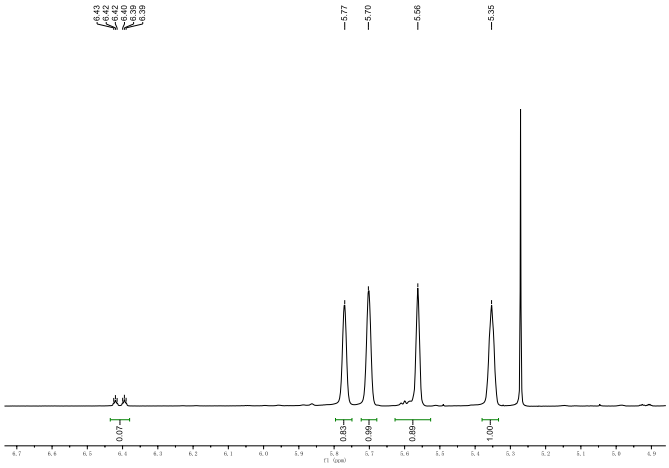
6.43
6.42
6.42
6.40
6.39
6.39
5.77
5.70
5.56
5.35
0.07
0.85
0.99
0.89
1.00
f1 (ppm)

2. Gold(I)-catalyzed cycloisomerization of enyne 5: enantioselectivity

IPrAuCl-catalyzed cycloisomerization of enyne 5:[5]

IPrAuCl (4.5 mg, 0.007 mmol, 2 mol%) and $AgSbF_6$ (2.5 mg, 0.007 mmol, 2 mol%) were introduced in a round bottom flask under an argon atmosphere and anhydrous CH_2Cl_2 (14.0 mL) was added. The solution was stirred at room temperature for 5 minutes, then enyne **5** was introduced (97 mg, 0.350 mmol, 1.0 eq, 0.025 M). The reaction mixture was stirred at room temperature for 3 h with the completion of the reaction being monitored by TLC. After completion, the solution was filtered through a pad of silica and the pad was washed with diethyl ether. The solvent was removed under reduced pressure and the crude mixture was purified by flash chromatography on silica gel (pentane/Et_2O : 85/15) to afford the racemate (±)-**7** (78 mg, 0.282 mmol, 80%) as a white powder.

Chromatogram was recorded on a CO_2 supercritical fluid chromatography (SFC) using AD-H column, pressure: 100 Bars, with a debit of 5 mL/min and 4 % MeOH as eluent at λ = 254 nm. (±)-1,6-dimethyl-3-tolylsulfonyl-3-azabicyclo[4.1.0]hept-4-ene **7** was obtained. See Figure S22.

***(α-ICyD)AuCl**-catalyzed cycloisomerization of **5**:*

(α-ICyD)AuCl (46.5 mg, 17.4 mmol, 5 mol%) and $AgSbF_6$ (6.0 mg, 17.4 mmol, 5 mol%) were introduced in a round bottom flask under an argon atmosphere and anhydrous CH_2Cl_2 (13.9 mL) was added. The solution was stirred at room temperature for 5 minutes, then enyne **5** was introduced (96 mg, 0.347 mmol, 1.0 eq, 0.025 M). The reaction mixture was stirred at 40°C for 18 h with the completion of the reaction being monitored by TLC. After completion, the solution was filtered through a pad of silica and the pad was washed with diethyl ether. The solvent was removed under reduced pressure and the crude mixture was purified by flash chromatography on silica gel (pentane/Et_2O : 85/15) to afford **7** (80 mg, 0.289 mmol, 83%) as a white powder. The enantiomer (+)-(R,R)-**7** (43% ee) was obtained as the major isomer.

$[\alpha]^{20}_D$ + 40.5 (*c* 0.62, $CHCl_3$). {$[\alpha]^{20}_D$ (***ent*-7**) – 93 (c 1.07, $CHCl_3$) for 88% ee (1S,6S)}[23]

Chromatogram was recorded on a CO_2 supercritical fluid chromatography (SFC) using AD-H column, pressure: 100 Bars, with a debit of 5 mL/min and 4 % MeOH as eluent at λ = 254 nm. (+)-1,6-dimethyl-3-tolylsulfonyl-3-azabicyclo[4.1.0]hept-4-ene **7** was obtained as the major enantiomer. See Figure S23.

(β-ICyD)AuCl-catalyzed cycloisomerization of 5:

(β-ICyD)AuCl (23 mg, 0.0073 mmol, 2 mol%) and $AgSbF_6$ (2.6 mg, 0.0073 mmol, 2 mol%) were introduced in a round bottom flask under an argon atmosphere and anhydrous CH_2Cl_2 (14.6 mL) was added. The solution was stirred at room temperature for 5 minutes, then enyne **5** was introduced (101 mg, 0.365 mmol, 1.0 eq, 0.025 M). The reaction mixture was stirred at r.t. for 15 h with the completion of the reaction being monitored by TLC. After completion, the solution was filtered through a pad of silica and the pad was washed with diethyl ether. The

solvent was removed under reduced pressure and the crude mixture was purified by flash chromatography on silica gel (Pentane/Et_2O : 85/15) to afford **7** (78 mg, 0.282 mmol, 77%). The enantiomer (+)-(R,R)-**7** (60% ee) was obtained as the major isomer.

$[\alpha]^{20}_D$ = + 59.3 (*c* 0.62, $CHCl_3$). For Chromatograms see Figures S24 and S25.

(γ-A,D-ICyD)AuCl-catalyzed cycloisomerization of 5:

Using **(γ-A,D-ICyD)AuCl** (25.4 mg, 0.007 mmol, 2 mol%), $AgSbF_6$ (2.5 mg, 0.007 mmol, 2 mol%) and **5** (100 mg, 0.36 mmol), the reaction mixture was stirred at r.t. for 15 h with the completion of the reaction being monitored by TLC. After completion, the solution was filtered through a pad of silica and the pad was washed with diethyl ether. The solvent was removed under reduced pressure and the crude mixture was purified by flash chromatography on silica gel (Pentane/Et_2O : 85/15) to afford **7** (77 mg, 0.28 mmol, 77%) as a white powder. (+)-(R,R)-1,6-dimethyl-3-tolylsulfonyl-3-azabicyclo[4.1.0]hept-4-ene **7** was obtained (7% ee).

$[\alpha]^{20}_D$ + 7 (*c* 0.95, $CHCl_3$).

For Chromatogram see Figure S26.

(γ-A,E-ICyD)AuCl-catalyzed cycloisomerization:

Using **(γ-A,E-ICyD)AuCl** (25.5 mg, 0.007 mmol, 2 mol%), $AgSbF_6$ (2.5 mg, 0.007 mmol, 2 mol%) and **5** (100 mg, 0.36 mmol), the reaction mixture was stirred at r.t. for 15 h with the completion of the reaction being monitored by TLC. After completion, the solution was filtered through a pad of silica and the pad was washed with diethyl ether. The solvent was removed under reduced pressure and the crude mixture was purified by flash chromatography on silica gel (Pentane/Et_2O : 85/15) to afford **7** (50 mg, 0.28 mmol, 50%) as a white powder. (±)-1,6-dimethyl-3-tolylsulfonyl-3-azabicyclo[4.1.0]hept-4-ene **7** was obtained (0% ee) as the racemate.

For chromatogram see Figure S27.

(α-BiCyD)AuCl-catalyzed cycloisomerization of 5:

Using **α-BiCyDAuCl** (19.2 mg, 0.007 mmol, 2 mol%), $AgSbF_6$ (2.5 mg, 0.007 mmol, 5 mol%) and **5** (100 mg, 0.36 mmol), the reaction mixture was stirred at 40°C for 15 h with the completion of the reaction being monitored by TLC. After completion, the solution was filtered through a pad of silica and the pad was washed with diethyl ether. The solvent was removed under reduced pressure and the crude mixture was purified by flash chromatography on silica gel (Pentane/Et_2O : 85/15) to afford **7** (63 mg, 0.23 mmol, 63%) as a white powder. (+)-(R,R)-1,6-dimethyl-3-tolylsulfonyl-3-azabicyclo[4.1.0]hept-4-ene **7** was obtained (26% ee) as the major isomer.

For chromatogram see Figure S28.

(β-BiCyD)AuCl-catalyzed cycloisomerization of 5:

Using **β-BiCyDAuCl** (22 mg, 0.007 mmol, 2 mol%), $AgSbF_6$ (2.5 mg, 0.007 mmol, 2 mol%) and **5** (100 mg, 0.36 mmol), the reaction mixture was stirred at r.t. for 15 h with the completion of the reaction being monitored by TLC. After completion, the solution was filtered through a

pad of silica and the pad was washed with diethyl ether. The solvent was removed under reduced pressure and the crude mixture was purified by flash chromatography on silica gel (Pentane/Et_2O : 85/15) to afford **7** (85 mg, 0.31 mmol, 85%) as a white powder. (+)-(R,R)-1,6-dimethyl-3-tolylsulfonyl-3-azabicyclo[4.1.0]hept-4-ene **7** (63% ee) was obtained as the major enantiomer.

$[\alpha]^{20}_D$ + 62 (*c*=1, $CHCl_3$).

Chromatogram was recorded on a CO_2 SFC using AD-H column, pressure: 100 Bars, with a debit of 5 mL/min and 4 % iPrOH as eluent at λ = 220 nm. (+)-(R,R)-1,6-dimethyl-3-tolylsulfonyl-3-azabicyclo[4.1.0]hept-4-ene **7** was obtained as the major enantiomer (63 % *ee*).

For chromatograms see Figures S29 ad S30.

(α-TriCyD)AuCl-catalyzed cycloisomerization of 5:

Using **α-TriCyDAuCl** (49 mg, 0.018 mmol, 5 mol%), $AgSbF_6$ (6.3 mg, 0.018 mmol, 5 mol%) and **5** (100 mg, 0.36 mmol), the reaction mixture was stirred at r.t. for 15 h with the completion of the reaction being monitored by TLC. After completion, the solution was filtered through a pad of silica and the pad was washed with diethyl ether. The solvent was removed under reduced pressure and the crude mixture was purified by flash chromatography on silica gel (Pentane/Et_2O : 85/15) to afford **7** (58 mg, 0.21 mmol, 58%, 0% ee) as a racemate.

Chromatogram recorded on a CO_2 SFC using AD-H column, pressure: 100 Bars, with a debit of 5 mL/min and 4 % iPrOH as eluent at λ = 220 nm. 1,6-dimethyl-3-tolylsulfonyl-3-azabicyclo[4.1.0]hept-4-ene was obtained as a racemic mixture (0 % *ee*).

See Figure S31.

^{1}H NMR of 7:

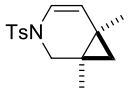

^{1}H NMR (400 MHz, $CDCl_3$) δ 7.69 – 7.58 (m, 2H), 7.34 – 7.27 (m, 2H), 6.24 (dd, *J* = 8.0, 1.2 Hz, 1H), 5.16 (d, *J* = 8.0 Hz, 1H), 3.76 (d, *J* = 11.4 Hz, 1H), 2.66 (dd, *J* = 11.4, 0.9 Hz, 1H), 2.40 (s, 3H), 1.10 (s, 3H), 1.09 (s, 3H), 0.71 (d, *J* = 4.3 Hz, 1H), 0.31 (dd, *J* = 4.3, 1.2 Hz, 1H); The spectral data for 1,6-dimethyl-3-tolylsulfonyl-3-azabicyclo[4.1.0]hept-4-ene correspond to those previously reported.[24]

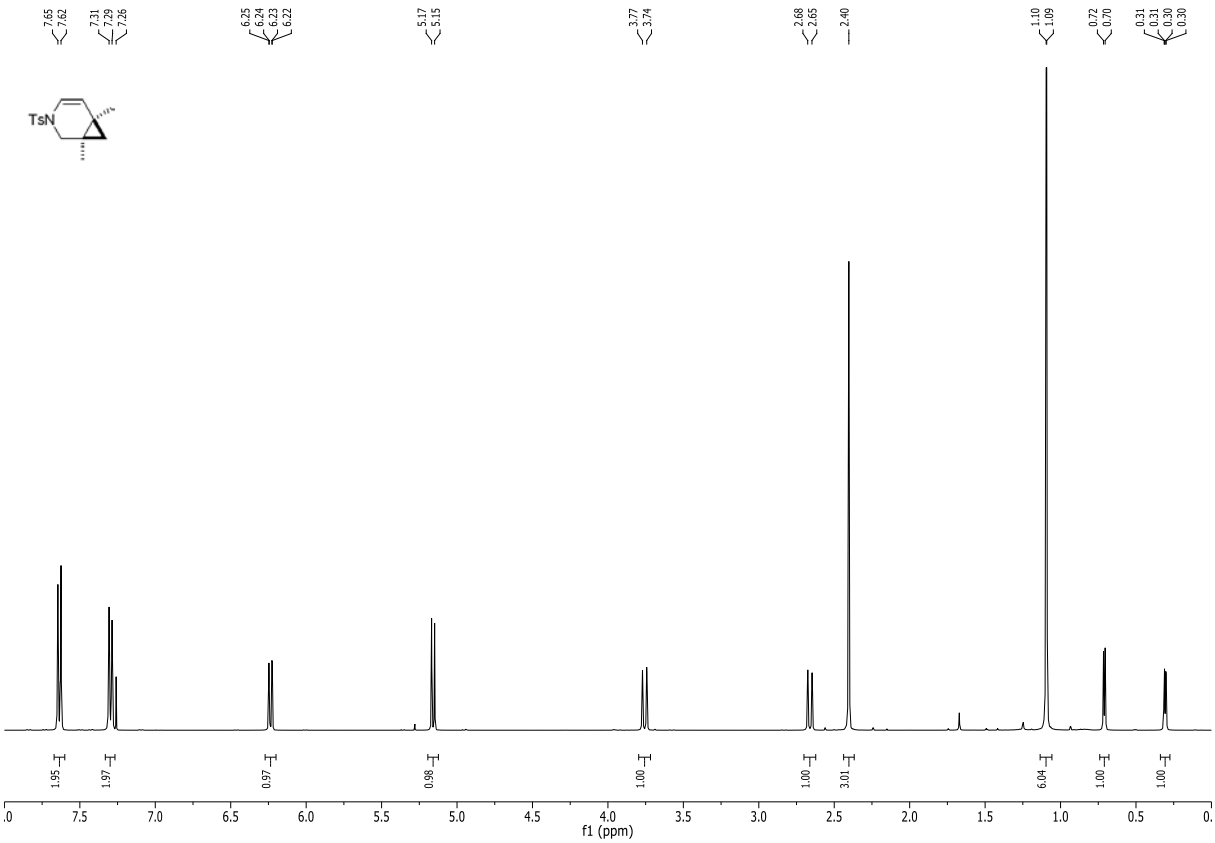

3. Gold(I)-catalyzed cycloisomerization of enyne 6: enantioselectivity

IPrAuCl-catalyzed cycloisomerization of 6:

Using IPrAuCl (3.9 mg, 0.006 mmol, 2 mol%), $AgSbF_6$ (2.1 mg, 0.006 mmol, 2 mol%) and **6** (100 mg, 0.30 mmol). The reaction mixture was stirred at rt for 3 h. After completion, the solution was filtered through a pad of silica and the pad was washed with diethyl ether. The solvent was removed under reduced pressure and the crude mixture was purified by flash chromatography on silica gel (Pentane/Et_2O : 85/15) to give (±)-6-methyl-1-phenyl-3-tolyl-3-azabicyclo[4.1.0]hept-4-ene (**8**) (74 mg, 0.22 mmol, 74 %) as a pale yellow solid.

(±)-6-methyl-1-phenyl-3-(*p*-tolylsulfonyl)-3-azabicyclo[4.1.0]hept-4-ene **8** was obtained (0% ee).

For chromatogram see Figure S32.

(α-ICyD)AuCl-catalyzed cycloisomerization of 6:

Using **(α-ICyD)AuCl** (15.6 mg, 0.006 mmol, 2 mol%), $AgSbF_6$ (2.1 mg, 0.006 mmol, 2 mol%) and **6** (100 mg, 0.30 mmol). The reaction mixture was stirred at 40°C for 15 h. After completion, the solution was filtered through a pad of silica and the pad was washed with diethyl ether. The solvent was removed under reduced pressure and the crude mixture was purified by flash chromatography on silica gel (Pentane/Et_2O : 85/15) to afford **8** (78 mg, 0.23 mmol, 78 %) as a pale yellow solid. (+)-(R,R)-6-methyl-1-phenyl-3-tolyl-3-azabicyclo[4.1.0]hept-4-ene (**8**) was obtained (48% *ee*) as the major enantiomer.

For chromatogram see Figure S33.

(β-ICyD)AuCl-catalyzed cycloisomerization of 6:

Using **(β-ICyD)AuCl** (18 mg, 0.006 mmol, 2 mol%) and $AgSbF_6$ (2.1 mg, 0.006 mmol, 2 mol%) and **6** (100 mg, 0.30 mmol). The reaction mixture was stirred at rt for 15 h. After completion, the solution was filtered through a pad of silica and the pad was washed with diethyl ether. The solvent was removed under reduced pressure and the crude mixture was purified by flash chromatography on silica gel (Pentane/Et_2O : 85/15) to afford **8** (99 mg, 0.29 mmol, 99 %) as a pale yellow solid. (+)-(R,R)-6-methyl-1-phenyl-3-tolyl-3-azabicyclo[4.1.0]hept-4-ene (**8**) was obtained (80% *ee*) as the major enantiomer.

For chromatogram see Figure S34.

(γ-A,D-ICyD)AuCl-catalyzed cycloisomerization of 6:

Using (**γ-A,D-ICyD)AuCl** (14.4 mg, 0.004 mmol, 2 mol%), $AgSbF_6$ (1.4 mg, 0.004 mmol, 2 mol%) and **15** (70 mg, 0.21 mmol), the reaction mixture was stirred at rt for 15 h. After completion, the solution was filtered through a pad of silica and the pad was washed with diethyl ether. The solvent was removed under reduced pressure and the crude mixture was purified by flash chromatography on silica gel (Pentane/Et_2O: 85/15) to afford **8** (48.8 mg, 0.15 mmol, 70%) as a pale yellow solid. (+)-(R,R)-6-methyl-1-phenyl-3-tolyl-3-azabicyclo[4.1.0]hept-4-ene **8** was obtained (22% ee) as the major enantiomer.

$[\alpha]^{20}_D$ + 49 (*c* 0.97, $CHCl_3$). {$[\alpha]^{20}_D$ = + 155 (c 1.3, $CHCl_3$) for 82% ee (1R,6R)}

For chromatogram see Figure S35.

(γ-A,E-ICyD)AuCl-catalyzed cycloisomerization:

Using **(γ-A,E-ICyD)AuCl** (16.7 mg, 0.005 mmol, 2 mol%), $AgSbF_6$ (1.6 mg, 0.005 mmol, 2 mol%) and **6** (83 mg, 0.24 mmol), the reaction mixture was stirred at rt for 15 h. After completion, the solution was filtered through a pad of silica and the pad was washed with diethyl ether. The solvent was removed under reduced pressure and the crude mixture was purified by flash chromatography on silica gel (Pentane/Et_2O: 85/15) to afford **8** (40 mg, 0.28 mmol, 50%). (-)-(S,S)-6-methyl-1-phenyl-3-tolyl-3-azabicyclo[4.1.0]hept-4-ene **8** was obtained (43% ee) as the major enantiomer.

$[\alpha]^{20}_D$ = -89 (*c* 0.5, $CHCl_3$).

For chromatograms see Figures S36 and S37.

^{1}H NMR of 6-methyl-1-phenyl-3-tolyl-3-azabicyclo[4.1.0]hept-4-ene **8:**

^{1}H NMR (300 MHz, $CDCl_3$) δ 7.89 (d, *J* = 7.6 Hz, 1H), 7.46 (t, *J* = 7.4 Hz, 1H), 7.33-7.21 (m, 7 H), 6.47 (d, *J* = 7.9 Hz, 1H), 5.40 (d, *J* = 7.9 Hz, 1H), 3.81 (d, *J* = 12.0 Hz, 1H), 3.19 (d, *J* = 12.0 Hz, 1H), 2.61 (s, 3 H), 1.19 (d, *J* = 4.6 Hz, 1H), 1.02 (d, *J* = 4.5 Hz, 1H), 0.89 (s, 3H). The spectral data for 6-methyl-1-phenyl-3-(*p*-tolylsulfonyl)-3-azabicyclo[4.1.0]hept-4-ene correspond to those previously reported.[25]

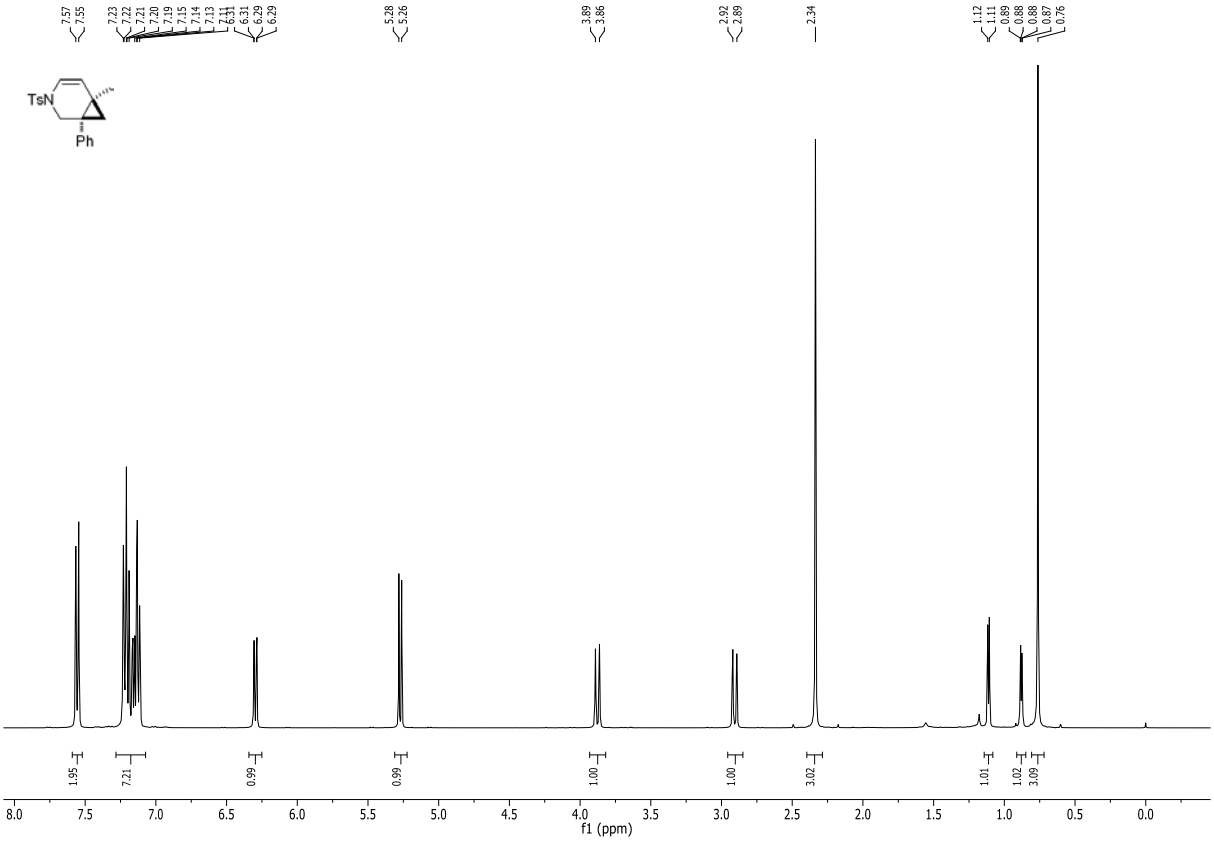

***4. Absolute configuration of (+)-6-methyl-1-phenyl-3-(p-tolylsulfonyl)-3-azabicyclo[4.1.0]hept-4-ene* (8)**

Analytical chiral HPLC separation for compound **8**

• A sample of a racemic mixture of **8** is dissolved in hexane/isopropanol 90/10, injected on the chiral column, and detected with an UV detector at 254 nm and polarimeter. The flow-rate is 1 mL/min.

Column	Mobile Phase	t1	k1	t2	k2	α	Rs
Chiralpak IF	Heptane / 2-PrOH / dichloromethane (90/5/5)	7.70 (-)	1.61	8.7 (+)	1.95	1.21	2.74

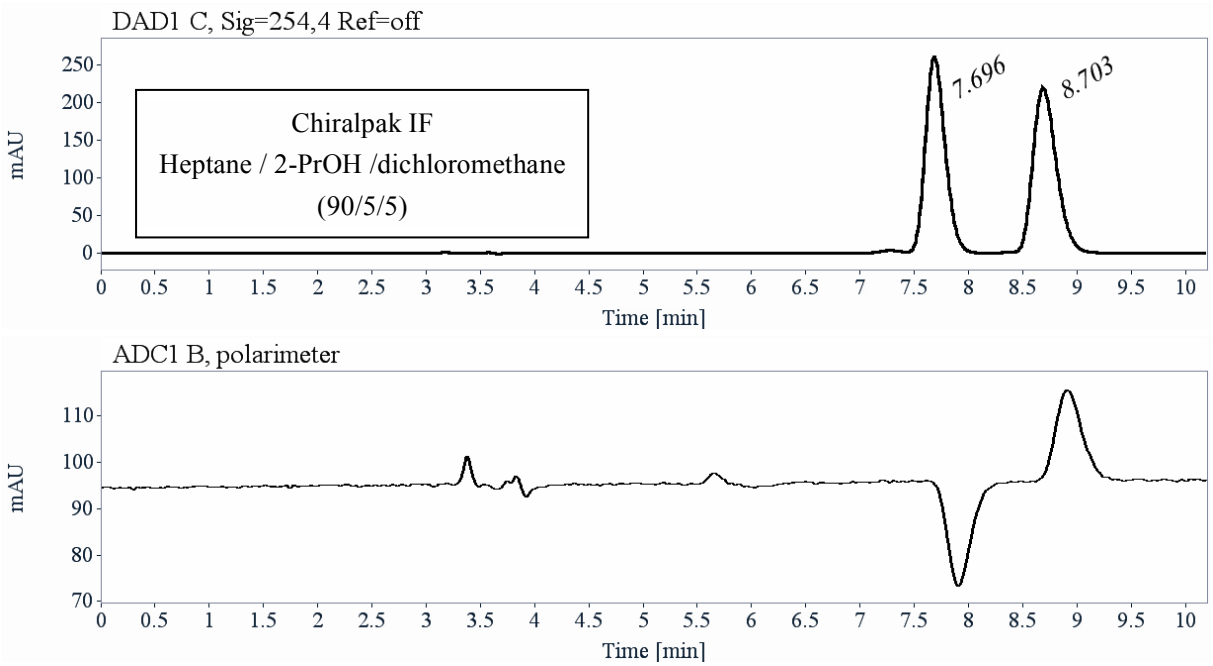

Signal: DAD1 C, Sig=254,4 Ref=off

RT [min]	Area	Area%	Capacity Factor	Enantioselectivity	Resolution (USP)
7.70	3291	49.77	1.61		
8.70	3321	50.23	1.95	1.21	2.74
Sum	6612	100.00			

Semi-preparative separation for compound **8** :

• Sample preparation: About 80 mg of compound **8** are dissolved in 15 mL of mixture of hexane/isopropanol/dichloromethane 70/10/20.

• Chromatographic conditions: Chiralpak IF (250 x 10 mm), hexane / 2-PrOH / dichloromethane (90/5/5) as mobile phase, flow-rate = 5 mL/min, UV detection at 254 nm.

• Injections: 100 times 150 mL, every 3 minutes.

• First fraction: 32 mg of the first eluted ((-, pol)-enantiomer) **(-)-8** with ee = 98%

• Second fraction: 28 mg of the second eluted ((+, pol)-enantiomer) **(+)-8** with ee > 99.5%

• Chromatograms of the collected fractions:

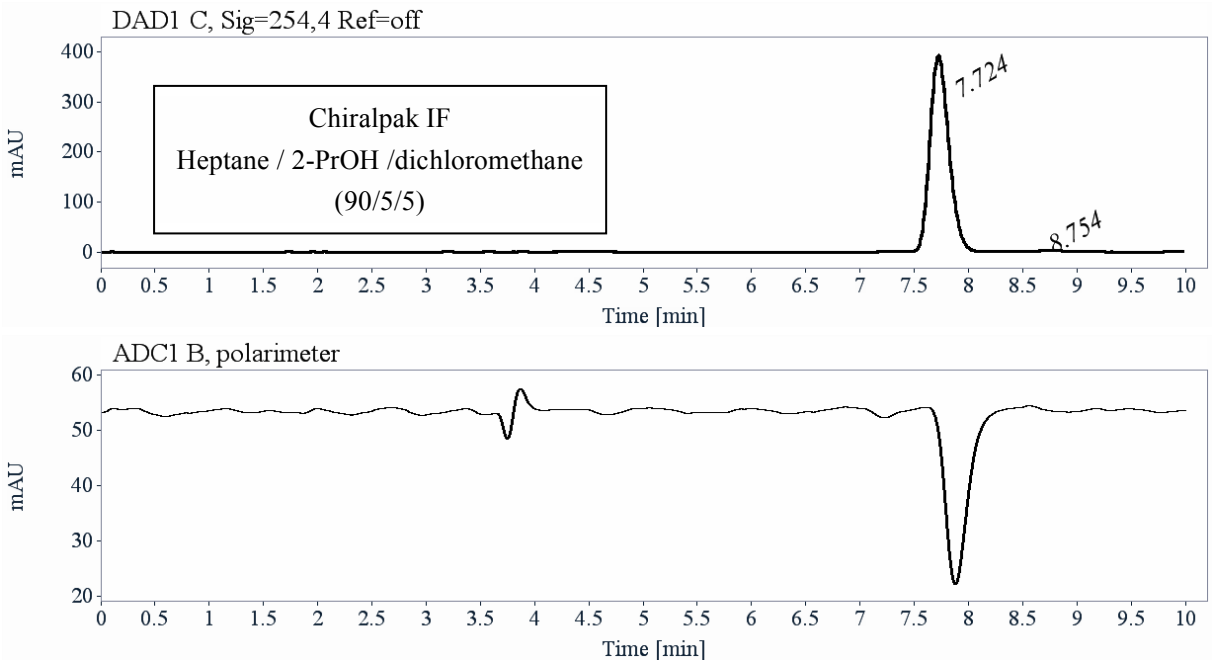

RT [min]	Area	Area%
7.72	4800	99.00
8.75	48	1.00
Sum	4848	100.00

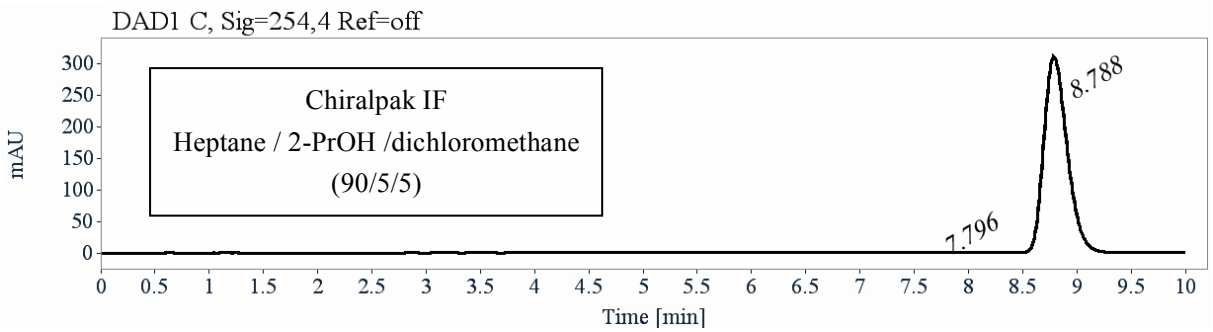

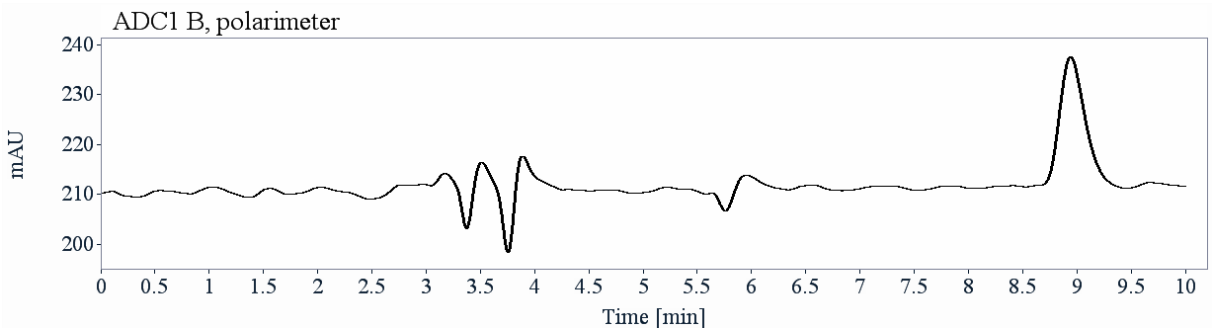

RT [min]	Area	Area%
7.80	7	0.15
8.79	4634	99.85
Sum	4641	100.00

Single crystals of compound (+)-**8** ($C_{20}H_{21}NO_2S$) were crystallized from acetonitrile. A suitable crystal was selected and mounted on a SuperNova, Dual, Cu at zero, AtlasS2 diffractometer. The crystal was kept at 223.00(10) K during data collection. Using Olex2[26], the structure was solved with the ShelXT[27] structure solution program using Intrinsic Phasing and refined with the ShelXL[28] refinement package using Least Squares minimisation.

Absolute configuration of (+)-6-methyl-1-phenyl-3-(p-tolylsulfonyl)-3-azabicyclo[4.1.0]hept-4-ene (+)-8

Crystal Data for $C_{20}H_{21}NO_2S$ (*M* =339.44 g/mol): orthorhombic, space group $P2_12_12_1$ (no. 19), *a* = 7.1089(3) Å, *b* = 13.2422(5) Å, *c* = 19.3781(7) Å, *V* = 1824.20(12) $Å^3$, *Z* = 4, *T* = 223.00(10) K, μ(Cu Kα) = 1.658 mm^{-1}, *Dcalc* = 1.236 g/cm^3, 5284 reflections measured (8.086° ≤ 2Θ ≤ 127.176°), 2961 unique (R_{int} = 0.0276, R_{sigma} = 0.0387) which were used in all calculations. The final R_1 was 0.0496 (I > 2σ(I)) and wR_2 was 0.1379 (all data).

Refinement model description

Number of restraints - 0, number of constraints - unknown.

Details:

1. Fixed Uiso
 At 1.2 times of:
 All C(H) groups, All C(H,H) groups

At 1.5 times of:
All C(H,H,H) groups
2.a Secondary CH2 refined with riding coordinates:
C4(H4A,H4B), C6(H6A,H6B)
2.b Aromatic/amide H refined with riding coordinates:
C1(H1), C2(H2), C9(H9), C10(H10), C11(H11), C12(H12), C13(H13), C15(H15), C16(H16), C18(H18), C19(H19)
2.c Idealised Me refined as rotating group:
C7(H7A,H7B,H7C), C20(H20A,H20B,H20C)

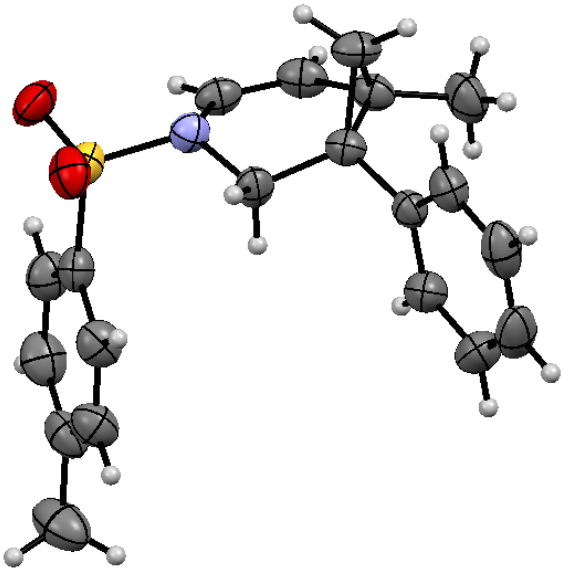

Crystal data and structure refinement for **(+)-8**[†]

Identification code	vmav441plus
Empirical formula	$C_{20}H_{21}NO_2S$
Formula weight	339.44
Temperature/K	223.00(10)
Crystal system	orthorhombic
Space group	$P2_12_12_1$
a/Å	7.1089(3)
b/Å	13.2422(5)
c/Å	19.3781(7)
α/°	90
β/°	90
γ/°	90
Volume/Å^3	1824.20(12)
Z	4
ρ_{calc}g/cm^3	1.236
μ/mm^{-1}	1.658
F(000)	720.0
Crystal size/mm^3	0.28 × 0.24 × 0.05
Radiation	Cu Kα (λ = 1.54184)
2Θ range for data collection/°	8.086 to 127.176

[†] CCDC 1523722

Index ranges	$-6 \le h \le 8$, $-15 \le k \le 15$, $-22 \le l \le 21$
Reflections collected	5284
Independent reflections	2961 [R_{int} = 0.0276, R_{sigma} = 0.0387]
Data/restraints/parameters	2961/0/219
Goodness-of-fit on F^2	1.088
Final R indexes [I>=2σ (I)]	R_1 = 0.0496, wR_2 = 0.1349
Final R indexes [all data]	R_1 = 0.0522, wR_2 = 0.1379
Largest diff. peak/hole / e Å^{-3}	0.58/-0.26
Flack parameter	0.00(2)

Fractional Atomic Coordinates (×10^4) and Equivalent Isotropic Displacement Parameters (Å^2×10^3) for **(+)-8**. U_{eq} is defined as 1/3 of of the trace of the orthogonalised U_{IJ} tensor.

Atom	*x*	*y*	*z*	U(eq)
S1	5824.5(15)	6195.9(7)	3794.3(5)	42.0(3)
O1	4747(6)	7050(2)	3588.7(17)	56.5(9)
O2	7658(5)	6035(2)	3509.8(16)	51.0(8)
N1	4571(5)	5190(3)	3589.8(17)	37.9(7)
C1	2587(6)	5242(3)	3641(2)	41.0(9)
C2	1527(6)	4438(4)	3546(2)	44.2(10)
C3	2295(6)	3429(3)	3369(2)	40.7(9)
C4	3585(6)	3404(4)	2742(2)	46.2(10)
C5	4428(5)	3318(3)	3449.4(18)	35.3(8)
C6	5454(5)	4210(3)	3756(2)	39.4(8)
C7	1040(7)	2528(4)	3510(3)	58.5(12)
C8	5287(5)	2343(3)	3687(2)	36.2(8)
C9	6218(6)	1702(3)	3230(2)	44.2(9)
C10	7135(7)	856(4)	3471(3)	58.2(13)
C11	7157(7)	636(4)	4167(3)	63.2(14)
C12	6230(8)	1259(4)	4619(3)	59.2(12)
C13	5292(7)	2105(3)	4387(2)	48.4(10)
C14	6040(6)	6213(3)	4700(2)	39.7(8)
C15	7393(6)	5637(3)	5024(2)	47.2(9)
C16	7506(7)	5629(4)	5731(2)	52.2(10)
C17	6281(6)	6201(4)	6132(2)	51.3(10)
C18	4945(7)	6776(4)	5796(3)	55.7(12)
C19	4786(7)	6790(3)	5088(3)	50(1)
C20	6429(9)	6183(6)	6908(3)	73.9(16)

Anisotropic Displacement Parameters (Å^2×10^3) for **(+)-8**. The Anisotropic displacement factor exponent takes the form: $-2\pi^2[h^2a^{*2}U_{11}+2hka^*b^*U_{12}+\ldots]$.

Atom	U_{11}	U_{22}	U_{33}	U_{23}	U_{13}	U_{12}
S1	49.1(5)	33.2(5)	43.7(5)	4.1(4)	5.8(4)	-1.4(4)
O1	79(2)	38.0(15)	52.3(17)	11.9(13)	-0.2(16)	6.0(15)
O2	48.7(16)	50.4(18)	53.8(16)	-2.8(13)	14.5(14)	-11.7(14)
N1	34.8(17)	36.9(16)	42.1(16)	1.3(13)	0.2(13)	3.3(14)
C1	38(2)	46(2)	38.6(19)	3.6(16)	0.5(16)	12(2)
C2	31.0(19)	61(3)	41(2)	-0.2(18)	1.3(16)	7.9(18)

C3	32.0(19)	50(2)	40.0(19)	-1.6(17)	-4.6(16)	1.2(17)
C4	51(2)	56(2)	31.6(18)	-0.8(17)	-4.4(17)	9.9(19)
C5	33.1(18)	40.4(18)	32.4(17)	-0.3(15)	-1.0(15)	1.3(16)
C6	33.1(19)	33.5(18)	52(2)	1.4(17)	-5.9(17)	3.9(15)
C7	44(2)	57(3)	74(3)	-3(2)	-10(2)	-14(2)
C8	33.1(18)	32.5(18)	43(2)	-1.3(15)	-6.5(15)	-3.4(14)
C9	40(2)	41(2)	51(2)	-7.0(18)	-0.2(18)	-5.3(18)
C10	44(2)	41(2)	90(4)	-13(2)	-3(2)	1.5(19)
C11	54(3)	36(2)	100(4)	7(2)	-20(3)	4(2)
C12	71(3)	48(2)	59(3)	12(2)	-17(2)	0(2)
C13	54(3)	45(2)	45(2)	1.4(18)	-8(2)	-2.0(19)
C14	40.9(19)	31.4(17)	47(2)	-2.0(15)	3.6(16)	-2.2(17)
C15	41(2)	48(2)	53(2)	-8.0(19)	2.6(19)	8.0(19)
C16	43(2)	60(3)	53(2)	-5(2)	-6(2)	1(2)
C17	45(2)	58(3)	50(2)	-10(2)	1.4(18)	-15(2)
C18	55(3)	53(3)	59(3)	-14(2)	12(2)	3(2)
C19	49(2)	41(2)	60(3)	-4.1(19)	2(2)	9.3(19)
C20	67(3)	104(4)	51(3)	-13(3)	3(2)	-20(3)

Bond Lengths for **(+)-8**

Atom	**Atom**	**Length/Å**	**Atom**	**Atom**	**Length/Å**
S1	O1	1.423(3)	C8	C9	1.394(6)
S1	O2	1.431(3)	C8	C13	1.392(6)
S1	N1	1.651(4)	C9	C10	1.378(7)
S1	C14	1.761(4)	C10	C11	1.378(8)
N1	C1	1.416(5)	C11	C12	1.371(8)
N1	C6	1.477(5)	C12	C13	1.379(7)
C1	C2	1.317(7)	C14	C15	1.379(6)
C2	C3	1.483(6)	C14	C19	1.395(6)
C3	C4	1.524(6)	C15	C16	1.372(7)
C3	C5	1.531(5)	C16	C17	1.392(7)
C3	C7	1.514(6)	C17	C18	1.381(7)
C4	C5	1.501(5)	C17	C20	1.506(7)
C5	C6	1.511(5)	C18	C19	1.377(7)
C5	C8	1.501(5)			

Bond Angles for **(+)-8**.

Atom	**Atom**	**Atom**	**Angle/˚**	**Atom**	**Atom**	**Atom**	**Angle/˚**
O1	S1	O2	120.0(2)	C8	C5	C3	121.1(3)
O1	S1	N1	106.50(19)	C8	C5	C6	110.8(3)
O1	S1	C14	108.4(2)	N1	C6	C5	113.3(3)
O2	S1	N1	106.21(18)	C9	C8	C5	121.5(4)
O2	S1	C14	107.8(2)	C13	C8	C5	119.7(4)
N1	S1	C14	107.25(17)	C13	C8	C9	118.6(4)

C1	N1	S1	118.8(3)	C10	C9	C8	120.3(4)
C1	N1	C6	116.8(3)	C9	C10	C11	120.5(5)
C6	N1	S1	115.3(3)	C12	C11	C10	119.5(5)
C2	C1	N1	121.4(4)	C11	C12	C13	120.8(5)
C1	C2	C3	123.3(4)	C12	C13	C8	120.2(4)
C2	C3	C4	115.2(4)	C15	C14	S1	120.5(3)
C2	C3	C5	115.3(4)	C15	C14	C19	120.2(4)
C2	C3	C7	116.8(4)	C19	C14	S1	119.3(3)
C4	C3	C5	58.8(2)	C16	C15	C14	120.0(4)
C7	C3	C4	118.8(4)	C15	C16	C17	121.1(5)
C7	C3	C5	119.3(4)	C16	C17	C20	120.3(5)
C5	C4	C3	60.8(2)	C18	C17	C16	117.8(4)
C4	C5	C3	60.3(3)	C18	C17	C20	121.8(5)
C4	C5	C6	119.6(4)	C19	C18	C17	122.3(4)
C4	C5	C8	120.5(3)	C18	C19	C14	118.5(4)
C6	C5	C3	116.3(3)				

Hydrogen Atom Coordinates (Å×10^4) and Isotropic Displacement Parameters (Å^2×10^3) for **(+)-8**.

Atom	***x***	***y***	***z***	**U(eq)**
H1	2019.53	5856.71	3743.19	49
H2	231.16	4505.89	3593.27	53
H4A	3565.94	2802.06	2456.46	55
H4B	3777.16	4029.95	2491.88	55
H6A	5498.83	4132.75	4253.86	47
H6B	6739.06	4212.27	3587.64	47
H7A	838.61	2465.9	3998.44	88
H7B	1631.24	1926.64	3339.56	88
H7C	-146.97	2621.82	3282.63	88
H9	6220.69	1845.27	2760.44	53
H10	7743.99	428.85	3162.6	70
H11	7794.6	70.6	4327.99	76
H12	6234.55	1108.5	5087.44	71
H13	4661.9	2517.86	4698.54	58
H15	8229.83	5254.05	4764.11	57
H16	8415.14	5233.7	5946.11	63
H18	4123.96	7167.63	6056.84	67
H19	3861.81	7175.51	4873.54	60
H20A	6490.79	5496.2	7064.09	111
H20B	5344.89	6505.95	7104.43	111
H20C	7544.13	6536.02	7048.53	111

5. NMR studies. Kinetics of Au-catalyzed enyne cycloisomerizations.

Determination of initial rates.

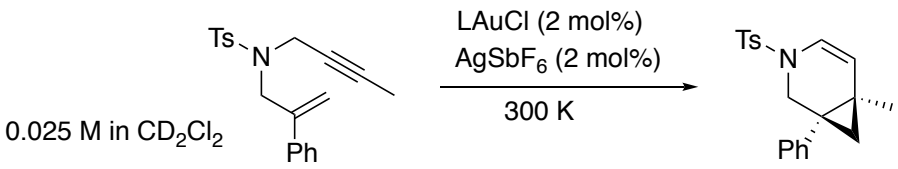

General considerations: All reactions were carried out in a NMR tube with a concentration of enyne **6** of 0.025 M and 2 mol% of catalyst. These conditions correspond to the standard conditions used in this study for the cycloisomerization reactions of enynes **5** and **6**. For all experiments $AgSbF_6$ and Au^I complexes were weighed in a glovebox with exclusion of moisture and O_2. CD_2Cl_2 was introduced under argon atmosphere. For each experiment, a fresh mother solution of $AgSbF_6$ at a concentration of 0.01 M was prepared by diluting 6.9 mg (0.02 mmol) of $AgSbF_6$ in 2 mL of CD_2Cl_2. The solution was kept away from light until addition into the NMR tube. A solution of enyne **6** at a concentration of 0.0312 M was also prepared under argon by diluting 10.6 mg (0.0312 mmol) of **6** in 1 mL of CD_2Cl_2.

*Cycloisomerization catalyzed by **(α-ICyD)AuCl**.*
A solution of **(α-ICyD)AuCl** at a concentration of 0.0033 M was prepared under argon by diluting 7.15 mg (0.002 mmol) of **(α-ICyD)AuCl** (Mw = 2679.3) in 0.8 mL of CD_2Cl_2.
In a NMR tube flushed with argon, were introduced 25 mL of $AgSbF_6$ 0.01 M in CD_2Cl_2 (0.086 mg, 0.25 mmol) and 75 mL of **(α-ICyD)AuCl** 0.0033 M in CD_2Cl_2 (0.67 mg, 0.25 mmol). The mixture was stirred for 15 min with exclusion of light and 0.4 mL of enyne 0.0312 M (4.24 mg, 12.5 mmol) were added. An inner tube containing the internal reference (1,4-dimethoxybenzene in CD_2Cl_2) was placed in the NMR tube. After closing, the sample was introduced in the spectrometer for analysis. In this case, no conversion was observed after 16 h at 300 K (initial rate $r_0 = 0$).

*Cycloisomerization catalyzed by **(β-ICyD)AuCl**.*
A solution of **(β-ICyD)AuCl** 0.0033 M was prepared under argon by diluting 6.24 mg (0.002 mmol) of **(β-ICyD)AuCl** (Mw = 3127.8) in 0.6 mL of CD_2Cl_2.
In a NMR tube flushed with argon, were introduced 25 mL of $AgSbF_6$ 0.01 M in CD_2Cl_2 (0.086 mg, 0.25 mmol) and 75 mL of **(β-ICyD)AuCl** 0.0033 M in CD_2Cl_2 (0.78 mg, 0.25 mmol). The mixture was stirred for 15 min with exclusion of light and 0.4 mL of enyne 0.0312 M (4.24 mg, 12.5 mmol) were added. An inner tube containing the internal reference (1,4-dimethoxybenzene in CD_2Cl_2) was placed in the NMR tube. After closing, the sample was introduced in the spectrometer for analysis. ^1H spectra were recorded with a 5-min interval for 3 h, then with a 15-min interval for 12 h. The results are presented in **Figure S18**.

*Cycloisomerization catalyzed by **(IPr)AuCl**.*
A solution of **(IPr)AuCl** 0.01 M was prepared under argon by diluting 6.2 mg (0.01 mmol) of **(IPr)AuCl** in 1 mL of CD_2Cl_2.

In a NMR tube flushed with argon, were introduced 25 mL of $AgSbF_6$ 0.01 M in CD_2Cl_2 (0.086 mg, 0.25 mmol) and 25 mL of **(IPr)AuCl** 0.01 M in CD_2Cl_2 (0.15 mg, 0.25 mmol). The mixture was stirred for 5 min with exclusion of light. 0.4 mL of enyne 0.0312 M (4.24 mg, 12.5 mmol) and 50 mL of CD_2Cl_2 were added. An inner tube containing the internal reference (1,4-dimethoxybenzene in CD_2Cl_2) was placed in the NMR tube. After closing, the sample was introduced in the spectrometer for analysis. ^1H spectra were recorded with a 5-min interval for 3 h. The results are presented in **Figure S19**.

TON studies

*Cycloisomerization catalyzed by **(β-ICyD)AuCl**.*

A solution **of (β-ICyD)AuCl** 0.0033 M was prepared under argon by diluting 6.24 mg (0.002 mmol) of **(β-ICyD)AuCl** (Mw = 3127.8) in 0.6 mL of CD_2Cl_2.

In a NMR tube flushed with argon, were introduced 25 mL of $AgSbF_6$ 0.01 M in CD_2Cl_2 (0.086 mg, 0.25 mmol) and 75 mL of **(β-ICyD)AuCl** 0.0033 M in CD_2Cl_2 (0.78 mg, 0.25 mmol). The mixture was stirred for 15 min with exclusion of light and 0.4 mL of enyne 0.0312 M (4.24 mg, 12.5 mmol) were added. An inner tube containing the internal reference (1,4-dimethoxybenzene in CD_2Cl_2) was placed in the NMR tube. After closing, the sample was introduced in the spectrometer for analysis.

Once all the enyne **6** was consumed, 9 additional equivalents of enyne **6** (38.2 mg, 115 mmol) were directly introduced in the NMR tube under argon. The reaction was stirred at room temperature for 18 h and ^1H NMR clearly showed the disappearance of all the substrate (see figure below, spectrum a). 10 additional equivalents of enyne **6** (42.4 mg, 125 mmol) were subsequently added and, after stirring at room temperature for 48 h. The ^1H NMR spectrum (see figure below, spectrum b) shows a conversion of 85% with 15% of remaining starting material (^1H NMR signals annotated (°)). The final conditions correspond to an enyne concentration of 0.5 M and a catalyst loading of 0.1 mol%, giving a TON of 850 and an ee of 79%. A this high concentration, the solution becomes very viscous.

*Cycloisomerization catalyzed by **(IPr)AuCl**.*

A solution of **(IPr)AuCl** 0.01 M was prepared under argon by diluting 6.2 mg (0.01 mmol) of **(IPr)AuCl** in 1 mL of CD_2Cl_2.

In a NMR tube flushed with argon, were introduced 25 mL of $AgSbF_6$ 0.01 M in CD_2Cl_2 (0.086 mg, 0.25 mmol) and 25 mL of **IPrAuCl** 0.01 M in CD_2Cl_2 (0.15 mg, 0.25 mmol). The mixture was stirred for 5 min with exclusion of light. 0.4 mL of enyne 0.0312 M (4.24 mg, 12.5 mmol) and 50 mL of CD_2Cl_2 were added. An inner tube containing the internal reference (1,4-dimethoxybenzene in CD_2Cl_2) was placed in the NMR tube. After closing, the sample was introduced in the spectrometer for analysis. Once all the enyne was consumed, 9 additional equivalents of enyne **6** (38.2 mg, 115 mmol) were directly introduced in the NMR tube under argon. The reaction was stirred at room temperature for 18h and ^1H NMR clearly showed the disappearance of all the substrate (see figure below, spectrum c). 10 additional equivalents of enyne **6** (42.4 mg, 125 mmol) were subsequently added and, after stirring at room temperature for 24 h. The ^1H NMR spectrum (see figure below, spectrum d) shows a conversion of 80% with 20% of remaining starting material (^1H NMR signals annotated (°)). The final conditions correspond to an enyne concentration of 0.5 M and a catalyst loading of 0.1 mol%, giving a TON of 800. (**Figure S20**)

6. DFT calculations

DFT calculations were performed with the Turbomole package, version 6.4.12 The B3LYP functional[29] was used for all the calculations, and complemented by the D3 semi-empirical dispersion scheme.[30] The Def2-SV(P) gaussian type basis set was used to describe orbitals.[31]

Supplemental References

[1] T. Lecourt, A. J. Pearce, A. Herault, M. Sollogoub, P. Sinaÿ, *Chem. Eur. J.* **2004**, *10*, 2960-2971; E. Zaborova, Y. Blériot, M. Sollogoub, *Tetrahedron Lett.* **2010**, *51*, 1254-1256.

[2] S. Guieu, M. Sollogoub, *J. Org. Chem.* **2008**, *73*, 2819-2828.

[3] E. Deunf, E. Zaborova, S. Guieu, Y. Blériot, J. Verpeaux, O. Buriez, M. Sollogoub, C. Amatore, *Eur. J. Inorg. Chem*, **2010**, *29*, 4720-4727;

[4] A. J. Pearce and P. Sinaÿ, *Angew. Chem., Int. Ed.* **2000**, *39*, 3610-3612; S. Volkov, L. Kumprecht, M. Budešínský, M. Lepšík, M. Dušek, T. Kraus, *Org. Biomol. Chem.* **2015**, *13*, 2980-2985.

[5] M. Guitet, P. Zhang, F. Marcelo, C. Tugny, J. Jiménez-Barbero, O. Buriez, C. Amatore, V. Mouriès-Mansuy, J.-P. Goddard, L. Fensterbank, Y. Zhang, S. Roland, M. Ménand, M. Sollogoub, *Angew. Chem. Int. Ed.* **2013**, *52*, 7213-7218.

[6] C. Egloff, R. Gramage-Doria, M. Jouffroy, D. Armspach, D. Matt, L. Toupet, *C. R. Chimie* **2013**, *16*, 509-514.

[7] A. Collado, A Gomez-Suarez, A. R. Martin, A. M. Z Slawin, S. P. Nolan, *Chem. Commun*. **2013,** 49, 5541-5543;

[8] R. Visbal, A. Laguna, M. Concepcion Gimeno, *Chem. Commun*. **2013,** *49*, 5642-5644;

[9] P. Mathew, A. Neels, M. Albrecht. *J. Am. Chem. Soc*. **2008**, *130*, 13534-13535.

[10] G. Guisado-Barrios, J. Bouffard, B. Donnadieu, G. Bertrand. *Angew. Chem., Int. Ed*. **2010**, *49*, 4759-4762.

[11] O. Schuster, L. Yang, H. G. Raubenheimer, M. Albrecht, *Chem. Rev.* **2009**, *109*, 3445-3478 ; M. Albrecht, *Adv. Organomet. Chem.* **2014**, *62*, 111-158.

[12] V. V. Rostovtsev, L. G. Green, V. V. Fokin, K. B. Sharpless, *Angew. Chem. Int. Ed.* **2002**, *41*, 2596-2599.

[13] I. Tabushi, T. Nabeshima, H. Kitaguchi and K. Yamamura, *J. Am. Chem. Soc.* **1982**, *104*, 2017-2019; K. Fujita, A. Matsunaga, H. Yamamura and T. Imoto, *J. Org. Chem.* **1988**, *53*, 4520-4522; E. Fasella, S. D. Dong and R. Breslow, *Bioorg. Med. Chem.* **1999**, 7, 709-714; D.-Q. Yuan, T. Yamada and K. Fujita, *Chem. Commun.* **2001**, 2706-2707; M. Fukudome, D.-Q. Yuan, K. Fujita, *Tetrahedron Lett.* **2005**, *46*, 1115-1118; H. Yu, D.-Q. Yuan, Y. Makino, M. Fukudome, R.-G. Xie, K. Fujita, *Chem. Commun.* **2006**, 5057-5059; D.-Q. Yuan, Y. Kitagawa, K. Aoyama, T. Douke, M. Fukudome, K. Fujita, *Angew. Chem. Int. Ed.* **2007**, *46*, 5024 –5027; M. Jouffroy, R. Gramage-Doria, D. Armspach, D. Matt, L. Toupet *Chem. Commun.,* 2012, 48, 6028-6030.

[14] O. Bistri, P. Sinaÿ, M. Sollogoub, *Tetrahedron Lett.* **2005**, *46*, 7757-7760; O. Bistri, P. Sinaÿ, M. Sollogoub, *Chem. Commun.* **2006**, 1112-1114 ; O. Bistri, P. Sinaÿ, M. Sollogoub, *Chem. Lett.* **2006**, *35*, 534-535; O. Bistri, P. Sinaÿ, M. Sollogoub, *Tetrahedron Lett.* **2006**, *47*, 4137-4139; O. Bistri, P. Sinaÿ, J. Jiménez Barbero, M. Sollogoub, *Chem. Eur. J.* **2007**, *13*, 9757-9774; E. Zaborova, M. Guitet, G. Prencipe, Y. Blériot, M. Ménand, M. Sollogoub, *Angew. Chem. Int. Ed*. **2013**, *52*, 639-644; B. Wang, E. Zaborova, S. Guieu, M. Petrillo, M. Guitet, Y. Blériot, M. Ménand, Y. Zhang, M. Sollogoub *Nature Comms.* **2014**, *5*, 5354.

[15] S. Guieu, M. Sollogoub, *Angew. Chem. Int. Ed*. **2008**, *47*, 7060-7063

[16] M. Petrillo, L. Marinescu, C. Rousseau, M. Bols, *Org. Lett.* **2009**, *11*, 1983-1985.

[17] S. Hanessian, C. Hocquelet, C. K. Jankowski, *Synlett* **2008**, 715-719.

[18] G. Gil-Ramírez, E. C. Escudero-Adan, J. Benet-Buchholz, P. Ballester, *Angew. Chem. Int. Ed.* **2008**, *47*, 4114-4118.

[19] B. Bertino-Ghera, F. Perret, B. Fenet, H. Parrot-Lopez, *J. Org. Chem.* **2008**, *73*, 7317–7326.

[20] Hoye, T.R.; Suriano, J.A. *Organometallics* **1992**, *11*, 2044-2050.

[21] Nieto-Oberhuber, C.; Munoz, M.P.; Lopez, S.; Jimenez-Nunez, E.; Nevado, C.; Herrero-Gomez, E.; Raducan, M.; Echavarren, A.M. *Chem. Eur. J.* **2006**, *12*, 1677-1693.

[22] Gryparis, C.; Efe, C.; Raptis, C.; Lykakis, I.N.; Stratakis, M. *Org. Lett.* **2012**, *14*, 2956-2959.

[23] T. Nishimura, Y. Maeda, T. Hayashi, *Org. Lett.* **2011**, *13*, 3674-3677.

[24] A. Fürstner, H. Szillat, F. Stelzer, *J. Am. Chem. Soc.* **2000**, *122*, 6785-6786.

[25] T. Shibata, Y. Kobayashi, S. Maekawa, N. Toshida, K. Takagi *Tetrahedron* **2005**, *61*, 9018-9024.

[26] O.V. Dolomanov, L.J. Bourhis, R.J. Gildea, J.A.K. Howard, H. Puschmann, *J. Appl. Cryst.* **2009**, *42*, 339-341.

[27] G.M. Sheldrick, *Acta Cryst.* **2015**, A71, 3-8.

[28] G.M. Sheldrick, *Acta Cryst.* **2015**, C71, 3-8.

[29] a) Becke, A. D. *J. Chem. Phys.* **1993**, *98*, 5648–5653. (b) Becke, A. D. *Phys. Rev. A* **1988**, *38*, 3098–3100. (c) Lee, C.; Yang, W.; Parr, R. G. *Phys. Rev. B* **1988**, *37*, 785-789.

[30] Grimme, S.; Antony, J.; Ehrlich, S.; Krieg, H. *J. Chem. Phys.* **2010**, *132*, 154104–154104.

[31] Schäfer, A.; Horn, H.; Ahlrichs, R. *J. Chem. Phys.***1992**, *97*, 2571–2577.